The Role of Neutrophil Elastase in Abdominal Aortic Aneurysm and Aortic Dissection

Stuart Pearce

Primary Supervisor: Professor Qingzhong Xiao
Secondary Supervisor: Dr Pedro Cutillas

Submitted to Queen Mary University of London in partial fulfilment of the requirements for the Degree of Doctor of Philosophy

---

William Harvey Research Institute

STATEMENT OF ORIGINALITY

I, Stuart Pearce would like to confirm that all efforts and experimental results stated within this thesis is my own, or where others have collaborated and contributed this will be acknowledged. Knowledge drawn upon from previous works will also be acknowledged.

I have done my utmost to ensure the originality of this work, along with the ethical and legal validity also, infringing upon no copyright, intellectual property or exposing any confidential materials within human experiments.

I accept that the College and University has the right to employ plagiarism techniques to check the originality of this work and that this work has not been submitted to any other institution for degree-awarding purposes.

As Author, the copyright of this thesis and the information contained rests with me, and no publication of part of this work may be published without my prior consent.

COLLABORATIONS AND CONTRIBUTIONS

MRI programming assistance and teaching was carried out by the Cancer Imaging group, part of the John Vane Research Centre. Following initial aid with set up and teaching, all scans and development were performed independently with troubleshooting aid from Sven Macholl and Joseph Brooks.

Assistance with Proteomic work was carried out by the group of my secondary supervisor, Dr Pedro Cutillas. Protein preparation and analysis assistance was also carried out by Professor Xiao and the research group, most namely Dr Wei Wu.

Human Works was performed in conjunction with the Barts BioBank resource and St Georges Hospital Medical School.

<u>Papers Published during this PhD:</u>

Genetic and Pharmacologic Inhibition of the Neutrophil Elastase Inhibits Experimental Atherosclerosis

Journal of the American Heart Association -February 2018

Guanmei Wen , Weiwei An , Jiangyong Chen , Eithne M. Maguire , Qishan Chen , Feng Yang , Stuart W. A. Pearce , Maria Kyriakides , Li Zhang , Shu Ye , Sussan Nourshargh , and Qingzhong Xiao

Foam cell formation: A new target for fighting atherosclerosis and cardiovascular disease

Vascular Pharmacology- August 2018

Eithne M.Maguire, Stuart W.A.Pearce, QingzhongXiao

The Role of Matrix Metalloproteinase in Abdominal Aortic Aneurysm and Aortic Dissection

Pharmaceuticals 2019, 12(3), 118; https://doi.org/10.3390/ph12030118

Eithne M. Maguire, Stuart W. A. Pearce, Rui Xiao, Aung Y. Oo and Qingzhong Xiao

PowerPoint and Poster Presentations of PhD Research:

William Harvey Research Day, 2017- Poster

Stuart Pearce, Joseph Brooks, Dan Chen, Eithne McGuire, Qingzhong Xiao

William Harvey Research Day, 2018- Poster

Stuart Pearce, Joseph Brooks, Eithne McGuire, Shiiping He, Qingzhong Xiao

William Harvey Spring Conference, 2018- Presentation

Stuart Pearce, Joseph Brooks, Eithne McGuire, Shiiping He, Qingzhong Xiao

University of Kentucky- Cardiovascular Research Day, September 2018- Poster Presentation

Stuart Pearce, Joseph Brooks, Eithne McGuire, Shiiping He, Mei Yung Qingzhong Xiao

British Atherosclerosis Society and the British Society of Cardiovascular Research, 2019- Poster Presentation

QMUL-3Rs Research Day, 2019

Stuart Pearce, Joseph Brooks, Eithne McGuire, Shiiping He, Qingzhong Xiao

ACKNOWLEDGEMENTS

Throughout my time at Barts, I have had a huge amount of support from my friends, family and Prof. Xiaos' lab group, all of which I would like to thank as without them this would not have been possible. I would like to specifically thank Prof. Xiao in his support of me as my supervisor. Furthermore, I would like to mention people from 87, SGS, Eyott Gardens, Jamie and Rajaei, for putting up with my moods, when things went less smoothly in the lab or I was having my surgeries and getting frustrated that I couldn't work, and for generally being there and being great friends. Thank you, I will forever be grateful

ABSTRACT

Background:

Abdominal Aortic Aneurysm (AAA) affects 4-5% of men over 65, and Aortic Dissection (AD) is a life-threatening aortic pathology where 75% of patients die within 2-weeks post-onset. Relatively little is known about the underlying mechanisms, which warrants further investigation. Neutrophil Elastase (NE) is an enzyme with roles in priming of the immune system, clearance of large pathogens and remodelling of extracellular-matrix proteins, all influential in AAA and AD. The Angiotensin II (Ang II) and Calcium Chloride (CaCL2) procedures provide methods to model the AAA pathology within small rodents, which enables the study of the disease. Furthermore, the β-aminopropionitrile monofumarate (BAPN) model provides an animal model which mimics the AD pathology and allows in-depth study of both changes in mortality and pathological severity.

Within AAA and AD, there is known to be a large immune system implication in the production and development of both pathologies, with enzymatic activity seemingly pivotal in the initiation of the AD and AAA phenotype. With the impact of enzymes such as immune cell-derived matrix metalloproteinases (MMPs)-2 and -9 studied in depth. Neutrophil Elastase (NE) is an, as yet, unstudied enzyme within these processes.

Purpose:

Current treatment regimen for AAA and AD both have significant flaws and is entirely surgical, with most at-risk groups being elderly and treatment consequentially of increased risk of complications. Surgical intervention has complex post-operative care considerations, with reintervention and morbidity being high within the following weeks after the procedures take place. Understanding of the underlying mechanisms

contributing to AAA and AD is poor and therefore designing a pharmacological agent to improve therapy is difficult. Understanding the role of NE and its implications within AAA will allow us to identify whether it has an impact within the pathology and, if so if it is an appropriate target for therapeutic intervention.

Therefore, the primary aims of this project was to identify if Neutrophil Elastase is involved within the AAA and AD processes, to detect via what mechanism it may act and if NE is a potential novel drugs target for treatment of AAA and AD.

Methods and Results:

To study if NE gene expression is regulated by AAA pathologies, *in Vitro* experiments were conducted with multiple cell lines (human aortic SMCs, Raw264.7 macrophages and HuVECs). Data from RT-qPCR analysis was insignificant and failed to show a relation between NE, MMP2 and MMP9, when cells were treated with Angiotensin II (Ang II) and Calcium Chloride, respectively.

Development of an MRI scanning technique to monitor the progression of AAA overtime was undertaken. A semi-automatic methodology was developed with representative and highly reproducible results achieved. This enabled the detailed study of animals whilst undergoing AAA-induction procedures, namely the CaCl2 and Ang II animal models.

By utilising two *in vivo* models, so far we have observed a significant difference that the two Aneurysm models result in lower AAA incidence within NE deficient mice, with infrarenal aortic expansion significantly reduced. Investigations into flow and other dynamic aspects of the vessel differ between animal models and consequentially need to be furthered but at present no significant differences were observable. Underlying mechanisms for AAA and NEs contribution towards the pathology were assessed, with novel associations between NE and MMPs identified as well as the

involvement of proteins such as TBL1x, Caveolin-2 and COPS8 following proteomics analysis techniques.

Similar results were seen within AD experimentation, with knockout of NE resulting in significantly lower mortality and vessel dissection rate. Similar histological staining patterns were observed within this model when compared to the two AAA animal models. This suggests a potential common pathway between the two that results in aortic medial degradation, and rupture of the vessel.

Early Human translational experiments were carried out with a AAA patient audit, there were no significant findings that correlated any basic blood profile characteristic to size or progression of AAA. This work was continued, working with Barts BioBank Resource to obtain tissues from surgical repair patients. Diseased tissues displayed expression of NE with small areas of staining being seen alongside MMPs, such as within the remodelled medial portion of the vessel, similar to that of previous mouse works. Furthermore, blood serum samples from patients had no significant change in level of NE when compared to Healthy Controls.

Conclusion:

This study identifies NE as having potential therapeutic applications if similar results are seen within pharmacological inhibition of the enzyme as were produced as a result of genetic knockout in mouse studies, especially within AD models. Early Translational experimental results have not been as promising, but more work is needed to fully understand whether NE could play a similar role within the Human condition and therefore warrant further study as a potential drugs target, although current results need to be developed prior to this.

Wider Implications:

Findings outlined within this thesis suggest NE has a potential role within both AD and AAA pathologies, with implications in the regulation of MMPs as well as potential direct enzymatic action within the modification of extracellular matrix proteins regulated within the AAA and AD conditions. Results so far show areas of promise, and with further investigation, NE inhibition could be established as a therapeutic option for AAA and/ or AD. In order to establish the link further, there is a need to determine if pharmacological knockdown of NE can produce the same results as those seen within *in vivo* experiments where genetic knockout was established.

LIST OF ABBREVIATIONS

AAA	Abdominal Aortic Aneurysm
AAS	Acute Aortic Syndrome
AD	Aortic Dissection
Ang II	Angiotensin II
AP-3	Associated Protein-3
ApoE	Apolipoprotein E
BAPN	Beta-Aminopropionitrile Monofumarate
CaCl2	Calcium Chloride
CAD	Coronary Artery Disease
CaPO4	Calcium Phosphate
CD	Cluster of Differentiation
CNC	Cardiac Neural Crest
COPD	Chronic Obstructive Pulmonary Disorder
CT	Computerised Tomography
DNA	Deoxyribose Nucleic Acid
ECM	Extra Cellular Matrix
ER	Eoestrogen Receptor
ERK	Extracellular Signal Related Kinase
EVAR	Endovascular Aortic Repair
GWAS	Genome-Wide Association Study
IF	Immunofluorescence
IL-6	Interleukin-6
LDL	Low-Density Lipoprotein
LDLR	Low-Density Lipoprotein Receptor
LPS	Lipopolysaccharide
LRP1	Low-Density Lipoprotein Receptor-Related Protein 1
MCP-1	Monocyte Chemoattractant Protein-1
MMP	Matrix MetalloProteinase
MPO	Myeloperoxidase
MRI	Magnetic Resonance Imaging
NE	Neutrophil Elastase
NE-/-	Neutrophil Elastase Knockout
NET	Neutrophil Extracellular Traps
NFKB	Nuclear Factor Kappa-Light-Chain-Enhancer of Activated B cells
NGAL	Neutrophil Gelatinase Associated Lipocalin
NLR	Neutrophil Lymphocyte Ratio
PBS	Phosphate Buffered Saline
PDGFR-B	Platelet-Derived Growth Factor Subunit-B
PVAT	PeriVascular Adipose Tissue
RAS	Renin-Angiotensin System

RNA	Ribonucleic Acid
SHF	Secondary Heart Field
TAAD	Thoracic Aneurysm Aortic Disection
TAD	Thoracic Aortic Dissection
TGF-B	Transforming Growth Factor- Beta
TIMP	Tissue Inhibitor of MMP
TLR	Toll-Like Receptor
VCAM	Vascular Cell Adhesion Protein 1
VSMC	Vascular Smooth Muscle Cell
WBC	White Blood Cell
WT	Wildtype

LIST OF TABLES

LIST OF FIGURES

TABLE OF CONTENTS

1 INTRODUCTION

An Abdominal Aortic Aneurysm (AAA) is the focal dilatation of the Aorta(1). Predominantly situated in the infra-renal segment(1), AAA is a localised weakening of the vessel wall which makes it prone to rupture (2). This pathology has a high mortality rate as a result and affects 4-6% of the male population and a smaller proportion of the female population also(3). The incidence of AAA is increased with Coronary Artery Disease (CAD) (4), family history and smoking(5), amongst others. However, the overall prevalence of AAA appears to be falling with a recent study indicating rates could be as low as 1.7% in a previously considered high-risk group(6). Contradicting this, rates of female AAA diagnosis has steadily increased to be not dissimilar to that of the male population, and screening programmes for middle-aged populations have been started in many countries, such as the UK. On top of this, rupture rates within the female population has been observed as much greater than that of the equivalent male counterpart(7). Consequentially, AAA is a significant health burden with relatively little known about the cause of the pathology.

The exact aetiology of AAA is unknown and current treatment sub-optimal, both of which highlight the need for a disease model that can produce a greater understanding of the mechanisms involved in the process. This could potentially lead to new therapeutic advances as currently open surgical repair and stenting via endovascular repair surgery (EVAR) has huge drawbacks and large risks, especially when the demographic AAA affects is taken into consideration. The pathological characteristics of AAA include collagen and elastin dysregulation(8), chronic inflammation(9),

smooth muscle apoptosis(10) and breakdown of the extracellular matrix in the surrounding areas of vasculature(11).

Chronic inflammation potentiated by the immune system is a process underlying the AAA phenotype(12). Immune driven production and activity of Matrix Metalloproteinases (MMPs) is highly up-regulated and appears decisive in the vessels expansion(9), potentiating the chronic inflammatory state, elevating numerous inflammatory markers(13). Inflammatory markers and chemokines are significantly up-regulated within AAA. Golledge et al. (1) have reported the increase in adhesion molecules and homocysteine, both of which add to the inflammatory process and are associated with conditions such as atherosclerosis. The function of Neutrophil Elastase (NE), a serine protease contained within azurophilic granules of neutrophils(14), has not currently been characterised within AAA. NE has been shown to play an important role in production of antimicrobial Neutrophil Extracellular Traps (NETs) and the developing stages of atherosclerosis(15), both of which have been suggested as predisposing or contributing factors to the AAA pathology. Resultantly, this enzyme could prove influential within the AAA pathology. Serine proteases have been observed to cleave Toll-Like Receptor-4 (TLR-4)(16), a receptor involved in inflammatory signalling, previously linked to AAA induction. Elastin degradation is a crucial step in the formation of AAA, a process performed by NE (17). Apart from its action on elastin, NE could act on other extracellular matrix (ECM) proteins, as well as non-ECM proteins, for instance, cytokines, chemokines, and receptors(17). Chua and Laurent (18), have outlined the roles of NE within lung degeneration and damage. Furthermore, still, this study was backed up by a number of other studies linking tissue-derived NE to inflammation with damaging and increasingly severe pathological features within

respiratory conditions(19,20). These studies have been furthered, with NE being targeted in respiratory conditions such as chronic obstructive pulmonary disease (COPD) and emphysema, with beneficial effects. A number of drugs have also been seen to interact with the enzyme and inhibit its effects, some of which have known circulatory implications, such as Atorvastatin (21).

NE is influential in the immune response to both gram-negative bacteria and fungi(16) and therefore strongly linked with potentiating inflammation. NE can exhibit effects both within cells and externally also, with associations with Associated Protein-3(AP3) determining its destination(16) (**Figure I**).

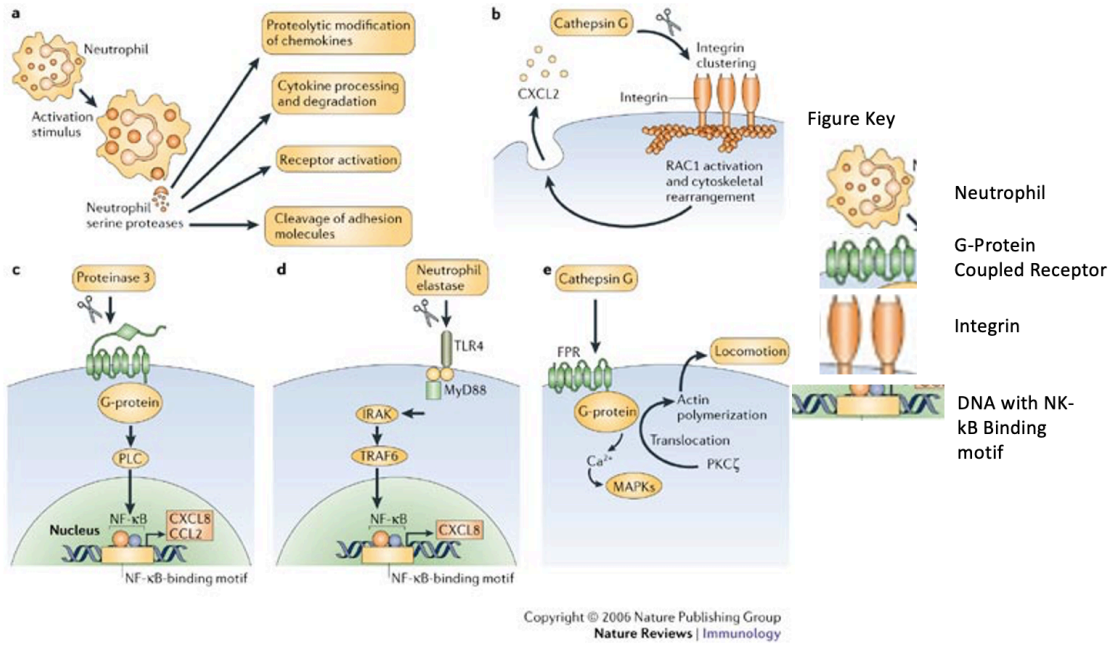

***Figure 1**- Action of Neutrophil Serine Proteases- The function of many serine proteases, including NE, including both intra- (a) and extra-cellular (b-e) effects. Some of these include interactions with immune and inflammation-associated receptors and molecules (15)*

Diagnosis of AAA is often incidental, with largely subclinical presentation. Screening programmes are in place for high-risk groups (males over 65 years old)(22). Treatment is limited, with various forms of surgery being the only course of action. This route is

not appropriate for all groups, with both EVAR and Open surgery having considerable associated risks. EVAR has a high re-intervention rate, 20% of patients within 5 years(23), whilst open surgery has a high mortality rate specifically in the peri-operative window(24). Development of alternate treatment regimens with less risk and lower invasiveness would improve patient outcome. To do this, a greater understanding of the pathology is needed. Human aneurysmal tissues give a good idea of the end-stage diseased state, but yield less of an insight into the disease aetiology. Therefore there is a need for the study of the early stages of AAA. This is near impossible *in vivo* within human studies or *in vitro* with human tissue samples, as early intervention is rare and consequentially minimal human tissue available from these time points.

With this aspect, the Angiotensin II (Ang II) and Calcium Chloride ($CaCL_2$) procedures provide a method to model the pathology within mice, enabling the study of the disease, especially at preliminary stages. $CaCL_2$ application provides a trigger that causes the induction of aortic aneurysms that can be used across a number of genetic mouse backgrounds. Unlike AAA itself, there is no differential response between genders, nor with hypercholesterolemic status. Angiotensin II provides a good model for aneurysm rupture and is currently one of the two most utilised models within the AAA research field.

In this PhD project, I will utilise both animal models of AAA (Ang II and $CaCL_2$) to study the potential role of NE in the pathology of AAA. A range of molecular and cellular biology techniques will also be applied, as well as *In Vivo* scanning techniques, to study the molecular mechanisms involved and the difference NE has to the condition. This project will allow for the study of the mechanisms underlying the AAA pathology

and possibly identify novel therapeutic targets. Small limitations of the models include discrepancies from the human phenotype such as the lack of; intra-mural thrombus, atherosclerotic background and AAA rupture, within the $CaCL_2$ model for example. However, there are a number of strengths to this model, enabling research into inflammation and inflammatory cell infiltration, neovascularisation of the area, loss of elastin and vascular smooth muscle cell (VSMC) content, plus significant increases in the levels of oxidative stress. NE has potential roles within a multitude of these characteristics and resultantly could highly influence the progression or induction of AAA.

1.1 AAA

MODELS OF AAA

AAAs are often categorised by the focal enlargement of the aorta to 1.5 times the size of the healthy or expected aortic diameter(25) usually within the infrarenal portion of the aorta. This increase in width is accompanied by the degradation of the medial segment wall, by invasion of inflammatory cells (26), as well as decreased structural organisation of both collagen and elastin. The initiator of these changes is as yet unknown, although the process has been associated with co-morbidities of heart disease as well as seen to be influenced by certain MMPs(27) and the low-density lipoprotein receptor-related protein 1 (LRP1) gene, amongst others variables. Effecting 4-5% of males over the age of 65 and 1.3% of women within the same group(28), this is a large clinical burden, especially as rates amongst the female population is on the rise(29), rupture risk is high, and pathology associated with intervention (endovascular aneurysm repair) still 23% (30).

Aneurysm is pathology where animal models have enabled a greater understanding of what we now accept to be a polygenic and multifactorial disease process. However, current models largely reproduce the findings co-founded when aneurysms are encountered, such as extracellular matrix degradation, altered collagen and elastin configuration and MMP modulation. The reason for a need for animal models within aneurysms is the lack of access to human aneurysm tissue that is not at the end-stage, post rupture. It is possible to obtain tissues from open repair surgery, but this is rare, and therefore studies on the tissues are extremely infrequent. Resultantly, there is a need for a model that combines multiple assaults to the aorta, revealing how the pathology progressively develops leading to rupture, and, creating a more representative environment in which aneurysms are formed. Consequentially this should yield more representative information on aneurysms, from which, we would be able to direct research with the aim of producing drugs or treatments using the information we have obtained, possibly improving treatment or lowering occurrence and therefore the clinical burden of aneurysms.

Currently, there are a number of animal models upon which aneurysms are studied. Each of these has aspects that they are representative of the pathology and others by which they are not. I will outline some of these benefits and flaws, including animal and process choice, with respect to the most commonly used and then conclude with what we can learn from these including what needs to be developed in order to gain a greater insight.

Based on their relevance to the clinical setting, with this being defined as the possibility to obtain information that will lead to new treatments, either due to developing greater understanding which provides the opportunity for the development of pharmacological agents as a result(31), or technical advancements that lead to

improved recovery, as seen in Wang et al. (32), the animal models of AAA will be reviewed in the following sections. Furthermore, I will regard models as representative of the pathology if they produce two or more of the four stages of aneurysm such as inflammation and dilation of the aorta(33).

1.1.1 Transgenic models

Transgenic animals allow the study of specific genes implication upon an organism as a whole as the genotype is altered across all tissues. From the removal of a single gene and its protein products, and by comparing the results to that of a control with the gene present we can conclude the effects that the missing gene has.

1.1.2 LRP1 Knockout

Low-Density Lipoprotein (LDL) LRP1 was the single gene to show up as relevant to incidence of aneurysm within a genome-wide association study (GWAS)(34), highlighting the relationship between this gene and the condition. Furthermore, studies upon LRP1 knockout mice have shown progressive development of aortic diameter increase(35). This model mimics the pathology seen within the human in some ways and therefore could be highly clinically relevant, due to its high age to aortic root diameter increase relation, similar to increased incidence of aneurysms within the ageing population(36). On top of this, there is the lack of need for invasive techniques, such as surgery or chemical exposure, which could potentially influence the inflammatory status of the animal and consequentially the aortic environment(37). On the other hand, LRP1 gene polymorphisms are not present within all aneurysm patients, with AAA being suggested to be a polygenic pathology(38). This limits the potential of this model as we know it to be inconsistent with observations of some patients. At the same time, this serves to highlight the problems with the use of animal models with

a view to carrying the information over to human disease. Differences in physiology between species can result in alternate causes for similar conditions.

1.1.3 Marfan's Model- FBN 1 Knockout

Marfans Syndrome is an autosomal genetic disease that results in defects of the connective tissue. Genetic abnormalities centre around the truncation or deletion of the Fibrillin-1 gene (FBN1). This condition results in severe connective tissue disorders, with AAA and other vessel abnormalities being a common presentation. Due to the wide-ranging presence within multiple tissues, the presentation of symptoms are similarly widespread, affecting the cardiovascular, visual and musculoskeletal systems. Development of the knockout mouse model of Marfans syndrome resultantly acts also as a method of studying AAA, however, the limitation of this model is clear, with not all AAA patients suffering from conditions such as Marfan's, or associated conditions that affect the FBN1 gene. Mutations of the FBN1 gene show full penetrance within humans, however, within the mouse model most significant phenotypic presentations include but are not limited to microfibrillar deposition, aortic wall deterioration and kyphosis. Differences in stage of onset are seen with C57BL/6 animals less effected and display later onset of symptoms in comparison to 129/Sv strains. Strong negative correlation is seen between the level of mutated FBN1 and phenotypic presentations. In a study of effected mouse families, a group heterozygous for the mutant FBN1 displayed rescuing effects of the healthy form of FBN1(39). Two forms of the mouse model are established with homozygous mgΔ and heterozygous $mg\Delta^{loxPneo}$, both of which have in-frame deletions of the exons 19-24 of the FBN1 gene. Aneurysmal features are produced within this model, with aortic degradation occurring over time. This degradation leads to dilation of the aorta and the aneurysmal phenotype by three

months of age, and associated levels of calcification observed(40). Whilst hemodynamic alterations associated with AAA have been observed within Marfan Syndrome sufferers, similar indications have not been observed within the mouse population as cardiovascular function was not found to be significantly different although there was an increased incidence of retrograde flow found within one study, however, this did not reach any level of significance(41).

1.1.3 Chemically induced models:

1.1.3.1 Angiotensin-II Infusion (AngII)

This is one of the most studied and well-established models of AAA. This model works on ApoE and Low-Density Lipoprotein receptor knockout (LDLR) background mice, relying on systemic exposure to Angiotensin II, released from a sub-dermal osmotic pump. Daugherty et al. have discussed thoroughly how the renin-angiotensin system (RAS) has a direct role in the formation of aneurysms, when angiotensin II is consistently up-regulated, within mice, and how this could be translatable to the human condition(42). In addition, drugs that act upon the RAS system have been repeatedly shown to decrease the rates of aneurysm(43), reinforcing the link between the two. The mechanism behind this model involves Angiotensin II, causing a decrease in Angiotensin type 1a receptor abundance and resultantly this is what causes the increase in aortic diameter(44)(45). However, this has not been shown to be the case within humans. In addition to this reported mechanism, Daugherty et al. report increase atherosclerotic plaques, haemodynamic changes and immune cell (macrophage) recruitment and stimulation(46), all of which often coexist with abdominal aneurysms, as well as hypertension. Many findings produced by studies using the ApoE ad LDL knockout background are not fully reproducible in non-transgenic animals, with

examples of contribution to the atherosclerotic burden, with the lipids becoming resident within aortic lesions(46). Multiple other similarities to other models, as well as the human pathology, have been described with the implication of this model, such as; progressive aortic expansion, focal disorganisation of aortic wall proteins, neovascularisation of the aneurysm region and adventitial build up in surrounding regions of the aorta (47)(48). However, this model may be more a measure of aneurysm regression and post insult dissection rather than aneurysm itself. Longer-term studies are needed to highlight the consequences on stability of this technique, as although decreased stability and increased rupture risk are reported (46), a number of human aneurysms are subclinical and do not rupture for extended periods, even though rupture rates are increasing(49), and therefore this model may not be representative for the human condition, especially as this model produces suprarenal abdominal aneurysms(50), in contrast to the stereotypical infrarenal aneurysms seen in humans. Although, on the other hand, genetic polymorphisms of enzymes concerned with the RAS have in the past been suggested to relate to different types of aneurysm(51) and aortic expansion rates, although some investigations have since disproved the aortic relation(52). Resultantly, as there are many conflicting standpoints regarding this models relevance to aneurysms, I am unsure of the representation of this model with regards to aortic aneurysms and subsequently, its clinical relevance of certain aspects have been disproven. However, I would still suggest this model to have a very strong relevance in understanding what causes ruptures to occur, meaning that although it may have less relevance in understanding the overall pathology, it may still have clinical significance in understanding what causes the fatal infarct.

1.1.3.2 Intra-luminal Elastase or collagenase

This enzymatic model has more frequently been used to induce aneurysms within large laboratory animals such as swine, with elastase and collagenase being used at times singularly and in conjunction, producing highly differing appearances of aneurysm(53). Within the study by Czerski et al., elastase and mechanical stretching alone, were seen to be insufficient at producing an aneurysm within the swine model, in comparison to the addition of collagenase that produce a marked increase above 70%, suggesting collagenase to be the active and bioactive enzyme within the model. On the other hand, elastase has been shown to reproducibly form aneurysms within the mouse model(54), highlighting differential responses between species. This is an important point as many models may be effective within one species, but if it is not a system that reacts in the same way as the human, it renders the investigation and model itself insignificant to humans clinically.

Importantly, this method has been compared to human tissues to see the relevance of the model, with respect to similar reactions occurring in human as in swine. Results suggested similar modulations of prominent biomarkers of aneurysm such as; increased MMP expression, increase cell size and spread as well as decreased proliferation(55), although this was shown in an *in vitro* representation of the *in vivo* model. However, this suggests that swine is very representative of human vascular conditions, with smooth muscle cells exhibiting the same behaviours in response to a stressor across the two species.

The mechanism behind this model is highly representative of pathology seen within the human. For instance, the alteration of the extracellular matrix and immune cell infiltration of the affected vasculature by macrophage and neutrophil immune cells(56). Resultantly, the model, is one of the most complete and representative models of the

human condition and in terms of clinical relevance this is an extremely thorough model as it combines two insults due to the haemodynamic changes and consequential sheer stresses that are elicited in response to the enzymatic treatment, as reported by Miskolczi et al. (57). However, this is a very acutely formed aneurysm, and therefore contrary to human aneurysmal formation, is not a chronic activation of inflammation and with gradual degradation and expansion of the vasculature. This I feel is under looked in many models as, although cheaper to simulate, if it is misrepresentative, clinical significance and the usefulness of the information yielded on aneurysm is diminished as the changes seen in acute phases will be very different to that in the chronic phase. Overall, I would say this was a good model of aneurysm initiation rather than the complete pathology aiming to be studied, furthermore still, due to the use of exogenous elastases and collagenases that mimic the functionality of NE, this model is inappropriate for use within this study.

1.1.3.3 Calcium Chloride ($CaCl_2$)

The Calcium chloride model has been extensively used within rodents(58)(27)(59)(60), however many small differences between techniques mean it is hard to draw overall conclusions as it is impossible to distinguish between what differences are due to technique discrepancies and what is due to true biological effects. Observational discrepancies, for instance, different average levels of calcification within the aorta can be dependent upon application technique of the $CaCl_2$(61). Alternately discordant average aorta diameter increases between strains(62), species(63), and even investigations result in the information gained from the separate investigations not being able to be extrapolated to the human clinical setting very easily.

Furthermore, the model has been developed to include secondary assaults upon the aorta. However this has led to a more representative model being produced(64), comparative histology and protein analysis is similar within updated models to what has been observed within human aneurysm tissue samples(65)(66). This updated calcium chloride model, acting alongside elastase or collagenase models, brings about increased elastin degradation, apoptosis, inflammation and MMP production, to a greater extent than solely calcium chloride(67)(64). Further aortic modifications have been seen, within more recently advanced methods, with a combination of calcium chloride and Phosphate Buffer Solution (PBS), which produces Calcium Phosphate ($CaPO_4$). Levels of apoptosis were seen to be 3.7 times within calcium phosphate treatment in comparison to that of calcium chloride by Yamanouchi et al. (68), along with other modulations of cell phenotype such as inflammation markers and calcification. This suggests the calcium phosphate model could be superior to calcium chloride. One huge weakness, however, is that this modified technique comparison mentioned was performed in cultures (*in vitro* techniques), namely cell culture of vascular smooth muscle cells, and not *in vivo* as numerous other calcium chloride studies(67)(64). This is influential in our ability to interpret the relation between comparable data sets, such as calcification and inflammation levels, as apparent differences may be due to cell culture and in vivo discrepancy rather than actual difference in induction of aneurysms or organism's response to treatment. Hence, the study by Yamanouchi et al. is a promising development, yet until verified *in vivo*, lacks the evidence needed for it to be considered as the current gold standard of chemically-induced aneurysm models.

	Arteriosclerosis and/or immune invasion	Aortic dilatation	Aortic wall proteins degradation	Haemodynamic alterations	Overall relevance
LRP1 knockout	Increased	Gradual increase	By PDGFRβ dysregulation	Not reported	3/4
AngII-infusion	Increased plaques and macrophage activation (46)	Receptor level modulation causing increase (44)	Focal dysregulation (47)	Some reported change (46)	4/4
Intra-luminal elastase/ collagenase	Reported in rabbits (69)	Receptor modulation	Elastin degradation and MMP production	Not reported	3/4
Calcium chloride	Inflammation, apoptosis and calcification	Varied levels of dilatation (62)(63)	Elastin degradation and MMP production	Not reported	3/4
Fibrillin-1 Knockout	Decreased stability of atherosclerotic plaques when on ApoE background, however, no innate	Significant and widespread	Widespread connective tissue abnormalities. With decreased presence	Increased aortic stiffness but no flow alteration	3/4

	increase of atherosclerosis or immune invasion(70)		of elastic lamellae(41)		

Table 1 *- Summary of mouse aneurysm models- includes features and basic mechanism by which they each model acts and their relevance to the study of AAA*

1.1.3.4 Surgical models

Many surgical techniques have been trialled to induce aneurysms, however, none as yet have been able to accurately replicate the pathology of an aneurysm. However, some have led to new methods of treatment being created due to the ability of people to practice repairs and novel repair techniques on large laboratory animal models such as swine and canine(32)(71). This, therefore, has produced potentially clinically important signs of progress in surgical techniques rather than the understanding of the pathology and pathophysiology, with haemodynamic changes, shear stress and overall larger animals being more comparable than mice to human physiology.

Overall, there are currently a number of different models by which aneurysms and specifically AAA are studied, the vast majority of these are performed upon small animals such as mice. This is economically the most viable due to the lower cost in comparison to larger animals such as pigs, however, there are many important drawbacks such as differences in immune system(72), which is especially relevant with suggested relations to genes such as Early Growth Response gene-1 (Egr-1)(73,74) and their subsequent relation to leukocytes(75), and this resultantly may influence pathology.

Conclusion

To conclude, there are currently many models of aneurysm within different size and species of animals, some of which are more representative of the human vascular system than others and therefore I would suggest that these are where the most clinically relevant information will come from. However, due to economic constraints, these models will be less widespread, as the swine model appears to mimic human vasculature and the response it elicits the most accurately. Swine are more expensive to keep and use but the potential benefit of using these animals is high.

The models studied above are some of a number of models that exist. However, these processes I believe to be the most often used and are the processes from which the large proportion of information regarding aneurysm originates. As explained, this does not mean they are faultless nor complete representations. Current models tend to focus on one specific insult producing the aneurysmal pathology, although some induce secondary changes, such as the hemodynamic stressors mentioned above(76). This I feel is where development needs to occur and has started to occur, with some intervention studies using a combination of models to see which produces the greatest change, close to the pathology of the human condition(53). The complete conditions of human pathology need to be looked into and recreated within a model that combines multiple stressors of different forms, as this is what has been suggested to create the disease within the clinical setting. We know this as many different alterations of numerous systems lead to modulation in aneurysm prevalence in the clinical setting. This occurs at times via interactions with other associated factors such as enzymes and inflammatory cells driving the chronic inflammatory process(77)(78)(79). Therefore multiple assault models could possibly yield us the greatest insight into how to treat, regress or inhibit the aneurysms we see widespread within the western population. At

present, I regard the Angiotensin II model of aneurysm as the best model of aortic rupture, and the Calcium chloride model as the best overall technique to induce the chronic inflammatory phenotype seen in the expanding and stable aortic aneurysms. Resultantly, these are the preferred models within my study.

Limitations

Current limitations to all of the above studies include the vast array of co-existing conditions that often preclude and compound AAA. Atherosclerosis and AAA are vastly intertwined with the majority of AAA patients exhibiting widespread atherosclerosis. None of the current models mimic this unless perform under high fat diet or western diet conditions on an ApoE knockout background. This in itself has some flaws, however is currently the best alternative found within the field as it allows production of the AAA phenotype on top of the underlying conditions such as atherosclerosis and associated CVD. Beyond atherosclerosis, neovascularisation and calcification, both often observed comorbidities are rarely replicated within animal models of the disease. Calcification is seen within calcium chloride, and has even been observed within elastin perfusion techniques within larger animals _, however this is a rarely observed aspect of animal models that is overlooked, as high levels and incidence exist within the true AAA population (81). Although, atherosclerosis and calcification are limited, neovascularisation is limited to human aneurysm studies (82), although VEGF inhibition within AngII experiments did have efficacy at reducing rates of aneurysm. Angiogenesis is observed widely within human AAA samples, and is understood to occur in the regions of inflammation and hypoxia, to the extent where it becomes erroneous. Often associated with areas of thick ILT, angiogenesis can be driven in these areas by production of factors such as hypoxia inducible factor-1alpha produced by the VSMCs. This influential mechanism potentiates the expansion of the

vessel as further factors such as nitrous oxide are released by hypoxic areas in an attempt to counter the level of low perfusion. Consequently, as this mechanism is not widely seen within animal models it is a glaring limitation and shortfall within the animal model representation of the disease.

In conclusion, whilst animal models are a very good method by which AAA may be studied, there are significant limitations to the translatability to the human phenotype, with key characteristics and processes lacking within many of the models. Consequently, multiple studies are needed with more than one model being employed prior to any conclusions being able to be drawn or applications made to the human pathology.

1.1.4 Review of Calcium Chloride Induction

The $CaCl_2$ Abdominal Aortic Aneurysm induction method provides a controlled and reproducible protocol, with greater localisation of the active agent in comparison to other models. Inflammation is limited to the area of interest and therefore minimal change to the animals overall inflammatory status occurs. In contrast to other AAA models, such as Angiotensin II infusion, the $CaCl_2$ model produces an aneurysm in the same anatomical location as within the human pathology. This makes it more relatable to the clinical setting. These characteristics allow for the study of AAA development, as well as monitoring the progression of the pathology. One limitation is the low rate of rupture in comparison to other techniques. By utilising this technique, we will be able to study the early changes in the vessel that cause the formation of the AAA phenotype. From this, we are able to identify proteins and cells involved in the formation as well as detect potential novel targets for treatment.

Controlling administration of Calcium Chloride is one of the largest areas of variability within this procedure, and along with it comes a number of risks. Localisation of the Calcium needs to be controlled as if the solution comes in contact with other organs in the area widespread calcification and consequential complications can occur. These can lead to delayed recovery and the death of the animal in some cases. To minimise this possibility calcium chloride-soaked filter paper was used, as this contains the solution and only allows the application to occur at the surface it is placed upon. Positioning and removal of the filter paper can occur easily with tweezers, this further reduces the risk of erroneous application.

Following on from this, handling of organs, specifically the intestines, can produce a number of problems. Handling of the delicate mesentery can be an area by which mortality is increased. If the mesentery is disrupted or damaged, blood supply to the intestinal tract is impeded. This can lead to hypoxia of the affected area. If blood supply is not restored, which is often the case, the affected area will undergo necrosis. This in many cases leads to death of the animal. To avoid this, incisions should be made away from the midline and saline-soaked gauze used to gently handle the movement of the entire intestine as one. This minimises disruption to the area and its bloody supply, whilst still being able to cleanly access and dissect the aorta.

Aortic measurement is one of the most important steps within the entire process, as without accurate measurement of the vessel all data is invalid and inaccurate. A number of options are available including video micrometry, ultrasound and MRI. All of these have different strengths. MRI is the highest resolution of the three techniques, however, length of time and level of invasiveness are much greater with this technique also.

Video micrometry enables measurement of the vessel during surgery, however, this means that to gather expansion data you must first re-dissect the aorta. Resultantly, to measure different time-points AAA progression you have to use multiple animals. Ultrasound is by far the quickest procedure and non-invasive, allowing relatively fast data collection and minimising the number of animals needed. Whilst ultrasound data is of a lower resolution compared to other techniques, it gives a good representation of lumen size.

This protocol allows for a reproducible, sterile and largely representative model of AAA within the mouse. This will allow for the study of AAA and allow for the potential identification of new therapeutic targets, stemming from a more thorough understanding of the mechanism behind the AAA pathology. Variability in the application process that existed in the previous model has now been minimised within this updated protocol.

Calcium chloride directly activates matrix metalloproteinase (MMP-2 and -9) activity within the area of application via interaction between the divalent cations within the molecule and the tissues itself. This, in turn, causes the calcification of elastin and general vasculature(83), as well as the breakdown of the extracellular matrix (ECM) components. These events kick-start a cycle of apoptosis within vSMCs and structural breakdown that induces inflammatory cells to activate and invade both medial and adventitial layers of the aorta (84). These processes are largely caused by action and internalisation of calcium crystals respectively(84). By doing so this heightens the level of dysregulation within the ECM, and in turn, perpetuates the activation of MMPs. Further inflammatory processes cause oxidative stress levels to increase, causing the induction of proteins such as elastase, further adding to the cycle of deterioration within

the vessel wall. Neutrophil elastase, as yet to be studied with relation to this field is another potential regulator of many steps within this process.

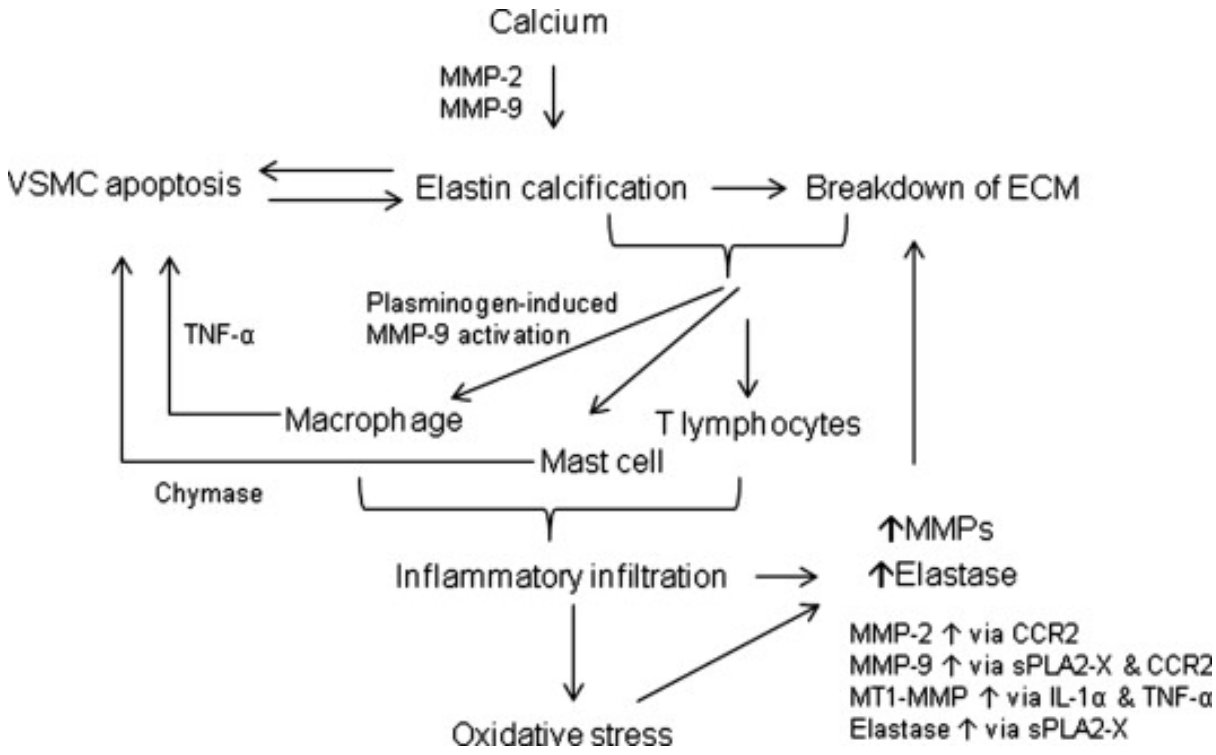

***Figure 2**- Flow diagram outlining the role of $CaCl_2$ application within the In Vivo model of AAA, including proteins and cells involved, as well as processes that occur due to application of $CaCl_2$. (84)*

This procedure will allow for the study of the AAA phenotype, enabling progression in the understanding of the pathology. This protocol produces many of the same features seen within human AAA tissues, such as localised chronic inflammation, neovascularisation of the area and a decreased elastin content within layers of the vasculature. The precise location can differ minimally, as well as the model lacking some characteristic features of human AAA. These include; intra-mural thrombus, atherosclerosis and eventual rupture of the aneurysm itself. Some of these discrepancies can be rectified, such as by using Apo-E knockout mice, so that atherosclerosis is present within the model.

1.1.5 Comparison of Human and Mouse AAA

As highlighted above, there is significant benefit from studying animal models in order to achieve a greater understanding of the AAA pathophysiology. However, at the same time, whilst there are great benefits and similarities, disparities between animal models and the human condition exist. For instance, SMC and medial depletion and destruction respectively, are evidenced within both human and the majority of animal models(1,53). Further, remodelling of the elastic lamellae is a key pathological feature in both also. The production of an inflammatory environment is an essential element of AAA formation, and is observed within aortas isolated from both animal and human studies. Building on this however, is the significant presence of atherosclerosis within human patients(85), however this has not been fully replicated within *in vivo* studies, although ApoE knockout and high fat diet mouse protocols attempt to address this shortcoming in the field(46). Where instances of atherosclerosis are recreated within animal models, a greater level of representation of the human phenotype is produced. In these instances, a higher presence of the Intra-Luminal Thrombus (ILT) is observed which has a significant impact within the human condition and less seen within animal models. The ILT is a site of protease production, such as the production of MMPs(8). These are largely due to the high concentration of WBCs that are contained within the ILT and lead to further deterioration of the adjacent vessel wall(8). WBCs such as neutrophils, macrophages and mast cells have all been observed to influence the phenotype within both human and animal studies, with knockout of these cell types leading to significantly smaller or less incidence of AAA(15,86,87). Such WBCs lead to action upon cells and proteins of the vessel, leading to deterioration of the aortic wall structure and structural proteins, as well as depletion of VSMC numbers, again a feature of AAA present in both human and some animal models of AAA. The source of these WBC has been a source of investigation, with the discovery of Adventitial Tertiary Lymphoid Organs (ATLOs) and the understanding of its role developed over more recent years. ATLOs develop at the site of chronic inflammation,

produced through lymphoid neogenesis(88), and are responsible for adventitial inflammation and subsequent destruction of the medial portion of the aorta(89). The formation of these vessels is a consequence of VSMC stimulation, producing CXCL13 and CCL21 chemokines and stimulation of ATLOs. Production of ATLOs allows for passage of WBCs through the media and into the adventitial portions of the vessel(90). Multiple cell types home to these ATLOs structure within the atherosclerotic and AAA diseased portions of the vessel wall, namely WBCs such as Neutrophils, B- and T-cells, with the consequent destruction of the surrounding vessel due to release of cellular contents, such as proteases and the induction of an inflammatory environment. These structures are only significantly present in the human phenotype, although they have been outlined within the animal but at present only recognised within ApoE-/- severely atherosclerotic mice(88), which can be utilised alongside some models of AAA such as the AngII model.

The AngII model of AAA has many similarities to the human phenotype, however whilst it possess significant aortic expansion, inflammatory infiltration, structural protein destruction, VSMC depletion and ILT production amongst others, one of the most important aspects of the pathology is the chronic expansion seen in the human condition which fails to resolve and is stable for, at times, many years. Within this model, large expansions are seen often within the suprarenal portion of the aorta and have a high risk of rupture around week three of the protocol. Comparatively, within human conditions, the expansions are more often seen in the infrarenal segment and can are typically far more stable, moving through expansive and stable periods, often asymptomatic for many years. Similarly, within the AngII model expansions are accompanied with elastic lamellae breakdown and dissection of the intimal and medial layers of the aorta. Comparatively in the human condition, expansion of the aorta does not have to be accompanied by dissection, a characteristic which is often absent within stable AAA presentations.

One further aspect of Human AAA is that of VSMC apoptosis, the process by which cells undergo self-programmed death in order to remodel and regulate mass or architecture of tissues(91). This phenomena has been evidenced within the aorta, and more specifically gives rise to the medial depletion of VSMCs within a diseased aorta such as within AAA(91). VSMCs are a source of elastin, a key component of a healthy vessel(92). Studies by Cao et al. studying tissues of human AAA origin display that regulation of apoptosis pathways, such as the p53 pathway by miRNAs (such as miRNA 504, in this instance), occurs within AAA and manipulation of this system is intrinsic to the production of the pathological phenotype(92). Beyond the production of elastin, VSMCs produce ECM, another important component to a healthy vessel(93), loss of both ECM and elastin are key in the depletion and degradation of the vessel architecture that leads to the AAA phenotype. The regulation of VSMC apoptosis within human tissues and AAA was backed up by subsequent studies within the AngII mouse model, within increased TUNEL staining evidencing the significant medial VSMC apoptosis within tissue samples(94)(95). Control and restriction of VSMC apoptosis has been observed to reduce incidence and severity of AAA, which in turn highlights the importance of the mechanism within the AAA condition(94,95).

In summation, there are many differences between the human and animal model phenotypes produced, and whilst there are many similarities continued development of animal models and methods by which AAA is studied is required in order to further understand the pathology.

1.2 Aortic Dissection

Aortic Dissection (AD) is another potentially lethal aortic pathology with acute onset and minimal prior symptoms. Effecting between 5 and 30 people per million, dependant on background, this pathology has a significant prevalence and as yet only a vague

understanding of the underlying pathology. AD has at times been included within the category of Acute Aortic Syndrome (AAS), which include Thoracic Aortic Dissection (TAD), Intramural Hematoma and Penetrating Aortic Ulcer. AD is part of a spectrum of thoracic aortic pathologies that are monitored for clinical outcomes and management, this monitoring helps to form the most up to date research from which predictors of survival, demographics and management originate. Whilst AAA is one of the most researched topics covered within the AAS bracket, AD has significantly higher rates than ruptured AAA, with an estimated 3.5 dissections yearly within each 100000 of the population. However similarly to AAA rates among the male demographic are also significantly higher when compared to the same disease rates within the female population.

AD has been categorized in a number of ways dependant upon the region affected and severity, however, the differing categorizations have distinct peaks in age of incidence. The most common classification system utilized is the Stanford Classification system, whereby Type A, Type B and Type C, are used to describe aortas where the dissection affects the ascending and descending, ascending only and thoracic aorta respectively(96). This enables for distinction and differentiation to occur between patients' pathologies, as this is often indicative of both the eventual treatment required as well as the likely clinical outcome. Alternative classification systems, such as the De Bakey classification system, with Type 1, Type 2 and Type 3 referring to AD involving the entire aorta, solely the ascending portion or the dissections that spare the ascending portion or the arch (most commonly descending or thoracic aneurysms).

Demographic of AD patients differ between groups, with recent studies observing that Type A patients are typically younger than those affected by Type B, with a new 10-year disparity in the average ages of onset(97). One common underlying co-morbidity,

the presence of hypertension, is recorded in both Type A and B patients, with over 75% of the studied cohort presenting with the condition. Furthermore, other similarities include the sudden onset of symptoms with sudden chest pain being felt and described in at least 85% of patients. The precise location of the pain patients present with is often an indicator of which Type of AD they are suffering from. Type A patients most characteristically present with sudden central chest pain solely, with back and/ or abdominal pain more consistent with Type B and C categorizations. The initial pain patients present with can change over time, as the dynamic nature of the pathology can lead to worsening or spreading pain as the vessel dissects over time(98). Monitoring of the pathology can be adjudged in more ways than solely referring to patient pain levels or location, as blood tests for such markers as d-dimer, soluble elastin fragments and smooth muscle myosin heavy chain proteins have been linked with both identification of AD and used as an indicator of a worsening pathological phenotype(99).

With the change in classification come differences in survival rates, prognosis and treatment. The different regions of the aorta involved are the main determinant of the type of treatment required(96). Dissections in the initial portion of the aorta, namely the ascending and aortic arch will most likely require surgery and are the most lethal. Surgical interventions, much similar to AAA, consist of either open repair or endovascular reparative surgical interventions. Dissections involving the more distal portions of the vessel may be monitored and treated more conservatively with blood pressure modifying drugs and beta-blockers or such drugs that limit the increase in heart rate. More distal portions, namely the descending and thoracic aorta can also be operated on, however, this is usually reserved for cases where complications arise or are expected, such as in instances where other vascular pathologies may interfere with the process and exacerbate one another, for instance with AAAs. Type A AD sufferers

have a much higher likelihood of also being effected by AAA, with 12.4% of Type A patients suffering from both within one study, compared to just 2.3% in Type B patients(100). In patients not undergoing treatment, type of AD has a large impact upon clinical outcome. Half of Type A patients die in the first three days post dissection, in comparison to Type B patients who fare much better, with Type B patients have around a 90% survival rate at 1-month post-onset of dissection(101).

1.2.1 Hemodynamic changes

Aortic dissection exhibits large differences in aortic flow in comparison to the healthy vessel. Due to the highly pulsatile flow, pressure and sheering forces that are present within the aorta, the vessel wall is placed under large amounts of stress. This increase in stress is highest within the ascending portion of the aorta and proximal descending portion of the aortic arch, and furthermore still greater within the external surface of the arch. This was superbly modelled by Qiao et al. (102) who demonstrated that these areas of higher pressure and stress coincided with the portions of the vessel that also suffer most greatly from conditions such as atherosclerosis and most importantly AD. At the same time, they were able to demonstrate that there was an increase in both transit and contact time of blood cells, within the same area. Disturbances of the intima led to turbulent and vortexed flow, coinciding with the previously mentioned regions of high risk of atherosclerosis and atheroma.

1.2.2 Pathology

A healthy artery is comprised of three basic layers all serving different purposes that collectively work to aid the function of the vessel. The innermost layer of the aorta and all arteries is the intimal layer which lines the vessel forming the point of contact between the blood and the vessel itself. This lining is predominantly endothelial cells

and basement membrane that anchors the cells into place. The intima is the portion of the vessel that is stripped from the remaining layers of the aorta, this can occur at various landmarks along the vessels' course however areas of high shear stress and turbulence are at increased risk due to these factors having a large influence on the pathology's initiation. As a result, the locations surrounding the heart and aortic arch are the most at-risk portions of the vessel, however, dissection is not limited to these areas. Within histological sections a break in this layer can be seen, leading to the production of an entry point by which the blood enters the vessel wall. From this point, the blood enters and serves to strip the proximal portion of the vessel wall of intimal coverage. This can extend both distally and proximally to the intimal tear. The stripping of the intimal layer can lead to the production of both a true and false lumen, seen when the vessel is visualized by either histological sectioning or scanning methods. Within the false lumen, blood can pool with highly pulsatile turbulent flow entering from the dissection site. This turbulence and pooling only serves to exacerbate the degradation and damage done to the vessel, leading to expansion and progression of the tear. The production of the true and false lumen phenotype, also known as double barrelling less often leads to complete rupture as opposed to dissection that causes pressure to be placed onto the external adventitial side of the aorta. The productions of these tears are due to unknown causes, however, large extracellular matrix modifications are believed to precede the intimal tearing(103). ECM proteins namely, elastin and collagen are highly deregulated by processes not yet fully elicited within the cystic medial necrosis process. This is common to a number of ECM conditions often of genetic origin, such as Marfan's syndrome (Fibrillin-1 deficiency) and Ehlers-Danlos syndrome (structural collagen insufficiency of various genetic origin), both of which will be discussed further later(104).

The secondary layer is the medial portion; this layer undergoes huge amounts of degradation and modification during the AD process. In a healthy state, the vessel should contain the main cell types that give the vessel its tensile strength and elasticity, namely smooth muscle cells and the multiple layers of the elastic lamina held together by connective tissues. This layers degradation as the smooth muscle cell component of the vessel become increasingly depleted due to apoptosis is considered the primary causal factor of AD and the eventual rupture of the vessel(99). These processes are largely driven by inflammatory processes that trigger apoptosis and the destruction of medial components. Inflammatory cells that are heavily involved with the occurrence of AD are macrophages and lymphocytes, which have both been identified in a number of studies within the medial space although these often are most concentrated within the adventitial segments of the vessel(105). As the pathology progresses the effects of inflammation and inflammatory cells have on the structure of the vessel increases, with the destruction of elastic tissues and compaction of elastic plates increasing. This change is irreversible and leads to the release of some markers of AD, as mentioned above. Markers such as D-dimer and pro-B type natriuretic peptide rise following initiation of dissection and do not fall after the chronic phase of pathology(106). This is in contrast to most vascular pathologies such as AAA which has similar rises in D-dimer, however, in chronic aneurysm patients, this marker is only transient with levels resolving and falling back to expected levels(106). This is used in the diagnosis of the pathology assisting with diagnostic scanning such as Ultrasound, MRI and CT.

Finally the adventitial layer, the least altered in structure during the AD process, however, this portion of the vessel has been seen to contain the predominant inflammatory cells(107). Whilst the medial dysregulation occurs it appears that inflammatory cells migrate into the adventitial portion of the vessel whereby they exert

their pro-inflammatory effects. Key inflammatory mediators such as MCP-1 and IL-6 predominantly occur in this portion of the vessel as outlined by Tieu et al. (107), who goes on to suggest that the production of such molecules leads to the recruitment of macrophages causing the interaction between these inflammatory cells and adventitial fibroblasts. These interactions serve to stimulate the migrating monocytes of the area, driving macrophage differentiation by paracrine signalling, with factors derived from the adventitial fibroblasts. In turn, these processes also serve to produce MMPs, a key player in the breakdown of the vessel walls integrity with substrates including both collagen and elastin, both of which are diminished within the deteriorating wall. Resultantly, whilst the adventitial structure remains largely intact during AD the same portion is being more and more accepted as the hub for pro-inflammatory molecule production and resultantly is highly influential in the production and development of a number of vascular diseases, not limited to but including AD.

Medial degradation coupled with SMC apoptosis is the primary cause of TAD and causal in the eventual rupture of the aorta. A large inflammatory component exists, with inflammatory cells and mediators key in the regulation of these processes. Macrophages and lymphocytes, largely localized within the adventitial portion of the vessel, cause the release of many enzymes and proteins, such as c-type natriuretic peptide, b-type natriuretic peptide and d-dimer. These proteins have particular expression patterns across acute and chronic dissection patients, elevating during acute phases of rupture. These patterns of increased expression do not resolve after repair. Such Inflammatory activity is much higher in aortic walls of clinically symptomatic patients. This increase leads to weakening of the aortic media. This weakening includes the loss of smooth muscle cell density as well as ECM disorganization and disruption, such as the

fragmentation of elastin layers. These main change pre dissection are confounded by mucopolysaccharides causing loss of elastic tissues and compaction of elastic plates. These symptoms were observed in patients with bicuspid valve problems which is an associated comorbidity to the TAD pathology.

1.2.3 Genetics

Aortic dissection has a large genetic influence with a number of inherited syndrome and familial traits making up a significant proportion of the treated patient demographic. Within the general population that suffer from AD almost a quarter of these have a family history of AD within 3 generations(108). The specific genes that cause the dissection are yet to be fully understood however it is believed to be an autosomal dominant mode of inheritance with incomplete penetrance. Many studies have had to objective of deciphering the precise genes responsible for familial AD, currently, the most significant studies have highlighted a number of genes, most interestingly MMP-3 and -9, TIMP-2 as well as gene loci 5q13-14 to name a few(109)(108)(110). The same studies have also highlighted loci implicated within the syndromes associated with AD, far more is known about these syndromes and the genetic foundation of them, this will be discussed further below. The onset of AD within the Familial demographics of those affected by AD is over ten years younger than that of the sporadically occurring AD sufferers. With the average age of onset standing at 55.4 years of age in comparison to 65.7 within the familial and sporadic groups respectively(111). Furthermore to the age of onset the region of the aorta that is most commonly and severely affected by AD is also dramatically altered. Within Familial AD half of the incidence occurs within the descending aorta, in comparison,

47.5% of cases affected the same area in sporadic groups. In contrast, the ascending aorta is only implicated in 20% of familial AD dissections compared to 82.1% showing aneurysm-like expansion within the sporadic group, but only 17.9% displayed clear dissection(111). The change in occurrence between the familial and sporadic groups compared to the syndrome groups differentiates and determines the optimal clinical management of each patient. Beyond differences in management survival rates differ within each group. Preliminary research being undertaken at the University of Kentucky have shown that both the different regions and layers of the aorta affected is likely due to differential responses of the cells to alternate stimuli is highly influenced by their embryological origin(112)(113)(114). The aortic arch smooth muscle cells are derived from three separate embryological origins: Second Heart Field (SHF), Cardiac Neural Crest (CNC) and somites (113). The SHF makes up the aortic root and the most proximal portion of the aortic arch. This then has a crossover zone with the CNC, overlapping each other initially before solely the CNC continues to solely form the ascending aorta and the majority of the arch itself. In the crossover zone, the SHF makes up the majority of the external media, with CNC derived cells populating the luminal inner portion of the media. The descending aorta then is made up predominantly of somite cells. As you can see within the demographic data, distinctive areas of the aorta are affected differently. The study by Sawada et al. displayed that the cells derived from the SHF coincide with the outer medial deformation, seen within mouse studies, however not confirmed to be similar within the human aneurysm and AD pathology (112). This could shed light on why the different genetic differences lead to the pathology presenting within the different portions of the aorta. Syndrome related expansion and AD is predominantly located within these areas. Marfan Syndrome and Ehlers-Danlos Syndrome aortic remodelling largely occurs within the aortic root,

whereas Turners and Loeys-Dietz syndrome happen slightly more distally in the ascending portion(**Table 2**) (104,109). However both of these areas are still composed of SHF derived cells, this suggests that the origin of the cell could have a distinct impact of pathological outcome. This work is in its infancy and mechanisms of action need to be elicited and verified however this is an area of research that is becoming increasingly of interest due to its potential in targeted treatments.

Table 2- Summary of genetic conditions that lead to a significant increase in AAA incidence

Genetic Disorder	Gene Affected	Protein Expression	Mechanism of Action	Clinical Presentation
Marfan Syndrome	FBN1	Expression of mutant fibrillin-1	Mutation of cbEGF domains lead to defective protein folding and defective secretion, leading to defective myofibril formation and TGF-β signalling	Widespread vascular alterations with frequent dilation and dissection of the aorta(115)
Ehlers-Danlos Syndrome	COL5A1, COL5A2	538 genes expression modulated, 368 overexpressed and 180	Decreased stability of mRNA and	Descending and abdominal

	AND COL3A1	under expressed, including; non-functional COL5A1 allele and COLLV haploinsufficiency, whilst COL5A2 mutations affecting collagens structural integrity	premature dissembly of collagen, leading to hypermobility and poor wound healing	aorta rupture(104)
Loeys-Dietz Syndrome	TGFBR1 and TGFBR2	Production of TGFBR1, TGFBR2, SMAD3, TGFB2, or TGFB3 gene occurs at comparable levels but lacking function	Unregulated TGF signalling, causing greater intensity of TGF signalling, disrupting ECM formation	Rapidly expanding aneurysm with high incidence of dissection(116)
Familial Aortic Aneurysm and Dissectio	TGFR2, MYH11 and ACTA2	ACTA2 point mutation leads mutant protein expression in Smooth muscle α-2 actin protein	ACTA2-defective sarcomere function	Ascending aortic aneurysm and dissection(110)

n Syndrome				
Turners Syndrome	45X	Partial or complete absence of an X chromosome	Cystic medial necrosis	Increased AAA incidence(117)

Syndrome related AD has a very different penetrance and impact upon life span in comparison to Familial and Sporadic AD. For instance, one of the most well-known syndromes where AD impacts patients is Marfans Syndrome. A defect in Fibrillin-1, leading to a severe connective tissue disorder that results in very tall, pigeon-chested and hypermobile joints amongst others(115). The most significant and life-threatening change is the cardiovascular changes that result from the defect in Fibrillin 1 production. The genetic defect causes alterations in TGF-β signalling, this impacts vascular production with enlarged vessels, namely the aorta being a result. This expansion results in aneurysm and aortic dissection in most instances with this often being the cause of death for Marfans patients. Aneurysm and AD is most commonly seen within the aortic root and descending portion of the aorta, with 100% of descending expansions studied showing signs of AD within a recent study, compared to just 12.8% within the aortic root or ascending expanded areas(118). Furthermore, the expansion of the aortic root was alarmingly quick, increasing on average 0.26cm a year(119). This incredibly high level of dissection carries a huge mortality risk. Other syndromes such as Turners Syndrome and Ehlers-Danlos Syndrome have similar risks. Turners Syndrome is caused by the complete or partial loss of a chromosome, resulting in a 45X genotype(117). This can occur across the whole body, as well as in a mosaic

form. The mechanism by which AD affects Turners Patients is not yet clear, however, significant cystic medial necrosis has been documented within these patients and, as discussed earlier, is a known precursor to AD(105). Furthermore, Ehlers-Danlos syndrome is caused by a mutation to one of a number of genes, with each effected gene causing slightly altered phenotypes and inheritance of symptoms as a result(104). Collectively, the patients with this syndrome have a number of connective tissue related symptoms, with chronic pain, premature osteoarthritis, multiple dislocations of joints and scoliosis being some of the more common symptoms. Like with inheritance, life expectancy is variable depending on the specific gene or genes mutated, with some variants having normal life expectancy. However, mutations with associated vascular pathologies life expectancy is significantly shortened(120), largely as a result of the vascular deformation or associated conditions that are produced as a result.

1.3 PROTEASES IN AAA

AAA is a pathology in which a number of degradative processes occur. Chronic inflammation leads to dysregulation, depletion and disruption of structural proteins, cell content and extracellular matrices respectively. A large proportion of said processes are enzyme driven. This chapter will summarise the many roles of proteases within the development of AAA, outlining what is currently established within the literature and highlighting potential aspects in which proteases could have a further potential role.

A AAA is the focal dilatation and weakening of the aorta, making it prone to rupture, significantly increasing mortality. There is known to be a large immune system implication in the production and development of the pathology, with enzymatic activity evidently pivotal in AAA initiation. NE is an, as yet, under-studied enzyme

within this process. Preliminary investigations suggest the current *In Vivo* AAA models to modulate levels of key proteins such as MMP-2 and -9 as well as NE. All of these proteases degrade the ECM, immune receptors and structural proteins that give rise to the vasculatures scaffold.

1.3.1 MMPs

MMPs are a class of endopeptidase proteins (121), all with different proteolytic abilities and functions within physiological processes, such as angiogenesis (122), but also pathologies, such as cancers (122) and cardiovascular disease (123).

They consist of 24 different endopeptidases and are all enzymatically active giving them the ability to process the entirety of the ECM. MMPs are able to control the microenvironment surrounding cells, which in turn alters their viability within it (124). They also alter the internal environment of cells by modulating signalling in and around the cell membrane (124). Having such an important role in physiology, deregulated MMPs can strongly contribute towards disease pathology and its progression, such as in AAA.

Originally grouped by the substrate that they degrade, namely collagenases, stromolysins and gelatinases, following the discovery of more members, a numbering system was adopted with groupings only made with relation to structure. Each MMP contains a conserved signal peptide along with a pro-domain and catalytic domain, within each different sub-group, such as in gelatinases for instance. Added regions are present and required for the breakdown of each respective substrate. Other features include hinge regions and Furin-recognition motifs in different subsets.

As noted, the MMP family is a diverse group of proteins, both structurally and functionally. They serve to regulate and breakdown the ECM, with substrates and

localisation of activity greatly differing between the MMPs. Some are secreted, whilst others membrane-bound. The MMPs that have been shown to be most relevant to aneurysm are MMP-2, -9 and -12 (27)(58). These, respectively, are structurally, gelatinase and archetypal type MMP proteins that are secreted and cleaved at both ends into an active component. This cleavage can be triggered by alternate MMPs or other factors found in the ECM, such as the MMP-9 activation by MMP-2, activated protein C (125) or the presence of Zinc (121). MMP-2 and -9 degrade collagen (largely collagen IV and V) and gelatin, and MMP-12 degrades elastin.

MMP-2 and -9 are seen as important contributors to AAA. Longo et al. (27) demonstrated the combinational effect of localised activation of MMP-2 and 9, before going on to look into the relation between MMP-12 and AAA (58). Whilst MMP-2 and -9 were showcased to be crucial for the creation of the aneurysm phenotype, MMP-12 knockout studies were seen to minimise aortic expansion seen within the surgically-induced aneurysm models. These two MMPs are of great significance and are required for the production of the AAA phenotype, it has been observed that both mesenchymal cells and macrophages produce these enzymes, with both needed in order to produce the AAA phenotype seen in studies of the condition(27). These studies examined the phenotypic differences made histologically by the presence of MMPs. MMP-12 loss had a dramatic difference, most notably on elastin structures within the vasculature (58). Similar structural defects were also evident in MMP-2 and MMP-9 knockouts. However, the significant differences exhibited between the three separate knockouts were that in MMP-12 models, recruitment of macrophages into the aortic wall was notably disrupted. In MMP-2 and -9 knockout mice, macrophages were recruited to levels similar to the ones seen in wild-type littermate controls, but instead, the degradation of elastin was defective(27). These findings demonstrated that important

AAA milestones, such as macrophage activation and recruitment, as well as elastin dysregulation are regulated by separate MMPs. Furthermore, these datasets highlighted the key immunological component of aneurysms and that level of macrophage recruitment and activation can be relatable to aortic diameter. This has been reproduced and further looked into, with suggestions of multiple immune cells such as neutrophils, amongst other cell types, possessing varying degrees of influence over the initiation and development of the pathology (126).

A number of pathways that are also involved in AAA are responsible for up-regulation of MMPs (127). Aortic histological samples have shown that such MMP up-regulation accompanies the dysregulation of collagen fibres (128). Other activating influences include MMPs being up-regulated by the Egr-1, ERK and NF-kB transcription factors (73), these are induced at times of inflammatory stress.

Specific MMPs have also been shown to sustain fibroblasts that perpetuate inflammation in conditions such as Rheumatoid Arthritis (129). Fibroblasts produce MMPs in different conditions; primary cardiac fibroblasts respond to lipopolysaccharide stimuli and produce, via activation of ERK pathway, a number of growth factors, as well as the discussed MMPs, MMP-2 and 9 (130). Ehrlichman et al. and Zhang et al. have demonstrated the involvement of the ERK pathway within AAA (131) (132). ERK also perpetuates the induction of Egr-1, mediating the increase by promoting Egr-1 up-regulation(133). Egr-1, specifically within myeloid-derived cells, is crucial in the formation of aneurysms in Calcium-Chloride derived models(134).

MMP-2 and -9 have been shown to be down-regulated in elastase-infused female mice at 14 days when compared to males at the same time point. This finding correlated with the decreased aortic diameters taken from random females at the same stage. Additionally, this data was inversely and proportionally correlated to the presence of

oestrogen receptor-α (ER-α), where oestrogen had been used as a protective agent against aneurysm formation. Alternate studies have also supported this idea, linking low oestrogen levels to increased rates of aneurysm (135). Furthermore, population statistics have shown that women overall, have a much lower occurrence of aneurysms than men (28), although this point of view has started to change with population data arising from Scandinavia contrasting these results(6). Supporting this alternative school of thought, the majority of mice studied within laboratories of some of the most highly regarded researchers into aneurysm use female mice preferentially within studies.

Contribution of MMPs towards the AAA pathology may not stop at ECM breakdown, elastin and collagen dysregulation, immune recruitment and priming. Dysregulation of MMP levels have been shown to also cause cerebral aneurysms (136). It has been noted that increases in MMP expression are not matched by rises in the levels of Tissue Inhibitor of Metalloproteinases (TIMPs). The presence of MMP-to-TIMP mismatch implies an increase in MMP activity, which is a widely reported finding, from multiple AAA studies (137). The increased activity comes from MMP protein up-regulation, as a result of altered MMP gene regulation. As mentioned earlier, MMP expression is modulated in part by the Egr-1 transcription factor. Evidence for this finding comes from fibroblasts within early stages of inflammation (138), macrophages and smooth muscle cells, amongst others (139). Interestingly, in chronic inflammatory conditions, of which AAA is considered one, Egr-1-induced MMPs are continually activated, which could potentiate the pathology (139).

1.3.2 The Role of Neutrophil Serine Proteinases in AD and AAA

NE is a serine protease harnessed within azurophilic granules, produced by neutrophils and macrophages alike(140). The deposition of such granules elicits an array of reactions, such as elastin breakdown, initiation and modulation of inflammatory

signalling and production of NETs. A number of said proteins and processes are relevant to AAA and the chronic inflammatory environment involved within the pathology. Whilst the link between NE and AAA has not yet been well established, this protease has many characteristics that make it a strong candidate for further study. With so many links to pathways and molecules associated with the AAA pathology, I will aim to shed light on the role NE plays within the pathology.

Inflammatory signalling and immune cell invasion is intrinsic to the AAA phenotype. A number of papers have shed light upon many different aspects of these processes; NEs influence on cleavage of TLR4 for instance. TLR4 cleavage leads to potent inflammatory cascade activation, which is, in part, responsible for the expansion of the aorta. Furthermore, the anti-microbial functionality of the serine protease serves to eradicate microbes and triggers mechanisms for clearing. NE enables the release of chromatin from neutrophils to engulf and nullify the microbes that are otherwise unable to be dealt with. NETs have been seen within histological samples of AAA, and blockage of the process has led to eradication of expansion within *in-vivo* models of aneurysms(141)(142).

NE, as well as having direct effects upon structural proteins and receptors has indirect functionality, acting to potentiate and exacerbate the roles of other proteases and proteins shown to be intrinsic to the development of AAA. Dysregulation and breakdown of elastin, collagen and other ECM proteins are some of the most well-studied and documented functions of NE(140,143), whilst all present and imperative for the development of AAA. Taking all of this into consideration, this area is an area of interest relevant to AAA and is currently understudied, I will aim to address some of the gaps in knowledge within this area as part of this series of works.

As mentioned above, NE is part of a family of enzymes with close relation to Cathepsin G (CG) and Proteinase 3 (P3), known as the Neutrophil Serine Proteinases (NSPs). PR3 is expressed within a number of cells, largely of the granulocyte lineage(144), and can exist as both a membrane-bound enzyme(145) or in a secreted form(146). PR3, whilst expressed on some subsets of neutrophils, is able to be secreted from granules into the ECM, known as inducible PR3(146). Whilst PR3 has many similarities to NE, such as an enlarged binding region, there are also some distinct differences. These include large differences in the subsites of the binding site, such as the inclusion of three charged residues (Lys99, Asp61 and Arg143) within the binding site itself. PR3 has capabilities differing from other NSPs, due to its ability to reach deeper portions of the vessel in comparison to alternate NSPs and exert its catalytic effects (144). Furthermore, PR3 has many roles within inflammation and the apoptosis of the immune cells themselves, regulating immune processes and prolonging neutrophil lifespan by inhibition of the caspase-3 dependent apoptosis pathway(147)(148). Within AAA, NSPs such as PR3 have been suggested to play a role within the development of the pathology, with decreased levels of their inhibitor leading to worsening of the phenotype produced(16). Within the same study, CG was noted for its direct contribution to the AAA pathology, notably its direct actions upon elastin within the breakdown of the substance within the vessel wall of the aneurysmal aorta.

Similarly to PR3, CG can be produced in a number of different cell types, including both Neutrophils and Mast Cells(86). CG has a multitude of direct actions upon the AAA process, with the ability to modulate MMP-1, directly degrade the ECM, induce SMC apoptosis and contribute to angiogenesis, all key features of AAA(86,149). CG was initially identified within the immunological response as part of large pathogenic clearance, within the NETosis process (150). NETosis has been identified as a

contributory mechanism by which AAA occurs, highlighting the relevance of CG and the NSPs within the AAA process(151).

NSPs are not the sole influential group of enzymes within the AAA and AD processes, with a multitude of proteases associated with the pathologies, a selection of which will be raised and discussed within the following section.

1.3.3 Sources of AAA-related proteases

The proteases involved within the AAA pathology come from a number of differing sources. SMCs, WBCs and even perivascular adipose tissue (PVAT), are all known to contribute significantly to the degradative environment. Each tissue contributes specific proteases that selectively break down the ECM of the aorta and help form the pathological phenotype.

SMCs have been well studied within basic physiology and have now begun to be studied in association to the AAA pathology. SMCs aid the healthy aorta by producing the essential structural proteins, namely elastin and collagen, which provide support for the cellular content of the vessel. As well as these structural proteins that are produced, proteins with enzymatic function are also produced. In the case of SMCs, these are predominantly MMPs, which serve to degrade the same structural proteins the SMCs produce in order to support a healthy microenvironment. Within the AAA pathology, the balance of these two functions is both delicate and pivotal. Dysregulation of this equilibrium causes the disruption of the ECM, evident within samples of AAA tissue. This appears to be influential, if not essential, in the progression of the AAA pathology. Many aspects of the immune system have been evidenced to influence AAA, both from in vivo and in vitro tissues. Golledge, amongst others, has extensively shown the

impact of immune cells, namely macrophages and neutrophils, and the role that they play in the causation of the AAA phenotype. Production of molecules, such as Neutrophil-Gelatinase Associated Lipocalin (NGAL), by neutrophils, act to potentiate the abilities of vessel damaging proteases, such as MMPs. MMPs also have inhibitors, most influential in AAA are TIMP-1 and TIMP-2, which inhibit MMP-9 and MMP-2 respectively(143). Macrophages are another leukocyte that has the potential to produce and influence the AAA phenotype, with similar work by Daugherty and Golledge amongst others shedding light on the potent proteins that they express and roles that they play within the breakdown of the vasculature(1,48,152). Not only does the macrophage lead to vasculature damage, but it also has key roles within initiating chronic inflammation, ECM breakdown and further problems such as SMC death(153). All of these are known markers for AAA and are seen within the early stages of the pathology. Macrophages and later foam cells that build up in various regions of the vessel wall activate macrophages. These cells have been stained within the adventitia, whilst the cells were also discovered within the media. These cells, recruited by inflammatory signals such as MCP-1 and IL-6, then serve to potentiate the immune recruitment and activation of the innate immune system via CD14 activation of TLR4 and TLR2 (152). Following this activation we see a further up-regulation of monocyte recruitment and infiltration, leading to a self-perpetuating cycle of increased inflammation and immune cell invasion. Large quantities of proteolytic enzymes are produced as a result of this consistent invasion and production of an inflammatory environment, furthermore still, some proteases have been reported to elicit similar effects to that of bacteria and immune cells. For example, NE has been shown to activate TLR4 leading to increased function, triggering downstream effects with decreased need for a ligand such as LPS or CD14(154), as cleaved fragments become

active peptides. This complex immune component has begun to be studied within a number of differing contexts related to AAA, from vessel wall tissue to the relatively new area of perivascular fat. Mast cells and T-cells, along with the previously discussed macrophages and neutrophils, have been found within these areas and are now thought to contribute to the production of the AAA pathology(155).

Perivascular fat, or PVAT, as it is referred in most literature, has roles related to cell trafficking and blood flow in and around the neovascularised areas of the aorta(155). AAA is an exception to the normality of WBCs invading tissues within small capillary networks and post-capillary venules, with the vessel lacking these features. Angiogenesis is a feature of AAA, and neovascularisation of the area leads to intricate networks of vessels around the aneurysmal area(156). These small vessels adventitia are encompassed by PVAT, in different quantities depending on health state. This fat is highly vascularized and appears to influence flow and function within the vessels passing through and surrounding it via a vasocrine system(157). This modulation, dependant on the health of the vessel can lead to endothelial dysfunction and immune cell invasion to the areas surrounding the vessel(158). This has been hypothesized as a contributor to the AAA pathology. Proteases originating from the macrophage and neutrophils, which are now free to move into the areas surrounding the adventitia, are then able to start breaking down the ECM, triggering apoptosis of the SMCs and contributing to the inflammatory background of the area, which in turn recruits further immune cells. This process kick-starts the weakening of the vessel wall and the eventual formation of the ballooned vessel wall.

In summary, proteases have been shown to be involved in many different aspects of the AAA phenotype. Many proteases have known functions within the process such as the

well-studied MMP family, however others, such as NE, are still to be fully explored within the AAA setting. Protease complexes modulate the activity of these enzymes and the abundance of complexes is based in part upon the expression of regulators, which in healthy physiology is tightly regulated, but appears erroneous in instances of AAA. Proteases are expressed in large parts by the WBCs, and these enter the tissues via small vessels under the control, in part, of PVAT, cytokine signalling and inflammatory signals. This leads to the production of an inflammatory environment, within which the degradation of the aortic wall occurs. More detailed study is needed, especially in the case of less well-known proteases, such as NE, and their role within the pathology. Following this, we may be able to understand the mechanism by which AAA occurs to a greater extent.

1.3.4 PDGFRB- a key receptor in protease expression

PDGFRB, is a receptor that is intrinsic to vascular health. This includes binding to a number of growth factors, namely PDGF-B and –D amongst others. Resultant conformational changes that ensue trigger the receptors kinase domain which has widespread implications on intracellular enzymatic activities and can initiate the potentiation of AAA-associated proteases, transcription factors and proteins as a result (159). Ephrin-B2 is one key regulator of platelet-derived growth factor receptor b (PDGFRb) distribution in the VSMC plasma membrane, endocytosis, and signalling in a fashion that is highly distinct from its role in the endothelium. Absence of ephrin-B2 in cultured VSMCs led to the redistribution of PDGFRb from caveolin-positive to clathrin-associated membrane fractions, enhanced PDGF-B-induced PDGFRb internalization, and augmented downstream mitogen-activated protein (MAP) kinase and c-Jun N-terminal kinase (JNK) activation but impaired Tiam1–Rac1 signalling and proliferation. Accordingly, mutant mice lacking ephrin-B2 expression in vascular

smooth muscle developed vessel wall defects and aortic aneurysms, which were associated with impaired Tiam1 expression and excessive activation of MAP kinase and JNK which in term regulate key protease activity e..g. MMPs (160). Published data suggests that ephrin-B2 is an important regulator of PDGFRb endocytosis and thereby acts as a molecular switch controlling the downstream signalling activity of this receptor in mural cells. (160)

Platelet-derived growth factor receptor-B (PDGFRb) has intrinsic roles within the maturation and development of the cardiovascular system within embryogenesis and knockout of the protein leads to reduction of VSMCs and pericytes. Interruption of pericyte growth and viability impacts the production of capillary cell walls and leads to the production of microaneurysms within the capillary network (161). Loss of the PDGFRβ protein consequentially decreases the functionality of multiple organs including the brain and the heart. Containing intracellular kinase activity, once internalised within the VSMC PDGFRb induction can increase the activity of MAP-kinase and JNK, both highly influential in AAA. Consequentially due to lack of PDGFRb presence and subsequent kinase activity, AAA and other vessel wall defects can ensue as a result. Furthermore, PDGFRβ has known interactions with LRP1, and again this influences kinase activity downstream with regards to MAPK. However, the level of influence and direction of mediation is highly debated with some studies observing the suppression of MAPK and other stimulation when the two interact. Alternately, LRP6 has a negative effect on PDGFRβ levels which in turn diminishes levels of VSMC proliferation(160).

1.4 ROLES OF NE IN IMMUNITY AND DISEASE

Whilst there have been many known proteases associated with the AAA phenotype, novel proteins and new associations with already identified enzymes are being made all of the time. As we begin to unravel the contributing mechanisms to AAA we understand the processes and roles certain proteins have within the phenotype. For instance, the previously mentioned MMP9 that has a huge impact on the production of the AAA phenotype is now known to be regulated in part by an array of miRNA proteins, namely miR-133b, miR-133a, miR-331-3p, miR-30c-2 and miR-204 which were all downregulated within human AAA aortic samples (162). Furthermore, some proteins and even cell types with known function in other areas are now beginning to be evidenced as to playing an influential role within the AAA condition(163). For that reasoning, it is valid to look into other areas of research with associations to the pathological processes occurring within AAA for a deeper insight into the currently poorly mapped out mechanisms controlling aneurysm development. For instance, NE is a molecule with known roles in pathology, immune implications and regulation of key molecules such as some of the aforementioned proteases(17,143,164). Resultantly being an enzyme of interest and a candidate for further study.

NE is an enzyme contained predominantly within azurophilic granules of the Neutrophil prior to degranulation into the cellular surroundings; however latest research is suggesting its ability to be produced by other cell types most abundantly within other white blood cell subtypes(17). Azurophilic granules harness a number of proteases, two of which highly structurally related to NE. Cathepsin G and Proteinase 3 are both serine proteases that work in conjunction with NE within microorganism clearance within the phagolysosome(154). NE was firstly known to degrade elastin, however further studies have gone on to identify the enzymes ability to cleave many other extracellular matrix proteins, enzymes, cytokines and adhesion molecules, a

number of which with relevance to AAA. MMP2 and MMP9 are both able to be cleaved by NE(165)(143), along with TLR4 and VCAM-1 amongst many others(166), all of which have known roles within the production of AAA. NE cleaves peptide bonds by arrangement of a catalytic trio of protein residues, a property conserved within the chymotrypsin family of serine proteases that it belongs.

Inactive NE is synthesized in the endoplasmic reticulum prior to activation and packaging into azurophilic granules. The activation and packaging step is dependant upon processing of the peptide. Firstly dipeptidyl peptidase I cleaves the signal sequence to activate NE, following on from this NE can be further modified with alterations made to the carboxy-terminal. The secondary modification of NE, whilst not necessary for activity, aids trafficking of the enzyme to azurophilic granules with non-cleaved versions directing the molecule to the plasma membrane. This direction alters NE ability to function within a number of immune and disease-related mechanisms(167). For instance, NE has a significant role within the deployment of NETs as well as the previously mentioned role within clearance of pathogens within phagolysosomes. NETs are web-like structures composed largely of chromatin that bind to pathogens in order to aid the clearance of larger pathogens. NE and other mediators such as myeloperoxidase (MPO) and protein-arginine deiminase type-4 which are responsible to trigger the release and decondensation of the later released chromatin(14). Whilst the process is predominantly beneficial, links to disease have started to emerge. Roles within cancer metastasis and thrombosis have been documented, whilst links to AAA have also emerged.

NETosis is the tertiary mechanism of defence of neutrophils, with the release of chromatin, containing antimicrobial properties and proteins, in an effort to trap and nullify pathogens(168). However, problems arise from the failure to clear such

chromatin, as this leads to the triggering of the host immune system against the proteins and cellular components expelled during the release of NETs(168), in turn this can lead to disease and has associations with AAA(142). Within this process, beyond the decondensation mechanism, ROS are produced in order to target and eradicate the pathogen. NADPH oxidase complexes drive this, through activation upon initiation of NETosis, this converts to Hydrogen peroxide. This is subsequently broken down by MPO and in turn stimulates the release of NE containing granules, which proceed to stimulate the degradation of histones and allow for the release of chromatin(95). NE and MPO are then able to attach to NETs when the nuclear membrane of the effected cell disintegrates. This both stabilises and increases the antibacterial properties of the released NET. This process, due to the membrane rupture mechanism, leads to the death of the neutrophil(169).

The role of NE within pathology is far better documented and well understood in other areas, most prominently COPD(164,170). Within COPD NE is understood to drive many of the processes where the lung and its microstructure deteriorate, leading to the fall in indicators such as FEV_1 with the rise in NE levels. This was first determined as a result of poor pulmonary health within patients suffering from α-1 anti-trypsin deficiency, a known inhibitor of NE. These patients presented with early-onset symptoms and far more severe phenotypes within patients suffering from both the deficiency and COPD. With the loss of α-1 anti-trypsin, even healthy individuals suffer signs of COPD and associated diseases due to the proteolytic breakdown that results from unregulated NE expression(171).

Resultantly, with NEs known roles within COPD as well as a number of associated contributing elements of AAA, namely; immunity, inflammation and ECM

degradation, further investigation into the role of NE within AAA appears necessary to elicit its full role within the disease.

1.4.1 The role of Neutrophils in AAA

Of the multiple WBCs that are known to have a role within the AAA pathology, most prominently studied being the macrophages, neutrophils are a less studied subgroup of WBCs, previously regarded as having limited role largely contained to phagocytic actions. However, identification of neutrophils and their roles within inflammation have been brought to light, with roles relating to release of reactive oxygen species and neutrophil proteases into the medial vessel wall and throughout the intraluminal thrombus specifically(87).

Neutrophils are recruited into tissues at times of acute inflammation, performing phagocytosis and pro-inflammatory functions with an aim to recruit further more specialised cells and promote clearance or resolution of infection or injury, respectively. Initial extravasation is a more complex process than previously thought, with cells forming a ‘tether and slingshot’ mechanism to be released from the bloodstream. Neutrophils follow multiple gradients of chemokines, initially following intermediate signals before progressing to further localised pathogen chemoattractant mechanisms (172). This chemotaxis is controlled by MAP-kinases amongst other mechanisms. This function highlights MAP-kinases importance and level of control over cellular activities. Beyond homing of the neutrophils and their basic functions as an immune cell, neutrophils produce numerous proteins and proteases that serve to prime the differing arms of the immune system by methods of activation and release of such mediators.

Neutrophil associated proteins such as D-Dimer and MPO, have been discussed as potential markers of AAA as a result of their correlation with the AAA pathology. Further, DPPI, dipeptidyl peptidase 1, a neutrophil-associated enzyme, was key in the production of experimental AAA, with knockout studies of the gene responsible for its expression abolishing the pathology (142). This strengthens the growing argument from within the literature that there is a key influence from neutrophils within the AAA pathology and its evolution. Supporting this, observations of neutrophil recruitment to the aneurysmal site, along with their activation resulting in NETosis, a characteristic discovered in both animal model and human AAA tissues. With relation to this study, it has been outlined that DPPI is responsible for release of key NSPs, such as NE and Cathepsin G in mature neutrophils.

Expression of NE within neutrophils-

Following bacterial infection, NE is known to be released into the extra-cellular space in order to aid in the battle against such pathogens. Release of NE produces increases in proinflammatory cytokines, namely TNF-alpha, MIP-2 and IL-6 via the NK kB pathway, this has been shown to improve immune function and consequently improve mortality rates (173). This is likely due to the evidenced recruitment properties of the aforementioned molecules which increase neutrophil translocation to the infected site. Stored within neutrophil granules at high concentration NE is released and exerts anti-microbial properties, often in conjunction with NETs. However, NEs increased production of pro-inflammatory molecules mRNA can be limited by the presence of silvestat, which stunts the enzymes catalytic activity. This catalytic activity enables the induction of protein expression, including IL-8 expression mediated by TLR4(174). Multiple studies have outlined the role of NE and its relevance in the production of pro-

inflammatory molecules such as IL-8, IL-6, MIP-2 and TNF-alpha in various cell types, most importantly macrophages. As such, NE appears to have TLR4 cleavage properties, which in turn produces active fragments with biological mRNA expression modulation potential, investigations into whether other serine proteases possess similar ability to achieve these results are being looked in to (174).

As well as having a direct role in AAA formation, by influencing structural proteins via processes such as proteolytic action and NETs, neutrophils can govern the production and release of key cellular mediators such as chemokines and cytokines. This can take the form of Interferons and Interleukins, with increased expression of type-1 IFN mRNA found in both tissues and serum of afflicted patients. The discovery that NETs and interferon alpha not only play a critical role in promoting experimental AAA but are also increased in human AAA suggests a high level of influence, and targeting of neutrophils and the cell type associated proteins may slow the expansion of AAA (142).

Beyond cellular mechanisms of AAA, matrix proteins are importantly regulated within the AAA process, with modifications to the arrangement of collagen and elastin being two of the key steps to AAA production. These changes can, in part, be brought about by neutrophil action, with proteolytic degradation of elastin a known function of NE , a neutrophil derived protease. Furthermore, neutrophils have been suggested to support further production of proteases within the ILT, with large-scale production of MMPs and cytotoxic molecules that in turn degrade the vessel wall and deplete the vascular integrity by inducing VSMC damage (175)

As identified above, neutrophils have key roles within the formation of AAA and its pathological phenotype. Neutrophils are located largely within the ILT and adventitial portions of the pathological vessels. Studies into neutrophil expression patterns within AAA made the observation of key regulators of AAA such as NGAL, MMPs and MPO,

amongst others, were largely expressed within the ILT, and most specifically the luminal portions of the thrombus. NE, an enzyme with involvement within a number of the processes associated with AAA, such as NETosis and chronic inflammation, is the focus of this work. NE and its role within AAA is less well defined and has the potential to have significant impact on the AAA pathology due to its multiple relations to initiating molecules and mechanisms of AAA such as direct elastin degradation. Whilst neutrophils are traditionally seen as responders to acute inflammation, evidence suggests them to have a role within chronic inflammatory processes and the potentiation of a worsening phenotype long term within aspects of the pathology such as the high concentration of neutrophils identified within the ILT. Current research into neutrophils and their role within AAA demonstrates impaired neutrophil recruitment can lead to improved AAA outcomes, at least within animal models (176).

2 HYPOTHESIS & AIMS

HYPOTHESIS

The foundation for this is the known contribution elastin breakdown and immune cell recruitment has to both the AAA and AD pathologies, taking into account the impact NE is proven to elicit on elastin, and involvement NE has been shown to have on relevant immune-related receptors, such as TLR4 amongst others. More directly, NE has a key role in NETosis(142), a phenomenon recently put forward as a further contributing aspect to the AAA pathology. Medial dysregulation and apoptosis are largely responsible for changes that lead to AD, with NE having known influence within these processes. Furthermore, NE can modulate MMPs which are known triggers of AD(177).

The hypothesis of this PhD study is that NE is involved in a mechanism contributing to AAA production and stability and that by knocking out this enzyme rates of AAA will be decreased. Similarly, we predict AD to be influenced by NE in a similar fashion to AAA. Consequentially, we hypothesize that NE will become a novel drugs target for the treatment of AAA and AD.

AIMS

- ⇒ To produce a protocol to monitor and measure AAA expansion and characteristic features, such as blood flow alterations, vascular remodelling and vessel pulsatility changes.
- ⇒ To understand the effect changes in expression levels of NE has on AAA and AD-associated proteins, such as MMPs, on a cellular and tissue level
- ⇒ Study the effect that the loss of NE gene has within Angiotensin-II and Calcium Chloride models of aneurysm
- ⇒ Study the effect that the loss of NE gene has upon TAD within animal models
- ⇒ If a difference is discovered, identify the mechanism by which NE contributes to the production of the AAA and AD pathologies.
- ⇒ Verify if knowledge gained from this study may be translatable to the Human conditions

3 General Materials and Methods

3.1 Cell Culture

Culturing of a number of cell lines occurred, predominantly; Human Umbilical Vein Endothelial Cells (HuVECs), Human Smooth Muscle Cells (hSMCs) and mouse macrophage cell line (RAW 264.7). These cell lines were chosen due to their relevance to the AAA pathology. By studying HuVECs we were able to elicit an understanding of how the vascular endothelium reacts to inflammatory insults utilised within the different models of AAA. hSMCs, from the aortic vascular bed, were cultured to give us information on the changes of expression that occur within the smooth muscle component of the vasculature. Finally, RAW 264.7, a monocyte-macrophage cell line, will give us a general comprehension of how an integral part of the inflammatory cell component is implicated within the models.

HuVEC cells were cultured in T75 flasks on a surface of 0.04% gelatin in Medium 199, 10% FBS and Antibiotics, until 60% confluent prior to use for experiments. hSMC and Raw264.7 cells were also cultured within T75 flasks within DMEM media, 10% FBS and Antibiotics, reaching 75% and 60% confluence respectively before experimental usage.

3.1.1 In Vitro Calcium Chloride and Angiotensin-II Experiments

All experiments reported below used the same protocol of AngII exposure. Cells were grown in 12-well plates overnight, with 500µl of media (Dulbecco's Modified Eagle Medium (DMEM)(Sigma Aldrich UK) or Medium 199, 10% fetal bovine serum (FBS)(Sigma Aldrich UK), 1% L-glutamine (2.5mM), Penicillin (100U/ml), Streptomycin (0.1mg/ml)(Sigma-Aldrich UK)) containing AngII diluted within the

relevant growth media to specific concentrations. Cells were left for 48, 24, 4, 2 and 1 hours under treatment conditions before immediately being harvested.

Within reported data, $CaCl_2$ exposure was for a period of 5,15 or 30 minutes, with media refreshed and cells recovered for 8hours following this before harvest. Multiple concentrations of $CaCl_2$ were trialled.

In Vivo models of AAA are used in order to gain a greater understanding, as currently there is limited knowledge with relation to the initiation and progression of the pathology. The degradation of elastin, collagen and other structural proteins, is a widely accepted early-stage event in the formation of the aneurysmal phenotype. NE is an enzyme able to degrade some of these proteins and is therefore, the initial protein being explored with relation to AAA.

Translating the *In-Vivo* models of aneurysm into an *In-Vitro* method by which we can look at the impact each method has within each cell-type is first needed. By establishing an *In-Vitro* model, we will be able to measure a number of AAA associated proteins, such as MMP2 and MMP9, as well as the level of expression NE.

In-Vitro exposure to Calcium Chloride was varied as to best assess which duration caused expression most akin to that of the aneurysmal phenotype seen within animal models. *In-Vivo*, exposure has been reported to range from 6 to 15 minutes. Resultantly, similar time-points were trialled, as well as longer durations of exposure in order to mimic the chronic pathology AAA is regarded as.

In-Vitro exposure to Angiotensin II (AngII), is a much more well-established protocol and therefore less variation in conditions were needed to be trialled. Current literature was followed as a guideline of appropriate concentrations for use within experimentation.

A time course of the varying effects differing concentrations has on expression of the relevant genes was carried out in both models. Utilising RT-qPCR, modulations in the gene expression were determined and compared.

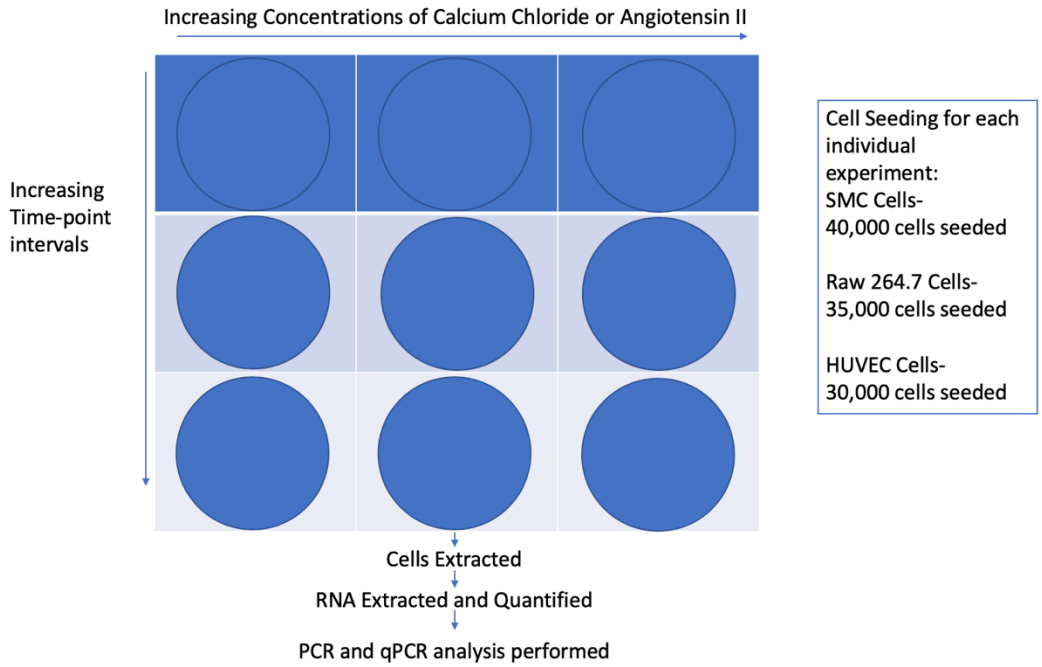

***Figure 3**- Schematic diagram of the seeding and treatment of cells using Ang II and $CaCl_2$. Cell seeding describes cells seeded within each well on a 12-well plate. Each individual well contained one cell type, treated with one stimulant for one time duration. Each set of conditions was performed in triplicate for each set of parameters.*

3.2 Animal Husbandry

All mice were housed in accordance with the regulations specified within the Animals Scientific Procedures Act 1986, with all experiments being approved by the Home Office prior to commencement of all procedures. This included the housing of animals in ventilated cages with controlled lighting, light and dark cycles of 12 hours each, with temperature regulated between 20 and 23 degrees. Food and water were available *ad libitum*, with standard chow diet available at all times. With the commencement of any highly invasive procedure, such as the Calcium Chloride model of aneurysms, mice

were individually housed in order to minimize the risk of breakage or biting of sutures causing infection or disembowelment. Upon the completion of all experiments, mice were humanely culled by Schedule 1 procedures most commonly CO_2 chamber followed by cervical dislocation.

3.3 MOUSE STRAINS

3.3.1 C57/BL6-ApoE Knockout mice:

ApoE deficient mice on a C57BL/6 background were originally purchased from Charles River Laboratories (Margate, UK) before inbred breeding in house to expand the colony took place. All Control mice were of this background due to the pro-atherosclerotic phenotype that is a consequence of the genetic deficiency. This is representative of the demographics of AAA sufferers.

3.3.2 NE Knockout mice:

These mice are deficient in the ELANE gene responsible for the production of NE. $Elane^{-/-}$ mice from The Jackson Laboratory, 006112 mice were bred with C57/BL6-ApoE Knockout mice to produce a double knockout for both ApoE and NE genes as described in our previous study(167). Genotype was confirmed following birth of litters, with mice separated into cages based upon gender and genotype. All mice were caged with littermates of similar gender and genotype. These mice were confirmed to be deficient for both NE gene and protein.

Within all AAA protocols, mice of both genders were aged until 8-weeks old prior to the commencement of $CaCl_2$ or AngII protocols, outlined below. Alternately, for BAPN induced AD studies, mice were placed upon protocols at 3 weeks of age and limited to the male population of pups.

3.4 GENOTYPING

All mice underwent genotyping in the period prior to weaning from mothers at the 3-week postpartum period. DNA of each mouse was isolated from tail tips of the mice, with samples digested overnight at 55 degrees in 250µl of lysis buffer containing 100mM Tris-HCL (pH 8.5), 5mM EDTA, 200mM NaCl, 0.2% SDS and 100µg/ml Proteinase K. Following lysis, contaminant debris was pelleted by centrifugation at 17000 RCF for 10 minutes. Supernatant was transferred into new sterile labelled tubes and the pellet discarded. Isopropanol was added to each tube (250µl per tube) with gentle vortexing carried out in order to precipitate DNA. This DNA was further centrifuged, again at 17000 RCF for 10 minutes, with supernatant discarded, washing in an ethanol gradient and air-drying. Following this wash and drying, the pellet containing DNA was suspended within sterile DNAse free H_20.

PCR reactions were performed to identify the genotype of each mouse, with primers selective for the NE Knockout and Control mice utilized within each reaction. PCR cycle details, as well as further information regarding the primers used within each reaction, are detailed below in **Table 3**.

Table 3- *PCR details utilized within the PCR and qPCR experimentation, including primer information, cycle details and size of gene targeted.*

Gene (reference)	Primer type	Primer name	Melting temp.	Sequence 5'→ 3'	Amplicon size (bp)
NE	Common forward	oIMR7065	60.2°C	TGC ACA GAG AAG GTC TGT CG	-
	WT reverse	oIMR7064	59.8°C	GGA ACT TCG TCA TGT CAG CA	230
(Mouse Mutant Resource, 2012)	KO reverse	oIMR8162	65.4°C	TGG ATG TGG AAT GTG TGC GAG	310

Reagents (units)	Stock conc.	Final conc.	Volume (n = 1, μl)
dH_2O	-	-	8.2
SYBR green mix (×)	2	1	10
Forward primer (µM)	5	1×10^{-4}	0.4
Reverse primer (µM)	5	1×10^{-4}	0.4
cDNA (×)	20	1	1
Total Volume			**20**

Step	Temperature	Time	Cycles
Initial denaturation	94°C	5 minutes	1
Denaturation	94°C	30 seconds	30 (NE) 35 (CX_3CR1)
Annealing	60°C	30 seconds	
Extension	72°C	30 seconds	
Final extension	72°C	5 minutes	1
Storage	4°C	hold	-

Step	Temperature	Time	Cycles
Initial denaturation	95°C	15 minutes	1
Denaturation	95°C	15 seconds	40
Annealing/Extension	60°C	1 minute	
DNA dissociation	95°C	15 seconds	1
	60°C	15 seconds	1
	95°C	15 seconds	1

PCR amplification enabled the expansion of genetic materials, following this the amplified mixture was mixed with loading buffer prior to vortexing to ensure sufficient mixing occurs. This was then placed within wells of 10% self-poured polyacrylamide

gels, with the gel ran within an electrophoresis unit it 1x Running buffer at 100 volts for 45 minutes before being stained and visualized for identification of genotype.

3.5 Angiotensin-II Model of Aneurysm

The procedures for AngII-induced AAA were similar to previous studies with modifications(178)(46). Specifically, animals were selected for this procedure based upon genotype, age and gender. All mice were kept with littermates, in cages of no more than 6 mice, until insertion of an osmotic pump (Alzet, model 1004, 0.11µl/hr). All mice studied were scanned using an MRI (1Tesla), prior to pump insertion, and injected with 90µl Galbumin (BioPal) solution, diluted 1:10 Galbumin stock: saline) immediately preceding imaging. Isoflurane anaesthesia (Piramal Critical Care Ltd) is used to sedate animals during the scan, with heart rate and breathing rate monitored throughout the scan. This scan gives us a composite image that is then reconstructed in order to give us volumetric data of the infrarenal portion of the aorta, as well as diameter measurements of specific places along the course of the aorta, for comparative reasons when compared against scans on the same animal at later time points.

Pumps were inserted sub-dermally, being placed into the excess skin fold of the abdominal wall, entering via a small incision at the back of the neck. Connective tissue is loosened using blunt dissection sub-dermally within the skin folds. The pump is inserted lid first and lubricated using saline, to minimize chances of contents leaking or dislodgement of the central pin before sutures close the wound. Following the procedure, animals were individually housed and recovered, whilst being checked daily for health and condition. There is a high risk of complications, especially in the first 5 days of Angiotensin-II administration, therefore close attention to the condition of the animal is essential so that it does not undergo any unnecessary pain or prolonged

complications. A hypertensive phenotype is produced within this period and remodelling of the vasculature ensues over the next few days and weeks. Dilation of the vessels, tissue remodelling and endothelial dysfunction or loss occurs. Following this aneurysm formation can occur, generally within the last week of incubation with the hypertensive agent.

Mice are left for 28 days post-implantation of the pump, before removal and a second MRI taking place. Pumps must be removed prior to MRI taking place for the safety of the mouse, as the steel pin within the pump is magnetic and therefore the magnetic forces within the MRI would attract this, causing potentially fatal problems. Monitoring of the animals' aorta can occur during the 28 day time period but must be in the form of ultrasound scanning. This occurred in a cohort of the mice within this study. During ultrasound scanning, ensure that the probe is never focused over the pump, as this can affect flow rates and has the potential to cause deviation in the level of angiotensin within each mouse. This is monitored and controlled in each mouse relative to body weight at a dose of 1.44 mg/kg/day AngII (Sigma Aldrich) diluted in saline (Sigma Aldrich). The weights of the mice are measured and recorded prior to pump filling, at the halfway stage and prior to the final MRI scan. This allows for the pumps to be filled with a specific concentration of Ang-II solution so that the correct dosage is administered to each mouse.

The second MRI scan is performed post-pump-removal, this enables comparison with the original ‘Week 0’ scan and for quantification of changes in infer renal aortic diameter and volume. From the reconstruction and individual sections produced by the MRI scan, we are able to determine the precise expansion of the vessel both in terms of diameter of the vessel and volumetrically. The use of Galbumin enables us to make luminal measurements that are as distinct as possible, as it highlights the areas in which

blood has pooled/ is present. One drawback to this technique is that, although we are able to distinguish between luminal and vessel walls, we may not be able to differentiate, with complete accuracy, between lumen, intra-mural thrombus and vessel wall. With this in mind, the use of ultrasound and MRI in conjunction with each other allows the verification of results at each time-point.

3.8 MRI SCANNING OPTIMISATION

Imaging of the abdominal aorta is complex due to it being a deep-lying structure, covered by a number of vital organs. This can distort the image in many methods of imaging, such as ultrasound. However, due to the MRI taking a series of sectional images, this minimizes such problems, with the magnetic forces being able to penetrate all tissue types, again unlike ultrasound, where sternum shadow can be a big issue with cardiac imaging especially. The clarity of the image needed to be optimized further, however, as with all MRI scans, the selection of the type of image and further optimization steps such as pixel size and field size adjustments. Furthermore, the type of scan needed to be decided too, with options of both T1 and T2 weighting. The T1 and T2 imaging selection decides whether tissues with high water content will appear bright or dark, and tissues with low water content dark or bright respectively. The ratio between echo time (Te) and repetition time (Tr) determines these differences in appearance. Sort Te and Tr gives you T1 weighted images and Long Te and Tr produces T2 weighted images. In order to make aortic images as clear as possible, to enable the most precise and accurate measurements of the infrarenal aorta, T1 weighted imaging was chosen after a trial of the two imaging techniques. T1 allowed the blood to be visualized as a bright field, enabling us to determine the borders of the vessel, and therefore the volumetric content. One issue that arose in the post imaging analysis was the blur created by distortion of the image, as the signal strength was not different

enough between the lumens border and the blood-filled lumen itself. This created the problem of potential inaccuracies in infrarenal quantification. To minimize this, a contrast agent was looked into, as this would increase the difference in signal between the vessel wall and the lumen of the vessel. Being able to distinguish between the two would allow us to see the changes in luminal size, the area of most interest. We would still be able to visualize the wall, with more detailed information regarding the vessel wall coming from alternate imaging, i.e. ultrasound. The options for contrast agents included gold nanoparticles and Gadolinium labelled albumin (Galbumin) amongst others. Due to its high molecular weight and therefore slow clearance, as well as cost restrictions, Galbumin was chosen as the preferred contrast agent. Galbumin was seen to be the most value for money and of sufficient quality to produce the difference in signal needed for the accuracy of quantification. Following the addition of Galbumin via tail vein injection, signal intensity within the aorta increased significantly and allowed for accurate measurement of the infrarenal portion of the aorta, as illustrated within **Figure 3**. Volume and dilution of this was altered and optimized to ensure the minimal amount was used, whilst maintaining optimal effect. This reduction ensured that the animal was administered the minimum quantity of the Galbumin and carrier substances, in case of adverse reactions.

3.8.1 Ultrasound Scanning

During this sequence of experiments, 2 different ultrasounds have been utilized, with the Vevo 770 and Vevo 3100. Initial scanning procedures were started on the Vevo 770, then after completion of pilot experiments involving the calcium chloride procedure all techniques transferred and updated utilizing the Vevo 3100 for increased

resolution and quality of the image. Ultrasounds intended use was to obtain information on the vessel wall, and later on information regarding flow.

Functionalities available on the Vevo 3100 included colour and pulse wave Doppler, as well as B-/M- modes. This allowed for a variety of additional assessments to be carried out. The intended use of the probe available is cardiac imaging, this means that frame rate is much higher to increase the pictures taken so that you can see the heart at all points of the heart cycle, however, this reduces resolution. This was able to be altered slightly, via modifications to the software controls such as gain, frame rate, pixel resolution, dynamic range and ultrasound focus depth. These adjustments allowed for clear images to be obtained at a greater depth within the animal, in comparison to cardiac imaging. From this, we were able to build protocols and troubleshoot the orientations of the ultrasound that was both reproducible and produced clear images. The clarity of M-mode imaging especially altered greatly with a change in orientation of the probe (See Below). Initial measurements were taken with the probe in a longitudinal orientation, whereas whilst in cross-section images produced far less noise and much more precise imaging. This meant the measurements of the vessel could more precise, increasing the accuracy of the study. From this increase in clarity, we can now precisely measure the artery at the point of max systole and diastole, giving us a measurement of the pulsatility of the vessel and how this changes over time in response to treatment. At the same time, we are consequentially able to measure vessel wall thickness as a result of the increases seen in the clarity of images. This increase enables the tracking of structures within the vessel wall through the pulse cycle. Resultantly, following aneurysm induction, we are able to monitor any changes in the composition and size of the vessel wall undergoes.

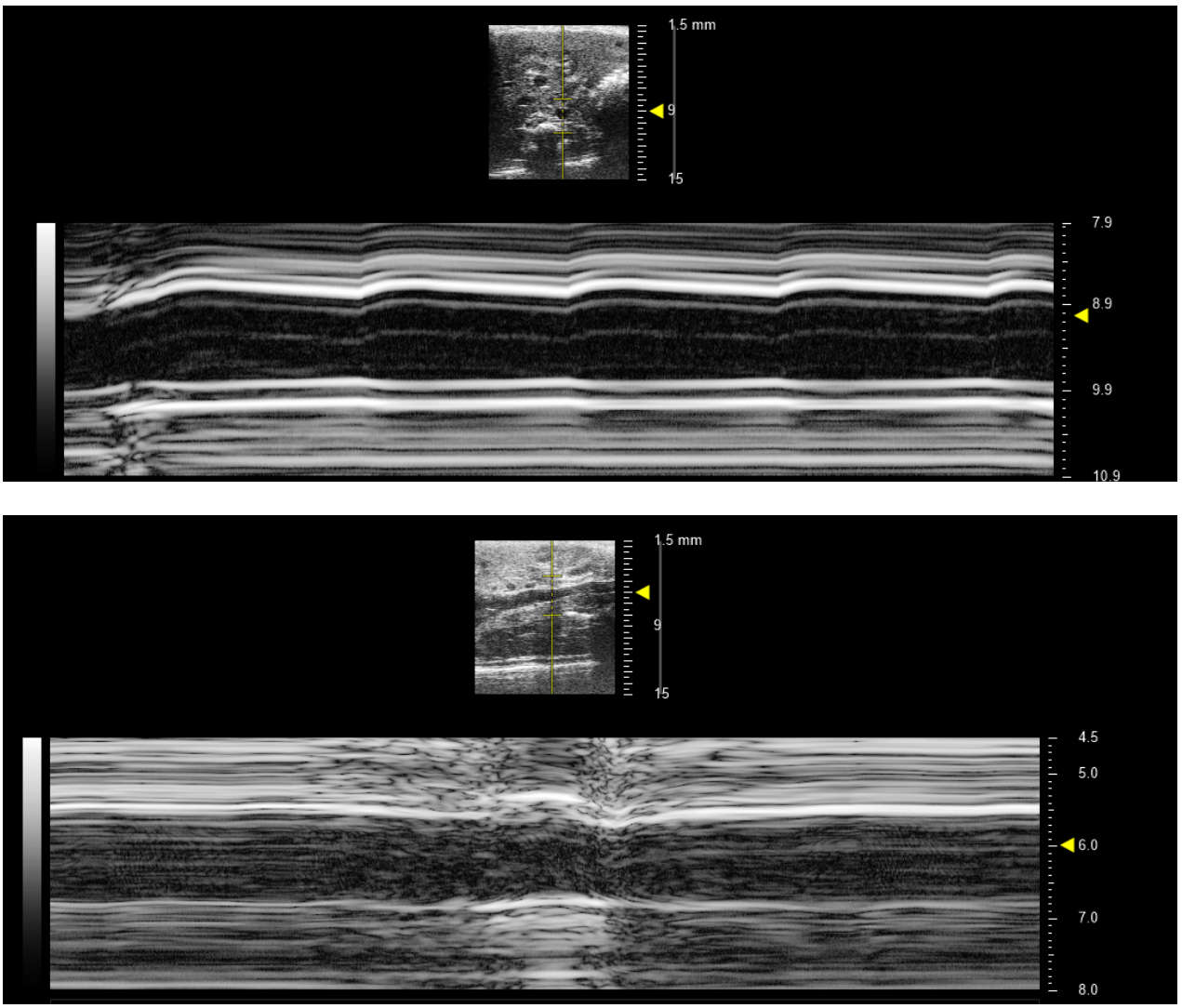

Figure 4*- Optimisation of ultrasound M-mode scanning. (Top) shows a cross-sectional view of the aorta with clear M-mode trace, enabling defined and accurate measurements. Note, the minimized levels of distortion enabling a clear vessel path shown as deep black (Bottom) a longitudinal image of the same infrarenal aorta within the same mouse, with a very noisy trace, this leaves it hard to distinguish between vascular wall structures and noise signals. US noise is shown as white speckled traces within the vessel path.*

3.9 RNA ISOLATION

Analysis of tissues from both AAA model, as well as Biobank collaborative works, were collected and preserved in liquid nitrogen immediately following harvest in order to ensure maximum quality of RNA. Snap frozen tissues were labelled and stored

within a -80°C freezer until extraction of RNA was possible. Upon removal from the freezer, tissues were placed on ice and transferred to a worktop. Sample vasculature was then transferred using tweezers from labelled tubes to 500µl Eppendorf tubes. This was dipped in liquid nitrogen with some liquid placed inside the tube to ensure complete freezing. At this point, a mini pestle was used to crush the tissue into a powder that remained within the Eppendorf. This powdered substance was then suspended within Trizol prior to further mixing by pestle on ice. Pestles were removed and thoroughly washed with detergent overnight to ensure no contamination of samples. Following treatment of all samples with Trizol, all solutions were centrifuged to pellet cellular debris. Centrifugation was carried out for 10mins at max speed, prior to the supernatant being removed and placed within fresh sterile Eppendorf tubes, leaving behind all pelleted materials. Isopropanol (200µl) was then added to these tubes and shaken to precipitate RNA. All precipitated RNA was then pelleted by a further 10 minutes of centrifugation at max speed. Pellets were then washed using an ethanol gradient before being left to air dry for 10 minutes. Following this, the pellet was resuspended in sterile H_20 and vortexed to ensure complete suspension.

3.10 PCR

Genes of interest, the most important markers of aneurysm and NE, were quantified by a series of PCR reactions. RT-qPCR enabled the relative quantification of each protein to be measured within both Tissue and Cell lysate samples following genetic material extraction from initial experimental tissues. The concentration of isolated RNA from tissues was quantified within each sample using the NanoDrop ND-1000 spectrophotometer, operating at 260nm. Concentrations were recorded for each sample before solutions were made up to 100ng in 20µl. RNA was converted into cDNA at this stage, utilizing PCR reagents outlined in the **Table 3**. Primers were designed to

specifically identify the genes of interest, and sequence for each primer is shown in the **Table 3**. Housekeeping genes GAPDH and 18s were used to control for sample variance and allow for the assessment of sample quality.

3.11 HISTOLOGY

Upon completion of all aneurysm-modelling experiments, the aorta was dissected, with photographs being taken to document the phenotype produced by all models in each genetic background tested. A subset of these mice aortas was taken at random for histological analysis. Mouse aortas were flushed with 4% PFA injected into the left side of the heart upon initial dissection to remove all the majority of luminal blood. Following this, a finer dissection was carried out and the aorta was removed completely, including heart and kidneys down to the aortic bifurcation at the femoral artery region. These vessels were then placed within labelled cryovials submerged in PFA and left overnight. The following day these were transferred to a similarly labelled cryovial, this time with distilled water to rehydrate the samples before again being left overnight. Fine dissections under microscopic aides were used to strip away connective tissues and fat from the vessel before mounting. Tissues were mounted within either OCT or Paraffin dependant on the stains they were to be subjected to. For OCT sections, dry ice was placed within a polystyrene container to provide a flat cold surface. An OCT mould was placed onto the ice to cool, prior to OCT being poured in and the vessel orientated within. This was then allowed to fully freeze, before being transferred to a -80°C freezer until the cutting of the samples. Paraffin tissues were treated similarly, with tissues embedded in paraffin and orientated as paraffin set within cooled moulds. Abdominal aorta sections were always orientated in a manner where the area of interest was cut first; which for the Calcium Chloride model was renal artery proximal aorta to first cutting surface and bifurcation section distal to the cutting surface, the suprarenal

portion closest to the cutting surface in AngII preparations and descending thoracic aorta first within BAPN models. Sections for all models were then cut to between 8-12μm thickness and mounted on poly-l-lysine coated microscope slides.

Immunofluorescence and immunohistochemistry staining were both employed to investigate the presence and localization of proteins relevant to the AAA and AD pathology, as well as the arrangement and structural differences that were seen respectively. Aortic sections were mounted onto poly-lysine coated slides following sectioning from with either paraffin or OCT frozen sections. Following mounting, sections were cleaned of mounting medium by washing or paraffin removal techniques. This consisted of washing the slides in PBS or the performing of antigen retrieval by heating methods. Following this, cells were then permeabilised with 250μl of 0.1% Triton in PBS for 3 minutes before washing in clean PBS. Blocking then occurred to minimize non-specific binding of antibodies, this was performed by incubating samples for 4 hours with blocking solution (5% BSA in PBS), followed by application of relevant antibodies for each protein being identified, enough to cover the sample. Slides were then placed within a humidified chamber and placed at 4 degrees overnight. The following day, slides were washed for 3 x 5mins in PBS, before incubation with the relevant secondary antibody for each protein. Secondary antibodies, specific to the species primary antibodies were raised in, were conjugated to a fluorophore so that antibody binding could be visualized and separately distinguished in double-stained samples. Secondary antibodies were incubated at room temperature for 90 minutes. Sections were also stained with DAPI in order to stain nuclear content for a further 10 minutes following the secondary stain. This was the final step prior to a wash and application of a coverslip to each section. Slides that had been covered were stored within a dark box prior to imaging on the EVOS microscope. 3 sections were applied

to each slide with one section being guarded from Antibodies for control purposes; this was used to set control exposure settings on the EVOS and to account for autofluorescence. Images were taken on the EVOS system with control levels set for all image settings for each objective used.

Immunohistochemistry techniques utilized included H&E, Sirus Red and Elastin staining. Slides were processed, sectioned and sectioning medium removed similarly to in immunofluorescence staining. Following these steps kits were used to stain for proteins and structures in accordance with information booklets provided. Following the completion of each staining protocol, slides were imaged using the GXM L3201 fluorescence microscope and camera. Structures were visualised and settings adjusted manually, with consistent image settings used throughout imaging.

Within elastin staining, quantification was utilised to determine the changes in the lamina arrangement with changes in distances between layers measured as a marker of degradation and medial damage. Using the GXM L3201 fluorescence microscope and camera, slides were analysed with micrometry performed on each slide to quantify the measurement from the inner to the outermost layer of elastin. These measurements were recorded both on-screen within the slide image, as well as recorded within an excel spreadsheet for statistical analysis.

3.12 STATISTICAL ANALYSIS

Statistical analysis was performed with the use of GraphPad Prism 7 software. All individual data-points were collated and subject to appropriate stats tests, based upon the sample size, data type and comparative groups. Assessment of distribution was assessed by the D'Agostino-Pearson omnibus K2 test. Where necessary statistical correction tests were also performed in order to get the most accurate p-value possible, where this is the case it will be stated within figure legends. A p-value of <0.05 was

considered to be significant in all test apart from proteomics data where a higher level of significance was used as a further cut off for identification of novel proteins implicated within the changes to pathological phenotype.

RESULTS

4 EFFECT MODELS OF AAA HAVE ON GENE EXPRESSION WITHIN CELL CULTURE

In order to examine the cellular processes induced during pathologies such as AAA, cell culture is utilized within many studies. Gene and protein expression within particular cell types relevant to the pathology being studied, in this instance SMCs, Endothelial and Macrophage cells. Application of AAA-inducing treatments similar to that utilized within AAA animal models can yield new information on the changes to expression levels in response to the stimuli within the different cell types. The two predominant animal models of AAA are the Ang II and $CaCl_2$ models, these were therefore mimicked *in vitro.*

Calcium Chloride application to the aorta *In Vivo* leads to the calcification and degradation of the structural integrity of the vessel. Consequentially, this produces an aneurysm within the area of application. Many cells are involved within this process, with known depletion of vascular smooth muscle cells, infiltration of macrophages and changes in protein expression within the endothelium. Resultantly, these cell types were looked at to elicit whether they expressed markers of aneurysm, namely MMPs, as well as Neutrophil Elastase (NE), in order to establish the main cell line responsible for producing the AAA phenotype and whether any relationship was present with NE.

Angiotensin II perfusion is another common technique used to study AAA, where Ang II-associated increases in blood pressure result in the eventual expansion of the aorta over a period of 4 weeks. This expansion of the aorta can occur at various locations *In Vivo. In Vitro,* Ang II has been used to mimic the model in order to look into protein expression changes at the cellular level. Ang II was used to verify results

seen within $CaCl_2$ experiments, ensuring that results were representative of the AAA phenotype rather than a result of model-specific changes.

The same cell lines were studied both sets of *In Vitro* work. Cell lines studied consisted of human Smooth Muscle Cells (hSMCs), Human Umbilical Vein Endothelial Cells (HuVECs) and a mouse monocyte/ macrophage cell line (Raw 264.7). These were chosen due to their high similarity to cell types affected in the AAA pathology.

4.1 Materials and Methods

Please refer to Chapter 3.1 for the materials and methods utilized within the following results chapter.

4.1 Results

4.1.1 Neutrophil Elastase is up-regulated by exposure to Angiotensin II and high concentrations of Calcium Chloride in hSMCs, Raw264.7 and HuVEC cells

Figure 5 showed that neutrophil elastase was upregulated in all cells in response to AngII, with sharp rises in expression following exposure for 4 hours or greater. The magnitude and timing of this expression change was cell type-dependent. HuVEC cells had the latest rise in NE expression, peaking at 2 days of exposure in all groups (**Figure 5A**). In contrast, Raw264.7 cells (**Figure 5B**) and hSMCs (**Figure 5C**) took far less time, with peaks seen at 4 hours and 1 day respectively, before NE expression dropped back down closer to basal levels. Similar trends were seen in cells response to $CaCl_2$ with Raw264.7 cells, having a premature peak in NE expression in comparison to other cell lines (**Figure 5E**). Highest concentrations of $CaCl_2$, the concentration used within *In Vivo* experiments, produced consistently higher levels of NE expression across the

majority of time points. Largest increases were observed within HuVEC (**Figure 5F**) and hSMC (**Figure 5D**) cell lines within both sets of experiments.

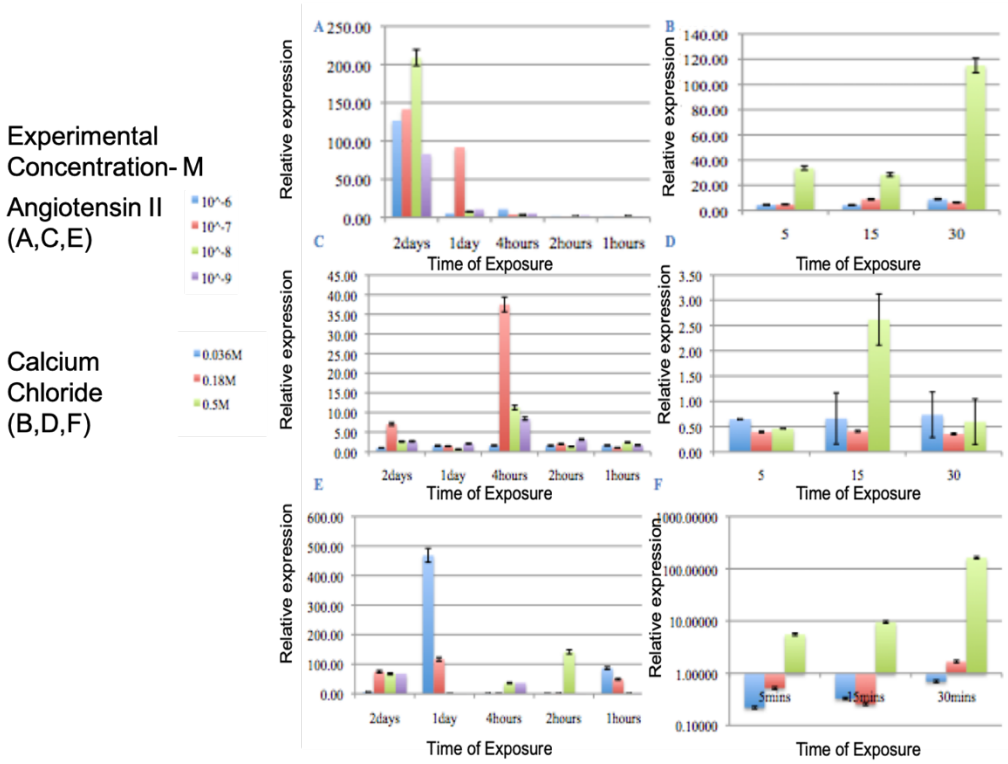

Figure 5- *Expression of Neutrophil Elastase across three cell lines at various time points and in response to the indicated concentrations (M/L) of Ang II (A,C,E) and CaCL2 (B,D,F), respectively. (n=3) A. HuVEC cells following AngII treatment (P>0.05), B. Raw264.7 cells following AngII treatment (P>0.05), C. hSMC cells following AngII treatment (P>0.05), D. hSMC following $CaCl_2$ treatment (P>0.05), E. Raw264.7cells following $CaCl_2$ treatment (P>0.05), and F. HuVEC cells following treatment by $CaCl_2$ (P>0.05). Note: the gene expression levels of cells with respective control (vehicle) treatments were normalised to 1.0 and error bars set as +/- 1 S.D. ANOVA statistical testing with Bonferroni correction for multiple analyses was used within the analysis of this series of experiments*

4.1.2 Exposure of Angiotensin II and $CaCl_2$ up-regulate expression of MMP-9 in hSMC and HuVEC cell lines

MMP-9 was induced after prolonged exposure to AngII within both HuVEC and hSMC cell lines. Angiotensin II experiments caused a gradual rise in MMP-9 expression in both cell lines, with minimal change in expression in the first hours of exposure, rising at day one and hour 4 in hSMC (**Figure 6A**) and HuVEC (**Figure 6B**) cell lines respectively. Overall, Peak expression was seen at day 2.

On the other hand, cells with short term of $CaCl_2$ exposure produced marked increases in express of MMP-9 within the 0.5M groups, while the expression levels decreased below control when low concentrations (0.036M and 0.18M) were used within HuVEC cell lines. More specifically, $CaCl_2$ experiments showed a stepwise expression pattern, increases in both duration of exposure and concentration caused marked augmentation to MMP-9 levels (**Figure 6C and 6D**). Highest expression was seen in the highest $CaCl_2$ at all time points. All groups showed increases in MMP-9 level with extended incubation with $CaCl_2$, this suggests both a dose a time dependance to MMP-9 expression.

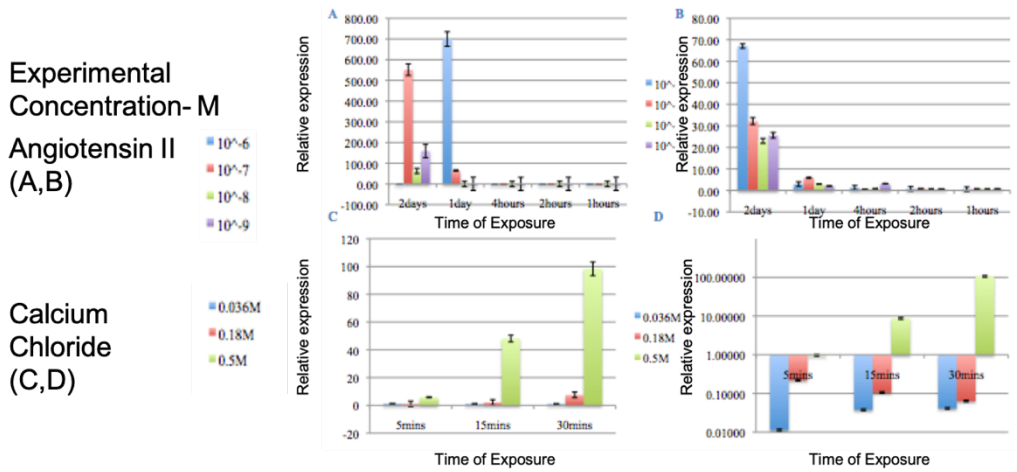

***Figure 6**- Expression of Matrix Metalloproteinase 9 in hSMCs and HuVECs, in response to varying concentrations of AngII and $CaCl_2$ during a timecourse of experiments (n=3). A. hSMC and AngII (P>0.05), B. HuVEC and AngII (P>0.05), C. hSMC and $CaCl_2$ (P>0.05) and D. HuVEC and $CaCl_2$ (P>0.05). Note: the gene expression levels of cells with respective control (vehicle) treatments were set as 1.0 and error bars set as +/- 1 S.D. ANOVA statistical testing was used within the analysis of this series of experiments*

4.1.3 MMP-2 expression is up-regulated in response to Calcium Chloride and Angiotensin II exposure

MMP-2 expression was augmented within all AngII experiments and displayed a dose and time-dependent expression pattern in two out of three $CaCl_2$ experiments.

An increased level of MMP-2 expression in all three cell lines treated with different concentrations of Ang II was observed at Day2, however, peak expression varied between cell lines (**Figure 7A-7C**). In general, peak expression was observed at day 2, day 1 and 4 hours for HuVEC (**Figure 7A**), hSMC (**Figure 7B**) and Raw264.7 cells (**Figure 7C**), respectively. Small increases were observed at other time points within the majority of concentrations studied.

$CaCl_2$ experiments demonstrated similar expression trends to that of MMP-9 within MMP-2. HuVEC cells decreased in MMP-2 expression in all tested conditions (**Figure 7F**), similar to the MMP9 expression observed in HuVECs treated with the lower two concentrations (0.036M and 0.18M) (**Figure 7D**). In hSMC (**Figure 7D**) and Raw264.7 (**Figure 7E**) cell lines, highest expression levels were seen within the highest concentration groups at each time point, and augmentation of time produced further increases in MMP-2 expression. MMP-2 expression appears dose and time-dependent within hSMC and Raw 264.7 cells in response to $CaCl_2$, however, HuVEC cells appear to be suppressed in their production under the same conditions.

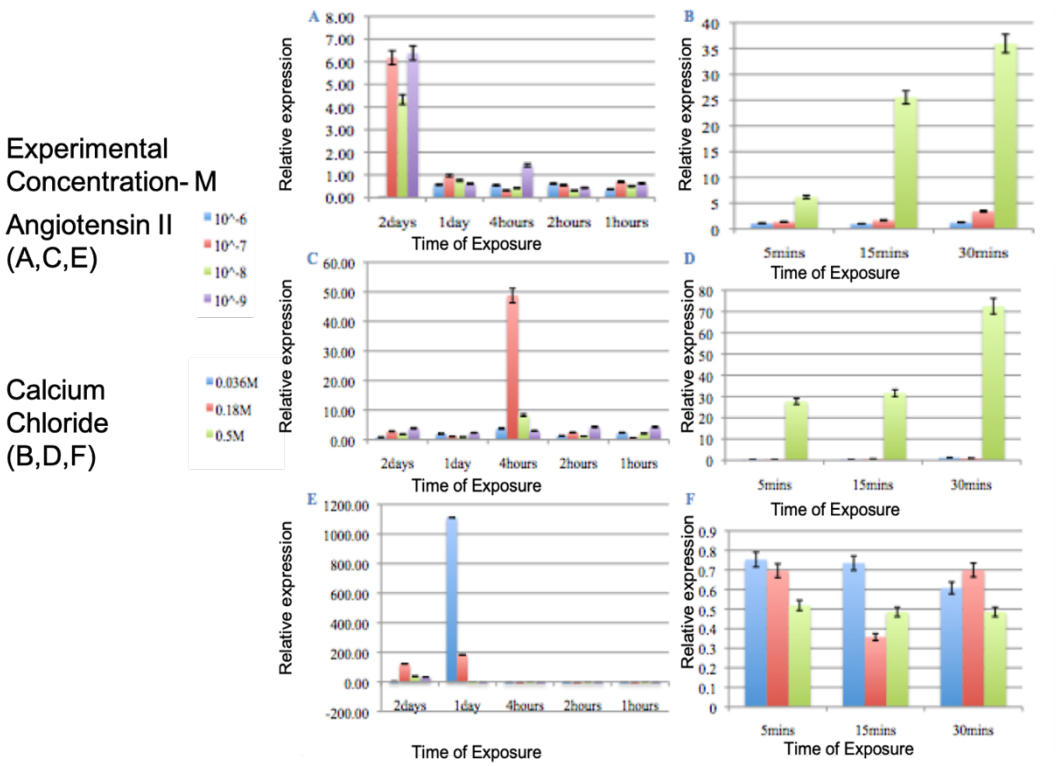

Figure 7*- Expression of Matrix Metalloproteinase-2 across three cell lines at various time points and in response to different concentrations of inflammatory stimuli (n=3). A. HuVEC cells following AngII treatment (P>0.05), B. Raw264.7 cells following AngII treatment (P>0.05), C. hSMC cells following AngII treatment (P>0.05), D. hSMC following $CaCl_2$ treatment (P>0.05), E. Raw264.7cells following $CaCl_2$ treatment (P>0.05), and F. HuVEC cells following treatment by $CaCl_2$ (P>0.05). Note: the gene expression levels of cells with respective control (vehicle) treatments were set as 1.0 and error bars set as +/- 1 S.D ANOVA statistical testing was used within the analysis of this series of experiments.*

4.2 Discussion

Results for all *In Vitro* work produced insignificant results, largely due to the high variability of expression. No significant conclusions can be drawn from these results. ANOVA testing was performed on all groupsets to determine if there were distinct differences between them, a P-value of<0.05 was not reached within any testing. A Kruskal-Wallace test would also be appropriate given the type of data and quantity, however, ANOVA is used more widely in the literature.

In-Vitro exposure to $CaCl_2$ was varied as to best assess which duration caused expression most akin to that of the aneurysmal phenotype seen within animal models. *In-Vivo*, exposure has been reported to range from 6 to 15 minutes. Resultantly, similar time-points were trialled, as well as longer durations of exposure in order to mimic the chronic pathology AAA. Exposure to $CaCl_2$ was trialled up to and including the same timeframe as the AngII model, however, from a study of the literature, we decided that having a model previously performed and more akin to the *In Vivo* model would be of greater benefit to our study.

In-Vitro exposure to Angiotensin II (AngII), is a much more well-established protocol and therefore less variation in conditions were needed to be trialled. Current literature was followed as a guideline of appropriate concentrations for use within experimentation.

A time course of the varying effects differing concentrations has on expression of the relevant genes was carried out in both models. Utilising RT-qPCR, modulations in the gene expression were determined and compared.

NE, MMP-2 and MMP-9 mRNA was detected within all cell lines, this follows on from publications supporting the production of these molecules in a variety of cell types, and modulated by $CaCl_2$ and AngII treatment. From the data collected, it is not possible to determine whether NE has any regulatory role within the expression of MMP-2 and -9. However, with that being said the level of enzymatic activity or protein expression has not been detected and is a significant limitation within this study. Consequentially, this could be considered as an area of potential development within future cell culture experiments of this nature. Performing Western blot analysis or immunofluorescent staining upon treated cells would be some of the potential methods by which this could be achieved.

4.3 CONCLUSION

In Vitro experiments based upon animal models are inconclusive and have not been able to determine a relation between NE and MMP expression, which is as yet not investigated within the AAA pathology. This was attempted to be studied within three cell types, with all gene-expression varied across time-points and concentrations of stimulant utilized. Further work is needed to elicit the full extent of this relationship and also its functional impact on the AAA pathology *In Vivo.* The next rounds of experimentation will address these issues in an attempt to address our primary aims and objectives.

4.4. LIMITATIONS

As mentioned briefly above in chapter 4.3, whilst efforts were made to identify the relation between NE and MMPs relevant to the AAA pathology, no successful conclusions were able to be drawn. As also identified above, further work is needed to overcome the limitations of this study, taking the initial work beyond gene expression analysis and onto analysis of protein levels within the same cell types. Further, the cells being utilised need to undergo greater levels of checks prior to utilisation for the experimentation. Whilst cell viability and health were checked by eye, under the microscope, further work needs to be carried out to verify cell state, such as senescence and cell viability to ensure the differences in the treatments and cell type have no significant impact on the cell number or health of the cells used within experimentation. In conclusion, there are a number of steps that should be taken within future experiments to ensure the full relationship between NE and MMP can be assessed.

Beyond this, the cell types utilised within this study may be improved upon, with the origin of cells selected improved upon. Currently used HUVEC cells could be replaced by endothelial cells of aortic origin, similarly Raw 264.7 cells which are a Abelson

leukaemia virus transformed cell line derived from BALB/c mice and therefore alternatives may be more appropriate for the study of AAA. For instance, alternative cells used within the study of AAA and appropriate for usage here are THP-1 cells for studies focussed on human AAA. Furthermore, during this study HUVEC cells were derived from a single isolation and subsequent passages of cells and therefore whilst separate experiments were undertaken, the true N number for HUVEC experiments is and N of 1 due to the same original source, this may explain the extremely tight standard deviations observed.

5 MRI SCANNING PROTOCOL DEVELOPMENT- CRITICAL ANALYSIS OF NEW TECHNIQUE COMPARED TO ULTRASOUND

Abdominal Aortic Aneurysm (AAA) is one of the leading contributors to death in the western world, with 4-5% of men over 65 being affected by the condition. Relatively little is known about the underlying mechanism, and therefore further study is needed to elicit the cause and pathways contributing to the disease. Currently, Ultrasound (US) is considered the frontline technique for monitoring *In Vivo* progression of AAA within both Humans and animal models. However, multiple limitations exist with US scanning of small aortas. This work aims to study an alternative scanning protocol that produces a more comprehensive understanding of the vascular changes throughout animal models. To do this we will be utilizing low field Magnetic Resonance Imaging (MRI), in order to determine whether more reproducible and detailed surveillance of changes within the aorta can be achieved when compared to the current gold standard.

Using a 1T MRI Scanner, Gd-albumin blood-pool agent and semi-automated processing, reproducible volumetric measurements of the infrarenal aorta and identification of AAA were obtained in 10 mice infused with angiotensin II for four weeks. Compared to US

scanning, MRI scanning provided a much clearer image, more accurate measurement of small infra-renal aortas with higher reproducibility, and discovered a higher incidence of AAA. Importantly, volumetric measurements of aortas is only possible with MRI scanning, which is a key determinant for predicting AAA rupture, representing a potential new gold standard for AAA prognosis.

Monitoring of the AAA Pathology and other similar aortic abnormalities can be achieved utilising this protocol, yielding an enriched dataset in comparison to the most commonly utilised US.

As previously mentioned, Abdominal Aortic Aneurysm (AAA) is the focal dilatation of the Aorta. Predominantly situated in the infra-renal segment(1), AAA is a localised weakening of the vessel wall which makes it prone to rupture(2). This pathology has a high mortality rate as a result and affects 4-5% of males globally and a smaller proportion of females in the 65 years old and above population also(3). The incidence of AAA is increased with Coronary Artery Disease (CAD)(4), family history and smoking(4), amongst others.

The pathological characteristics of AAA include collagen and elastin dysregulation(8), chronic inflammation(9), smooth muscle apoptosis(10) and breakdown of the extracellular matrix in the surrounding areas of vasculature(11). The alterations lead to the expansion of the vessel beyond that of the normal aorta, sequentially weakening the vessel and consequentially increase the probability of aortic rupture, and mortality at the same time. Resultantly, screening programmes have been put in place in order to discover rapidly expanding vessels early, in order to minimise the chances of death. In line with the

introduction of screening programmes, death rates as a consequence of AAA have fallen in the UK(179). From such studies, the identification of numerous factors influencing the probability of rupture has become apparent, these include the aneurysmal maximum diameter, aneurysmal volume, location and gender(180,181). Some of these variables were already known to be risk factors for the AAA pathology, however, volume is an, at present, underutilised diagnostic tool. For the most part, current clinical practice relies upon the widely installed base of US scanners to identify patients that would benefit from higher resolution modalities such as CT or MRI. Consequently, translating factors as identified above by Tang et al(180). as well as Hatakeyama et al(182). into the clinics could result in improved diagnostic abilities with regards to risk of rupture. US is unable, at present, to implement these changes, with volumetric measurements beyond that of the capabilities of most US facilities, with limitations to simple diametric quantification, instead of the proposed volumetric change which is put forward as a potential new gold standard for AAA prognosis by Tang et al(180).

Magnetic Resonance Imaging (MRI) scanning is an alternate scanning method to US, that function by reconstructing a hydrogen signal that can be altered by scanning program parameters to give clear images of internal structures non-invasively. Optimisation of a scanning program can increase the clarity of specific tissue types, such as the usage of a blood-pool contrast agent. Within this study, we use such agents to highlight the aorta and the luminal changes that occur within it over time. Benefits and drawbacks of the utilisation of MRI in comparison to US are outlined later within the discussion of this paper.

The pathological characteristics of AAA, as mentioned above, lead to the production of a progressively expanding aneurysmal phenotype. One way to uncover such changes *in vivo*, non-invasively, is by molecular imaging. However, this requires the development of a suitable imaging agent and protocol. An example is the elastin binding MR imaging agent (ESMA)(181). Alternatively, anatomical imaging may be employed to visualise and quantify disease progression with the benefit of an easier implementation in other labs. This approach has been taken in this study.

Among the various anatomical imaging modalities, US scanning has been the preferred method for *in vivo* monitoring of AAA in preclinical research, and high field MRI studies have also been reported(183,184). US is currently the preferred method within the clinical setting due to its low cost and speed. These techniques enable tracking of macroscopic changes to the aorta, predominantly by quantifying the size of the lumen and alterations to the vessel wall path away from expected dimensions. Both modalities have been employed and adapted in this paper.

US is a common method of detection and tracking of mouse anatomy, where tissues such as smooth muscle and organs create different strength signals in scans in comparison to alternately composed substances e.g. blood. Advantages include; relatively low cost of the equipment and fast US scanning. Disadvantages are that (a) additional time is needed for preparation of fury mice, with US requiring shaving around the area of interest; (b) time is needed to find the probe angle for the least obstructed view of the aorta; (c) the field of view of a high-resolution ultrasound is relatively small and localised; (d) the data is easily

influenced by user technique i.e. suffers from inter-operator variability and thus lacks reproducibility between labs; (e) similarly, the data interpretation is performed by the operator which increases the chance of operational bias and misdiagnosis(185). Although such misdiagnosis could be minimised by verification of all scanning measurements by double measurement of each scan, utilising VevoLabs software, an improved alternative imaging technique is urgently needed in order to achieve more objective, reproducible and detailed surveillance of changes within the aorta over weeks, or even longer within the clinical setting.

In this chapter, we present the use of low-cost imaging modalities US and 1 T MRI with commercially available contrast agent to scan and monitor the aorta in AAA mouse models, which is directly translatable to the clinical setting. Comparison between 3D US and MRI imaging is beyond the scope of this paper. 3D US scanning is a relatively new technology with huge potential(186), however, comparatively few facilities currently posses such scanning capabilities. Aneurysms are visualized and their anatomical changes over time quantified via MRI images by custom-built semi-automated analysis. Use of analysis outlined in this paper could lead to improved surveillance of AAA patients and increase the predictability of AAA rupture.

5.1 METHODS

5.1.1 Animal Husbandry

Animals were housed according to the parameters set out within the materials and method chapter above (Chapter 3.2).

5.1.2 AngII-induced AAA

To model the AAA phenotype 8-week old ApoE$^{-/-}$ mice of mixed gender underwent AngII, dissolved in saline, infusion using Alzet Osmotic Pumps (Charles River) to infuse 1.44mg/kg/day (Sigma) for 28 days. Pumps were implanted subdermally into the dorsal neck region, under sterile surgical conditions. Mice were placed under anaesthesia by isoflurane carried in oxygen. The small incision is closed by discontinuous suture using 3.0 Vicryl. Following surgery, mice were individually housed and returned to chow diet and water ad libitum for the duration of experiments. Sham animal procedures had been carried out previously, and expansion of the aorta deemed negligible over the same time-course. Animals were weighed prior to pump implantation and at weekly intervals during the procedure, loss of weight was seen in response to AngII and no correlation between weight and aortic size was observed.

5.1.3 Ultrasound Scanning

Ultrasound was performed weekly, with baseline measurements being taken prior to pump implantation and continuing throughout the duration of the experiments, totalling 5 US scans per mouse. Mice were sedated by gaseous anaesthesia, isoflurane vaporised in oxygen as a carrier. Following sedation, all mice had all hair on their stomach removed by hair-removal cream (Veet) before being placed on a heated ultrasound platform. Paws were taped down to sensor pads to monitor heartbeat throughout the experiments. Pre-warmed ultrasound gel was then applied to the newly-bald area before the ultrasound probe (MX550D, VisualSonics) was mounted and placed over the animal's abdomen. The Vevo 3100 was used to perform all ultrasound scans and analysed with VevoLabs analysis software. Measurements were taken in both longitudinal and cross-

sectional planes within the Infrarenal portion of the aorta within each mouse. Diametric changes were quantified in the cross-sectional plane in a Catherine wheel-like fashion to account for non-uniform expansion of the vessel (see **Figure 2**). These were then compared to control scans for percentage expansion measurements.

5.1.4 MRI Scanning

MRI scanning was performed once before pump implantation (baseline) and once after pump removal and recovery from surgery, typically 2-3 days after the last US scan. The chosen pump model was not MRI compatible and therefore had to be removed before MRI scanning after AAA induction. Note: MRI compatible versions of Alzet pumps are not commercially available but in principle can be produced by replacing the steel rod regulator with plastic tubing. However, we believe that validation would be required that this modification does not interfere with pump flow rates and this study was simplified by using the original pumps instead. For each MRI scan, the mouse, average weight of 27g, was sedated by isoflurane in oxygen, injected into a lateral tail vein with 85 µl of Gd-Albumin (20 mg/mL, BioPAL USA, diluted with saline) and immediately placed on the MRI bed (Bruker BioSpin MRI, Germany) equipped with isoflurane anaesthesia, water-heating, respiration monitoring, controlled to 30-40 bpm (SA Instruments, USA), and solenoid whole-body RF coil. The bed was then inserted into the 1 T permanent magnet (Aspect Imaging, Israel) coupled to the ICON MRI console controlled by Paravision 6.0 software (Bruker). After scanner preparations, a fast low angle shot (FLASH) based localizer was acquired, a 3D scan volume placed over the whole abdominal area, and a T1 weighted 3D FLASH image acquired with echo time 4 ms, repetition time 30.6 ms, flip angle 40°, 8 dummy scans, image size 76x100x58 pixels, field of view 23.8x30x17.5 mm, isotropic 0.3 mm voxels, total

acquisition time ca. 10 min 36 secs. Scans were prospectively respiration gated to avoid motion artefacts and improve image quality.

Use of 1T MRI scanning equipment limited the resolution of images produced, however, imaging was optimised to provide sufficient quality reconstructions so aortic volume could be accurately and reproducibly measured. Contrast increased the accuracy of this protocol as lumen boundaries were much more distinct, in comparison to pre-contrast scans. Alternative scanning setting were also tested to find the best settings for scanning. Contrast consistently increased clarity and precision of scans and subsequent measurements,

The reconstructed MRI images (Paravision) were analysed in two steps in VivoQuant (Invicro, USA). First, data were preprocessed by a custom-written script performing bias field correction[17] (iterative Otsu with downsampling factor 2, max. iteration 50x50x50, converging threshold 0.5, control points 2x2x3, spline order 3) and image reorientation. Then, the infrarenal aorta was manually segmented into transaxial 2D slices between the lower renal artery and the bifurcation of the aorta into the femoral arteries. This dataset consists of 53 total slices compared to USs single slice, with a fixed smaller region of interest being selected. Resultantly this allowed for continuity between scans and controls for difference in aortic size at different parts of the aortic tree.

5.2 RESULTS

5.2.1 Gd-Albumin Increases clarity of scans and improves the accuracy of scan interpretation

The use of vascular contrast agent Gadolinium labelled albumin increased the clarity of the vessel lumen by increasing the signal in blood-rich areas. As seen in

Figure 8 initial scans produced obscure and vague outlines of the aorta lumen, however with the introduction of this blood pool contrast this was rectified and more typical clear lumen demarcations were evident. With the use of Gd-Albumin precise quantification of the infrarenal aorta became possible, and the possibility of signal gated readings becomes possible. No side effects were evident from the use of contrast reagents within any experimental procedure performed. No adverse effects are commonly noted within the literature on this subject either, thus making the procedure relatively safe and similar in severity of US scanning techniques.

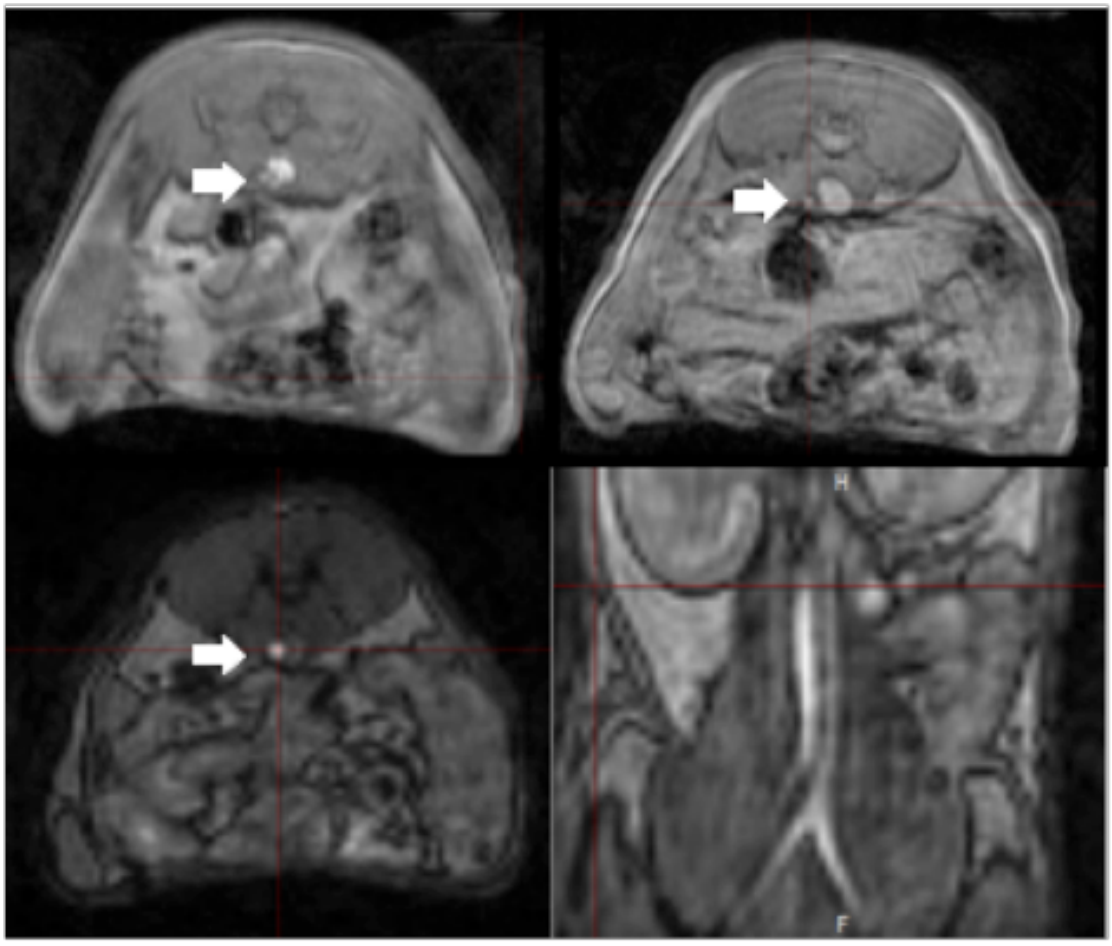

***Figure 8**- Representative images of imaging optimization, with each image showing the development of the protocol as outlines of the aorta become clearer (sequentially from Top*

to Bottom and Left to Right. White Arrows indicate the Aorta in each cross-sectional image, with original images obtained from VivoQuant analysis software.

5.2.2 Ang II infusion produces a significant expansion in abdominal aorta measured quantitatively by ultrasound and MRI

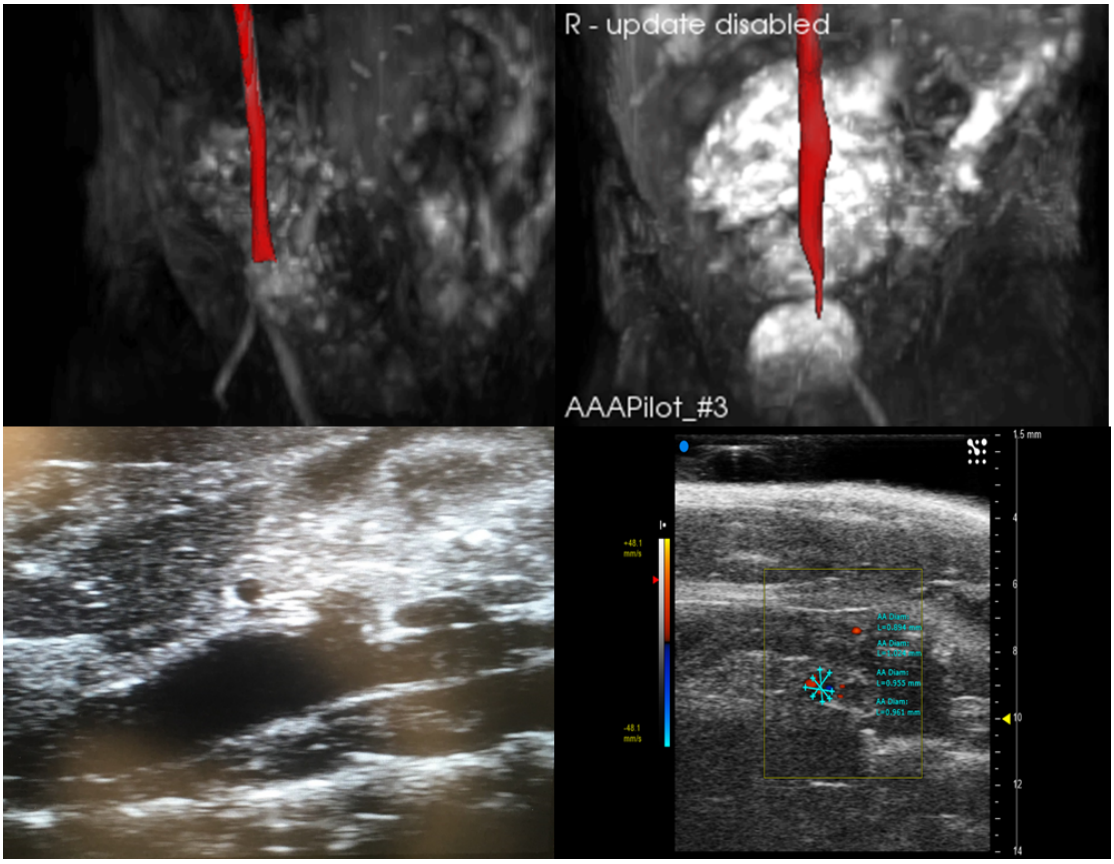

***Figure 9**- Composite image of MRI and US typical images. Top left, typical 3D reconstruction image for pre-AngII scan. Top left and right, typical 3D reconstruction image of the same mouse for pre- and post-AngII. Bottom left, Longitudinal aortic US scan with aneurysm in the 3rd week of AngII infusion. Bottom right, Cross-sectional US scan with Catherine wheel measurement, displaying the technique of diameter measurement used.*

A total of 10 mice underwent MRI scans of their aorta, all of which consequentially received AngII infusion of 1.44mg/kg/day for 28 days before undergoing a second scan. All 10 mice showed a marked increase in infrarenal volume, following similar trends to that of US scans. Aneurysmal enlargements within scan analysis

were detected by comparison to each respective baseline control scan. Use of contrast reagents enabled easy identification of the aorta and production of ROI's. The scanning technique was sensitive enough to pick up relatively small changes within the aorta, making it appropriate for use within the study of AAA. All animals showed to have expansion of the aorta, not all had aneurysms as defined by an increase of 50% in infrarenal aorta diameter measured by US and aorta dissection (see **Table 4 and Figure 9**).

Table 4- Summative Table of Results following the implementation of the Ang II procedure. Comparison of monitoring using all modalities possible, namely MRI in both 2D and 3D as well as post-mortem dissection to confirm diagnoses.

	Aneurysm	Rupture	No Aneurysm
Dissection	7	1	2
MRI- Average Infrarenal 3D Volume Percentage Expansion	140% (7 aneurysms detected by MRI scanning)	N/A	118% (2 volumes fell below 20% expansion threshold)
US- Average Aortic Diameter Increase	199.92% (5 Aneurysms detected by US scanning)	N/A	131.51% (4 below 150% expansion threshold)
MRI- 2D Average Aortic Diameter Increase	169.83% (6 Aneurysms detected by 2D MRI scanning)	N/A	118.62% (3 below 150% expansion threshold)

5.2.3 Use of MRI scanning can produce 3D reconstructions of the abdominal aorta and subsequent aneurysms

Following MRI, scans are performed and processed in VivoQuant. This software can automatically produce a maximum intensity projection (MIP) in 3D of the selected scan area (**Figure 9** top panels). Within each scan, you are able to view results within 3 planes as well as how this relates to the 3D MIP. By selecting ROIs

you are also able to highlight relevant areas within both sectional scans and 3D MIP reconstructions. This functionality allows for measurements of the Infrarenal aorta in both 2D and 3D. Both direct measurements of aortic diameter are possible, as well as volumetric measurements of the same vessel.

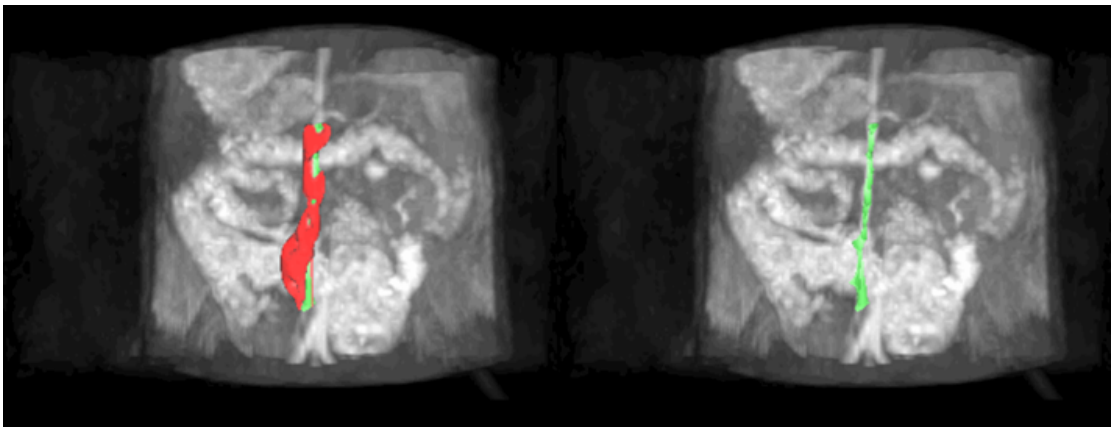

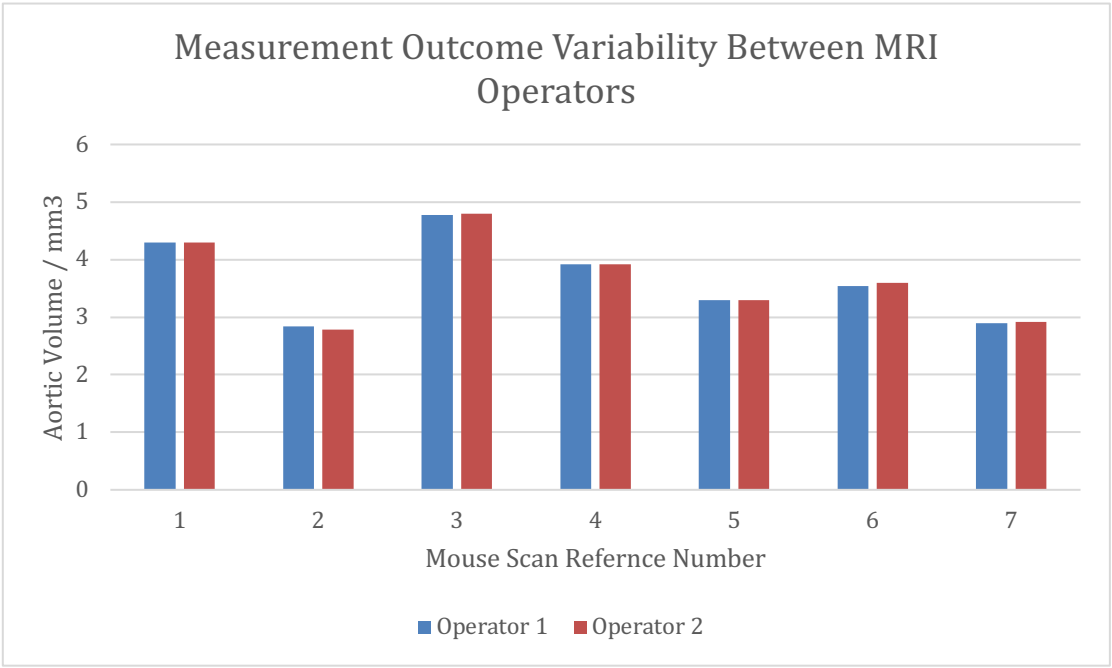

Figure 10*- Top- Images depicting how Otsu's iteration analysis can outline and quantify the aorta in a semi-automated fashion following basic user training. Red indicates the freehand operator-defined potential aortic area. Green indicates the true aortic region as determined and optimized by Otsu's iteration analysis. Bottom- Inter-operative variability highlighting similarities between datasets (P= 0.3602, paired two tailed t-test)*

5.2.4 Semi-automated format of MRI post optimisation allows for low-level training to scan the aorta

Minimally trained researchers were able to perform MRI scanning and achieve sufficient quality outcomes as induction. Training on how to set basic parameters, such as; area of interest, wobble calibration, localiser and quantity of contrast reagent, was undertaken and following this independent operation of scanning was able to be achieved (**Figure 10**). Following on from this the processing of the MRI files and identification of the aorta within all subsequent scans were carried out. The interpretation of scans took place on a post-analysis computer, where further training took place for analysis. Again, this training was basic and largely comprised of anatomy and VivoQuant software training.

5.2.5 Proposed AAA definition for MRI scanning

By utilising our optimised MRI scanning protocol, aortic expansion after exposure to AngII for four weeks is easily identified (**Figure 12**). The average increase in infrarenal volume was 33% above that of baseline as measured by MRI scanning. Since the MRI analysis protocol measures infrarenal volume change, the current definition of an aneurysm is not compatible. Current guidelines define an AAA as "a vessel diameter 50% greater than expected or its previously determined size", this is incomparable to the measurements taken by the MRI as aneurysms occur in many forms, however, most are saccular or fusiform aneurysms, and therefore are limited to a relatively small region of the vessel. Resultantly, as the volumetric measurements are taken over a whole segment, only part of which is aneurysmal, the volume in many cases will not reach this 50% increase threshold. Consequently, 'the 50% increase threshold' cannot be used to define an AAA in the volumetric measurement by MRI, and the definition of an aneurysm will have to be reassessed when a vessel is quantified. Instead, we observed

an excellent agreement between the volumetric data measured by MRI and the final aortic dissection data. Importantly, based on the AAA incidence observed from aorta dissection, we could set a '20% increase of aortic volume' measured by MRI as a 'threshold' to define an AAA in MRI scanning, which results in 100% agreement between two methods (aorta dissection and MRI) in identifying AAA incidence. This threshold was determined by assessment of dissection and comparative analysis of accompanied scans. This value falls from traditional 50% cut-offs due to the length of the expansion and total infrarenal aorta being taken into account within this instance. In essence, as the whole infrarenal aorta is rarely effected and therefore would decrease the overall expansion percentage, this has been accounted for within the cut-off value. By utilising the 20% as a cut-off we are able to highlight incidences of significant remodelling, the protocol may later be updated to isolate solely the area of expansion however this level of sophistication is yet to be achieved(**Figure 11**) (**Table 4**).

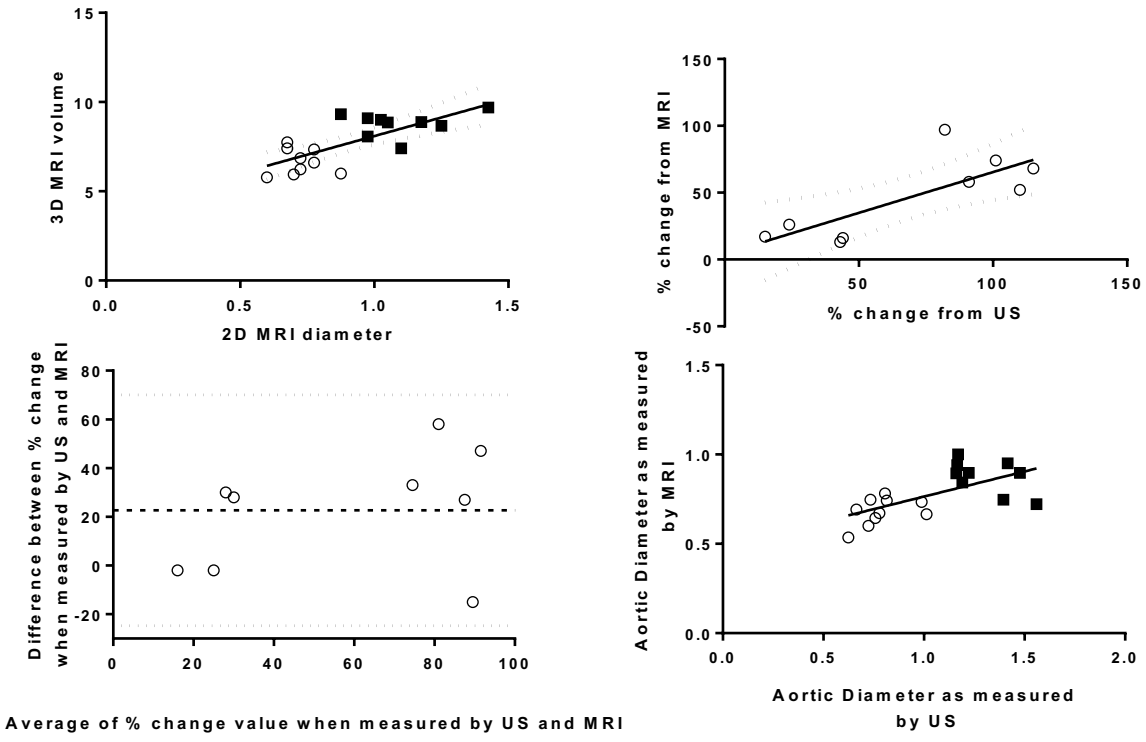

Figure 11- *Comparison of infrarenal aorta expansion (percentage) measured by US and MRI. Measurements for each mouse are given and comparison for each mouse within each form of measurement are presented. (Top Left) Correlation between 2D (mm) and 3D (mm^3) MRI measurements, with distinct Pre and Post- AngII exposure evident, r^2= 0.5467, P= 0.0005. (Top Right) Percentage change in aortic size, as measured volumetrically by MRI (mm^3) and diametrically by US (mm), r^2= 0.6003, P= 0.0142. (Bottom Left) Bland Altman plot displaying the relative difference between US and 3D MRI measurement percentage change. (Bottom Right) Comparative Graph of 2D Measurements performed by both MRI and US (mm), r^2= 0.6487, P= 0.0027.*

5.2.6 Measurements of aorta expansion by MRI and US are comparable

When comparing MRI and US measurements, the overall trend was similar, however, some discrepancies were seen between the two (**Figure 11**). Measurement units for each differed, with MRI involving volumetric measurements and therefore quantified in mm^3, in comparison to US diameter measurement quantified in mm. Resultantly, as the overall length of infrarenal aorta differs between animals it is hard to quantify how similar these two modalities are in their results. Consequently, percentage expansion was used to monitor the changing of the vessel from in both techniques. Data shown in **Figure 11-Top Right** revealed a good agreement between the two techniques was

observed.

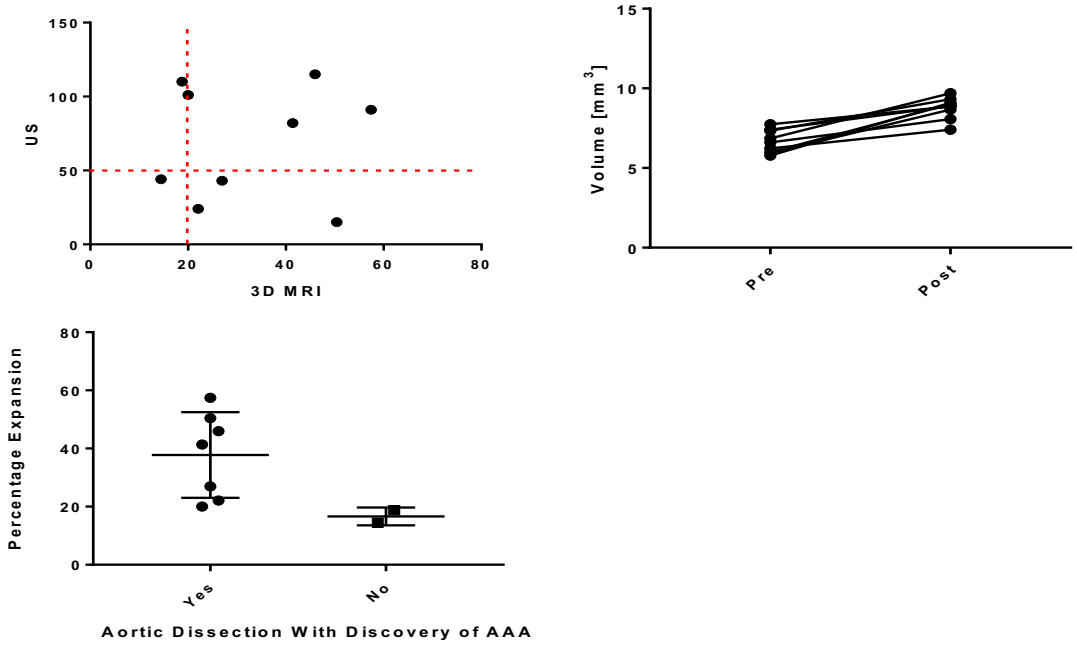

Figure 12*- Top left- Percentage Change of aortic diameter (US) and volume (3D MRI) respectively, with current 50% threshold for AAA marked for US and suggested 20% similarly for 3D MRI illustrated with a dotted red line. Top Right- Aortic Volume Measured by 3D MRI, with paired data change shown Pre and Post exposure to AngII. Bottom Left- Comparison of 3D MRI percentage expansion and dissection outcomes for presence of AAA. N=9 animals, scanned both before and after exposure to AngII for four weeks*

To verify one technique against the other, 2D sections from Infrarenal aortic scans were taken and measured for vessel expansion. These comparisons were performed on scans from the same mouse at the same time-point and within the same region, using biological landmarks for reference. Resultantly, 2D percentage measurements could be generated and compared across the two modalities. As is evident from the resulting graph, there are very similar trends seen across the two datasets (**Figure 11**). Classification of aneurysmal vessels by 2D measurements were improved (6 aneurysmal, 3 non-aneurysmal) with expansion trends within other vessels showing a similar trajectory. Overall, expansion rates were highly comparative between modalities. 3D analysis was used to further enhance the

dataset, giving greater information on the changes occurring to the vessel. As outlined earlier, volumetric changes could provide important information on rupture risk and therefore verification as to whether this is possible within a mouse model would be seen as a step forward for AAA monitoring.

Although largely good agreement between the two techniques was observed, a clear disagreement was also observed between them in term of the AAA incidence. Particularly, we observed one animal displayed a very high aorta expansion (>50% increase) measured by MRI, while exhibited a subtle change (<10% increase) measured by US. This could be due to either US operational error, missing the aneurysm and therefore the enlargement. Alternately, if this was a diffuse AAA, small changes to the diameter but prolonged areas of the vessel affected could increase the volume by a far higher percentage than the increase seen in diameter.

5.3 Discussion

Current clinical protocols of US are limited, and this update in MRI procedure may now allow for utilisation of low-field MRI to provide greater detail in a reproducible and affordable manner. Current scanning of the Infrarenal aorta may need to be adapted, with scan area extended to include suprarenal regions. This is possible by expanding the region of interest or performing a secondary scan for the alternate area. With a change in volume being an indicator of AAA rupture, with further study, we could determine a volume increase threshold by which

aneurysms are classified as at risk of rupture (180). This would be beneficial in the clinic as with semi-automated quantification, this could lead to basic preliminary diagnostic markers and prognosis indicators, similar to that seen with blood test biomarkers or ECG traces.

Moreover, if the volumetric measurement by MRI is to be utilised as a clinical or even research tool, quantification in both a 2D and 3D format could result in the most comprehensive analysis method, and by doing this allows for detection and monitoring of both diffuse and saccular enlargements of the vessel. Currently, if you were to use 'the 50% rather than the 20% expansion threshold', a large number of false-negative outcomes would be produced. It is possible that a redefined area could be used, post-secondary scanning, where retrospective measurement of a specific adjustable area within control scans and measurement of equivalent areas within follow-up scans takes place. This would only be possible within preclinical studies.

As mentioned above, there is the possibility for this protocol to be scaled up to the clinical setting. This work within small rodents, utilising a 1T MRI scanner, would be directly translatable to the clinical setting if an alternate contrast agent, approved for human use, could replace the Gd-Albumin bolus administered to each mouse. These agents are widely available and already in use within the clinical setting. Alternately, the use of RF pulses to generate contrast within more powerful MRI scanners could also produce similar results, a functionality not possible within the 1 T scanner utilised. Possibilities for this include other gadolinium-based agents as well as alternate albumin binding contrast agents, as exemplified within studies discussed by Habets et al.(187), however, alternate

lower molecular weight contrasts could be utilised as clearance within humans is much lower than rodents.

MRI produces images reconstructed from the hydrogen signal that is modulated by several effects (local hydrogen concentration, structure, T1 and T2 relaxation times, etc.) and several experimental parameters, such as magnetic field strength, pulse sequence, scan parameters e.g repetition and echo time, to name a few. Image contrast can be enhanced by the injection of a contrast agent. Advantages compared to US are that (a) with a given protocol (like a chosen set of pulse sequence parameter values) the acquisition is fairly user-independent and thus reproducible; (b) the positioning of the animal within the RF coil is relatively stable and has little influence on the image quality as long as the area of interest is approximately in the RF coil centre; (c) a larger area (even whole-body) can be imaged with high spatial resolution. Subsequent detailed image analysis can then extract robust measurements of AAAs. Disadvantages and our solutions to them are that (a) MRI systems and their maintenance are expensive, but a low cost 1 T MRI system can produce reliable and reproducible data, as outlined in this study. (b) Time and effort is required to optimise the imaging protocol, however, this is a one-off development effort with time being minimised by building upon already existing protocols. (c) Contrast agent may have to be administered, however, this was a simple intravenous injection minutes before image acquisition, we observed no side effects, and the cost was acceptable. Furthermore, if RF pulses were used to generate contrast in more powerful scanners, this would not be necessary. (d) Subjects need to be permitted to enter the magnetic field, however, in this study, the surgically inserted osmotic pumps for continuous release of Angiotensin-II

were not MRI compatible so MRI could only be done before pump insertion and after their removal. (e) Image acquisition is more time consuming than US scanning, although with optimisation of scans this time discrepancy is minimal and a richer data set is obtained. (f) Image analysis may be time-consuming and introduce operator variability. To address this final point, the design of a semi-automated process by which quantification of the aorta could occur quickly and easily with minimal training took place. VivoQuant (Invicro LLC, Boston) enabled the semi-automation of quantification steps, utilising the increase in signal in aortic areas, largely due to the contrast used. In order to implement gating thresholds, for the identification of the aorta, segmentation through image thresholding took place. This takes advantage of the grey levels within an image and is particularly good at differentiating an object from background. It is fast and computationally simple. Otsu's method, the method chosen to calculate the thresholding in this study, uses integration to find the global minimums(188). This means that Otsu's method could be used for unsupervised computation with no prior knowledge of grey levels of the object. This allows for a mathematical strict way to calculate the thresholding from a given histogram. Following this, there were no significant differences found between the sequential analysis of the same dataset by multiple operators, as depicted in **Figure 10**.

AAA are typically located in mice pararenal and in humans more specifically infrarenal aortic locations. Ultrasound is able to scan both areas of the aorta when adjusting the angle and orientation of the probe to avoid other tissues masking a clear view of the aorta. However, this adjustment can restrict the field of view such that small expansions like saccular aneurysms may be missed. This carries the risk

of incorrect AAA quantification and even misdiagnosis. Another limitation of US is that the orientation of the acquired images varies somewhat for each individual scan in the same subject. Thus, surveillance scans over time compare slightly different views of the aorta. This makes the diagnosis less precise and more subtle changes may be invisible. Observed changes in vessel size may be an artefact, producing a false positive, caused by the limited reproducibility of scans. Similarly, the aorta diameter can change rapidly along the blood vessel even within healthy mice, or generally in diffuse aneurysms also in humans. Moving the US probe along the aorta by few millimeters then has a significant impact on the measured aorta diameter. The result of each scan is hence associated with a considerable error in such cases. Resultantly, MRI gives an alternative, solving a number of the previously mentioned operational errors that can occur. MRI gives you a rich 3D dataset, this can give all quantitative US data values, with additional information about the surrounding regions of the vasculature and changes in the form of the overall vessel being captured.

Alternate scanning methods that could produce similar datasets were considered, such as Computed Tomography (CT). However, MRI is superior to CT for soft tissue imaging and (unlike CT) produces the images using non-ionising radiation(185). Large areas of the mouse can be imaged in a single scan, allowing better understanding of the effects of AAA models on the full organ system, as well as giving anatomical references that will aid definition of the aorta in the mouse. MRI also allows high-resolution imaging and small structures, such as the aorta, and potential aneurysms are distinguishable on a low field MRI.

5.4 Conclusion

Ultimately, this technique allows users to monitor aneurysms in an unbiased and reproducible manner, with the use of relatively low-field MRI technology, making it a new option within the study of AAA and other such diseases.

Quantitative imaging with low-field MRI is now possible for study of vessels as small as a mouse aorta. Changes as small as a fraction of a millimetre are detectable with the use of a blood-pool agent. There is the potential for this technique to be scaled-up into clinical use. Using this method and low-powered setup, far more in-depth study of the aorta could occur, with lower levels of training and equipment experience needed. Data generated is of superior reliability and accuracy, than that of currently utilised 2D ultrasound data, as quantification area is much more tightly controlled and therefore all scans and measurements can be taken in precisely the same region. 3D reconstruction of the aorta, as well as multi-plane viewing options, furthermore gives you a visual representation of the whole vessel in comparison to cross-sectional images provided by US. With this added information, improved scanning and quantification of each vessel and its changing morphology could contribute to improved diagnosis for potentially lethal events, most notably AAA rupture.

6 NE DEFICIENCY IS PROTECTIVE AGAINST AAA INDUCTION BY CALCIUM CHLORIDE

AAA is an aortic pathology that affects a significant portion of the population, largely of the male and ageing demographic, with large studies reporting 4-5% of males

affected, a figure that can increases to around 8% of men over 65 according to alternate studies(189). The most commonly affected region of the aorta within the human condition is the infrarenal aorta, with expansion occurring between the renal arteries and femoral bifurcation. A number of animal models were used to model the pathology of AAA, however, the $CaCl_2$ model of AAA procedure is one of the most specific in terms of regionality. Within the protocol, $CaCl_2$ is applied directly to the adventitia of the vessel, with this applied area being selectively affected by consequent changes. The application of $CaCl_2$ leads to localized triggering of inflammation by the activation of MMPs via divalent cationic activation. The activation of MMPs leads to cleavage of extracellular matrix proteins such as collagen and elastin, the cleaved bi-products cause inflammatory cell recruitment and activation whilst MMPs alternate effects on transcription factors such as NFkB as well as the activation and release of pro-inflammatory cytokines which again(190), in turn, promotes the inflammatory environment causing the destruction and degradation of the vessel wall. One significant benefit of this model is the localization of the inflammation, mimicking the human pathology unlike the Ang II model, which causes systemic changes to the animal in order to produce a less localized but more aggressive aneurysm phenotype. Whilst both have their place in AAA research, it could be argued that they represent different phases of the pathology, with the $CaCl_2$ model mimicking the chronic stable phase that is the predominant phenotype seen within AAA monitoring and investigations. As a result, this model does not result in rupture, and there have not been any reported cases of rupture being the cause of death within this procedure when used alone, however, when used in combination with an elastase or collagenase infusion rupture has been reported. The $CaCl_2$ model has been championed and most extensively carried out by the lab of Dr J Golledge. This has led to extensive progression within the understanding of the

AAA field. Large advances in the understanding of inflammatory markers, structural remodelling and specific cellular involvement within the development of AAA have been thanks to the use of the $CaCl_2$ model.

This round of experimentation will produce a deeper understanding of NEs role within both the initiation of AAA, as well as the chronic inflammatory stable phase of the pathology. NE already has a known role within NET formation and a role of NETosis within AAA has been put forward; suggesting NE will play a role within the overall pathology. However as yet, this role is undefined, and its influence is even less clear. Beyond AAA NE is known as a driver of pathology within COPD, with functionality in the degradation of elastin and destruction of the lung and consequentially the potential for NE to play a similar role within AAA is high. Furthermore, NE already has a known role within atherosclerosis, with knockout of the enzyme by pharmacological and genetic means inhibiting experimental induction of atherosclerosis(167). Particular attention will be paid to the changes to the structural changes that are produced between Control and NE knockout mice, as this is the area in which NEs known functions are predicted to have the greatest degree of influence.

6.1 Material and Methods:

Please refer to Material and Methods chapter previously for an in-depth overview of general materials and methods utilized in this round of research.

6.1.1 Calcium Chloride Model of Aneurysm

A Pilot study comparing Wild type ($ApoE^{-/-}/NE^{+/+}$) to NE Knockout ($ApoE^{-/-}/NE^{-/-}$) mice subjected to $CaCl_2$ induced-AAA procedures was carried out as previously described by Wang et al. (84). Briefly, $CaCl_2$ was administered at 0.5M for 2x7mins (Sigma Aldrich), under general anaesthetic (gaseous isoflurane), directly to the aorta within the Infrarenal portion of the aorta halfway between the renal arteries and femoral

bifurcation, as seen in **Figure 13**. Measurements of this area were taken, by abdominal Ultrasound scanning technique, prior to surgery and repeated at various time-points following the operation to monitor the expansion of the vessel over time. The use of Ultrasound minimises the number of animals used, in accordance with the 3Rs.

A follow-up study comparing the same two groups of mice, undergoing the same treatment was carried out. Initial Infrarenal measurements were made using Magnetic Resonance Imaging (MRI) in place of Ultrasound and repeated biweekly to monitor the changes in the aorta. At week 6 all animals were finally scanned, before being culled and dissected for analysis of tissues.

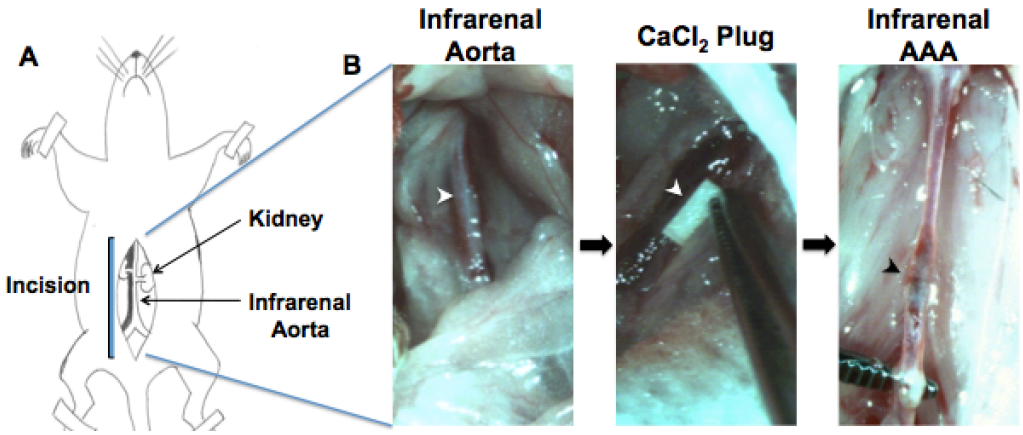

***Figure 13**- Schematic of the Calcium Chloride model of aneurysm procedure, outlining the various steps of surgery and the end result. A- Sketch of mouse orientation and region effected within the procedure. B- Step-wise time points from isolation- application- dissection of the infrarenal aorta. White arrows indicate area of calcium chloride application, Black arrow indicates the same area and identification of AAA*

6.2 RESULTS

6.2.1 MRI monitoring of Calcium Chloride Model of AAA shows altered expansion trends with NE Knockout and Control Mice

The $CaCl_2$ Model was employed and monitored in a time-course fashion over the 6-week time period that the protocol lasts. Mice were scanned in accordance with scanning protocol in the 2 days prior to the commencement of the $CaCl_2$ model. Following on from this time point, mice underwent the procedure and were scanned bi-weekly. This enabled the identification of the specific time point at which the vessel underwent the greatest level of change. As we can see from scanning, the rate at which the vessel diameter expands significantly increases after the 4^{th} week of the procedures induction. Within the first month, there is low-level changes to the vessel and gradual expansion before a more significant and exaggerated change at the 4-week stage. This trend was replicated within both experimental groups, with NE knockout mice rising earlier however not reaching the same peak at week 6 when compared to the Control group.

Whilst the infrarenal (IR) volume of the aorta was similar between the two groups at week 0 of experimentation, this was not the case following AAA induction with the NE knockout group expanding on average at a quicker rate than Controls. However, from the week 4 point onwards Control mice experience a later rise in aortic diameter increase with the gap between the two experimental groups growing drastically from week 4 to 6. Expansion of the IR volume was almost three times greater within the Control group when compared to the NE knockout group. An increase of 0.3 mm^3 was witnessed within the NE Knockout group as opposed to 0.92 mm^3 seen in Control groups, this average expansion was an increase of 9% and 29.4% respectively. However

no significant difference was observed between the two groups when compared (**Figure 14**). Comparatively, the incidence of AAA was shown to significantly differ between the same two groups (**Figure 15**).

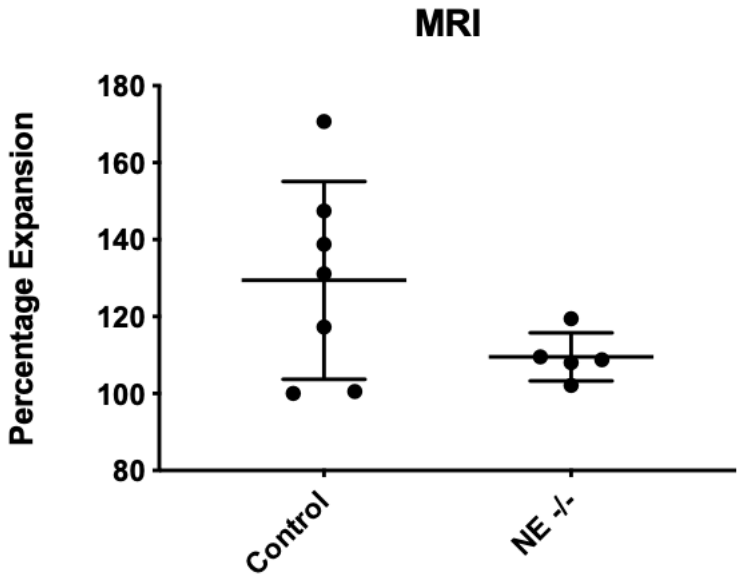

***Figure 14**- Comparison of percentage aortic expansion within $CaCl_2$ treated mice of the WT Control genotype and NE Knockout genotype (P=0.0988, Unpaired t-test, error bars display +/- 1 S.D, Largest Horizontal bar represents the mean percentage expansion in each group N=7 WT Control and N=5 NE-/-)*

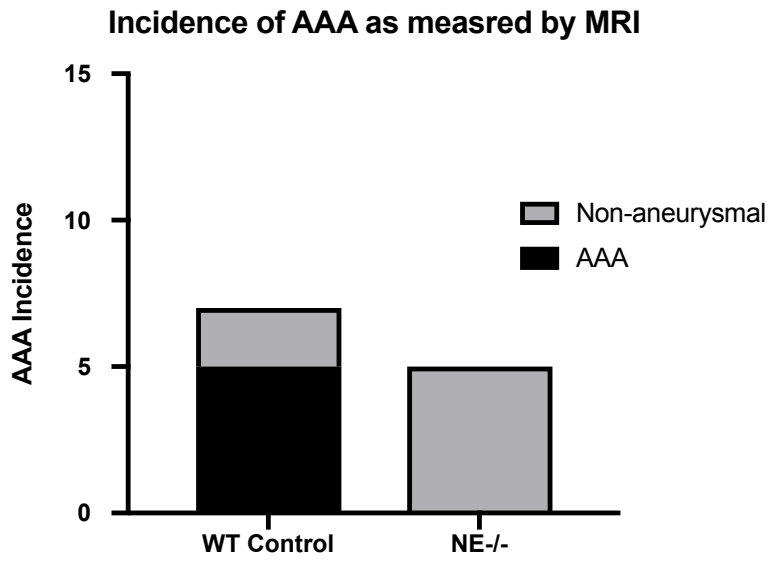

Figure 15*- Incidence of aneurysm following $CaCl_2$ treatment as measured and determined by MRI analysis of all animals, comparing aortic scans at week 0 and week 6 of aneurysm protocol. WT Control- 5 out of 7, NE-/- - 0 out of 5 (P=0.0278, Fishers Exact Test)*

6.2.2 Ultrasound analysis of the aorta verified results seen with MRI, with larger increases in aortic diameter seen within Control mice compared to NE knockout mice

Similarly to MRI analysis, US scanning was performed in the days prior to the $CaCl_2$ model being carried out. Following the procedure, scans were performed biweekly with images taken in many ultrasound-scanning modes and saved for future analysis. This enabled the identification of both functional and structural changes in the vessel over the time course. Diametric quantification by means of US is the current clinical guideline for diagnosis and director of management for AAA. US results displayed expansion was present within both Control and NE knockout groups, however, the rise seen within Control mice was on average four times that seen within NE Knockout mice. Average expansion of 0.10mm and 0.41mm were quantified within NE Knockout

and Control mice respectively, with measurements being taken within the same scanning period and analyzed in a blinded fashion to minimize any operator bias. This expansion was equivalent to 14.4% expansion of the aorta in NE Knockout mice and 51.5% within WT Controls (**Figure 16)**.

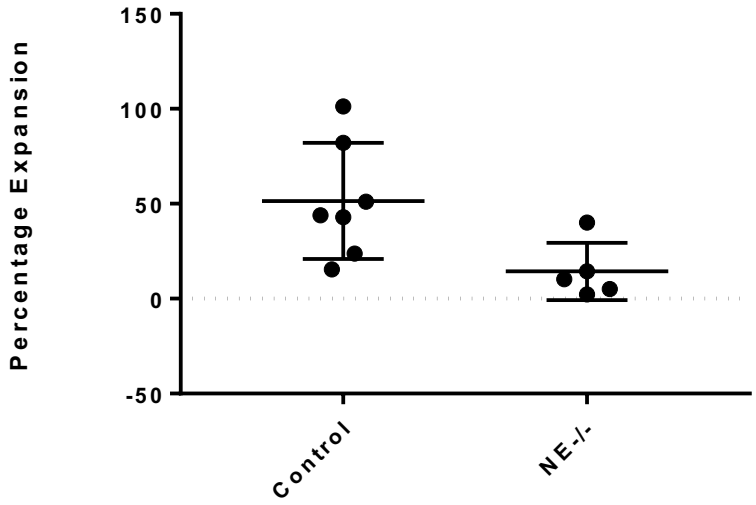

Figure 16*- Percentage Expansion of mouse aortas following US scanning at week 0 and week 6 of $CaCl_2$ treatment. Largest Horizontal bar represents the mean percentage expansion in each group (P=0.0324, Mean +/- 1 S.D, Unpaired t-test N= Control- 7, NE-/- -5)*

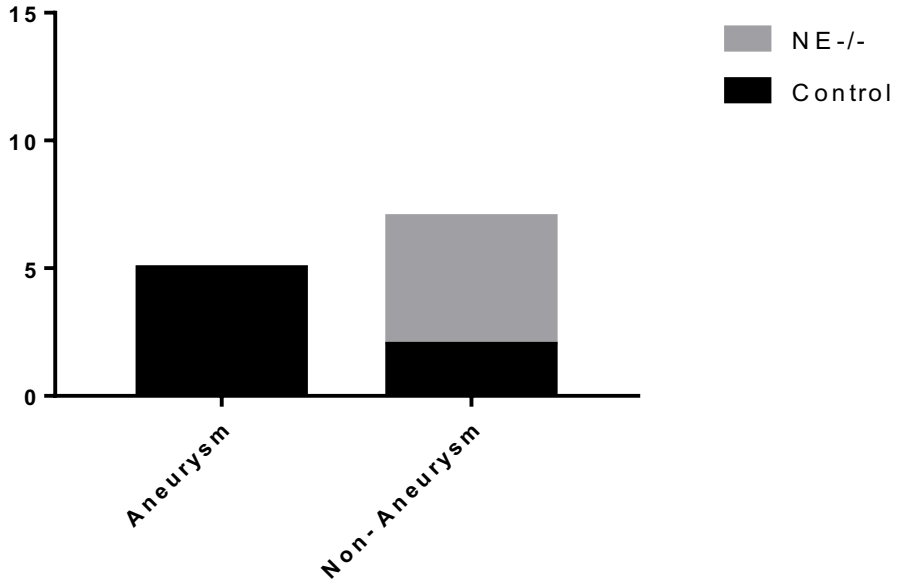

***Figure 17**- Incidence of AAA as determined by US scanning techniques at week 0 and week 6 of $CaCl_2$ treatment. Largest Horizontal bar represents the mean percentage expansion in each group (P=0.0278, Fishers Exact Test, N= Control- 7, NE-/- - 5)*

6.2.3 Aortic pulsatility change was not significantly different between Control and NE knockout mice 6 weeks post-application of Calcium Chloride

During scans at week 0 and final scans at week 6, the vessel's pulsatility was assessed, with the pulsatility being determined by tracking the movement of the aortic wall within the heartbeat cycle at both instances. M mode traces of each scan were assessed using VevoLabs analysis software, with video traces of the infrarenal aortic wall enabling quantification by tracking maximum and minimum diameters and calculating results from these measurements. Within the two groups, there were significant increases in pulsatility within the Control group, with all animals pulsatility increasing across the 6-week period. This was not the case within NE Knockout mice with some mice displaying a decrease in the same characteristic (**Figure 18**), however generally this measurement also increased across the time period similar to that of Control mice. Although predominantly an increase was found within both cohorts the difference observed within Control group was far greater than those of the NE knockout animals. NE Knockout mice only increased negligibly, 3.3%, whereas Control mice increased by 43.9%.

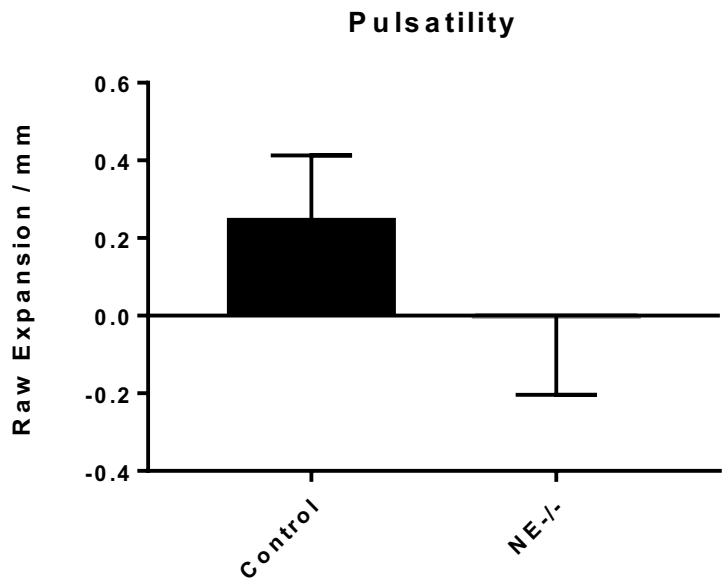

Figure 18*- Changes in Pulsatility of vessels following $CaCl_2$ treatment (P=0.588, unpaired t-test, mean +/- 1 S.D, N= Control- 7, NE-/- - 5). Each aorta was measured at maximum expansion and minimum contraction over 3 heartbeat cycles whilst mice were under sedation to a specific heart rate range and temperature.*

6.2.4 Dissection of Control and NE Knockout mice replicate findings of both MRI and US modalities, with expansion seen more prominently within Control animals.

Following the completion of the 6-week $CaCl_2$ protocol, all mice were culled via Schedule 1 methods. Following this, mice were immediately grossly dissected with the vasculature isolated and removed from the carcass. Removed vasculature was then finely dissected, with images taken.

Within dissections, the infrarenal region of the vessel was the most remodelled portion, with evidence of the direct and localized application of $CaCl_2$ to the exterior of the vessel obvious within many vessels. Expansions were seen in Control mouse vessels in the mid infrarenal aorta, however, no similar expansions were seen within the NE Knockout mice. The predominant effect of the $CaCl_2$ procedure was the observed change in luminal path which was evident under closer inspection and easier to

visualize whilst blood was still present within the vessel. This was seen as an expansion in a highly localized area of the aorta, as seen in **Figure 19**.

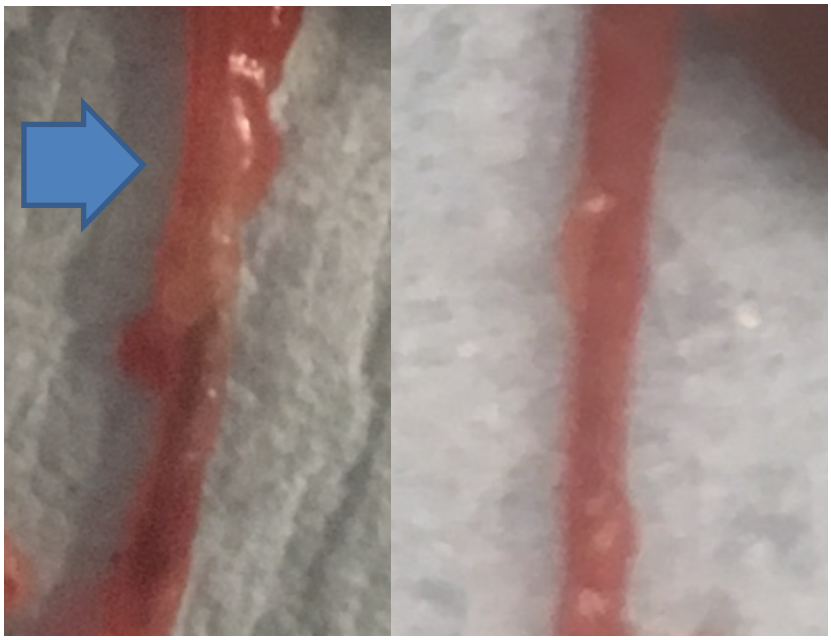

***Figure 19**- Representative differences in aortic morphology as displayed by dissection images. WT Control mice had observed expansions in the region of $CaCl_2$ application (Left, blue arrow indicating a region of expansion), whereas no significant increases were seen within the same infrarenal portion of NE Knockout mice (Right)*

No mice showed any signs of expansion or vessel remodelling in regions not treated with $CaCl_2$, with all vessels displaying a clean, uniform and continuous vessel wall in shape and cellular appearance when inspected under a microscope.

6.2.5 RNA analysis of dissected aortas display differential expression of MMPs within NE Knockout mice

Tissues generated from the Calcium Chloride procedure were taken, following fine dissection, for utilization within RNA analysis. RNA analysis allows for a snapshot of gene expression changes within tissues that have undergone different treatments or in

this instance when of differing genotypes in response to the same treatment. In order to preserve the RNA within tissues, all fine dissection occurred immediately, and each respective dissected aorta snap-frozen prior to processing.

Consequent RNA analysis by qPCR outlined clear differences and similarities in the expression of particular cell types, proteins and enzymes. Observations included the significant loss of MMP2 in line with NE ($p<0.05$) (**Figure 20**), in comparison to expression of MMP8 where there was no significant, changed seen across the aortas isolated (N=3 per group). Similarly, markers for endothelial cells (CD144) were also found to be comparable between Control and NE Knockout groups.

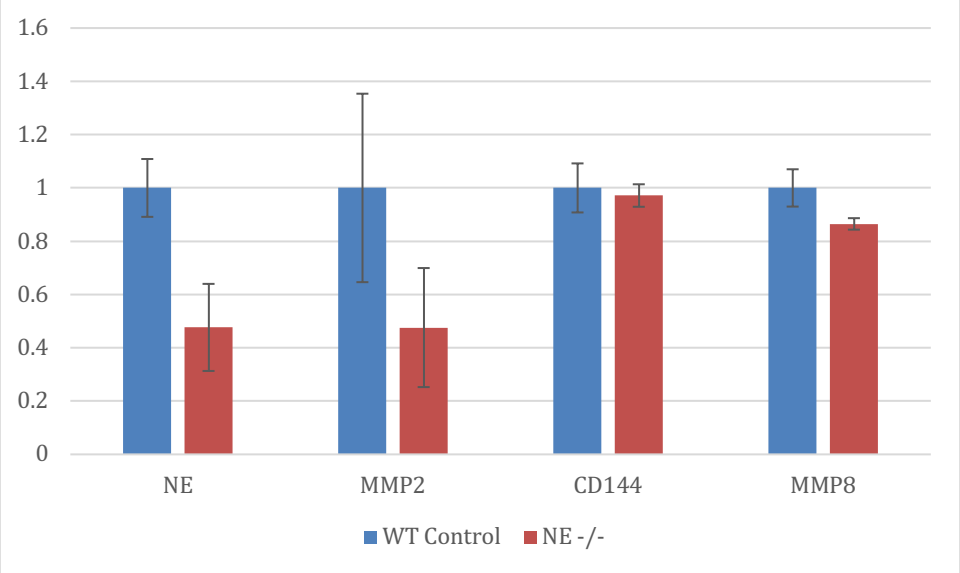

***Figure 20**-RNA analysis results of q-PCR from WT Control and NE Knockout Aortas following $CaCl_2$ treatment at week 6 of the protocol. NE, MMP2 and MMP8 have observable reductions in levels between the WT and NE-/- groups, whereas CD144 shows no change. N=3 per group, mean +/- 1 S.D*

6.3 Discussion and Limitations

Throughout this Chapter, studies to elicit whether NE contributes to the AAA pathology and how it takes its effect was undertaken. Consistently within experiments, there is evidence to suggest NE may play a role within the production of AAA within the $CaCl_2$ model, as changes in expansion and incidence rates within AAA models indicate.

However, due to the number of animals utilised within this study remains relatively low, these outcomes are preliminary and require validation by increase in the N number. Furthermore, changes in RNA analysis results between the two groups point towards MMP difference being influential, suggesting a link between NE and MMPs, possibly similar to that discussed within the COPD condition. Again, further investigation is needed to understand the full impact of NE and the mechanisms by which NE produces an effect due to a limited number of repetitions. The observed effect is dissimilar to a pilot study which utilized the elastase model of AAA-induction(142), however considering the use of an elastase to replace another elastase, I feel this is not surprising, and with further study, the argument for that paper to be disregarded will be strengthened. Beyond this, inhibition of NE has previously been observed to decrease the levels of circulating cholesterol within animal studies(167). Consequently, reduced levels of circulating cholesterol, reduced inhibition of cholesterol efflux from macrophages and consequent decreased levels of atherosclerosis and inflammation would have a beneficial impact on AAA incidence and could explain the outlined decrease in pathology incidence.

Although some evidence to suggest a role within AAA was identified, serious limitations of some experimentation exists. With reference to qPCR results outlined within **Figure 20**, the detection of NE was unexpected, as all mice were subject to repeated genotyping. This could imply the jeopardization of sterility and consequent contamination. The insertion of the neomycin selection cassette into exon 2 has historically led to no protein expression, this was confirmed with no evidence of significant NE staining within relevant NE knockout samples and genotyping of mice at birth. Verification of this should however be carried out in order to reassess the

source of NE material prior to the acceptance of results stemming from this specific aspect of experimentation.

Further to this, the results discussed above within this chapter require validation and an improved understanding of the mechanism by which the potential effects are occurring. For instance, there is a definite need for further clarification of the effect brought about by loss of NE within this AAA model. Techniques such as histological staining are needed to be undertaken prior to concrete conclusions being made.

6.4 CONCLUSION

Throughout this chapter, we have started to understand the role of NE within AAA. Experiments in some instances did not reach significance. These prelininary results suggest inhibition of NE is protective against the induction of AAA. RNA analysis of end-stage tissue led to the observation of a reduction in MMP expression with loss of NE, this could be a potential mechanism by which loss of NE exerts its effect. Further work is therefore required to verify these results with the use of an alternate model of AAA.

7- NE GENE INACTIVATION IS PROTECTIVE AGAINST INDUCTION OF AAA BY ANGIOTENSIN II

Whilst previous experimentation has eluded to NEs role within AAA, both within *in vitro* and *in vivo*, confirmation with a further animal model that is considered the most comprehensive is required before definitive conclusions are drawn. Currently both cell culture experiments and the calcium chloride model point towards NE playing a significant role within the modulation of AAA-associated markers and generation of AAA itself.

The Angiotensin II model of AAA is a widely used procedure, previously unused within our laboratory group. Ang II is infused via an osmotic pump, over a 28-day period, positioned within the sub-dermal pouch of the rodent. Early on in this time period, the infusion of the agent causes activation of the AT1a receptor and consequential significant increase in blood pressure of the animal; this is a commonly observed risk factor for AAA and occurs within the first few days with results lasting the duration of the time course. Over the next month, vascular remodelling occurs within the recipient animals. Included in this remodelling is cardiac hypertrophy and, of most interest in this investigation, aneurysms. Aneurysms- the enlargement of a vessel by 50% or greater beyond that of a healthy vessel, can be witnessed in as much a 70% of animals undergoing 28-days of Ang II infusion, dependent upon operator. The location of these enlargements most commonly occur in the suprarenal or thoracic portion of the aorta, however, they can bridge the renal arteries and form a fusiform aneurysm in severe instances. With the expansion of the vessel come a number of risk factors for mortality, these include both aortic dissection and rupture. Aortic Dissection is the splitting of the

vessels intima away from the medial and adventitial portion of the vessel resulting in the production of a false lumen. Aortic Rupture has even further complications, where the luminal contents break through the weakened and expanded vessel wall. Rupture results in death in approximately 80% of cases where the sufferer is not already in medical care. These expansions and changes can be a result of changes in flow within the vessel, as well as inflammatory cell infiltration and degradation of the vessel wall. All of these factors have known roles within the initiation and progression of AAA and are present within the tissues generated from the Ang II model. NE may have roles within some of these processes and potential to impact the pathology, with already reported roles of NE within the cleavage of ECM proteins. Resultantly, use of the Ang II model of AAA upon a NE knockout background could elicit further information that aids in unravelling the AAA initiation and development process or even provide a drugs target for the pathology.

This model differs from the previously utilized $CaCl_2$ model, with the model mimicking a different phase and severity of aneurysm. Whilst the $CaCl_2$ model replicates the stable chronic phase of the condition, the Ang II model produces the more acute dissection and rupture-prone phase of the pathology. As a result, the results are occasionally dissimilar if the aspect being investigated is relevant only within a particular phase of the process. However, both models have the ability to produce significant advancements in the understanding of the mechanisms underlying AAA.

Following similar AAA studies that utilized the Ang II model procedure, the field has moved on hugely. The role of MMPs and TIMPs in AAA were outlined by utilization of this model, as well as inflammatory signalling mechanisms such as Toll-like Receptors, micro RNAs involvement within AAA and even drug trials for inhibition of AAA before progression to human trials. Resultantly, this can be viewed as a gold

standard within the field for mimicking the disease and consequentially should yield the largest insight into the role of NE within the pathology, in turn answering one of our main hypothesis. Predominantly this round of experimentation is aimed to answer the research question of how is NE implicated within AAA. This will be addressed by the use of genetic knockout of NE within the animal model, as well as the use of subsequent tissues generated to look at the changes in further proteins with the use of histological staining and RNA analysis.

7.1 Material and Methods:

For detailed information on the Materials and Methods utilized within these chapters experiments, please refer to the Materials and Methods chapter above.

7.1.1Proteomics analysis

Proteomics analysis was performed to elicit and identify underlying mechanisms of any changes seen within the aneurysm model experiments. As NE is an enzyme produced predominantly by circulating blood cells, cells that can cross into the vasculature, the enzyme can interact with a number of cell-types and therefore has a wide scope for potential influence. Resultantly we employed a fractional extraction of the proteins to narrow down the areas in which NE was exerting its effects. Following in the footsteps of Didangelos et al. (11), the aortic tree of mice treated with AngII for 14 days, administered by osmotic pumps, was finely dissected before being processed. Two groups of mice were administered the same AngII treatment over the same time period, with Control Mice and NE knockout mice undergoing experimentation. Following treatment of mice with AngII and fine dissection of the aortic tree, the vessel was finely diced and placed into separate cryovials for fractional protein separation, in accordance with the Didangelos protocol(11). This protocol separates the sample into three protein subsets, with the three portions consisting of; loosely bound novelly synthesized

proteins, intracellular protein content and finally, extracellular matrix proteins. NE has the possibility to influence all three of the fractions, with results providing the basis for further experimentation to verify the results and their effects on the AAA phenotype.

Following the isolation of the three protein fractions, these are taken for proteomic mass spectrometry analysis. Protein samples were run on a self-made 10% acrylamide gel and stained by Coomassie blue staining to reveal all protein bands. This separates the proteins from the extraction buffers, removing impurities from the samples. Each protein lane was then cut and placed within sterile Eppendorf vials, before trypsinisation to remove the proteins from the gel. Following separation from the gel, proteins were dissolved in 10mM Urea and 0.05% SDS/ ammonium bicarbonate at pH 8, samples were then incubated for an hour at 50degrees. Following this, iodoacetamide was added and incubated for a further hour, at 21degrees. This left samples reduced and alkylated. Samples were then diluted to 1.2M urea/ 0.01% SDS. Trypsin was added to this mixture at a 1:50 ratio before overnight incubation at 37degrees. Mixtures were consequently dried in a SpeedVac, removing volatile salts and later re-dissolved in 100µl of 0.1% AcN/formic acid. Protein solutions were separated using an ABI 140C HPLC binary pump, with an SCX column. Elution gradient was 0%B to 20%B in 30mins and 20% to 100% B in 22mins. A consisted of 25% AcN/0.1% formic acid, with B 500mM KCl, dissolved within A at 20µl/min, with collection of fractions occurring at each minute. Reversed-phase liquid chromatography electrospray tandem mass spectrometry was subsequently undertaken.

Peptides present in the protein elution fraction were separated by nanoLC and sequenced using online tools (ESI-MS/MS). Eluted peptides were detected and sequenced by Q-tof equipment (Waters, Micromass, Manchester, UK) with a nanoESI ion source. MS/MS processing of all spectra was carried out using MassLynx software.

This produced the peak list, used to identify the proteins present. This was identified using the NCBI murine database. Mascot software (Matrix Science, UK) alongside Daemon software (Matrix Science). Results were then imported into an Excel spreadsheet for interpretation, this was considered significant when a Mascot score was greater than 25, in accordance to the method utilised within papers such as Naba et al. (191) . Mascot scores are used similarly to P-values, in the sense that they are used as a measure of likelihood that the result of the reading occurred by chance. A cut-off of 25 is used in this instance to have a high threshold by which the protein reading must improve upon in order to be considered as significant. This score is relative to how well the assessed ion MS/MS spectrum relates to the stated peptide it is being compared against. Through the use of a 25 cut off the level of false-positive results significantly falls. Identified proteins within the searches were then used to direct further works, such as western blot and histological analysis of AAA model samples.

7.2 RESULTS

7.2.1 Blood Pressure changes following Ang II administration was comparable between groups

The mechanism by which Ang II exerts its predominant effect of raising blood pressure in order to produce hypertension and latterly AAA is via the AT1a receptor. Other side effects of Ang II exposure exist and can impact the AAA pathology to a lesser extent, however, these are of less importance within this study as the AT1a receptor is widely accepted as the predominant mechanism of AAA causing hypertension within this model. Monitoring blood pressure change was imperative as the relation between NE and blood pressure regulation is currently unknown. Consequentially any alterations to the AAA phenotype seen with NE knockout mice could be a result of inhibition of

blood pressure by NE, compared to an actual role in inhibition of the pathological process and phenotype formation.

Tail-cuff blood pressure monitoring methodology was utilized, with 10 repeat measurements taken daily on 3 days in a week, before being averaged, removing outlying or interrupted readings. This procedure was repeated both the week before Ang II pump insertion, as well as during the second week of Ang II exposure. As is evident within the Graph below, significant increases in both systolic and diastolic blood pressure were recorded within both Control and NE knockout mice. Blood pressure increases were highly comparable between the Control and NE Knockout groups, with no significant difference was seen at any stage. Initial blood pressure values were minimally lower within the NE knockout cohort, however, failure to produce any significant difference between the NE knockout and control groups.

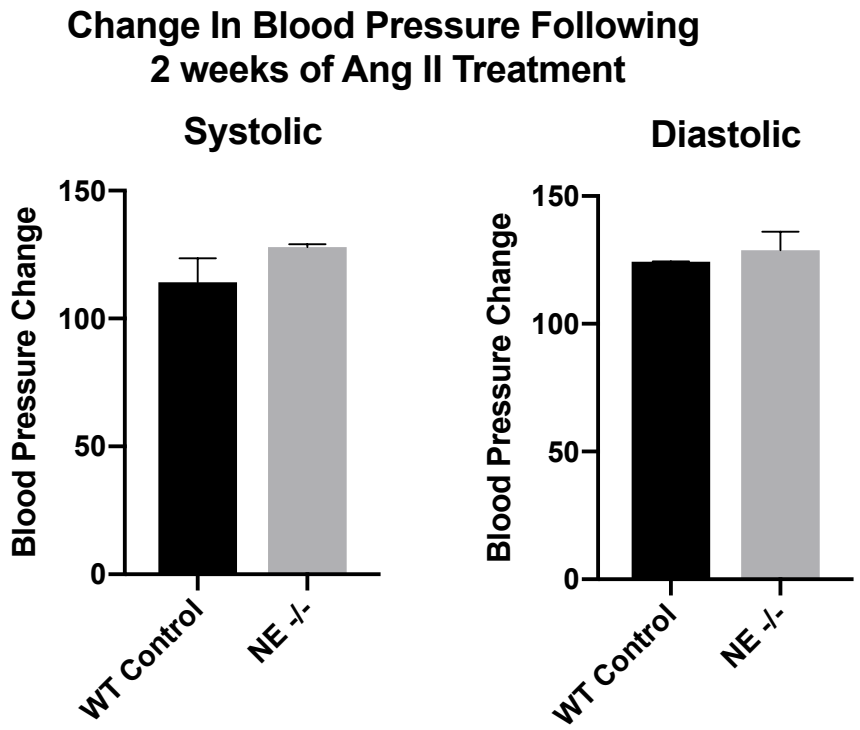

Figure 21*- Average changes in systolic and diastolic blood pressure in a cohort from the experimental group of mice following Ang II treatment as measured by tail-cuff analysis at week 0 and week 2 of the Ang II protocol. Results achieved by taking 10 readings per day,*

for 3 days per time point per animal. N= 3 per group (Systolic p=0.179, Diastolic p=0.466, Unpaired t-test, mean +/- 1 S.D.)

7.2.2 Changes in flow are seen from week two after Ang II administration within Control animals, but no significant change is visible within NE knockout mice

The use of Ultrasound to measure vessel dimensions and flow has been widely used within the cardiovascular field, both in research and clinically for many years. As a new technique being established within our research group, many scans were undertaken to learn and optimize imaging of the vessel in order to monitor the induction and progression of AAA over the 4 week period that the Ang II procedure is carried out, and one week prior for control baseline measurements. Ultrasound enables the visualization of flow with an algorithm attributing a colour to a certain velocity of flow, producing a colour image that visualizes the velocity of flow and the changes to this velocity that occur across a US image. Major arteries such as the aorta in healthy physiology are pulsatile, with flow being highly pressured and progressing in a laminar formation. This forms a target like signal, as the resistance of the wall slows the adjacent blood, whereas the centre of the vessel progresses unimpeded. However, in specific areas such as the aortic arch and also within areas of remodelling and pathology, this laminar flow is highly disrupted becoming turbulent. This turbulence can have adverse effects to the surrounding vessel and has been evidenced to contribute to pathologies such as AAA and atherosclerosis. Furthermore, the flow of a vessel can exemplify the health status of a vessel. For instance, with the example of aortic dissection and AAA where a false lumen can be created this can be clearly visualized within US scans. Within the pathology, where a break in the intimal layer allows blood to flow into the

medial space and pool within the area, large amounts of remodelling occurs and is a sign of worsening prognosis. Similar qualitative and quantitative assessments will be made and comparisons drawn between the Control and NE knockout groups across the entire timeline of Ang II treatment. Control scans prior to Ang II administration will be carried out and subsequent biweekly assessment of the aorta within each animal at numerous reproducible locations and in both cross-sectional and longitudinal planes, this enables a thorough time course overview of the changes the Ang II model has upon the aorta within mice, as well as the difference NE knockout elicits to the same process.

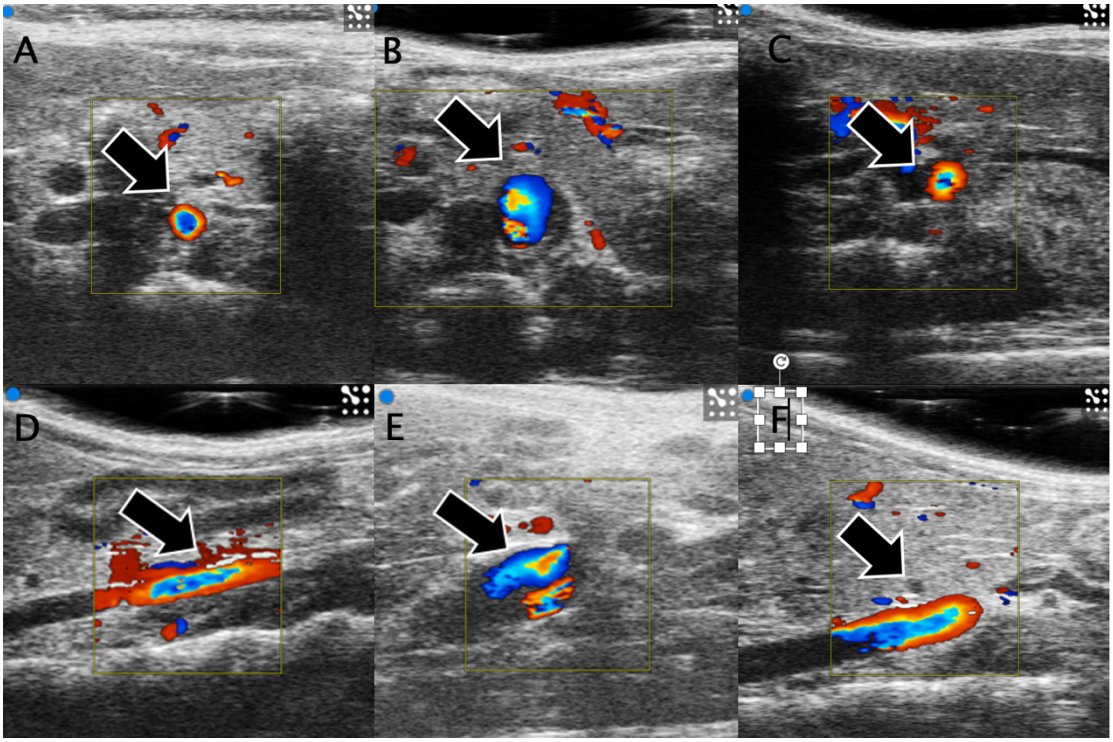

***Figure 22**- Colour Doppler analysis displaying the progressive changes in colour doppler image signatures at the various stages of aneurysm development within WT Control and NE-/- Mice. Arrow indicates the aorta in each image, top row is cross sectional view, bottom row shows the same mouse as top row but in longitudinal plane. A&D- Healthy laminar flow displayed by a target-like appearance in Doppler reading, identified by an arrow, seen within both WT and NE-/- mice at week 0, images from a WT control pre-implantation of Angiotensin pump. B&E- WT mouse 4 weeks post-Ang II pump implantation, disturbance of*

the clear vessel outline and laminar flow signature, with accompanied enlargement of the vessel. Disturbance of laminar flow observed with non-central peak in reading. Complete separation of flow with production of a false lumen shown by complete alteration in doppler signature with separation of blue and red signal. C&F- NE-/- Week 4 post-pump implantation, no widespread or notable change from images A&D, with similar doppler signal visualized and observed within all mice.

Within the study of Control mice and NE knockout mice, flow was consistently seen to be altered within Control animals however this change was minimized within comparable NE knockout mice. Laminar flow, represented by a target like image, was repeatedly found within all mice within Control scanning (**Figure 22, A and D**). At the 2-week stage of Ang II infusion, no change was seen within the NE knockout mice population, however, occasional early changes and distortions to laminar flow were identified within Control mice. Most commonly this was visualized in the pararenal portion of the vessel. Moving onto the end-stage 4-week point of Ang II infusion, small deviations from normal were seen, with NE knockout mice not displaying any significant changes in flow pattern when measured using Colour Doppler (**Figure 22, C&F**). However, the early changes witnessed at the 2-week stage within Control mice were exacerbated within Control mice at week 4 (**Figure 22, B&E**). The proportion of scans that showed early signs of remodelling had increased, and beyond this, a significant portion of the cohort had developed further with remodelling progressing into significant changes and in the case of 2 animals the production of a false lumen (**Figure 22, B&E**). This production of a false lumen resulted in significant turbulence as witnessed within the longitudinal section of imaging and the production of a secondary lumen with extremely low velocities of flow in cross-sectional planes.

7.2.3 PW Doppler results show changes in pulse waves within both groups

Alongside the use of Colour Doppler, the use of Pulse Wave Doppler allows the quantification of vessel pulsatility and visualization of the variability of a vessels blood flow over time. PW Doppler produces a trace of flow velocity at a particular point in the vessel over a period of time, producing a wave trace which displays the variability of the blood flow velocity over that set period. Different vessel characteristics such as size, pressure and health of the vessel alter the wave produced. From this wave, we are able to tell many things that can give a further insight into the health of the vessel and therefore this will be used as an indicator of disease progression as animals are monitored over the 4-week Ang II infusion period. Ultrasound analysis software can produce automated readings and values for factors such as vessel plasticity as a product of the PW characteristics; this also can give an indication of the level of remodelling or deterioration seen within a vessel when repeatedly measured in a time-course manner.

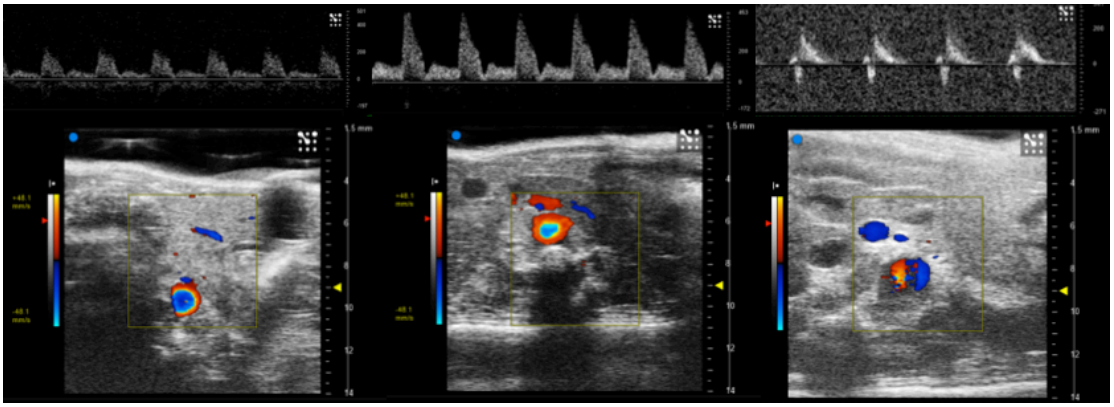

Figure 23*- Colour Doppler and PW Doppler analysis, displaying representative changes to both the colour doppler and PW doppler measurements at different stages of the aneurysmal phenotype within WT Control mice. Progressive changes range from untreated (Left), to early changes at week 2 (Centre) and Late stage of AAA (Right)*

Within the experimental groups' baseline, PW waves were highly similar and consistent with literature images. High peaks in vessel velocities followed by a sharp fall-off but

no backflow was seen within both Control and NE knockout groups at week 0. Following the administration of Ang II vessel readings significantly changed, with large levels of deviation from the healthy stereotypical PW wave seen within Control experimental mice, most predominantly within the highly remodelled vessels. At week 4 NE knockout mice had minor changes to the PW Doppler trace, with less sharp fall off after the velocity peak within the trace. Comparatively, Control mice showed an altered PW wave, with backflow present in most extensively remodelled vessels (**Figure 23**, right panel). The loss of the aortic flow signature in Control vessels at week 4 is a sign of deteriorating vascular health.

7.2.4 Both Aortic Diameter and Infra renal volume are significantly increased following 4 weeks of Ang II treatment

The Ang II model of AAA is a well-established technique that replicates the acute expansion and dissection phase of the aneurysmal pathology. The administration of Ang II and tracking of the changes to the abdominal aorta was made possible by use of both Ultrasound and MRI scanning techniques. Ultrasound enabled the detailed tracking of changes to aortic diameter, whilst MRI allows for volumetric measurement of the entire selected portion of the aorta at each time point.

Within Ultrasound analysis, mice were scanned prior to implantation of the osmotic pump and then biweekly following the insertion. As an aneurysm is defined as the enlargement of a vessel to greater than 50% of its original diameter, all measurements were taken and compared to relative control measurements. At week 0 infrarenal diameter measurements within both groups were comparable and a healthy outline of the vessel was observed within all mice across both Control and NE knockout groups. At week 4 the two groups have highly differing results, with the average

expansion within Control groups being around 70% above control scans compared to the 5% increase seen within NE knockout groups.

MRI results and scanning protocols were highly similar, however, due to the osmotic pump containing a metal rod, no week 2 measurement were taken and final scans were carried out following the removal of the pump. Volumetric expansion was diminished in comparison to diametric increases, however. When analyzing week 4 MRI measurements, average volume expansions within the Control group were around 35% increase, compared to the 5% of the NE knockout contingent. Variability of expansion seen was much larger within the Control aortas measured in comparison to NE counterparts.

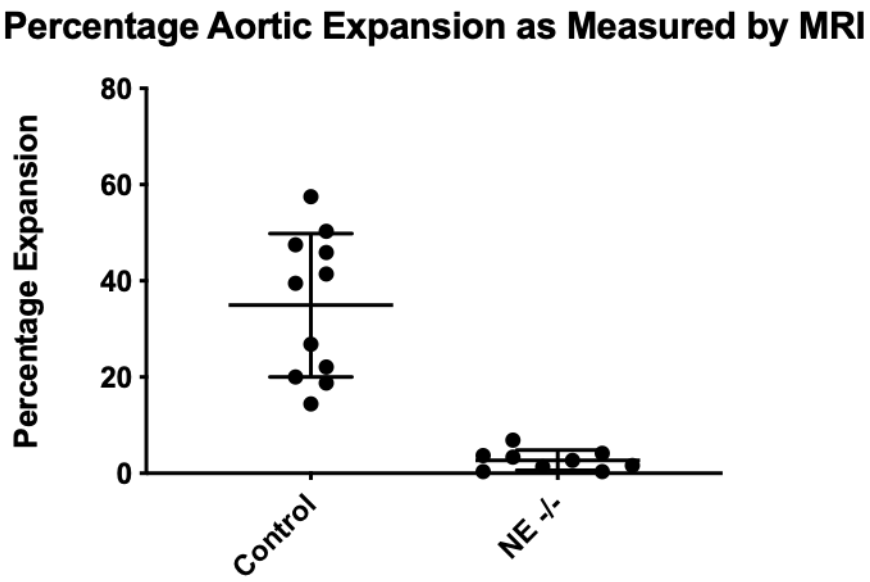

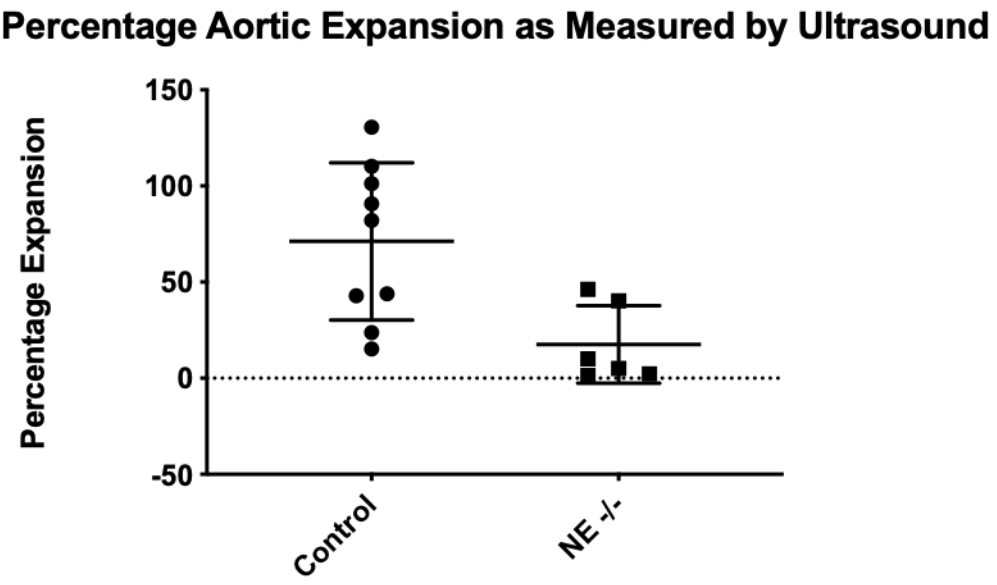

Figure 24*- Comparative graphs displaying the Volumetric differences between WT Control and NE Knockout groups following Ang II protocols. Top- displays differences between groups as measured by MRI (P=<0.0001, unpaired t-test). Horizontal Bar indicates average percentage expansion as measured by MRI, N= Control-11 NE -/- -9 Bottom- differences in aortic expansion between groups as measured by US (0.0112, unpaired t-test) Horizontal Bar indicates average percentage expansion as measured by US. N= Control- 9 NE -/- -6*

7.2.5 Fine Dissection of Mice post-induction of AAA models confirm findings of Ultrasound and MRI analysis

Within MRI and Ultrasound analysis, developed and outlined above, differences in aortic health were observed by both diagnostic imaging modalities. However, confirmation of this result by analysis of end-stage tissues was imperative to confirm the validity and reliability of the results. Following the termination of experiments at day 28, all mice were sacrificed by a CO_2 Schedule 1 procedure prior to dislocation of the neck to confirm death. Immediately following this rough dissection to remove the aorta of each animal was performed, with images being taken to confirm aortic health. Upon removal of the aorta from the heart to iliac bifurcation, finer

dissection was carried out to remove as much connective tissue surrounding the aorta as possible without damaging the vessel itself. The following figures show representative images of the results, with confirmation of the MRI and Ultrasound imaging results. Identification of some vascular expansions in regions outside to region of interest was also identified within Control groups, however, no areas of localized aneurysmal expansion were identified within the NE knockout group.

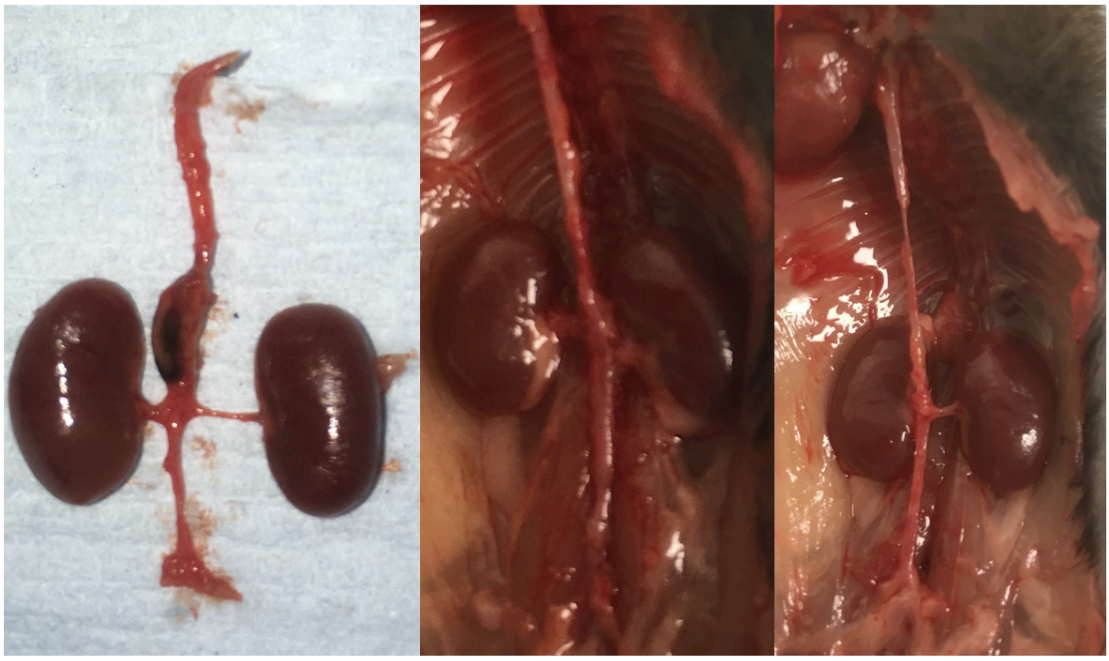

AAA Dilated Healthy

Description of Aorta	Percentage of Baseline Measurement as Measured by US
Healthy	<105%
Dilated	105-149%
Aneurysmal (AAA)	150%+

	NE-/-	Average Expansion	WT Control	Average Expansion
Healthy	3	2.883%	0	
Dilated	3	32.033%	4	31.471%
AAA	0		5	102.979%

***Figure 25**-Typical findings at post-mortem. Rough-dissection images following Ang II treatment, with large expansions observed within WT Control mice in 5 control animals (Left), diffuse minor dilation within WT mice in four control mice (Centre) and no similar expansions observed in NE Knockout mice (Right)*

7.2.6 Pulsatility of the Aorta differs in control and NE knockout mice with Ang II administration

During the progression of the AAA pathology, the ECM and structural proteins of the vessel such as elastin and collagen are hugely degraded. This degradation interrupts the normal functions and characteristics of the vessel, for instance, its ability to expand and recoil in response to pulses in blood flow. With the utilization of Ultrasound monitoring, the vessels elastic recoil can be monitored and compared across different time points within the same mouse and aortic location. Subsequent monitoring of mice from each cohort, both prior and following Ang II treatment was carried out. Analysis of the vessel location and image quality was imperative to being able to pinpoint minor changes within vessel characteristics as vessel characteristics are dynamic and change along the length of the vessel.

Vessel pulsatility was not significantly different when comparing NE knockout and Control groups across the 4 weeks of Ang II treatment. Baseline measurement comparisons between the Control and NE knockout mice showed a minor difference in the basal pulsatility of the vessel, (**Figure 26**), with NE knockout mice appearing to have a minimally more pulsatile infrarenal aorta when compared to Control counterparts, this was not significantly an different. However, the levels of pulsatility in NE knockout mice would fall below that of the Control mice following the complete 4-week treatment with Ang II. Overall the two datasets regarding vessel pulsatility were comparable.

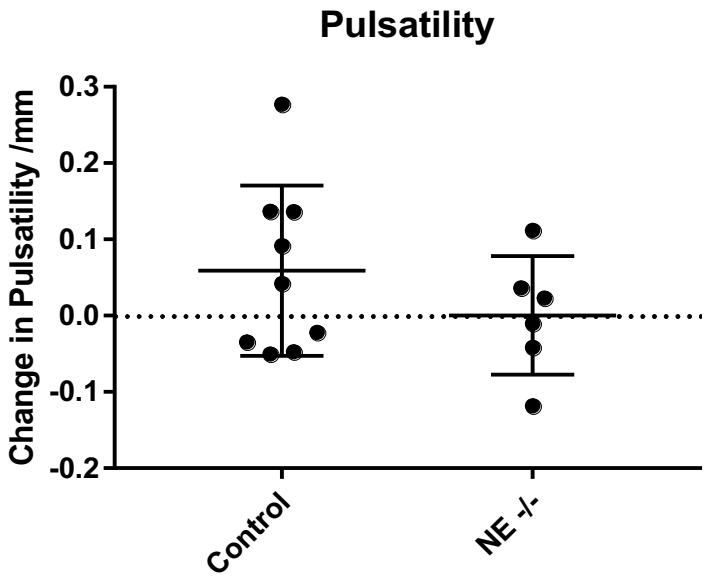

Figure 26*- Comparison of change in pulsatility of the aorta between each group following Ang II treatment, as measured by US techniques at week 0 and week 4 of treatment. (P=0.2854, Unpaired t-test, mean displayed by major horizontal bar+/- 1 S.D, N= Control- 9, NE-/- - 6). No Change is indicated by a dotted line*

7.2.7 Histological analysis displays the changes of vessel morphology, with Collagen and H&E staining displaying significant alterations between Control and NE knockouts in end-stage tissues

From the end-stage dissection, tissues were preserved and mounted within OCT or Paraffin in order to compare the cellular and structural changes as a result of Ang II treatment within the Control and NE knockout groups. H&E staining is a widely used within diagnostic histology as it visualizes the basic structures and components of the cells and tissues, with DNA material staining a purple colour and cytoplasm or collagen in a pink to red colouration.

Collagen is a well-known structural protein that helps to form the scaffold of the aorta. Remodelling of collagen and elastin is a well-known step within the

progression of AAA and even minor evidence of these changes should be visible within vessels that have not yet started to expand.

H&E staining displayed a clear deviation from normal structural arrangement within Control group animal tissues (**Figure 27 A**). These changes were visible within all three layers of the vessel, with dysregulation of the media and adventitia evident and the loss of the intimal landmarks such as the prominent elastic lamina. Furthermore, the adventitial layer of the aorta in control mice appears to have developed outwards in a regional-specific manner, as the coverage of this layer surrounding the vessel is not proportional around the entire vessel circumference. Whilst looking further into the medial portion of the vessel, you can see clear dysregulation of the extracellular structure. The elastic lamina is typically seen within a formation of defined continuous lines with consistent distances between the many layers, however, these have become broken and changeable in gaps between layers of elastin are highly inconsistent with loss of nuclear staining within the expanded regions (**Figure 27 A**).

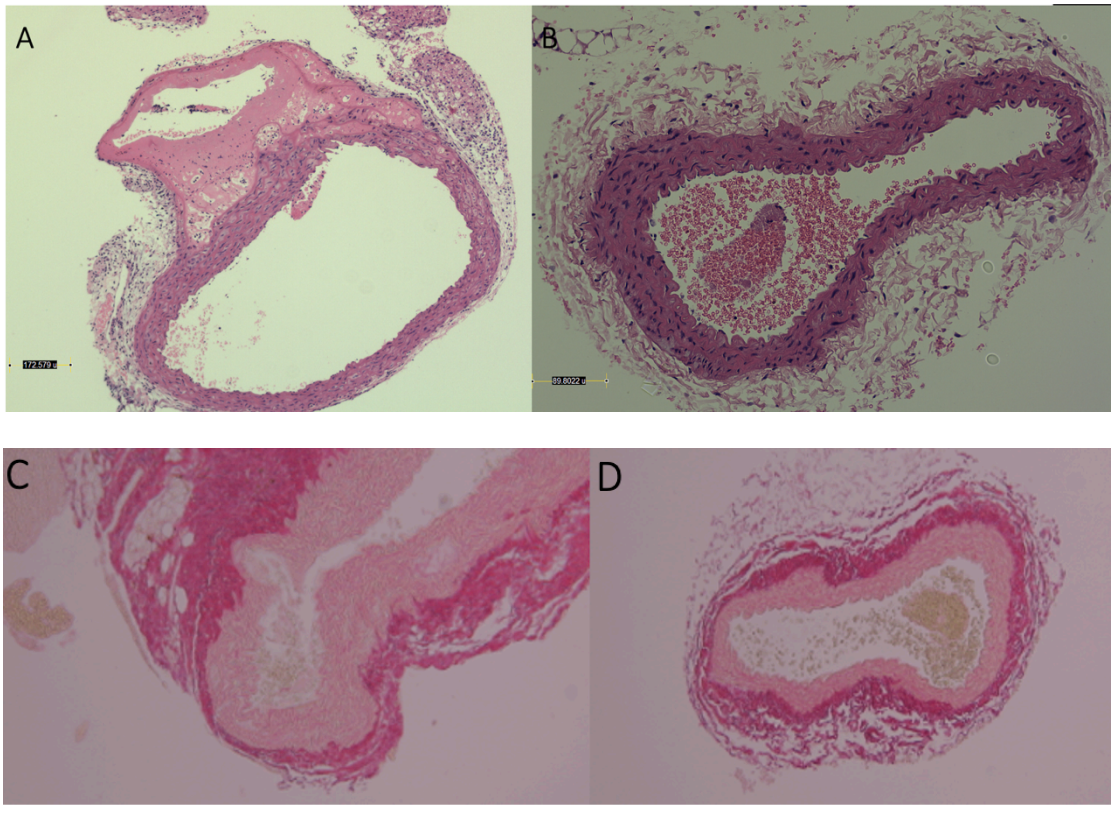

Figure 27*- H&E images of histological sections from both WT Control (A) and NE Knockout mice (B) following the completion of the 4-week protocol. Collagen staining by Sirius Red used within the bottom two rows. WT Control (C) and NE Knockout mice (D) are displayed, showing the erratic and irregular banding of proteins in C when compared to the uniform D image.*

In comparison to this phenotype observed with control mice, the NE knockout mice displayed minimal signs of remodelling, with all three distinct layers of the vessel intact and undisrupted (**Figure 27 B**). Clear elastic lamina folds are visible throughout the tissue sections, with consistent distances between the layers and no evidence of medial layer destruction. Intimal, medial and adventitial layers are consistent in form and depth throughout the sections prepared. No clear changes to adventitial layers can be seen. Intimal analysis shows some elastin folds have appeared to flatten slightly, however no breaks or loss of nuclei within the region can be seen.

Collagen staining shows highly similar patterns of remodelling when compared to the H&E analysis (**Figure 27 C&D**). Both Control and NE knockout mice show the different densities and forms of collagen present within the aorta. Intimal and medial layers stain lighter in comparison to the adventitial layer that is much deeper in staining colour. This difference in staining colour is also due to the differential uptake by type I and III collagen fibres that are visualized within Sirius red collagen stains. In WT Control mice (**Figure 27 C**), all the aortas displayed higher levels of remodelling within the intimal portion of the vessel, whilst the outer adventitial layer was far more similar to that of NE knockout mice (**Figure 27 D**). High levels of breakdown of intima layers and even exposure of the deeper layers at times where the luminal layers of collagen had been stripped away were observed in WT control mice. Such changes were never seen in NE knockout mice, with consistent coverage of the medial and adventitial layers

with luminal layers of collagen. One major shortcoming is the lack of scale bars in both **Figure 27 C & 27 D** due to problems with microscope scale bar accuracy at the time of the experiments, therefore whilst patterns of expression can be assessed no quantification or references to scale can be drawn.

7.2.8 Immunofluorescent staining confirmed upregulation of MMPs and presence of immune cells within the vessel wall

Dissected sections of the aorta were taken and preserved prior to mounting and sectioning within OCT or Parafin. These end-stage samples were sectioned by microtome before adherence to polylysine coated slides took place. These prepared slides underwent chemical antigen retrieval and were then able to be stained and imaged using immunofluorescent techniques in order to visualize specific proteins of interest, as well as said proteins localization and structure.

Within this experiment, we identified MMPs and immune cell invasion as an area of interest, with both being regarded as a key influence within the AAA pathology. Staining on these peptides occurred successfully with the secondary antibodies identifying diffuse expression within the vessel wall of aneurysmal tissues. Immune cell markers and MMPs were located most strongly within the adventitial portion of the vessel wall (**Figure 28**), with MMPs appearing less regionalized but imaged at greatest intensities within the same portion. Immune cell markers such as ly-6g were used to identify cells of immune origin.

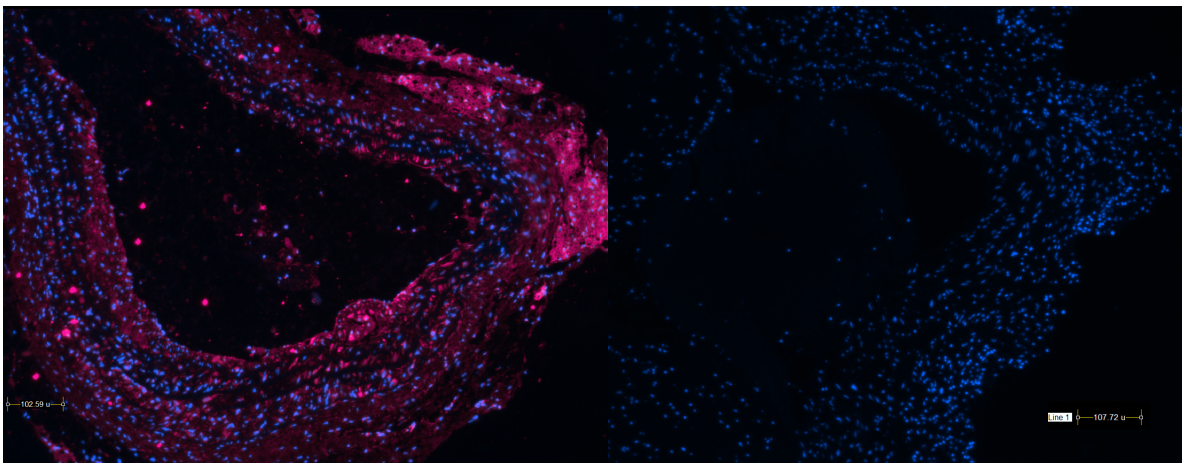

Figure 28*- Example images of immunofluorescent staining of MMP8 within WT aortas that had undergone Ang II protocols. This experiment was repeated 5 times across a selection of WT aortic section slides. All sections were counterstained with Hoescht nuclear staining, MMP8 (Pink), Left- x20 objective. Right- IgG Control from the same aorta but a number of sections along from immunostained region x 20 Objective.*

7.2.9 Fractional Distillation of the Aorta was achieved, separating vessels into three distinct groups of protein content

Following the continuously emerging result of NE playing a role within the initiation and development of AAA, there was a need to understand the mechanism by how NE was having an effect. RNA analysis had shed some light on the changes within end-stage tissues composition, in terms of differential expression of key enzymes such as MMP2. However, we suspect that this was the product of more subtle changes at an earlier stage of the pathological mechanism. In order to address this in detail, we wanted to decipher which area of the vessel NE was having its most potent effect, and what it was regulating or modifying at the same time. To do so fractionation of the aortic sample was needed. Following the protocol set out by Didangelos et al.(11), aortic tissue samples were processed in order to separate proteins from three differing origins.

Proteins were separated into; loosely bound newly synthesized proteins, intracellular proteins and finally extracellular matrix proteins. This occurred by a novel protein extraction process that enabled the precipitation of the relevant proteins at each stage.

After a few modifications to the protocol and optimization of the procedure, a successful extraction of all three fractions from within the same tissue sample was completed. Following this, the successful running of a gel was completed in order to separate all proteins contained within each sample. This displayed the abundance present within each fraction and each sample. Completed in triplicate, this allowed for the possibility of analysis of Control and NE knockout tissues by proteomics. Abbreviated results are included below in **Figures 29-31** and a more extensive summary is included within **Appendix 1-3**.

7.2.10 Proteomics analysis of the three generated fractions produced promising insights into proteins implicated in NEs protective role against AAA

As outlined above, following fine dissection of the aorta from three mice within both Control and NE knockout groups, fractional separation of the tissues occurred. Loosely bound and newly synthesized proteins, intracellular and extracellular matrix proteins were extracted into a total of eighteen samples for comparison between relevant fractions and genotypes. Due to us being more interested in the causal mechanism of AAA and the implications of NE within this process, all Ang II treatments were halted at the 14-day stage, prior to widespread modifications of the vessels. This was in order to identify the proteins that change early within the process and are causal in bringing about the phenotypical changes that we see later on within the AAA model. Following the extraction, gel separation of proteins followed by trypsinisation and mass

spectrometry techniques were used to identify the proteins present, as well as modifications to proteins such as phosphorylation of such molecules. All readouts from mass spectrometry analysis were assigned a Mascot score, with a threshold of 50 being used as a threshold of validity. From this list, analysis of change across the relevant samples were carried out, with a heat map generated in order to visualize changes, with fold change and p-values produced to determine the significance of these changes. Following on from this Volcano plots were utilized to determine the most appropriate proteins to follow up.

Resultantly, the volcano plot generated by the comparison of Extraction fraction 1 between WT and NE knockout mice undergoing the Ang II model of AAA yielded many positive results. Thresholds of change in both p-values and fold change were applied with some of the most significant changes seen in the proteins highlighted within the heat map below. Proteins such as VASP-like protein and DDRGK protein 1 were some of the most significantly different. However, when looking deeper into the data set, genes such as F-Box-Like/WD Repeat-Containing Protein, Transducin Beta Like 1 X-Linked (TBL1x), were highlighted as they had sufficient levels of significance whilst increased levels of fold change simultaneously (P=<0.0005). Thousands of proteins were analysed with only a small fraction of these regarded as significant when comparing the two groups extraction fractions.

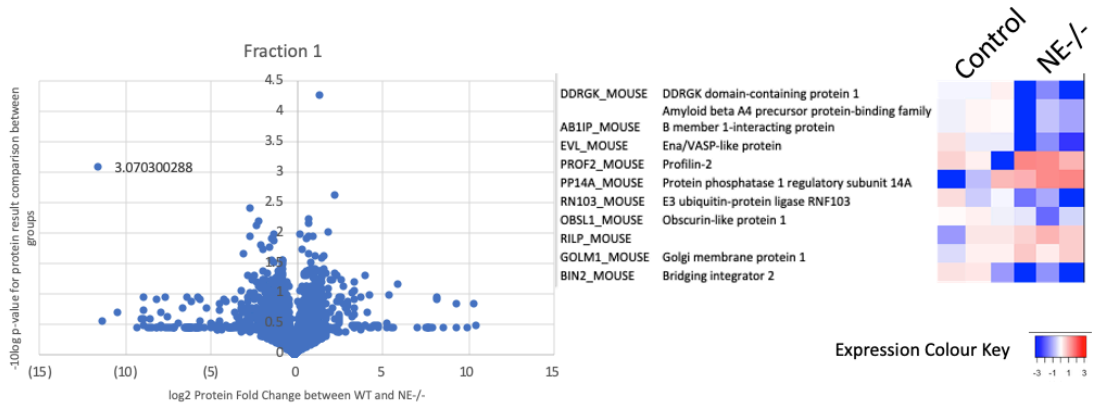

***Figure 29**- Volcano plot analysis of fraction 1 comparison between WT Control (lane 1-3) and NE knockout mice (lane 4-6). Top protein hits as ranked by mascot score and p-value between proteins identified within fractions from the aorta of the two genotypes*

The secondary extraction fraction provided similar results, with regards to the number of significant hits that were produced. However, the concentration of hits along the y-axis was far greater, with less of an effect size, if any, suggesting that changes for the majority of the intracellular proteins did not reach statistical significance. There were a number of proteins however that did deviate from the clustered group, as a result of a clear increase in fold change of the relevant proteins. This includes a protein of note in Caveolin-2, which was significantly different between the groups ($p = <0.05$) whilst a significant fold change was concurrently recorded.

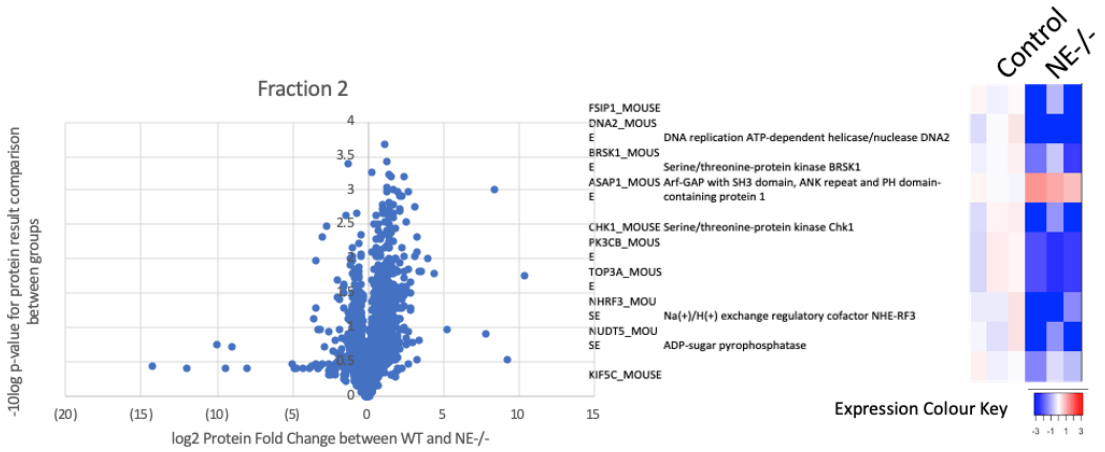

***Figure 30**- Volcano plot analysis of fraction 2 comparison between WT Control (lane 1-3) and NE knockout mice (lane 4-6). Top protein hits as ranked by mascot score and p-value between proteins identified within fractions from the aorta of the two genotypes*

Finally, the third extraction fraction contained the proteins that were identified to be within the extracellular matrix of the aortic tissues. Interestingly this fraction produced the most significant results in terms of p-value recordings. Similarly, the spread of the data points in terms of fold change were much more disparate and less concentrated around the origin in comparison to other fractions. Skew of the fold change was towards the negative with the most significant and greatest changes being found within this portion. Included in this was the protein COP9 signalosome complex subunit 8 (COPS8), a protein involved in the regulation of signaling pathways and modulation of enzymes involved in protein degradation.

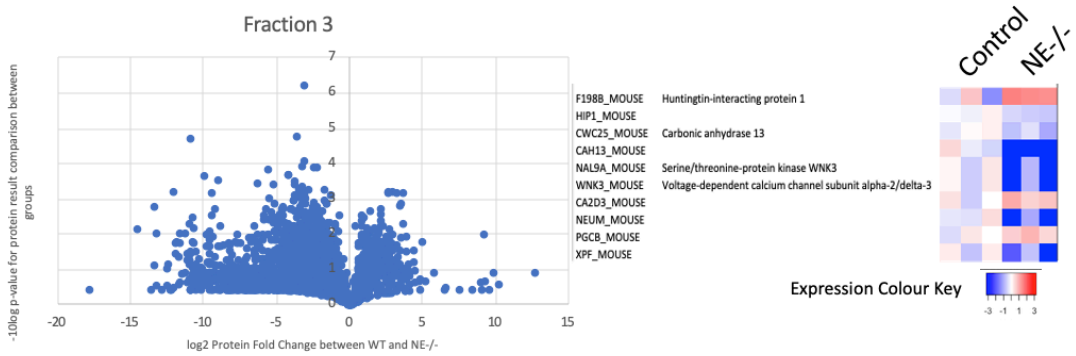

***Figure 31**- Volcano plot analysis of fraction 3 comparison between WT Control (lane 1-3) and NE knockout mice (lane 4-6). Top protein hits as ranked by mascot score and p-value between proteins identified within fractions from the aorta of the two genotypes*

7.2.11 Staining of Proteins identified within Proteomics analysis were verified as displaying differential expression between WT Controls and NE Knockout groups

Identification of proteins by proteomic analysis indicates various mechanisms by which NE could act. Volcano plots were used to narrow down the changes in aortic proteins to highlight the most significantly modulated proteins between the Control and NE knockout datasets. Following comparison of the fold change and p-value, identified proteins with marked differences were identified with greater detail, with research into each protein and their potential mechanism of involvement being assessed. Proteins that deviated from the group in the volcano plot were identified and researched for any past research, relevance to vascular function and similar proteins with known roles in pathology. One protein was chosen from each fraction to be verified, with the protein deemed to have most potential significance following evaluation chosen. TBL1x, Caveolin-2 and COPS8 were the respective proteins that were selected, before consequentially being stained for within histological sections from both WT and NE Knockout genotypes.

Initial staining resulted in TBL1x visualizing the differences in expression levels of the protein between WT and NE Knockout observed in proteomics data. Consistently, TBL1x displayed increased expression within NE Knockout aortas (**Figure 32B)** in comparison to the Control vessels **(Figure 32A)**. This difference was seen across all layers of the vessel however most significantly within the medial and adventitial regions within NE Knockout samples. Low levels of expression were seen within Control mice, however, this appeared to be isolated to the adventitial portion and highly concentrated within small areas, appearing to be intracellular (**Figure 32A)** rather than the more disperse expression seen in NE Knockout scans (**Figure 32B**), although some erratic staining was seen elsewhere which was considered signal from poor washing rather than true expression. Furthermore, lack of scale bar in **Figure 32A** decreases our ability to draw comparative conclusions between the two sections. Consequentially, thanks to poor washing and scale availability this should be repeated prior to conclusions fully being drawn, even though proteomics and western blot data supports this result. Western blot protein analysis led to observations of higher levels of TBL1X within NE Knockout tissues when compared to WT controls (**Figure 32C**).

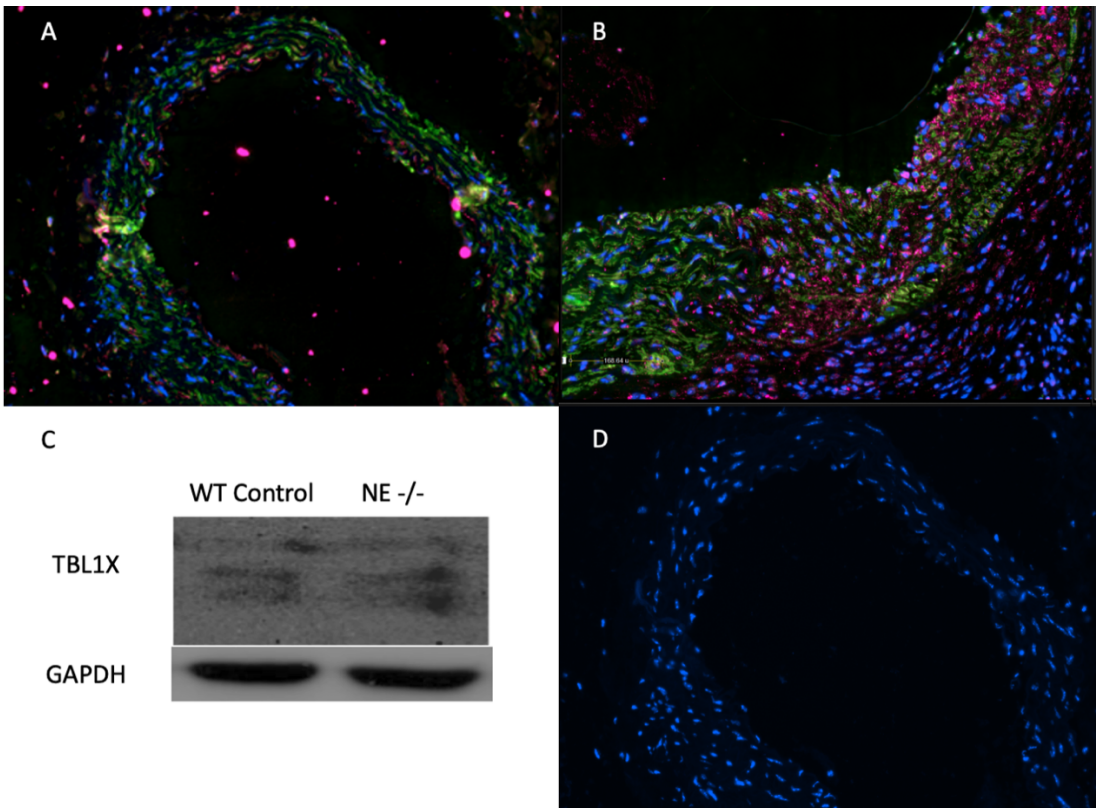

***Figure 32**-Staining of TBL1x (Far-Red) in WT Control (A) and NE Knockout (B) aortic sections following Ang II infusion for 4 weeks, counterstained with Hoescht nuclear staining (Blue) and SMC (Green). Western Blot data for TBL1x within Ang II treated aortic tissue lysates, WT Control and NE Knockout (C). IgG Control (D)*

Caveolin-2 was another protein identified within proteomics analysis. Resultant staining saw Caveolin-2 visualized within both Control (**Figure 33A**) and NE Knockout sections (**Figure 33B**), with significantly higher expression observed within NE Knockout mouse sections. Caveolin-2 was visualized within intimal portions of Control vessels most strongly, similarly, this same pattern was observed with NE Knockout mice which displayed predominantly intimal expression of Caveolin-2 however more intense expression and expression within intimal areas, with lower levels of medial expression also visualised. Increased staining intensities within the endothelial-intimal and adventitia layers was apparent in the vessels of NE Knockouts mice (**Figure 33B**). Expression of Caveolin-2 was not found to be dramatically

different within the medial portion of the vessels studied. The same outcomes were observed with utilisation of Western Blot techniques (**Figure 33C**).

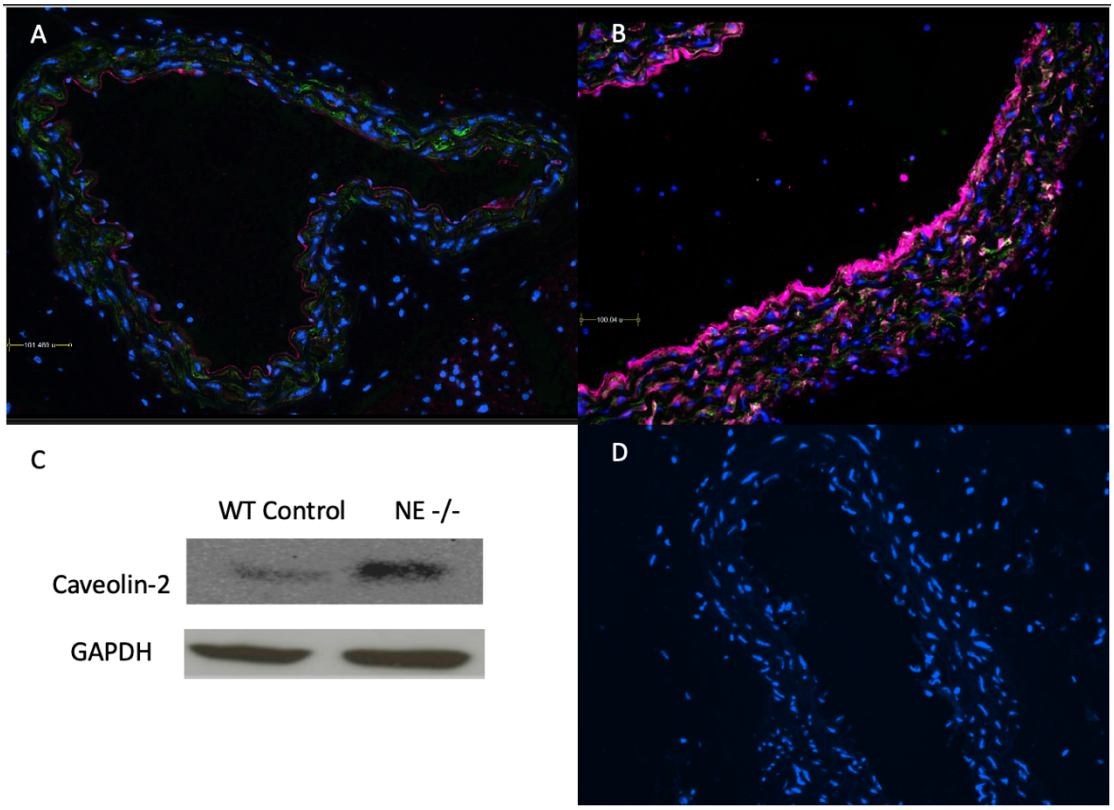

Figure 33- *Staining of Caveolin-2 (Far-Red) in WT Control (A) and NE Knockout (B) aortic sections following Ang II infusion for 4 weeks, counterstained with Hoescht nuclear staining (Blue) and SMC (Green). (C) Western Blot data for Caveolin-2 within Ang II treated aortic tissue lysates with respective loading controls for comparison (D) IgG control for images taken above of the Caveolin-2 stained sections*

Finally, COPS8 was the third protein investigated following identification of a significant difference in expression between Control (**Figure 34A**) and NE Knockout (**Figure 34B**) aortas after both have undergone Ang II treatment. Resultant staining was highly representative of the proteomics data with clear differences between Control and NE Knockout mice, similarly, western blot analysis (**Figure 34C**) further strengthened this observation. WT Control mice displayed very low levels of COPS8 within stained sections, with very low levels visualized within the adventitial portions of vessels

stained. Alternately, COPS8 were highly expressed within NE Knockout mice with significant expression within medial and adventitial portions of the vessel (**Figure 34C**) in all sections stained. Staining patterns of COPS8 in Control mice appears to show an intracellular pattern with expression localized surrounding nuclear stains and with cell-like outlines visualized (**Figure 34A)**. Alternately, NE Knockout mouse sections displayed a more nuclear pattern of staining with expression co-localizing with the nucleus predominantly (**Figure 34B**).

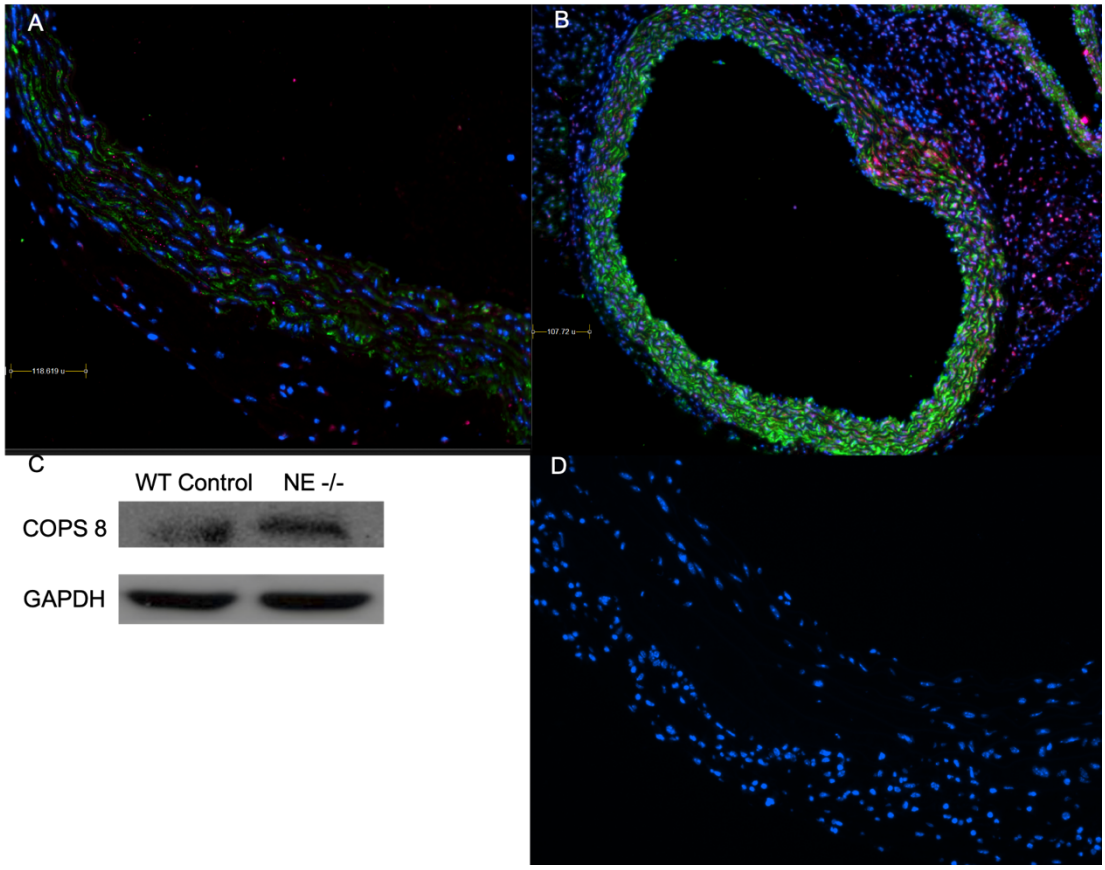

Figure 34*- Staining of COPS8 (Pink) in WT Control (A) and NE Knockout (B) aortic sections following Ang II infusion for 4 weeks, counterstained with Hoescht nuclear staining (Blue) and SMC (Green). (C)Western Blot data for COPS8 within Ang II treated aortic tissue lysates from WT Control and NE Knockout. IgG control images for COPS8 images (D)*

7.3 Discussion and Limitations

From the studies currently undertaken, the role NE plays within the development of AAA within animal models is becoming more clear. Relations between the enzyme and the pathology that were outlined in the previous chapter were further backed up and confirmed with the use of a secondary animal model, namely the Ang II model. Furthermore, still, the model employed allowed for dynamic changes to be monitored such as blood flow patterns enabling us to understand in greater depths the differences between the two genotypes and likely where the changes lie. Continuing in this vein, following the completion of the model, further studies utilizing the tissues generated produced a greater insight into the molecular changes occurring within the model within both experimental genotypes, with the differences between each giving rise to new targets and molecules of interest for further study into the AAA pathology. Utilization of a proteomics approach enabled the possibility of identifying both known and novel peptides significant to the role of NE within the production of AAA. Confirmation of these peptides were necessary, and further work on these are still needed in order to fully understand the changes that are brought about as a result of the loss of NE within the AAA model.

Within early experiments, focusing on the changes in flow generated by the administration of Ang II, commonly observed readings for both Colour and PW Doppler were witnessed within all stages of the protocol within Control mice. However, the same was not seen within the NE knockout cohort in later stages of the study with later scans of NE knockout mice appearing highly similar to the week 0 and week 2 scans within Control mice, with no progression or development of the AAA phenotype and associated alterations in either Doppler modalities. This is most likely due to the lack of aneurysmal development seen within the NE knockout mice. This in itself could

be related to NEs known function within reverse cholesterol transport. Inhibition of NE has previously been observed to decrease the levels of circulating cholesterol within animal studies, a known risk factor for AAA development (167). Consequently, reduced levels of circulating cholesterol, reduced inhibition of cholesterol efflux from macrophages and consequent decreased levels of atherosclerosis and inflammation may potentially have a beneficial impact on AAA incidence and could explain the outlined decrease in pathology incidence within the NE knockout cohort. Changes in Doppler readings are highly dependant upon vessel characteristics, with any change in the vessel diameter, wall thickness or elasticity impacting greater on the flow occurring within the lumen of each respective vessel. Within the Control mice, the greatest changes in PW and Colour Doppler readings were witnessed within the most remodelled vessels, notably, the production of a false lumen created huge changes in the Doppler profiles. This phenotype was never seen within NE knockout mice. Consequentially there was no large disruption of flow and creation of turbulence, all of which alter the Doppler signal created.

Moving onto the changes seen with regards to the expansion of the aorta within each experimental group, significant differences were seen with marked increases in both diameter and volume of the aorta in Control groups. NE knockout mice showed minimal increase and this as highly comparable to procedural control mice, with no significant difference seen. This finding backs up the result of the Calcium chloride study of similar finding, as well as supporting the work of Yan et al. (192) which shows an influence of serine proteases within AAA, however, the same study does contravene the result that NE alone is responsible for this difference. Yan et al. employed a third protocol, the elastase-induced model of AAA, with a reduction in expansion following the knockout of serine proteases, of which NE is one. This study highlights the role of

NETs and concludes their importance within the initiation of AAA. NE is required for NET formation, and therefore one finding of this study does seem to conflict with the other. As the loss of NE alone was considered a secondary preliminary study, and within an elastase-induced model where an elastase was removed by genetic knockout, I am confident that the previous finding of NETs influence on AAA and NEs role within NET formation is the primary finding of this study and it supports similar findings of my current work. This further strengthens the argument that NE plays an influential role within the AAA pathology although alternate pilot research may contradict this argument. Due to the AAA model Yan et al. are employing, I feel the experimental design was inappropriate for purpose with replacement of an endogenous elastase with an exogenous elastase to study elastase influence.

Developing this study further, analysis of the end-stage tissues ensued. With known contributing mechanisms of AAA development already outlined by numerous studies by such research groups as Alan Daugherty(1), Jonathon Golledge (79)(193) and Lisa Cassis(152), the role of inflammatory mediators, MMPs and ECM breakdown in the production of AAA are highly supported and well documented. Consequentially we looked to determine any significant differences within these areas that were produced as a result of the loss of NE. Firstly ECM and structural protein changes were looked into with the use of H&E as well as Sirus Red staining for collagen. Remodelling of the structural fibres of the aorta is a significant milestone in the progression of the AAA pathology. Collagen is degraded and distorted, morphing from the expected wave-like formations to linear weaker organizations of the micro infrastructure. This change in structural formation rather than the density of collagen itself is believed to be the reasoning for the weakening of the vessel, with these changes reported in both Marfan and non-Marfan AAA patients. With regards to this, our study lends support to

this argument, with little to no changes apparent within the structure of the vessel of NE knockout mice, however widespread alterations to this organization within the Control cohort. Within both Collagen as well as H&E staining, all vessels displayed signs of demarcation of the differing vessel layers, however, this was distorted within Control mice in comparison to NE knockouts, another sign of deteriorating vessel health.

Proteomics data gave rise to proteins and other novel targets that were implicated within the differences seen between the NE knockout and Control phenotype. During this chapter, the optimization of fractional extraction of proteins from different components of the aorta was successfully carried out. Within the three fractions of; novel synthesized and loosely bound proteins, intracellular proteins and extracellular matrix proteins, thousands of proteins were identified with a shortlist of a few hundred proteins being significantly different between the two experimental groups. The highlighting of one protein from each fraction within this study was to confirm the validity of the findings. Volcano plots were used in order to best identify which proteins measured were most like to play a significant role, this was based upon them concurrently having a highly significant p-value and a large fold change. This enabled the identification of a few highly appropriate candidates for further investigation from a very large dataset. Subsequent immunofluorescent staining validated TBL1x, Caveolin-2 and COPS8 as potential proteins of interest with differences in expression observed during staining. These differences were varied in terms of effect, with COPS8 expression differing in cellular localization, however, Caveolin-2 produced significant differences in expression levels largely within the adventitial portion, both intra- and extra-cellular. All three investigated proteins were much more highly expressed with knockout of NE, this suggests that NE could cleave

or breakdown the proteins TBL1x, Caveolin-2 and COPS8. These three proteins, as well as a number of other proteins, could be novel substrates for NE, with roles within the AAA process and warrant further investigation. In summary, this work has identified proteins that could have a possible influential role within the production of the AAA phenotype which has thus far not been studied.

As mentioned, the proteins raised are yet to be studied, however, they do have known function within other pathological or physiological pathways. In the case of Caveolin-2, related proteins already have a known role within the AAA disease, as Caveolin-1 genetic knockout has already been outlined as influential within Ang II and Thoracic Aortic Dissection (TAD) procedures, with inhibition of the ADAM17 as the underlying mechanism of aneurysm induction(194). TBL1x has known roles within hormonal and transcription factor regulation but as yet no report to suggest its influence on related cardiovascular conditions(195). Whilst COPS8 has not had any significant link or study within the AAA or TAD pathology, unrelated work has elicited that COPS8, a G-protein coupled receptor mechanism, can indeed regulate NF-κB expression, which in turn has large ties to the AAA pathology(196). Similarly, work on TBL1x has yielded data suggesting an influential role of the protein on transcriptional activity, including modulations of NF-κB(197).

The use of NE inhibitors has recently been experimented with as a post-surgical option of pharmacological treatment within aortic dissection patients, with success within early phases of trials. However, these studies focused on the improvement of post-surgical coagulopathy rather than the initiating mechanism of the pathology, which is highly related to AAA(198). Positive results were obtained in terms of blood marker decreases seen and clinical outcomes, suggesting further study is warranted.

Furthermore, previous studies have shown similar degrees of positive benefit from NE inhibitors with respiratory symptoms following surgical interventions(199).

In summary, the findings outlined and discussed above are largely an observational dataset and require clarification, quantification and verification before they can be accepted as factually conclusive. Patterns identified within histological analysis require quantifiable comparison between the two groups, with statistical analysis to be performed on subsequent outcomes. This can be considered one of the greatest limitations of this dataset, with the observational nature limiting the conclusions able to be drawn.

7.4 CONCLUSION

Within this chapter, the role of NE in AAA has been investigated utilizing the Ang II model, with significant reduction in AAA arising as a result of genetic knockout of NE. Functional changes in vessel dynamics were observed and the pathway by which the effect was looked into. Expansion rates were significantly higher in Control animals when compared to NE Knockout mice, this occurred via a mechanism independent to AT1a-induced hypertension, as blood pressure changes were comparable. From this series of experiments, a difference in a MMPs -2 and -8 expressions, which have a known role in AAA induction, were found repeatedly. Furthermore, other possible mechanisms were looked into and novel pathways attempted to be identified via a proteomics approach. This work gave rise to the identification of a number of proteins, three of which were chosen for further investigation. All proteins highlighted by proteomics analysis were verified by immunofluorescent staining as well as Western blot analysis, with significant differences observed between genotypes. Further work is needed to elucidate the full influence these proteins have upon the AAA pathology.

8 THE ROLE OF NE IN THORACIC AORTIC DISSECTION

Aortic Dissection is the striping of the intimal layer of the aorta, most commonly within the ascending or proximal descending aorta, with tearing of elastic lamina resulting in the creation of a false lumen within the affected portion of the vessel. This pathology is associated with medial dysregulation, smooth muscle cell death and aortic rupture, with clinical outcomes ranging from chronic to acute, and survival rates currently poor if reparative surgery isn't immediate. The AD pathology has many underlying similarities to AAA, with a large inflammatory component. Neutrophils and macrophages have been identified within the adventitial portion of AD affected sections of the aorta, with MMPs also known to influence the pathological outcome. Consequentially NE could play an influential role within the pathology, its initiation and progression. From previous chapters we have demonstrated NEs role within the AAA process, identifying new proteins that are regulated within NE Knockout mice, who do not exhibit the same level of vascular modification as WT Controls. This chapter will examine whether NE has a similar role within the AD pathology with the use of the BAPN model of TAAD using juvenile mice.

8.1 MATERIALS AND METHODS

For information regarding the methodologies utilized within this chapter please refer to the Materials and Methods chapter above.

8.1.1 Aortic Dissection Model- BAPN

Animal models are a commonly utilized tool used to study pathology and help identify the underlying mechanism by which the pathology occurs. Within this study, the BAPN Thoracic Aneurysm Aortic Dissection (TAAD) model was utilized to look into if or

how NE plays a role within the pathology. BAPN is a lysyl oxidase inhibitor that when administered to a mouse, usually via the drinking water, inhibits cross-linking of elastin and collagen. The inhibition of this process results in severely weakened vasculature and often produces an enlargement within the aorta, most commonly seen within the descending thoracic region of the vessel. During further histological analysis dissection of the vessel can often be identified with significant medial degeneration and breaks within the elastin lamina visible. Aortic intramural hematoma can result from the intimal breaks seen, with this serving to strip the innermost portion of the vessel, again this can be seen within some histological sections.

Aortic Dissection was induced by administration of β-Aminopropionitrile Monofumarate (BAPN) at 1g/kg/day for 28days within drinking water as described in the previous studies(200). Mice were monitored closely whilst under experimentation, with the study comparing Wild type ($ApoE^{-/-}/NE^{+/+}$) to NE Knockout ($ApoE^{-/-}/NE^{-/-}$) mice. Mice were administered BAPN for the 28 day period, or until death, with the aortic arch and heart dissected (**Figure 35**) and either preserved for staining or snap-frozen for analysis of protein.

Measurement of aortas was quantified following fine dissection using microscopy and Image J software to look at relative differences between groups. Alternately, differentiation between the two groups was carried out by the production of a Kaplan-Meier curve. Differences in death rate were compared following cause of death being confirmed by a post-mortem dissection. Quantification of the Aorta occurs via the fine-dissection of the aortic arch and *ex vivo* measurements of the dissected arch, as seen below.

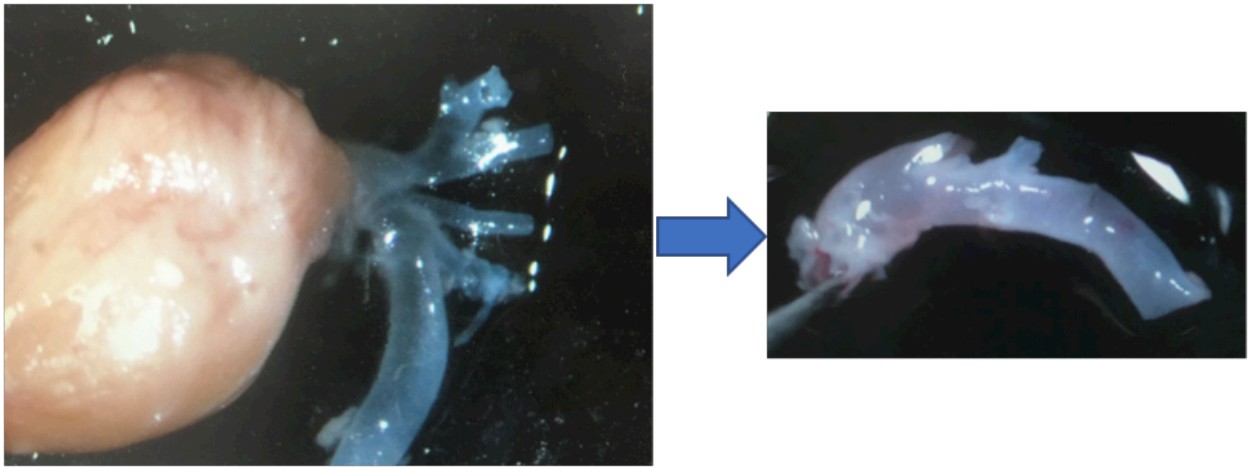

***Figure 35**- Video still images of BAPN model dissection (Left), with isolation of the aortic arch following fine dissection (Right)*

8.2 Results

8.2.1 Death as a result of aortic dissection and consequential rupture is significantly decreased in NE knockout mice within pilot experimentation

Within a pilot study comparing NE knockout mice (n=14) and Control mice (n=38), there was a significant difference seen between mortality rates of the two groups (p=0.0278) when compared by Log Rank statistical analysis. As seen within the Kaplan Meier graph (**Figure 36**) , all mice apart from one within the NE knockout contingent survived the full 28-day period, meaning a 92% survival rate under TAD conditions. In comparison, control mice had a much higher mortality, with only 60% of mice surviving under the same conditions. Deaths from the control group were all found to be of cardiovascular origin, namely Aortic Dissection (**Figure 36 and Figure 37**), identified by post-mortem dissection.

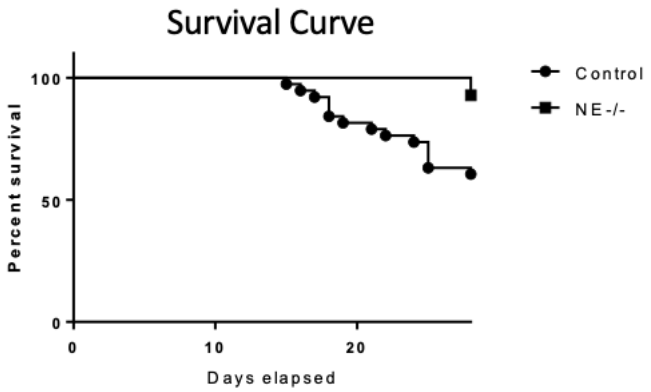

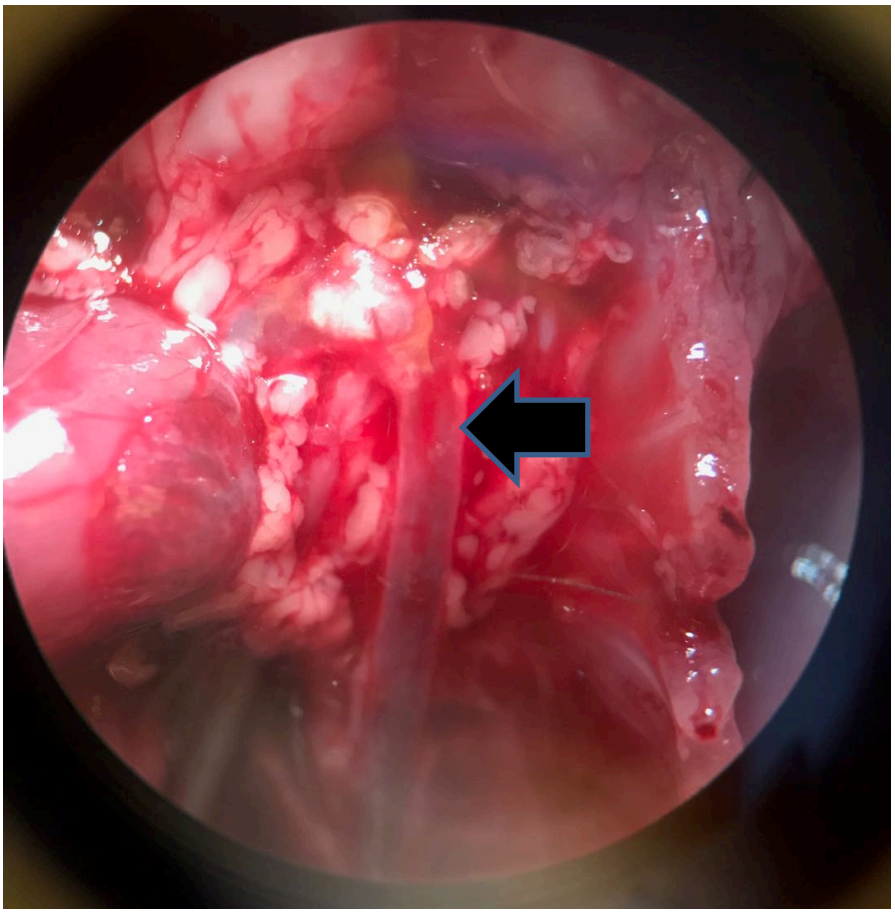

Figure 36*- (Top)- Kaplan Meier survival curve of BAPN-induced TAD mice, administered for 4 weeks to 3-week old mice. (P=0.0278, log-rank test, N= 14 NE-/- and 38 WT Control) (Bottom)- Post-Mortem dissection image for confirmation of cause of death. Black arrow demarcates the location of aortic dissection. No expansion within the thoracic region is visible, but a*

large blood volume was found within the region, followed by identification of rupture.

8.2.2 Intimal tears and Elastic Lamina changes were seen within the descending aorta and aortic arch following BAPN administration in WT but not in NE knockout mice

Following dissection and preparation, staining of the elastic lamina took place, with elastin and H&E staining used to examine its arrangement and condition. Quantification of the distance between internal and external lamina of the vessel was measured by video micrometry and image analysis software. Distance between internal and external layers within healthy procedural control and experimental WT Control mice were significantly changed ($p=<0.0001$), with a drastic increase seen in the size of the medial portion within the aorta of experimental WT Control mice at the same region of the vessel. Similarly, there was a significant difference observed between experimental WT Control and NE knockout mice. Furthermore still, there was no difference quantified between procedural control measurements and NE knockout measurements ($p=>0.05$) for sections taken from within the same portion of the aorta at the same time period of the protocol. Statistical analysis was performed by ANOVA methods.

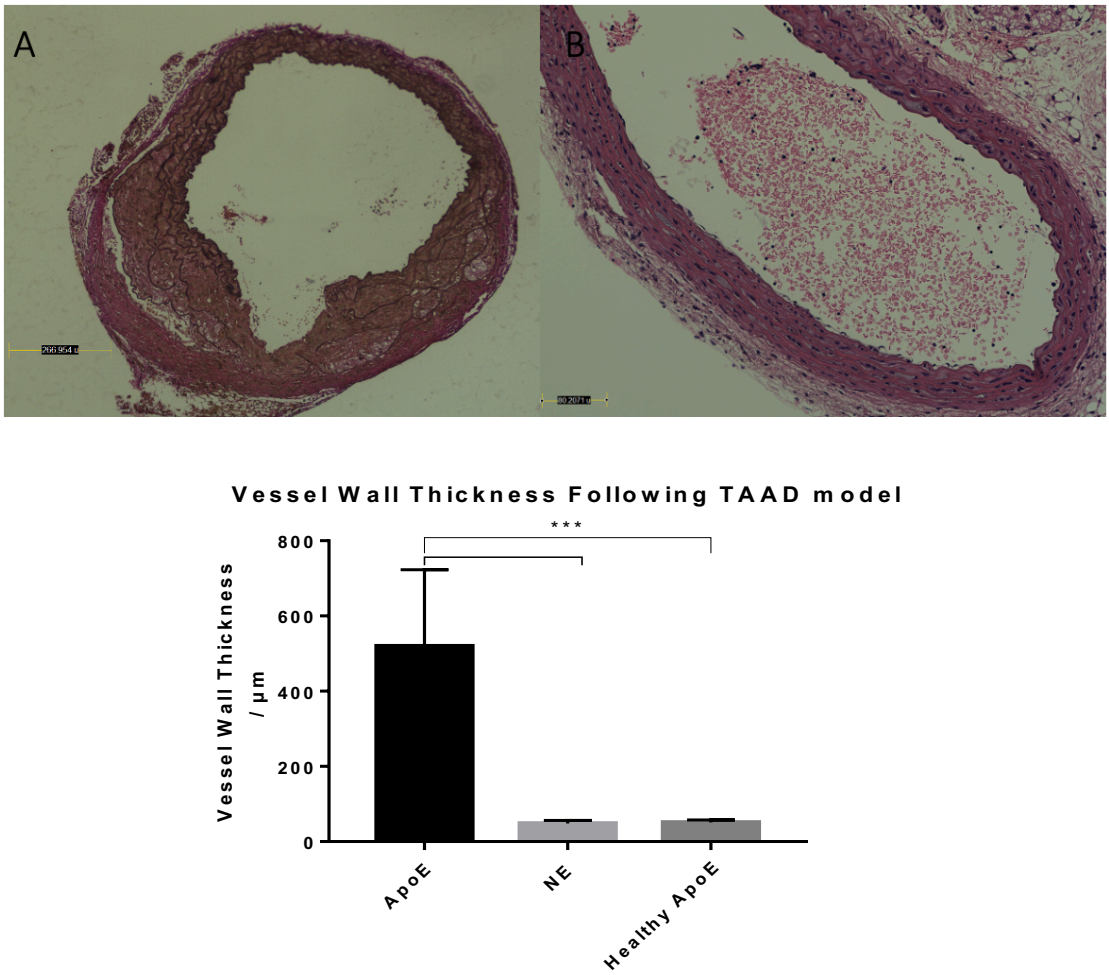

Figure 37*- Top- Representative images of H&E plus elastin stained aortic sections following 4 weeks of BAPN administration, with WT Control displaying dissection (A) and NE Knockout mice with a minimally modified vessel wall (B). Bottom- Quantification of the level of medial dysregulation by measurement of distance between internal and external elastic lamina. (p value= <0.005, Mean +/- 1 S.D. N= 3 per group, 3 slides per animal, ANOVA)*

8.2.3 Aortic dissection was observed in the majority of Experimental WT Control mice, with high levels of rupture also observed

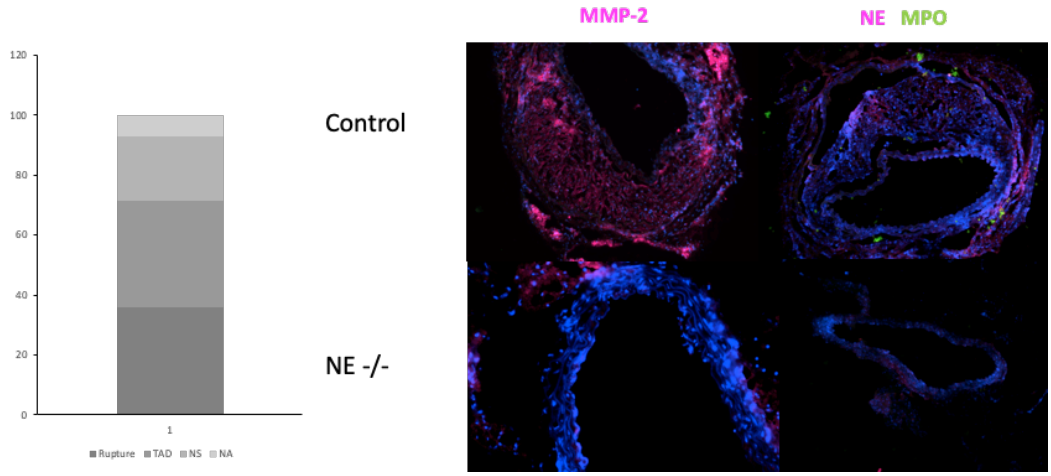

***Figure 38**- Left- BAPN treated WT Control mice analysis and categorized based upon fine dissection and aortic investigation, with categorization of each dissected aorta into Rupture, TAD, Non-Significant and Not affected. Right- Immunofluorescent staining of aortic sections within WT Control (Top) and NE Knockout mice (Bottom), with MMP2 (Left) and NE with MPO (Right)*

Within further rounds of experimentation, sections along the ascending, descending and aortic arch were cut, stained and studied in order to verify the elastin integrity, this was monitored throughout the vessel and across all genotypes. H&E with elastin staining was utilized to visualize these changes. Intimal tears were seen in 80% of aortas from the experimental WT Control animals (**Figure 38**), with more minor modifications to the elastin arrangement witnessed in a further 15% of aortic tissues in WT Control mice. In contrast, pilot NE knockout mice had no visible elastic lamina disruptions and minimal to no medial changes which were widely documented amongst the experimental WT Control mice. Only 5% of Experimental WT Control mice undergoing the BAPN model of Thoracic Aneurysm and Aortic Dissection were found

to not have undergone any noticeable level of vascular wall remodelling. On the other hand, the rate of rupture in the Experimental WT Control mice following the expansion of the pilot study was 35%. The NE experimental group was not expanded due to insufficient mouse litters.

8.2.4 Decreased expression of MMP-2, MMP-8, NE and Myeloperoxidase was observed in NE knockout mice.

Tissue sections from the ascending, arch and descending aorta following exposure to the BAPN TAAD protocol were stained for enzymes and proteins of interest. This was in order to gather further information on the process and mechanism by which differences in phenotype between the two experimental groups are being produced. Staining for NE also served as a validation for the genetic knockout strain being utilized within the study. No NE significant levels of NE were found to be expressed within any NE knockout cohort sections.

Further staining for MMP-2, notable for its association with vascular remodelling and ECM degrading potential was significantly up-regulated in the medial and adventitial portions of Experimental Control vessels (**Figure 40**). This staining pattern was seen most strongly in the more highly remodelled areas of the vessel, however it was still apparent in less modified areas although expression is seen at much lesser intensities. Whilst MMP-2 was present throughout the regions mentioned there were distinct portions of the vessel with raised signal, this suggests concentration is centred on and surrounding a source cell.

Another enzyme of interest with proteolytic capabilities was MMP-8, with staining being carried out on similar sections to that of the NE and MMP-2 stained samples. These ascending and descending aortic sections of both Experimental Control and NE knockout groups were stained for MMP-8 with signal being significantly decreased within Experimental NE knockout group sections. Both groups displayed some degrees of signal, however, the pattern of expression is much more diffuse and intense within the sections of WT Control mice. MMP-8 expression appears to very localized to single cells within the adventitial portion of the vessel in NE knockout mice. Similarly, the predominant staining for MMP8 in WT Control arteries was also within the adventitial region, however, this is not highly localized and instead spreads across much of the adventitia and as well as the media layers of the vessel (**Figure 38**). The most intense signal produced was located at the innermost portion of the adventitia where the elastic lamina ends. Unlike within NE knockout sections, the diffuse expression of MMP-8 in WT Control arteries suggests that it is secreted into the extracellular space as opposed to being contained within a cell in NE knockout arteries.

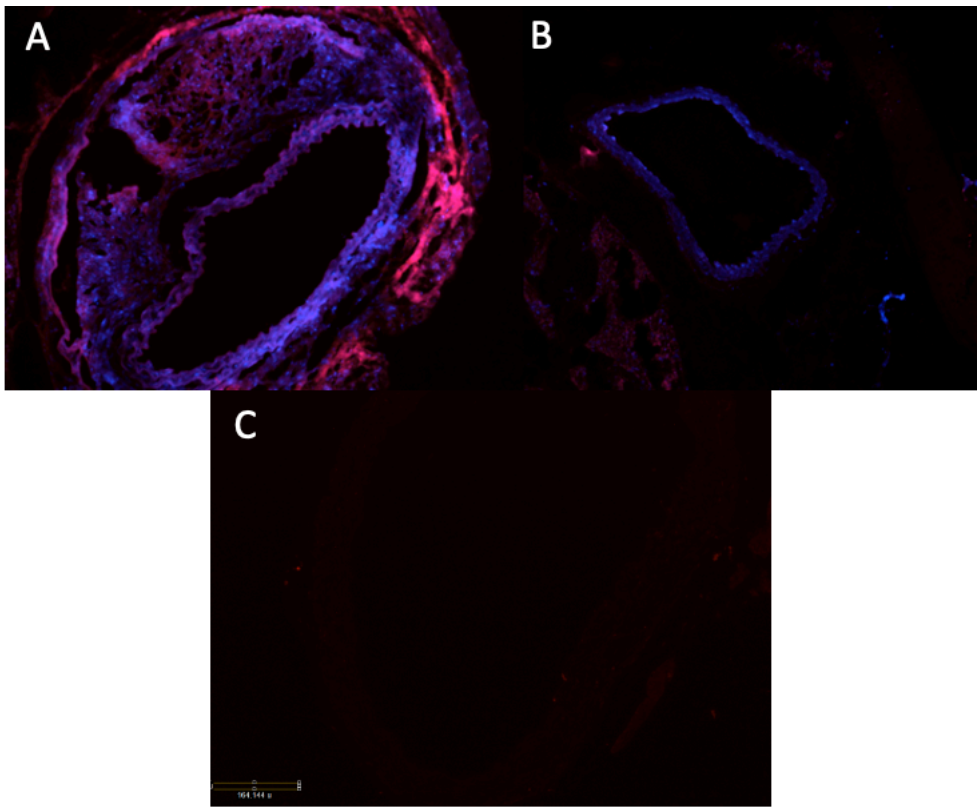

Figure 39*- Immunofluorescent staining of aortic sections within WT Control (A) and NE Knockout mice (B), with MMP8 (pink) counterstained with Hoescht (Blue)- IgG Control- Hoescht absent (C)*

8.3 Discussion

In Summary, this study displays that TAAD can be modelled *in vivo* in a reproducible manner that mimics the human pathology, with localized aortic remodelling and cardiovascular events produced in a number of instances. After the establishment of this model within the group, the Pilot study utilizing WT Control and NE knockout mice alluded to protection from TAAD as a result of the NE gene inactivation. However, due to the low numbers associated with the NE knockout group, as a product of insufficient breeding, this is only an early forecast. Further work is needed to attribute the significant impact of NE upon these conditions, no matter how promising early data is. The TAAD model produced highly comparable results to peer-reviewed

published work, with rates of AD discovered within 80% of histological sections within the WT Control cohort in comparison to published rates of 80% and 81% in papers from Jia et al. and Kurihaha et al. respectively. Rates of death as a result of complete rupture were reported as 40% within both of these papers, as well as within our own study. This suggests that the TAAD model is working reproducibly and comparably to other groups.

In continuation, following the Pilot study, the TAAD model was continued with the aim of looking further into the mechanism behind the pathology. Several proteins were stained for and look to play a role within the development of AD. MMP-2, MMP-8, and MPO were all stained with decreased intensity and frequency within end-stage of NE knockout arteries compared to that of WT mice. This suggests that all of these molecules are likely modulated by NE during TAAD formation and progression. The location of these molecules varies, with MPO appearing to remain intracellular in comparison to MMP-2, and MMP-8 which are a lot more diffusely stained for, suggesting secretion of these enzymes occurs into the extracellular space. These findings agree well with current literature, such as Atherosclerosis attributing Aortic Dissection to MMP-9 levels (177) Similarly, MMP-2 has been well documented as a major contributor to the aneurysmal phenotype in AAA research for a prolonged period with field-leading labs such as that of A. Daugherty and J. Golledge both highlighting its role within murine aneurysm models(46,79). Furthermore still, MPO is used as a marker for neutrophils, their role has been well documented within literature and the localization of this cell type and other immune cells, within the adventitial portion of the vessel as it is undergoing remodelling is to be expected. Building on this point, it has been reported within our own group that MMP-8 and NE aid in the process of macrophage polarization and foam cell formation, respectively(167,201). Building on

this point, knockout of NE interferes with reverse cholesterol transport which impacts upon circulating cholesterol. Levels of circulating cholesterol, macrophage polarisation and foam cell formation beyond this are all known to impact AAA formation and AD. Consequently, the implications on these processes may be the reason for decreased rates of AD and AAA, as discussed in section 7.3. Both MMP-8 and NE are present within the region of MPO expression as well as more diffusely. Both enzymes are known to be secreted and exert effects upon the ECM, with roles in matrix protein remodelling including that of collagen and elastin.

8.4 CONCLUSION

In this experiment, a reproducible methodology for studying TAAD was set up. This model then allowed for the studying of the role NE and other associated proteins play within the TAAD pathology. NE, MPO, MMP-2 and MMP-8 were all shown to be up-regulated in WT Control sections in comparison to NE knockout samples. Within a Pilot study of NE knockout mice, no remodelling was seen within the aorta, in contrast to the 80% AD rate and widespread medial remodelling reported within Control samples, more work is needed to develop this Pilot in order to draw definitive conclusions on the knockout of NE and its impact upon the AD.

9 CHARACTERIZING BASIC BLOOD TEST RESULTS AND AN INVESTIGATION TO IDENTIFY A NOVEL BLOOD MARKER OF AAA PROGRESSION

Due to the large risk of rupture and apparent ever-growing incidence of AAA within western populations, AAA screening programs have been implemented across the UK in order to aid in the diagnosis and consequential early treatment of the pathology. Aimed at most at-risk groups, the AAA screening program monitors the aortic health of men above the age of 65. All men are invited to attend as they turn 65 and anyone who missed or have not previously been tested are able to opt-in at any point. Participants are then scanned using ultrasound to identify any abnormalities in aortic dimensions. The Ultrasound scanning process is a non-invasive procedure taking less than 30 minutes to carry out, this results in high compliance, as it is minimally disruptive. Repeat monitoring is offered every 3-6months for minor enlargements of the vessel, whereas larger expansions of the aorta are referred for further investigations, most commonly resulting in surgical intervention. Patients with rapidly growing AAA may also be flagged by the screening program for further investigations as these patients are also deemed to be of high rupture risk. As a result of the screening program, it has been suggested that patients scanned and identified by the program have half the risk when compared to unmonitored patients(202).

Following the implementation of the screening program 11 years ago, over 700 000 men have been investigated as part of the nationwide program(202). Following this over 1000 men had their aneurysms surgically repaired after a large aneurysm was discovered as a direct result of the scanning, this was in the first 5 years alone.

Resultantly, there is a growing body of data that gives us information on the prevalence of the condition within the UK. Furthermore, we also manage to get more qualitative data on the condition of the aorta with the degree of expansion and rate of surgical intervention. For instance, of the 700 000 men in the above 65 group scanned, only 1.34% of these had an aneurysm measuring above the 2.9cm expansion. Patients with aneurysms considered as larger than >5.4cm hit the threshold used to define a large aneurysm. Within the initial cohort of scans resulting in 1000 referrals of patients deemed to possess a large aneurysm, the false-positive identification within these patients was only 3.2%. Of the remaining group, 870 underwent successful surgical interventions for AAA repair. Intervention rate within this group was over 91% with post-operative death standing at less than 1%. Results suggest the screening program to be successful with studies undertaken by the National Institute for Health Research with a decrease in AAA rupture incidence from 7.1 per 100 000 to 2.6 per 100 000 person-years within a study of 23,300 participants. Continuing on from this decrease, it is calculated that the screening program prevents over 10 ruptures per year within the same group and consequentially saves both lives as well as money.

During the investigations taken place as part of the AAA screening program, many other patients undergo other tests, as males aged 65 and over are at risk for a number of conditions not solely AAA. Resultantly, blood tests and similar diagnostic tests are often performed around the same time as initial scans. From there, we can get a basic overview of an individual's inflammatory status and cardiovascular health. As part of this experiment, we were able to correlate blood markers and screening results. Blood markers have been used to monitor the progression of cardiovascular disease in a number of conditions, such as post-myocardial infarction where troponin levels are used as an indication of cardiac health as it is selectively released at times of cell

damage or death. Furthermore, other conditions such as Chronic Obstructive Pulmonary Disorder, a disorder where NE has a significant influence, have started to develop similar monitoring tests using blood markers. Neutrophil to Lymphocyte ratio (NLR) has increasingly been utilized as a monitoring tool and indicator of disease progression. Within numerous studies, NLR has gained support as a marker and diagnostic tool, as its high prognostic accuracy and lack of need for further testing makes it a cost-efficient, quick and accurate marker that can aid in the diagnosis of patients. Consequentially following these results, we were interested to see whether the same patterns were evident with AAA patients and therefore whether NLR could be used as an indication of AAA progression. At the same time, we wanted to investigate the possibility of other basic blood test results being used as a biomarker for disease progression. This includes the quantity of differing white blood cells, as well as their ratio to one another.

As it is well reported that AAA affects certain demographics more severely than others, we also utilized the clinical data gathered to test whether the same demographic was observed. As a result, we utilized clinical data to look into the demographics of people scanned at St. Georges Hospital London, largely as part of the nationwide AAA screening program, and following this aimed to investigate whether there were any diagnostic blood markers that could be implemented from basic blood test results, similar to that of NLR. Within the cohort of patients we were able to observe both stable and expansive aneurysms, beyond this we could track the change of expansive aneurysms across many years in some instances, tracking how the blood results altered across the same time period.

9.1 Materials and Methods

9.1.1 AAA- Patient Audit

In order to elicit whether there is a group of patients that have a distinct blood profile that is able to predict the likelihood of their aneurysm expanding, work with St Georges Hospital Tooting was undertaken looking into basic blood marker profiles with progression of AAA overtime. This was retrospective data collected from the AAA screening program based at St Georges, with permissions and ethical approval given by St Georges University and Consultants. Patients who matched the criteria of having undergone ultrasound scanning and blood tests within two weeks preceding the scan were selected. From these patients, history was searched, tracking both blood and scan results over time. This was performed for as long as there was a scan history. Blood test results and size of aneurysm at each point, as well as the date, were recorded for analysis. All blood markers consistently measured were recorded and analysed against the same patients' results at the time of subsequent scans. Relationships between markers were then produced in relation to aneurysm size and progression. Analysis of individual cell types was also undertaken, and ratios between cell types were also investigated for any potential relationship between them and aneurysm progression. Patients were divided into both static and expansive groups, with this dependent on status at each scan.

Later Biobank resources and blood samples from Aneurysmal repair patients would be compared against such groups in order to determine if NE level deviation has an impact on which group a patient falls into. This work will now be outlined below.

9.2 RESULTS

9.2.1 Age and gender differences seen within the general population are seen within St. Georges AAA Screening program data

Age and gender differences are often reported within patient cohorts and population statistics when assessing the most at-risk groups for AAA. Population data and statistics have been used repeatedly throughout medical research to spot correlation between variables in an attempt to identify most at-risk patients or to personalize treatment to patients based upon their specific needs. As mentioned previously, basic blood tests can give a large insight into a patient's inflammatory and general health status.

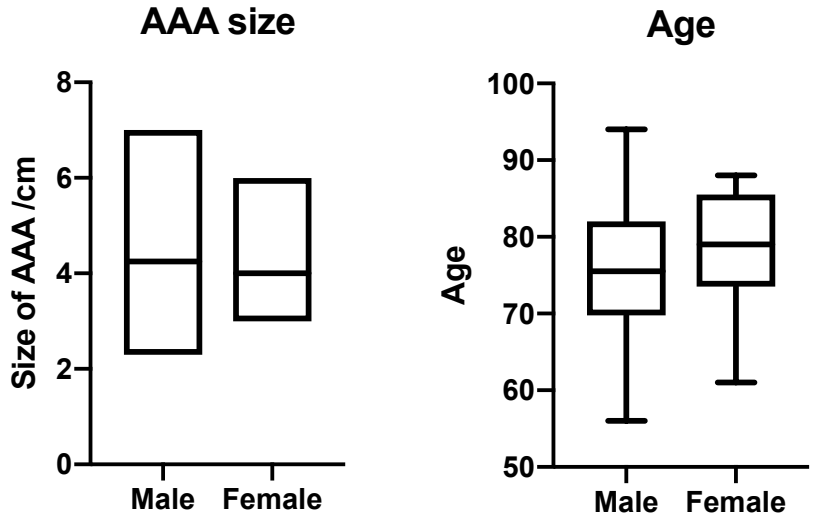

Figure 40*- Graphical comparison of demographic data of patients within the AAA screening program whose data is being utilized. Left, Size of AAA divided by gender displaying maximum, minimum and average size of AAA recorded (p=0.6083, unpaired t-test). Right, Age separated by gender, with maximum, minimum, Q1, average and Q3 shown by box and whisker plot (p=0.2520,unpaired t-test) N= 78 Male, 17 Female*

Results of basic demographic analysis followed expected patterns, with highly comparable age and gender values between the cohort and national population statistics. Resultantly, Males made up a larger proportion of the population, experiencing AAA at a higher frequency to females within the cohort studied. Furthermore still, an increase in age at final scan is associated with worsening phenotype at both initial and final ultrasound investigations. Significant correlation was observed within both stable and expansive cohorts when compared with AAA size (**Figure 41**)

***Figure 41**- Comparison of aneurysm size and age of the patient. Differentiation of patients by expansive (Red, p=0.0207, R^2=0.1363) and After-Stabilization (Blue, p=<0.0001, R^2=0.1034) Pearsons Correlation Analysis) N=95 Patients (50 Expansive, 45 Stable)*

9.2.2 Expansive and Stable aneurysm blood profiles are markedly different between groups, with most significant changes witnessed in monocyte populations from initial scans

Aneurysms are not continually expansive and can go through periods of growth and times of latency. Resultantly, the population cohort can be divided into separate groups by tracking the scanning outcomes at the 6-month intervals. Patients who undergo periods of aneurysm growth and stability were excluded from either group, in order to not interfere or skew with any significant patterns that may be seen within blood profile statistics. However, the excluded patients were looked at individually to see patterns that lead to changes in growth and similarly instability also.

Collated blood profiles consisted of the measurement of basic blood test parameters, with overall white blood cell (WBC) count and quantity of subpopulations of white blood cells measured, before averaging values across patients within each group. The white blood cell population that is implicated most strongly within inflammatory diseases, including AAA, is the macrophage/ monocyte. This variable was highly altered between Expansive and Stable groups; with Expansive patients displaying increasing monocyte levels per 6-month interval (+ 0.45 cells/ μl) when compared to their initial scan. Contrastingly, the opposite was observed within stable aneurysm patients. A decrease of 0.2 cells/ μl across the Stable group was measured when compared to their internal initial controls. Monocyte levels were the most dissimilar between the two groups, and the only WBC subpopulation to display the opposite result across the two groups. Alternately, leukocyte population measurements were highly similar across the two groups with differences between the two groups being as small as 0.05 cells/ μl. Leukocyte changes were seen to increase at a greater rate within the

Stable population compared to the Expansive group. Although unexpected, the Leukocyte pattern of a greater increase within the Stable group was not the only WBC population to increase. Neutrophils also saw an increase, which was also much greater than the increase seen within the Leukocyte population. Neutrophils increased by an average of 0.22 thousand cells/ μl per 6 months within the Expansive group; to almost 0.4 thousand cells/ μl per 6 months within the Stable group. This increase of 1.7 thousand cells/ μl per 6 months change was the most marked increase across the blood profile analysis when comparing Expansive to Stable aneurysm groups.

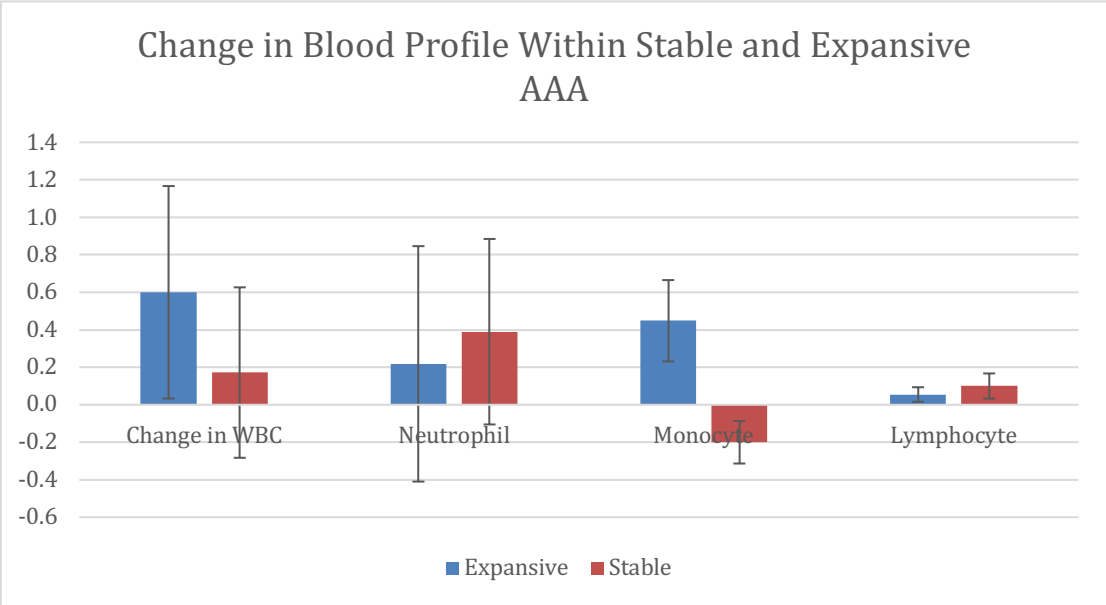

Figure 42-*Alteration in blood profile at 6-month follow up following diagnosis of AAA compared between Expansive (Left) and Stable groups (right). N=95 Patients (50 Expansive, 45 Stable) values represent a mean +/- 1 S.D.*

Overall White blood cell measurements go up drastically within the Expansive group when compared to the Stable group. This is largely in part to the huge change seen within monocyte results across the two groups, as both neutrophils and leukocytes actually increase further within the Stable group. However, due to large variance between patients there is no significant differences observed within this dataset. Much smaller variance is observed within the lymphocyte readings, however the neutrophils

readings are highly different between patients. Monocytes are most dissimilar with smaller levels of variation seen.

9.2.3 All WBC populations are altered in the expansive cohort with most significant changes seen in leukocyte and monocyte groups, however, no significant differences are seen between any WBC sub-population and Aneurysm growth

As mentioned above, WBC levels can be an indication of inflammatory status of a patient. AAA is categorized as a chronic inflammatory disease that leads to the expansion of the aorta. We now know that certain sub-populations of WBCs expand in response to infection and we also have determined that certain cell types play highly influential roles within the AAA initiation and progression process. For instance, macrophages and the proteinases that they produce significantly contribute to the remodelling of the ECM. By inhibiting the invasion of macrophages into vascular tissues or production of MMPs once they have crossed into the vasculature, you could inhibit the pathology at least within animal models of AAA.

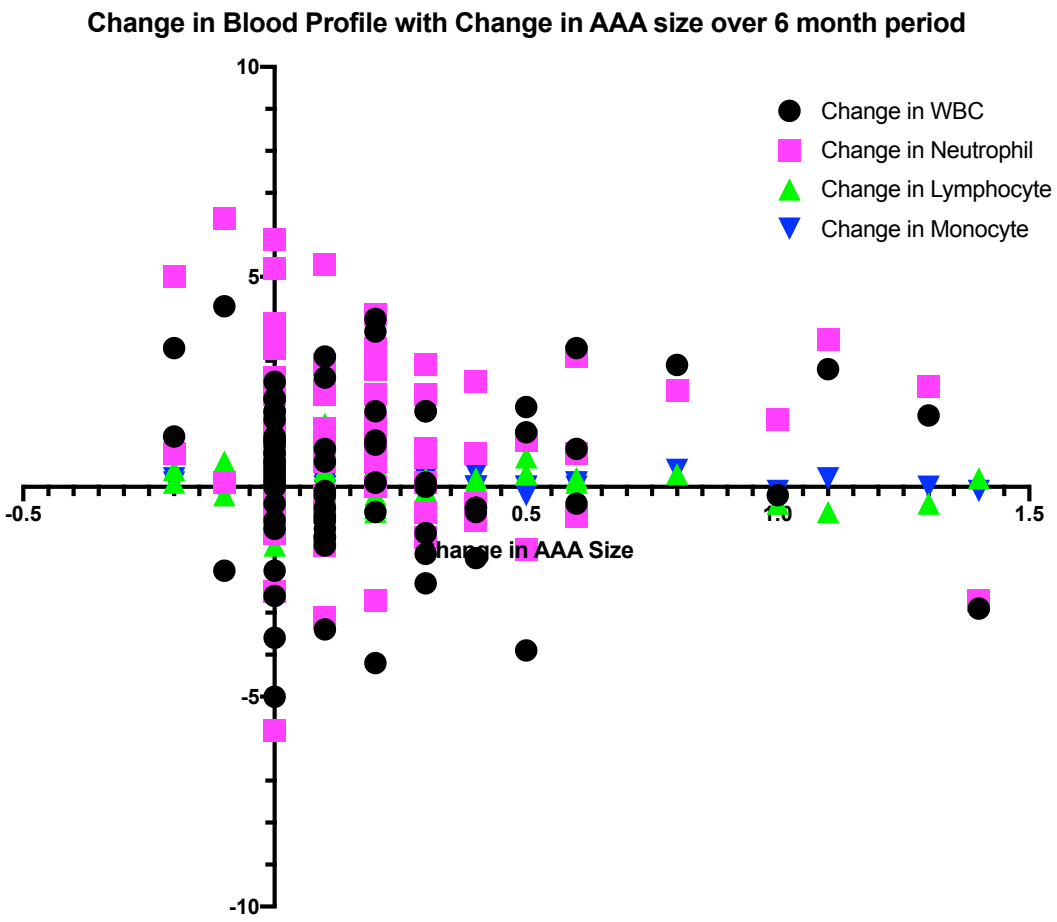

Figure 43*- Changes in size of aneurysm correlated with change in blood profile, with each white blood cell population illustrated with different trend lines. White blood cells (Black, p=0.9854), Neutrophils (pink, p=0.3718), Monocytes (blue, p=0.6020) and Lymphocyte (green, p=0.1813). Pearson Correlation analysis was performed but no significant relations were discovered. White Blood Cell- R^2=0.000004445 p=0.9854, Neutrophil- R^2=0.01051 p=0.3718, Lymphocyte- R^2=0.02339 p=0.1813, Monocyte- R^2=0.003597 p=0.6020. N= 50 patients per group*

All subpopulations of WBCs were modulated between the two AAA screening program groups of Stable and Expansive AAA, with monocytes significantly falling whereas neutrophils and leukocytes minimally increasing on average within the same patients. However, trends within the analysis of WBC populations and size elicit further

information on the relationship between specific cells and the relation to the expansion of AAA.

The monocyte cell population displayed the largest difference between Stable and the Expansive population; this trend was carried over within regression analysis. Expanding patients' data points produced a weak positive correlation (r^2= 0.0489) between monocyte count and aneurysm size. This trend was repeated using both final and individual time-point measurements in comparison to monocyte count (r^2= 0.0334 and r^2= 0.0489 respectively). Stable AAA patients produced a different trend; with negative or near flat correlation when comparing final aneurysm size against average monocyte count and aneurysm size and monocyte count at each time point, respectively.

Contrastingly, the remaining two WBC cell types display the opposing trait, with cell count decreasing as aneurysm size increases in both neutrophils and leukocytes. This trend is remarkably more drastic within leukocyte populations in the Expansive population of the screening program. Interestingly, the Stable group within the same analysis displayed a similar pattern although to a much less drastic extent with expected aneurysm size decreasing at a much steeper rate within the Expanding group in comparison to Stable cohorts, with over a three-fold difference being observed. Differences in neutrophil cell population between groups were even starker, with a small average AAA size fall but increases in the neutrophil cell population within Expansive cohort patients, this is compared to an increase in AAA size with neutrophil count inflation within Stable Aneurysm patients. This is an unexpected finding within both groups. However, when taking the entire dataset into consideration using a one timepoint analysis the pattern is altered significantly. Within neutrophil analysis AAA size increases with rise in WBC sub-populations (r^2= 0.018). Furthermore, Leukocyte

trends become far less angular, with correlation becoming almost flat (r^2= 0.0012) with no apparent relation being seen at the one-time point analysis.

9.2.4 NLR shows no change across a 6 month period when compared across cohorts and at both 6 month and longer-term time-points

NLR has been increasingly used as an indicator of Chronic Obstructive Pulmonary Disease (COPD), with great success. This low cost and low skilled investigation using blood biomarkers removes the need for further invasive, highly skilled and consequentially costly investigations within COPD patients. Neutrophil is highly implicated within the COPD phenotype and the progression of the disease. As a result, verification of whether the same observations in NLR could potentially be seen are worthwhile, as they have a high potential to save time and money within the NHS and further healthcare settings.

All patients who underwent investigation within the AAA screening and had follow up of 6 months or longer were used within this analysis. Initially, Stable cohorts were included to look at the spread in NLR value within this group, this enabled us to see whether this was clustered and highly similar. NLR values within the Stable group were calculated to fall within the 0.16 and 17.64, however, this is highly skewed by the upper-value outlier, which is markedly higher than the rest of the cohort. Excluding this value would produce a more representative range of 0.16-3.52 for the Stable population measured. However, similarly, the Expansive cohort had a value range of between 1.18 and 6.17, with peaks of 1.4 per 6 months expansion rate within this group as opposed to the 0 of Stable data points. Correlation for Expansive groups is very low, with r^2 values of 0.001 for comparison between NLR and long-term expansion rates and this value falls even

further when comparing the expansion rate observed within the first 6 months of observation and NLR, falling to an r^2 value of 0.000001 (**Figure 44**).

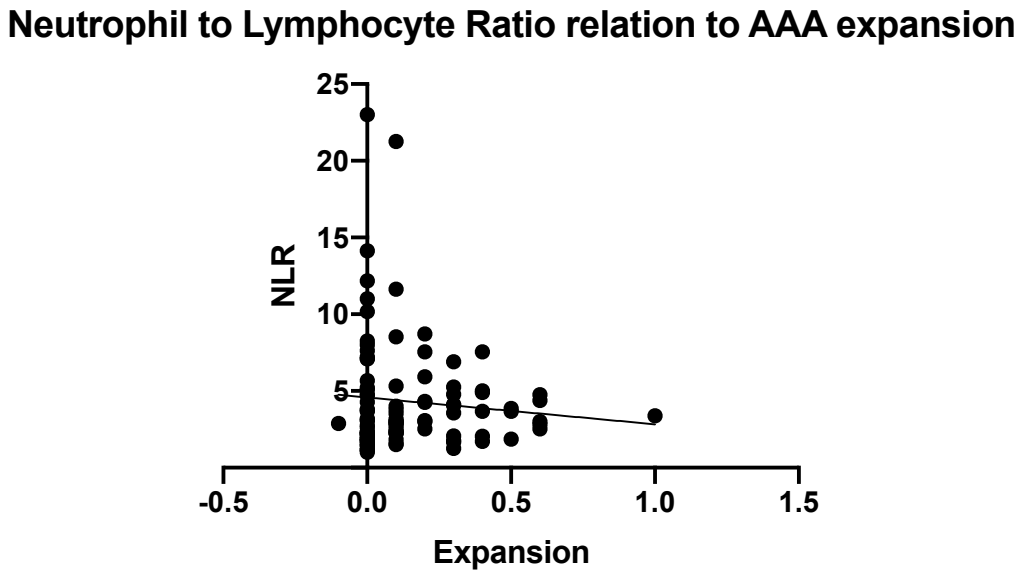

***Figure 44**- Neutrophil to Lymphocyte ratio compared to change in AAA size at the 6-month period post-diagnosis. (p-value= 0.3518, R^2=0.008851, Pearsons Correlation analysis) N= 95 patients*

9.3 Discussion, Limitations & Conclusion

Overall the results from Blood Profile analysis in relation to AAA size were not as expected with no significant correlation found, however not unexpected. No clear, strong and significant results were found within basic blood markers when compared to AAA size or progression of aneurysm. Some changes in patterns were seen within the Stable as opposed to Expansive groups, however, these were not significantly different. For population data, this audit was comparatively low in n number, power and true results may become more clear and apparent with an increase in this, however, at the moment, this is not something that is warranted based on current results.

These results when put into context with what is currently understood within the literature are surprising, as the pathology is accepted as a chronic inflammatory pathology with significant contribution from blood-derived cells(26,203). Furthermore, the manipulation of specific white blood cell populations in previous studies has highlighted the significance of their impact upon the initiation and progression of the phenotype. With regards to the previous data presented within this report, there are also some surprising contradictions, with significance reached in some early work on NE knockout mice in terms of preventing the incidence of AAA within animal models. For there to be no relation to WBC subpopulation levels, Age or Gender, the results appear to go against the majority of the other body of work carried out within this study, and what is also accepted within the literature as strong risk factors for AAA(1,65).

10 DEVELOPMENT- BARTS BIOBANK RESOURCE

Following the success of our *In Vivo* works, which suggests a role for NE within the production of the AAA phenotype, we endeavoured to verify that this result was translatable to the human pathology. It is already known that inhibition of NE within a clinical setting can lead to improved patient outcomes in COPD, and if high levels of NE were found within human AAA tissues it could identify NE as a potential target for AAA treatment. In order to carry out this round of experimentation, collaboration with the Barts BioBank Resource was developed. The Barts BioBank Resource enables collaboration between Clinicians and Researchers at QMUL and Barts in order to further research aims with the use of human tissues, pooling the skills or the Clinical and Academic staff within a singular project. In this instance, our Lab partnered with a group of Cardiovascular Surgeons in order to obtain tissues from AAA repair patients, giving us the ability to analyse and investigate the role of NE within the human AAA condition. This all occurred post-assessment of our research proposal by RedCap and attending meetings with the Barts BioResource panel to discuss the best way in which we could carry out experiments. This concluded in obtaining approval for our study along with ethics.

This study is the next step in determining whether NE has a role within AAA within the human and not just within the mouse models as determined earlier in our work. By carrying out investigations within the human we are able to conclusively determine whether NE is present and if there is a potential role for the enzyme with the production of the phenotype. Whilst *In Vivo* studies used are the gold standard for theoretical and academic purposes, information founded within murine models can be fallible and at times can fail to translate to the human equivalent pathology, this can be

due to a number of factors such as differences in immune systems or small variations between human and murine versions of the same proteins.

10.1 Materials and Methods

10.1.1 Biobank Resource Analysis

In order to look into the potential translational relevance of all *In Vivo* and previous works, collaboration with the Barts Biobank facility was organized. Barts Biobank work to provide contact between researchers and clinicians, this is so tissues can be made available for research purposes. In order to look into AAA and the association of the pathology with NE, contact with cardiothoracic surgeons at Barts hospital was made.

In order to verify whether the effect seen within *In Vivo* works were translatable to the human pathology, human samples were obtained from AAA patients undergoing aortic repair surgery at Barts Hospital, London. Surgeons were consulted, and patients consented for the permission to taken samples during already planned procedures. Patients were made aware that the taking of samples would not change the procedure that they were undergoing and would mean tissues would be analysed for NE expression in order to better understand the pathology. Any patients that were deemed unsuited due to comorbidities were not consented, and therefore no samples were collected. Ethical approval and approval for all work was approved as part of REDCAP application process, with project code NEAAA being utilized and approved at first instance.

Resultantly, weekly surgical lists were looked at to identify appropriate patients who were undergoing aneurysmal surgical intervention. Following this, patients were approached and consent for both blood and aneurysm tissue discussed. If permission

was granted, blood was collected from patients via a central line, and tissues were taken upon the opening of the aorta. Tissues were then divided and preserved in liquid nitrogen or PFA immediately, to ensure sample quality. Blood was immediately taken to the laboratory upon exiting surgery. At this point, blood was spun down at 1300g for 12minutes with supernatant removed in order to isolate the plasma, with cellular content discarded. This was then snap-frozen and stored at -80degrees until a cohort of patients had been collected for analysis. Following the collection of a patient cohort, plasma was analysed for NE expression and basic blood profiles. Tissues were processed alongside, with PFA submerged samples left overnight before rehydration and mounting in OCT prior to sectioning.

Once the tissues were taken, they were processed for analysis similarly to other tissues outlined above within alternate *In Vivo* experiments.

10.1.2 Neutrophil Elastase Fluorometric Analysis

In order to determine whether NE was elevated within human AAA repair patients, blood collected during work with the Barts Biobank were analyzed using an enzyme-based fluorometric assay. Blood taken from patients during surgery were spun down at 13000g for 12minutes in order to remove the cellular content from the sample. A 200µl aliquot of serum was taken before serial dilution was performed, with 9 final dilutions and final volume of 50µl per read sample. This was the performed for each patient within a 96-well plate and consequential steps were followed in accordance with Abcam kit instructions. Patient sample dilutions were then compared against a standard curve for NE. 96-well plates containing samples were read with output data analysed using GraphPad Prism statistical analysis software.

10.2 RESULTS

10.2.1 Extra Cellular Matrix proteins are deregulated within Human AAA tissue samples similar to that of AAA animal models

A part of investigations into verification of the translatability of our *In Vivo* findings, collaboration with the Barts BioBank resource led to the formation of collaborations with cardiovascular surgeons at Barts Hospital. Following agreement with these surgeons, patients upon their surgical lists were identified when determined appropriate and consented for inclusion within our study. Once patients had given consent and were undergoing AAA repair procedures, tissues were collected during the procedure. By taking both blood and aortic tissues we were able to identify both expression and localization of NE expression within relevant aspects of the AAA patients.

Patient aneurysm samples were collected and processed immediately following AAA repair surgeries, with tissues snap-frozen prior to being mounted within OCT and sectioned by cryo-sectioning methodologies. Sections were collected from the blade using poly-l-lysine slides before staining. Stains were applied to sections of aneurysmal and healthy internal control aorta in order to visualize the ECM proteins, namely collagen and elastin, before imagining using light microscopy techniques were employed utilizing the EVOS system.

Within staining for both Elastin and Collagen, AAA patient samples displayed high levels of medial dysregulation with diseased samples. Collagen patterns generated were non-uniform and disjointed wave-like structures with clear breaks and gaps in sections, dissimilar to continuous homogenous healthy regions. Collagen stained sections had clear areas of difference, with some regions of the vessel possessing more tightly arranged fibres compared to the areas of medial damage.

Within Elastin staining, a similar pattern was observed with the loss of consistent elastic banding seen within healthy vessels being replaced by highly fragmented patchy staining of elastin. The areas in which most fragmentation has occurred was localized to the portions of the media with most disruption to both Collagen and Elastin fibres, with some regions of stained sections appearing relatively more structured and healthy compared to others. In continuous homogenous healthy regions, elastin fibres are arranged in continuous bands as opposed to the fragmented appearance seen within the aneurysmal aortic tissues.

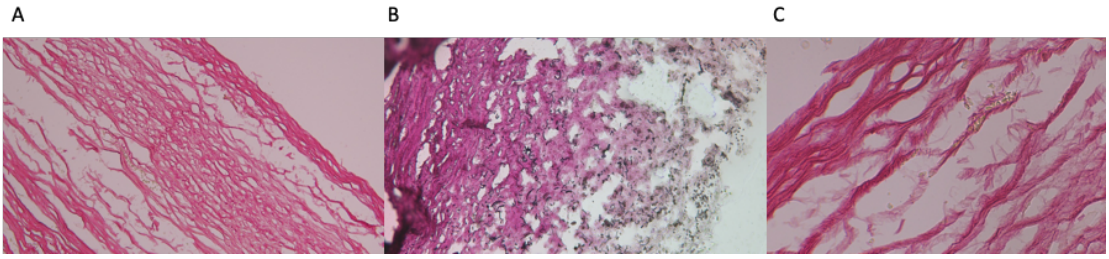

***Figure 45**- Human aortic samples from different patients, stained for (A) collagen, (B) collagen and elastin and (C) Collagen*

10.2.2 Healthy and aneurysmal aortic tissues have differential expression of NE and MMPs, with co-localization of the two enzymes found within areas of extracellular matrix breakdown

Following the staining of ECM proteins, the identification of NE within Human tissue samples was carried out in order to elicit whether NE could have a role within the human pathology. From works carried out within the Ang II *In Vivo* models, the staining of NE, as well as MMP-2 and MMP-9 were present within AAA sections. Human sections were stained for NE, MMP-2 and MMP-9 using antibodies from Abcam, with both staining positive within human aneurysmal aortic tissues. Both NE and MMP are apparent within areas of high medial degeneration and remodelling.

Furthermore, the two enzymes were co-localised at the points of the most prominent changes to the vessels structure, although the majority of MMP2 staining is dispersed and not colocalised to NE expression. Similarly, MPO and NE majority of expression is within different areas. MPO staining is highly localised to the intimal portion of the vessel and areas of significant damage such as the regions of dissection. NE is seen within the same areas however also more diffusely, most commonly situated surrounding unclear staining (**Figure 46**). In both instances the visualisation of the elastic lamina seems to be autofluorescence although the negative control counters this. It is possible that an inappropriate part of the tissue was used for this instance.

In comparison, this staining was not found within comparable staining of continuous homogenous healthy aortic tissues from the same patient. MMP2 staining also appeared more diffusely with areas of the enzyme scattered throughout the vessel wall, however, NE appeared far more localized within sections stained. Localisation of NE was contained to the cytoplasm in the majority of instances, however, there were exceptions to this with small regions of non-cellular NE staining (**Figure 46**).

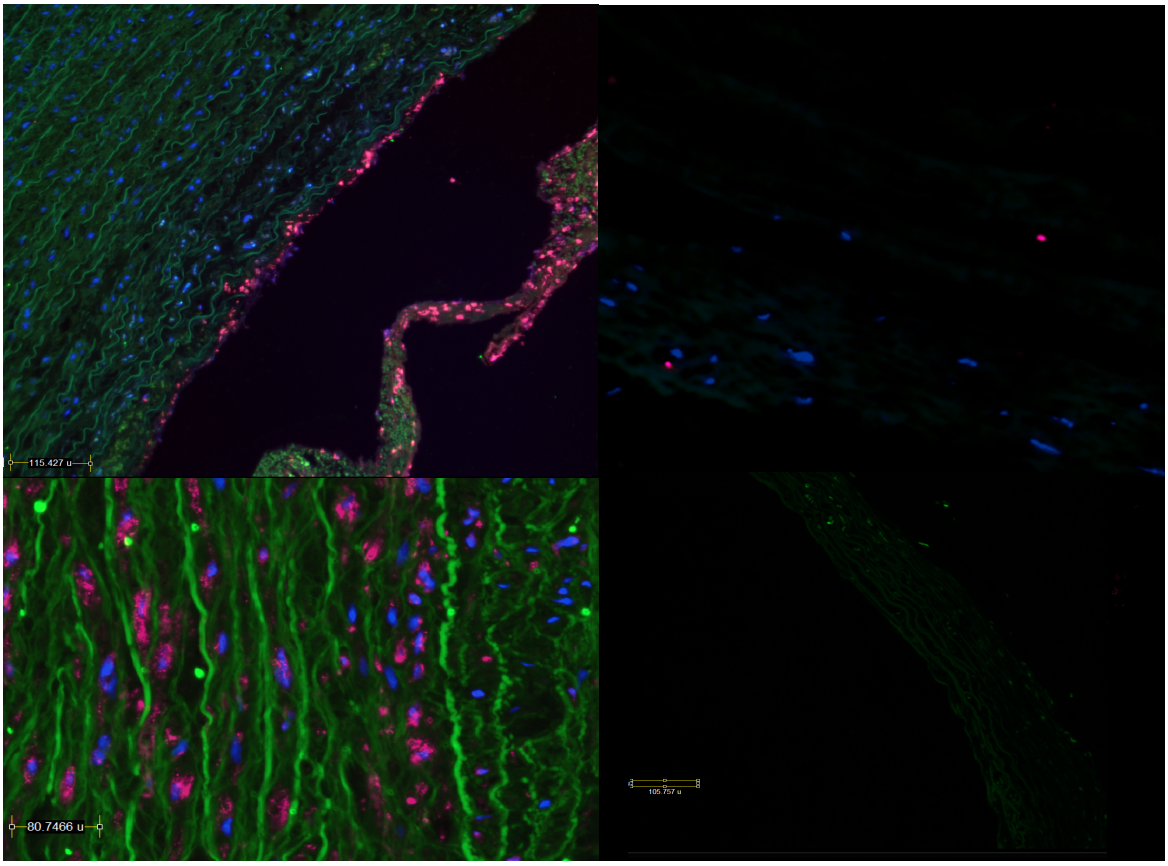

Figure 46*- Identification of NE, MPO and MMP-2 within human samples obtained during AAA repair surgery. Top Left- MPO(Red) and NE (Green) Top Right- Health Human Aorta stained for NE (Red) and MMP2(Green) Bottom Left- indicates area of MMP-2 staining with small portions of co-staining for NE(Red) and MMP2(Green). Bottom Right- Negative IgG Control*

10.2.3 Human blood samples collected from AAA repair patients displayed higher levels of NE activity when compared to Healthy Control blood samples

Fluorometric assay analysis of human blood samples collected from AAA repair patients and unaffected Control patients showed a higher level of NE activity in AAA surgical repair patients (n=5) than that of controls (n=3) (**Figure 47**). Samples fluorescence was measured in kinetic mode following the protocol set out in the Abcam

kit purchased. Reactions were measured in kinetic mode over the period of 30minutes to allow for the action of enzymes. On average, over double, the amount of activity was seen within AAA patients as opposed to Controls. Although dissimilar average values, significance was not reached, P=0.1699. AAA patient blood test values were largely within healthy ranges (**Table 5**), with little variability identified asides from within neutrophil and age variables.

Table 5- Demographic and Blood profile averages of AAA patients who underwent AAA repair surgery and donated tissue and / or serum for analysis.

Marker	Average Patient Value	Healthy Range
Age	54.4 (+/- 23.2)	
AAA Size (cm)	4.98 (+/- 0.64)	
Gender	Male- 78 (82.1%) Female- 17 (17.9%)	
WBC (cells/µL)	6.4 (+/- 0.7)	4-11
Neutrophils (cells/µL)	3.58 (+/- 1.39)	2-7.5
Lymphocytes (cells/µL)	2.2 (+/- 0.4)	1.5-4.5
Monocytes (cells/µL)	0.7 (+/- 0.2)	0.2-0.8
Eosinophils (cells/µL)	0.1 (+/- 0.0)	0-0.4
Basophils (cells/µL)	0.05 (+/- 0.05)	0-0.1

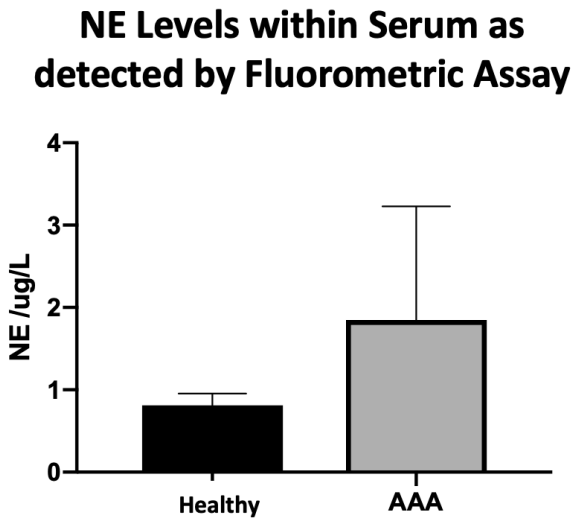

Figure 47*- Comparison of NE activity obtained from an 100microliter aliquot of serum from Control patients and AAA-repair patients (p=0.1699, t-test)*

10.3 DISCUSSION AND LIMITATIONS

Throughout the analysis of AAA patient repair tissues, NE was repeatedly found to be elevated on average within this group in comparison to the unaffected group used as a control, however significance was not reached within this study (**Figure 47**). ECM proteins were, as expected, highly remodelled within the diseased cohort with elastin fragmentation evidenced and H&E stains displaying the changes to vascular structures that occurred as a result of the AAA pathology (**Figure 45 &46**). These changes have been widely reported, suggesting our tissues are consistent and representative of AAA, consequentially we can assume further works to be indicative of the AAA phenotype, however, evidence of tissue damage as a result of the freezing process utilised may diminish the conclusions able to be drawn from this aspect of investigations (**Figure 45**). Further staining of tissues isolated from the same region of the same aorta was performed in order to increase the understanding of proteins involved within AAA and answer one of our primary research questions of 'Does NE play a role within the human AAA pathology'. Resultant staining suggests that NE is positively stained within areas of aortic remodelling, located predominantly within the medial and adventitial portions of the vessel. Staining of the enzyme was seen within areas of higher degrees of vascular change, although quantification is necessary to determine quantifiable differences, however comparatively no NE was stained for within healthy control portions of the same vessel (**Figure 46**). Furthermore, NE also co-stained with MMP2 similarly to staining carried out within *in vivo* murine models. This suggests that pathways responsible for the AAA condition identified in animal model work could be transferred across to the human pathology. This pattern of co-localization has been identified within other pathologies, most thoroughly discussed has been the role of NE within COPD and respiratory conditions. NE has been proven to activate MMPs(164),

leading to worsening of respiratory conditions where remodelling breaks down the functional structures of tissues. Furthermore, still, NE has been reportedly responsible for further potentiating the pro-MMP and pro-inflammatory environment, not only activating MMPs but degrading their inhibitors(204). The cause of this phenomenon has also been investigated, with risk factors for AAA such as smoking being a reported trigger(170).

Resultantly, work within this chapter points towards NE having a negative impact on the AAA condition, aiding in potentiating the degrading enzymes responsible for a large part of vessel damage. Changes in NE was tested with the taking of blood from AAA repair patients, in order to identify whether it was up-regulated within the most severe instances of AAA. Activity of NE was not significantly different between the two groups tested within a relatively small pilot study (**Figure 47**). This suggests that with the expansion of the work a significant difference could be observed between healthy controls and AAA patients. Developing this further could lead to the identification of NE as a biomarker of AAA progression, however, work is still too early to indicate whether this will be at all possible.

Limitations to this work however do exist, with the processing of the materials and tissues potentially influential in the outcomes produced. As seen within **Figure 45** and **Figure 46** there appears to be artefacts from the freezing process, damaging the tissue and leading to potential false conclusions. Beyond this, due to problems with the slide there are no scale bars for the same images contained within **Figure 45** and therefore we are able to draw little from this resource which could have provided invaluable information. Subsequent tissues stained within **Figure 46** come from a separate aorta and therefore were harvested at a different time, therefore it may be the case that this was unaffected, however as the protocol for processing remained consistent, it is

possible that this experiment result also has been skewed. Resultantly follow-up work to verify these results should be carried out, alongside quantification of any differences observed within IF staining.

10.4 CONCLUSION

Histological analysis of AAA-repair patient samples stained positive for NE and displayed patterns of a high level of remodelling, although quantification needs to be undertaken prior to conclusions being drawn. Minor areas of co-staining for NE with MMP2 was localized to the most damaged and remodelled regions of the stained vessels, however the majority of MMP expression was not adjacent to any NE signal. ECM proteins stained for displayed the highest level of remodelling within the medial portion of the vessel, the region where NE was most commonly stained. These patterns were not seen within healthy control sections, with ECM protein structure more consistent and regularly arranged, compared to AAA-repair patient samples. NE was not expressed within the healthy control samples stained, suggesting NE may play a role within the AAA phenotype in humans.

Further work with the blood of the same patients displayed no significant difference in activity of NE within AAA-repair patients in comparison to healthy controls. This dampens the argument that NE has an influence within the AAA pathology, however further work is needed in order to fully elicit the role of NE within the human pathology following contradictory previous results within alternate avenues of investigation.

11 GENERAL DISCUSSION

During this project, there was a number of key hypothesise addressed in order to understand the role of NE within AAA. Development of imaging methodologies were imperative for monitoring of vessels in a time-course manner, allowing for the observation of how the AAA pathology develops over time and any differences that occur as a result of the genetic knockout of NE. Following on from this, the understanding of NEs impact on AAA was the primary focus, with secondary and tertiary aims of improving our knowledge of the mechanisms that contribute to the AAA pathology and whether findings of our main investigations were translatable to the human condition.

Imaging modalities used within this group of work were all learnt and developed during this PhD. Both contrast-MRI and US imaging were utilised as they were regarded as the most appropriate methods to visualise vasculature changes and the changes in flow patterns that are associated with these. This was determined following research into alternatives, as well as consultation with the Cancer Imaging group. Optimisation of protocols and procedures were carried out in collaboration with the same group, in order to achieve the most accurate and thorough process. MRI reached the point where semi-automation became possible, eliminating operator bias whilst gathering vast information in a 3D format. Volumetric measurement of the vessel consequentially became possible, with this being suggested within the literature to be a better indication of rupture risk following analysis of clinical outcomes(182). However, at the same time, clinical observations are most commonly carried out with the utilisation of US due to the modalities improved ease of use, lower levels of training required and ability to gather functional and flow information on the vessel. Therefore,

a dual scanning protocol was carried out, to gain a greater data bank on each vessel. This meant the benefits of both methods were gained, with one method verifying the results of the other, with no discrepancies observed between the two.

The primary focus of this work was the understanding of NEs role within AAA. This developed from AAA to TAAD. Multiple animal models were employed, comparing WT with NE Knockout mice, in order to see the difference genetic loss of NE had. Initial AAA models both resulted in the observation that loss of NE was protective against the induction of AAA within animal models. Later, the same was seen within TAD and rupture, with loss of NE being protective against the remodelling and rupture seen within Control mice. These findings were developed further, with histology, RNA analysis and proteomics carried out to develop the understanding of how this result was occurring. Modulation of MMP2 and MMP9 were one pathway investigated, due to its huge significance in the initiation process(205). Changes in levels of expression were observed, with a reduction in NE Knockout sections observed. Furthermore, structural organisation was hugely significantly different and this was seen across the three models, a phenomena already established within human and animal model tissue dissection (11,206). Most notably within TAD, this was significantly different with medial degradation and dysregulation apparent within Control animals. Distance between internal and external elastic lamina were comparable between procedural controls and NE Knockout mice however both were vastly different from treated WT mice. Following the identification of these changes, we aimed to identify novel pathways using a proteomics approach (11). Fractionation of the aortic proteins into there portions allowed for the focused identification of both proteins and compartments of significant interest within the disease, these consisted of; loosely bound proteins and novel peptides, intracellular proteins and extracellular

matrix proteins. This approach and consequential analysis produced a number of proteins of interest, some of which were looked into further. COPS 8, Caveolin 2 and TBL1x were verified as being different between WT and NE Knockout mice. This suggests that these proteins may warrant further investigation.

11.1 Similar conclusions have been reached within $CaCl_2$ and Ang II experiments, with NE Knockout mice significantly less impacted by both models when compared to Control mice

The basis of this round of experimentation was to answer the research question of 'Does NE play a role within AAA?'. Experiments were undertaken within both Control and NE Knockout mice so that observations could be made that display the difference loss of NE makes within the AAA process. The $CaCl_2$ model and Ang II procedures were undertaken in order to verify the results of each respective model were physiological effects attributable to the AAA phenotype and not a consequence of NEs involvement solely within the models triggering mechanism. For instance, blood pressure measurements were carried out within Ang II experiments to ensure loss of the NE gene does not impede the rise in blood pressure that in turn results in the production of the AAA phenotype.

The conclusions drawn within both Ang II and $CaCl_2$ model experiments were highly similar. Induction of both models resulted in an aneurysmal phenotype being produced within the majority of Control mice, with significant expansions of the aorta observed by scanning and post-mortem dissection methods. However, within NE Knockout mice the occurrence of aneurysms was decreased with fewer expansions of the infrarenal aorta being produced or found within NE knockout experimental mice. Further

investigation as to the histological differences between groups resulted again in dissimilar results between genotypes, although quantification analysis is required prior to definitive conclusions being drawn. However, early indications suggest vessel structural proteins follow in the same pattern as seen within expansion results, with minimal alteration to collagen and elastin, both highly remodelled within the AAA phenotype (61,207). Histologically, NE Knockout mice that had undergone one of the AAA models appeared akin to procedural control mice. Changes in the elastic lamina that were seen within WT mice, with widespread elastin breakage and medial disruption, were absent within NE Knockout mice. Similar changes were also seen within collagen staining when comparing between the two groups, with collagen structure and arrangement preserved within NE Knockout mice while high levels of collagen dysregulation were evidenced in WT mice.

Within Ultrasound and MRI scanning quantification of aortic expansion, the same patterns emerged, with WT aortas expanding further than those of sex and age-matched NE Knockout aortas. Ultrasound scanning provided both quantitative and qualitative data, with Colour Doppler results visualizing hemodynamic changes occurring in the vessels over time. Quantitatively, US observed a much higher level of expansion within WT mice cohort in comparison NE Knockout cohort mice, this occurred in both AAA models. Similarly, MRI reported the same phenomena. However, within MRI studies the increase in infrarenal volume within $CaCl_2$ mice was lower than that seen within Ang II studies. This is most likely due to the higher localization of the $CaCl_2$ model (84), with application occurring to a select portion of the vessel in comparison to the global Ang II model, which has implications on the entirety of the mouse (46), with systemic pressure increasing and consequentially systemic consequence. Furthermore, the Ang II model is known to produce a far more severe phenotype in comparison to

the $CaCl_2$ model and therefore diametric expansion has the potential to be much greater generally between the two models. Qualitatively Colour Doppler US displayed the production of a false lumen in some instances within Control mice, with significant but less severe changes observed in other mice belonging to the Control cohort with Ang II infusion procedure, whereas minor to no Colour Doppler US changes were seen within NE Knockout vessels, matching the findings of Dissection investigations. Similarly, within $CaCl_2$ model experiments more severe disturbances to laminar flow were recorded within Control cohort scans in comparison to NE Knockout mice, although the changes in vessel dynamics were less severe within this model when compared to the Ang II results(208). Again, this could be a result of the model being more severe and often producing large volatile aneurysms prone to rupture in comparison to the more minor changes seen within the $CaCl_2$ model experimentation.

Overall, there were a lot of comparable results and findings from both rounds of investigation into the effects loss of the NE gene has within Ang II and $CaCl_2$ model procedures. The findings suggest loss of NE gene to be protective within AAA animal models. Loss of NE gene led to the abolishment of AAA within both Ang II and $CaCl_2$ models, this loss of aortic expansion was accompanied by the loss of hemodynamic changes when analyzed by US imaging modalities as well as the diminution of histological changes to the extracellular matrix proteins largely responsible for the development of the pathological phenotype.

11.2 Comparisons can be drawn between TAAD and AAA, with similar results seen within Pilot TAAD work and AAA models with relation to the impact of loss of the NE gene

Many of the observed contributors to changes seen within Control tissues and Control animal phenotypes have been highly similar between both the TAAD and AAA models. Involvement of MMPs, NE and immune cells has been visualized by histological and RNA analysis methodologies both within current studies and previous (209). On top of this, the results within some elements of study within NE Knockout mice have been of the same outcome, suggesting a common causal or at least contributory pathway that exists in both AAA and TAAD(111).

NE Knockout mice undergoing animal models for both AAA and TAAD both showed decreases in incidence of the respective conditions, with decreases or abolishment of vessel remodelling and downregulation of key proteases such as MMP-2, MMP-8, and MMP-9, all previously identified as pivotal within the underlying pathological mechanism(9,103). Further work is required for full understanding of the pathways linking these three molecules to NE in the aneurysm pathology as a whole, as without a conclusive idea on the underlying disease mechanism the identification and development of a successful clinical treatment is far less likely. The use of a proteomics approach within one of the models has identified potential novel targets for the furthering of this research, with TBL1x, Cavanin-2 and COPs-8 all significantly highlighted within fractional analysis of the aortic tissues generated within the Ang II model. However, this work is in its infancy, and translation of work to the human pathology is necessary in order to boost chances of being able to conclusively state the pathological mechanism underlying aneurysm development in the human.

Consequentially, work on NE and its potential role within AAA was carried out in the human in an aim to further the project and our understanding of the disease as a whole.

Final developments of the project allowed for the verification and translation of information developed within murine studies to the human pathology. An audit of blood profiles of an AAA screening program produced information on the complex nature of the disease. NLR and blood cell values were compared to expansion amongst other characteristics, with no significantly strong relationship identified, contrary to expectation. NLR is a highly accurate indicator of systemic inflammatory conditions(171)(210). The identification of a biomarker would greatly improve monitoring and diagnosis of AAA, with NE being a candidate for this. Consequentially, a pilot study looking at the expression of NE within human samples ensued. Tissues and blood were obtained from patients undergoing AAA repair surgery. The following analysis was focused on the expression on NE within both types of sample, with both staining positive for the enzyme, in contrast to healthy control tissues. NE and MMP2 were identified in regions of high dysregulation, as expected for MMP levels when compared to published literature(205), as identified by histological analysis. However, NE activity within AAA patients was on average similar within repair patients when compared to healthy controls, this was unexpected from previous results from this body of work but predicted by previous studies on NE in AAA (142). Development of this Pilot study is needed in order to identify whether this is a representative result, as due to the small sample size we are unable to put NE forward as a definitive biomarker. If upon expansion of the study, significance was reached, there is a possibility that this could have great potential and hold benefit for clinical diagnostics.

In summary, NE appears to play a role within the AAA animal model pathology, although no clear link can be claimed within the human phenotype. Genetic loss of NE is protective against animal models of AAA, with no significant increases in vessel diameter observed by MRI or US when compared with the procedural controls. Development and optimisation of MRI and US analysis allowed the study of vessels over the entire time course of experiments, with this protocol translatable to any size or power of vessel or MRI respectively. Greater understanding to potential contributing mechanisms was reached, with identification of new investigative targets within the AAA pathology achieved and confirmed by proteomics and histological analysis. The work *in vitro and in vivo* was continued in human studies with surprising results within pilot experiments. Further work is needed before we are able to suggest that NE has an real significance within the human pathological phenotype as *In Vivo* results did not translate to similar Human Pilot results.

11.3 STUDY LIMITATIONS

Throughout the experimental process, there are always investigations that are beyond the scope of the study that may yield beneficial information on the topic at hand. NE is implicated in a number of processes, many of which are discussed within this project. The primary focus of this work was to determine the role of NE within the AAA process, resulting experiments lead to the conclusion that genetic knockout of NE led to inhibition of AAA. This was followed up within preliminary Human works. The next step within this process would be to prove the human link further; as well as to ascertain whether the changes in phenotype seen within the 3 animal models studied were reproducible with pharmacological knockout of NE. By carrying out these two rounds of experimentation we would be able to determine the potential benefit that the

inhibition of NE could have on AAA treatment. One major limitation was the lack of significance within the AAA screening program data. Expansion of the human pilot study would enable the development of in depth analysis, helping to determine whether NE could be regarded as an indicative biomarker of AAA progression.

Whilst we have extensively outlined the benefit that loss of NE has within AAA models we have not taken it any further, for instance with the pharmacological knockout of NE. Use of a pharmacological agent to inhibit NE, within animal models initially, would help determine whether targeting the enzyme for therapeutic benefit would be a possibility. Both administration of NE prior to induction of AAA, as well as a regression study where any inhibitor was administered post AAA induction would produce a comprehensive overview of where NE has its greatest impact. Furthermore, this would give an indication of whether any treatment would need to be administered as a prophylactic to most at-risk groups, or if once aneurysms are identified a NE inhibitor could still be effective as a form of treatment. Within the second instance, the stabilisation of aneurysms and the consequential reduction of surgeries or death due to rupture would both be regarded as a positive and significant result, improving the current therapeutic options.

Furthermore, *In* Vitro results were inconclusive with no concrete significant differences observed, any hypothesis of a relation between AAA-markers and NE were not fully conclusive. Whilst these hypothesis were, in-part confirmed within AAA-models, continuation of this work looking into further markers could be of benefit to the understanding of the overall pathology. However, results produced within cell culture *in vitro* work are not always representative of the action of cells within a tissue system, as cell to cell, interactions can have a large influence on expression and reactions occurring within the cell. Therefore, whilst indicative and informative, verification of

in vitro results with *in vivo* works should always be considered as stronger evidence for transferable insights, especially within conditions involving a multitude of cell types. Similarly, *in vivo* works have their own downfalls, with murine immune systems, specific protein constitution and other processes differing from the human and consequentially direct translation from animal models to the human condition are not guaranteed. Consequentially, the gold standard of research is always proof of concepts, first developed within both *in vitro* and *in vivo* studies, within human experimentation. Whilst the production of insight into the function of NE with the AAA phenotype has been successful, the assessment of NE activity has been limited to human work. Transferring this to mouse procedures could further emphasise the differences between WT Controls and NE Knockout mice within affected tissues. RNA analysis and histology work on these tissues were indicative of increased levels of NE within the affected areas, however, furthering this with functional analysis would strengthen the argument for NE making a causative difference to the AAA pathology.

11.4 Future Directions

Within this work, NE has been put forward and illustrated as having a role within AAA and TAAD, the exact manner by which it takes its effect have been looked into with implications in the regulation of MMPs within the pathologies highlighted. However, further work to fully understand the mechanism behind AAA and TAAD, as well as NEs role within this, is still necessary. The highlighting of further implicated proteins, namely TBL1x, Cops 8 and Caveolin 2 are under investigation for their role within the NE associated mechanism and its relation to the aneurysm pathology at large. Whilst

NE has a high substrate promiscuity already established, it is highly possible cleavage of a novel protein or peptide sequence by the enzyme could be responsible for the physiological effects observed within animal models. Further analysis of proteomic results could potentially yield information regarding the modifications made by NE, and as a result, provide influential insights into aneurysm formation mechanisms.

Beyond work already underway, the use of currently utilised medicines that influence NE could have huge potential. Following the influence of genetic NE knockout upon the models of aneurysm, a pharmacological antagonist for the same enzyme should be looked into. Pharmacological agents already exist and have been used in academic studies with beneficial physiological effects(167). Beyond this trials of already approved human medicines, used within COPD and previously discussed conditions could potentially lead to repurposing of drugs. An intervention study, firstly within rodent models, using NE inhibitors whilst undergoing AAA and/or TAAD induction should be of utmost importance. This will confirm whether NE could be considered as a target for the production of a pharmacologic treatment of AAA. Utilisation of novel technology may be able to yield further information, such as 4D ultrasound imaging technology that could provide a dynamic reconstruction of the vessel over time. This new technology could provide flow information and allow in-depth mapping of how genes and proteins are regulated by the changes in vessel dynamics, alongside the already studied alterations in vessel wall conformation and diameter.

Following on from mouse studies, development of human translational work is imperative to understanding whether the results of obtained from animal investigations can be transferred to the human pathology and lead to eventual treatment. Patients suffering from COPD in severe instances were often found to have NE inhibitor deficiency, leading to worsening of the COPD condition. Studies within a similar cohort

of alpha-1 antitrypsin deficiency patients could provide a dynamic case study, with the potential to greatly increase our understanding of NE within the AAA pathology.

At this point in time, the aneurysm field needs extensive molecular science-based studies to further understand causal mechanisms of AAA, and consequentially understand the pathologies initiation and development process. From there we will be able to identify further candidate genes or proteins that have an influence on AAA, leading to the possibility of being able to control them and resultantly improve treatment of AAA.

Beyond clinical implications and translation to human therapeutic treatment, the identification of causal pathways would be a significant milestone in the study of AAA. Proteomics analysis produced novel therapeutic targets and potential mechanisms of the AAA process. Three of these proteins were verified to be implicated within differences seen between NE Knockout and Control tissues, however further study on TBL1x, Caveolin 2 and COPS8 could yet yield significant results with a large impact on the understanding of AAA as a pathology and the underlying mechanisms that induce and progress it. Undertaking of similar works done within this study but focusing on one of the alternate proteins would be appropriate for determining the impact of the protein upon the pathology. Production of genetic knockout mouse strains or initial work within cell lines could produce information on the impact of these proteins within specific cells involved within the AAA process.

12 CONCLUSION

In conclusion, during this study, we were able to demonstrate the influence of NE within the AAA pathology with genetic abolishment of the enzyme limiting the effects of three separate models of aneurysm *in vivo.* Following analysis of generated tissues, the link between NE and MMPs has been strengthened and appears to play an influential role within the AAA phenotype, as evidenced within histology and RNA analysis from Ang II, $CaCl_2$ and BAPN treated aortas. Furthermore, identification of novel target molecules within the AAA pathology was achieved via proteomic methodologies, before verification by western blot and immunostaining methods. NE appears to regulate an array of proteins, most noted within this study being TBL1x, Cops 8 and Caveolin 2, all with potential influence in the decrease of AAA incidence.

Translatability of the research into the human needs to be further developed and verified, currently, initial pilot human studies demonstrated NE staining with AAA patient tissues although no significant difference was determined between serum samples of healthy and AAA patients. Identification of NE co-localising with MMPs within human AAA samples were carried out suggesting the findings of *in vivo* studies could be applicable within the human condition.

These studies were carried out after the successful development of AAA imaging protocols that give automated and reproducible results. This enabled a non-biased analysis of the aorta within all mice over the time course of AAA models.

In conclusion, genetic knockout of NE inhibits AAA/TAAD production within animal models, occurring in part by regulation of MMPs, with the other potential mediators of the phenomena put forward.

13 REFERENCES

1. Golledge J, Muller J, Daugherty A, Norman P. Abdominal Aortic Aneurysm Pathogenesis and Implications for Management. Arterioscler Thromb Vasc Biol. 2006 Jan 12;26(12):2605–13.

2. Buijs RVC, Willems TP, Tio RA, Boersma HH, Tielliu IFJ, Slart RHJA, et al. Calcification as a risk factor for rupture of abdominal aortic aneurysm. Eur J Vasc Endovasc Surg Off J Eur Soc Vasc Surg. 2013 Nov;46(5):542–8.

3. Go AS, Mozaffarian D, Roger VL, Benjamin EJ, Berry JD, Borden WB, et al. Heart Disease and Stroke Statistics—2013 Update A Report From the American Heart Association. Circulation. 2013 Jan 1;127(1):e6–245.

4. Hernesniemi JA, Vänni V, Hakala T. The prevalence of abdominal aortic aneurysm is consistently high among patients with coronary artery disease. J Vasc Surg. 2015 Jul;62(1):232-240.e3.

5. Choke E, Vijaynagar B, Thompson J, Nasim A, Bown MJ, Sayers RD. Changing Epidemiology of Abdominal Aortic Aneurysms in England and Wales Older and More Benign? Circulation. 2012 Mar 4;125(13):1617–25.

6. Svensjö S, Björck M, Gürtelschmid M, Gidlund KD, Hellberg A, Wanhainen A. Low Prevalence of Abdominal Aortic Aneurysm Among 65-Year-Old Swedish Men Indicates a Change in the Epidemiology of the Disease. Circulation. 2011 Jun 9;124(10):1118–23.

7. Norman PE, Powell JT. Abdominal Aortic Aneurysm The Prognosis in Women Is Worse Than in Men. Circulation. 2007 May 6;115(22):2865–9.

8. Koole D, Zandvoort HJA, Schoneveld A, Vink A, Vos JA, van den Hoogen LL, et al. Intraluminal abdominal aortic aneurysm thrombus is associated with disruption of wall integrity. J Vasc Surg. 2013 Jan;57(1):77–83.

9. Gong Y, Hart E, Shchurin A, Hoover-Plow J. Inflammatory macrophage migration requires MMP-9 activation by plasminogen in mice. J Clin Invest. 2008 Sep;118(9):3012–24.

10. Thompson RW, Liao S, Curci JA. Vascular smooth muscle cell apoptosis in abdominal aortic aneurysms. Coron Artery Dis. 1997 Oct;8(10):623–31.

11. Didangelos A, Yin X, Mandal K, Saje A, Smith A, Xu Q, et al. Extracellular matrix composition and remodeling in human abdominal aortic aneurysms: a proteomics approach. Mol Cell Proteomics MCP. 2011 Aug;10(8):M111.008128.

12. Anidjar S, Dobrin PB, Eichorst M, Graham GP, Chejfec G. Correlation of inflammatory infiltrate with the enlargement of experimental aortic aneurysms. J Vasc Surg. 1992 Aug;16(2):139–47.

13. Henry CM, Sullivan GP, Clancy DM, Afonina IS, Kulms D, Martin SJ. Neutrophil-Derived Proteases Escalate Inflammation through Activation of IL-36 Family Cytokines. Cell Rep. 2016 Feb 2;14(4):708–22.

14. Metzler KD, Goosmann C, Lubojemska A, Zychlinsky A, Papayannopoulos V. A Myeloperoxidase-Containing Complex Regulates Neutrophil Elastase Release and Actin Dynamics during NETosis. Cell Rep. 2014 Jul 24;8(3):883–96.

15. Warnatsch A, Ioannou M, Wang Q, Papayannopoulos V. Neutrophil extracellular traps license macrophages for cytokine production in atherosclerosis. Science. 2015 Jul 17;349(6245):316–20.

16. Pham CTN. Neutrophil serine proteases: specific regulators of inflammation. Nat Rev Immunol. 2006 Jul;6(7):541–50.

17. Döring G. The Role of Neutrophil Elastase in Chronic Inflammation. Am J Respir Crit Care Med. 1994 Dec 1;150(6_pt_2):S114–7.

18. Chua F, Laurent GJ. Neutrophil Elastase. Proc Am Thorac Soc. 2006 Jul 1;3(5):424–7.

19. Idell S, Kucich U, Fein A, Kueppers F, James HL, Walsh PN, et al. Neutrophil elastase-releasing factors in bronchoalveolar lavage from patients with adult respiratory distress syndrome. Am Rev Respir Dis. 1985 Nov;132(5):1098–105.

20. Cailes JB, O'Connor C, Pantelidis P, Southcott AM, Fitzgerald MX, Black CM, et al. Neutrophil activation in fibrosing alveolitis: a comparison of lone cryptogenic fibrosing alveolitis and systemic sclerosis. Eur Respir J. 1996 May;9(5):992–9.

21. Kamio K, Liu XD, Sugiura H, Togo S, Kawasaki S, Wang X, et al. Statins inhibit matrix metalloproteinase release from human lung fibroblasts. Eur Respir J. 2010 Mar 1;35(3):637–46.

22. Silverstein MD, Pitts SR, Chaikof EL, Ballard DJ. Abdominal aortic aneurysm (AAA): cost-effectiveness of screening, surveillance of intermediate-sized AAA, and management of symptomatic AAA. Proc Bayl Univ Med Cent. 2005 Oct;18(4):345–67.

23. Jones WB, Taylor SM, Kalbaugh CA, Joels CS, Blackhurst DW, Langan III EM, et al. Lost to follow-up: A potential under-appreciated limitation of endovascular aneurysm repair. J Vasc Surg. 2007;46(3):434–40.

24. Brewster DC, Cronenwett JL, Hallett Jr. JW, Johnston KW, Krupski WC, Matsumura JS. Guidelines for the treatment of abdominal aortic aneurysms: Report of a subcommittee of the Joint Council of the American Association for Vascular Surgery and Society for Vascular Surgery. J Vasc Surg. 2003;37(5):1106–17.

25. Al-Omran M, Verma S, Lindsay TF, Weisel RD, Sternbach Y. Clinical Decision Making for Endovascular Repair of Abdominal Aortic Aneurysm. Circulation. 2004 Jul 12;110(23):e517–23.

26. Shimizu K, Mitchell RN, Libby P. Inflammation and Cellular Immune Responses in Abdominal Aortic Aneurysms. Arterioscler Thromb Vasc Biol. 2006 Jan 5;26(5):987–94.

27. Longo GM, Xiong W, Greiner TC, Zhao Y, Fiotti N, Baxter BT. Matrix metalloproteinases 2 and 9 work in concert to produce aortic aneurysms. J Clin Invest. 2002 Sep;110(5):625–32.

28. Scott RAP, Bridgewater SG, Ashton HA. Randomized clinical trial of screening for abdominal aortic aneurysm in women. Br J Surg. 2002 Mar;89(3):283–5.

29. Powell JT, Norman PE. Abdominal aortic aneurysm events in postmenopausal women. BMJ. 2008 Oct 14;337(oct14 2):a1894–a1894.

30. Edwards ST, Schermerhorn ML, O'Malley AJ, Bensley RP, Hurks R, Cotterill P, et al. Comparative effectiveness of endovascular versus open repair of ruptured abdominal aortic aneurysm in the Medicare population. J Vasc Surg. 2013 Dec 14;

31. Kurosawa K, Matsumura JS, Yamanouchi D. Current status of medical treatment for abdominal aortic aneurysm. Circ J Off J Jpn Circ Soc. 2013 Nov 25;77(12):2860–6.

32. Wang J-B, Zhou B, Gu X-L, Li M-H, Gu B-X, Wang W, et al. Treatment of a canine carotid artery aneurysm model with a biodegradable nanofiber-covered stent: a prospective pilot study. Neurol India. 2013 Jun;61(3):282–7.

33. Bergqvist D. Abdominal aortic aneurysms. Eur Heart J. 1997 Apr;18(4):545–6.

34. Golledge J, Kuivaniemi H. Genetics of abdominal aortic aneurysm. Curr Opin Cardiol. 2013 May;28(3):290–6.

35. Basford JE, Koch S, Anjak A, Singh VP, Krause EG, Robbins N, et al. Smooth Muscle LDL Receptor-Related Protein-1 Deletion Induces Aortic Insufficiency and Promotes Vascular Cardiomyopathy in Mice. PLoS ONE [Internet]. 2013 Nov 29 [cited 2014 Jan 4];8(11). Available from: http://www.ncbi.nlm.nih.gov/pmc/articles/PMC3843717/

36. Li X, Zhao G, Zhang J, Duan Z, Xin S. Prevalence and trends of the abdominal aortic aneurysms epidemic in general population - a meta-analysis. PloS One. 2013;8(12):e81260.

37. Kokot M, Biolik G, Ziaja D, Fojt T, Cisak K, Antoniak K, et al. Endothelium injury and inflammatory state during abdominal aortic aneurysm surgery: scrutinizing the very early and minute injurious effects using endothelial markers - a pilot study. Arch Med Sci AMS. 2013 Jun 20;9(3):479–86.

38. Wei Y, Xiong J, Zuo S, Chen F, Chen D, Wu T, et al. Association of polymorphisms on chromosome 9p21.3 region with increased susceptibility of abdominal aortic aneurysm in a Chinese Han population. J Vasc Surg. 2013 Dec 20;

39. Lima BL, Santos EJC, Fernandes GR, Merkel C, Mello MRB, Gomes JPA, et al. A New Mouse Model for Marfan Syndrome Presents Phenotypic Variability Associated with the Genetic Background and Overall Levels of Fbn1 Expression. Nogales-Gadea G, editor. PLoS ONE. 2010 Nov 30;5(11):e14136.

40. Pereira L, Lee SY, Gayraud B, Andrikopoulos K, Shapiro SD, Bunton T, et al. Pathogenetic sequence for aneurysm revealed in mice underexpressing fibrillin-1. Proc Natl Acad Sci. 1999 Mar 30;96(7):3819–23.

41. Mariko B, Pezet M, Escoubet B, Bouillot S, Andrieu J-P, Starcher B, et al. Fibrillin-1 genetic deficiency leads to pathological ageing of arteries in mice. J Pathol. 2011 May;224(1):33–44.

42. Daugherty A, Rateri DL, Cassis LA. Role of the renin-angiotensin system in the development of abdominal aortic aneurysms in animals and humans. Ann N Y Acad Sci. 2006 Nov;1085:82–91.

43. Hayek T, Attias J, Smith J, Breslow JL, Keidar S. Antiatherosclerotic and antioxidative effects of captopril in apolipoprotein E-deficient mice. J Cardiovasc Pharmacol. 1998 Apr;31(4):540–4.

44. Thompson RW, Curci JA, Ennis TL, Mao D, Pagano MB, Pham CTN. Pathophysiology of abdominal aortic aneurysms: insights from the elastase-induced model in mice with different genetic backgrounds. Ann N Y Acad Sci. 2006 Nov;1085:59–73.

45. Ouali R, Berthelon M-C, Bégeot M, Saez JM. Angiotensin II Receptor Subtypes AT1 and AT2 Are Down-Regulated by Angiotensin II through AT1 Receptor by Different Mechanisms [1]. Endocrinology. 1997 Feb;138(2):725–33.

46. Daugherty A, Manning MW, Cassis LA. Angiotensin II promotes atherosclerotic lesions and aneurysms in apolipoprotein E-deficient mice. J Clin Invest. 2000 Jun;105(11):1605–12.

47. Saraff K, Babamusta F, Cassis LA, Daugherty A. Aortic dissection precedes formation of aneurysms and atherosclerosis in angiotensin II-infused, apolipoprotein E-deficient mice. Arterioscler Thromb Vasc Biol. 2003 Sep 1;23(9):1621–6.

48. Rateri DL, Howatt DA, Moorleghen JJ, Charnigo R, Cassis LA, Daugherty A. Prolonged infusion of angiotensin II in apoE(-/-) mice promotes macrophage recruitment with continued expansion of abdominal aortic aneurysm. Am J Pathol. 2011 Sep;179(3):1542–8.

49. Cornuz J, Sidoti Pinto C, Tevaearai H, Egger M. Risk factors for asymptomatic abdominal aortic aneurysm: systematic review and meta-analysis of population-based screening studies. Eur J Public Health. 2004 Dec;14(4):343–9.

50. Lu H, Rateri DL, Cassis LA, Daugherty A. The Role of the Renin-Angiotensin System in Aortic Aneurysmal Diseases. Curr Hypertens Rep. 2008 Apr;10(2):99–106.

51. Chen Z, Ma J, Cen Y, Liu Y, You C. The angiotensin converting enzyme insertion/deletion polymorphism and intracranial aneurysm: a meta-analysis of case-control studies. Neurol India. 2013 Jun;61(3):293–9.

52. Yeung JMC, Heeley M, Gray S, Lingam MK, Manning G, Nash JR, et al. Does the angiotensin-converting enzyme (ACE) gene polymorphism affect rate of abdominal aortic aneurysm expansion? Eur J Vasc Endovasc Surg Off J Eur Soc Vasc Surg. 2002 Jul;24(1):69–71.

53. Czerski A, Bujok J, Gnus J, Hauzer W, Ratajczak K, Nowak M, et al. Experimental methods of abdominal aortic aneurysm creation in swine as a large animal model. J Physiol Pharmacol Off J Pol Physiol Soc. 2013 Apr;64(2):185–92.

54. Bhamidipati CM, Mehta GS, Lu G, Moehle CW, Barbery C, DiMusto PD, et al. Development of a novel murine model of aortic aneurysms using peri-adventitial elastase. Surgery. 2012 Aug;152(2):238–46.

55. Riches K, Angelini TG, Mudhar GS, Kaye J, Clark E, Bailey MA, et al. Exploring smooth muscle phenotype and function in a bioreactor model of abdominal aortic aneurysm. J Transl Med. 2013;11:208.

56. Halpern VJ, Nackman GB, Gandhi RH, Irizarry E, Scholes JV, Ramey WG, et al. The elastase infusion model of experimental aortic aneurysms: synchrony of induction of endogenous proteinases with matrix destruction and inflammatory cell response. J Vasc Surg. 1994 Jul;20(1):51–60.

57. Miskolczi L, Guterman LR, Flaherty JD, Szikora I, Hopkins LN. Rapid saccular aneurysm induction by elastase application in vitro. Neurosurgery. 1997 Jul;41(1):220–8; discussion 228-229.

58. Longo GM, Buda SJ, Fiotta N, Xiong W, Griener T, Shapiro S, et al. MMP-12 has a role in abdominal aortic aneurysms in mice. Surgery. 2005 Apr;137(4):457–62.

59. Yoshimura K, Aoki H, Ikeda Y, Fujii K, Akiyama N, Furutani A, et al. Regression of abdominal aortic aneurysm by inhibition of c-Jun N-terminal kinase. Nat Med. 2005 Dec;11(12):1330–8.

60. Isenburg JC, Simionescu DT, Starcher BC, Vyavahare NR. Elastin stabilization for treatment of abdominal aortic aneurysms. Circulation. 2007 Apr 3;115(13):1729–37.

61. Basalyga DM, Simionescu DT, Xiong W, Baxter BT, Starcher BC, Vyavahare NR. Elastin degradation and calcification in an abdominal aorta injury model: role of matrix metalloproteinases. Circulation. 2004 Nov 30;110(22):3480–7.

62. MacTaggart JN, Xiong W, Knispel R, Baxter BT. Deletion of CCR2 but not CCR5 or CXCR3 inhibits aortic aneurysm formation. Surgery. 2007 Aug;142(2):284–8.

63. Gacchina C, Brothers T, Ramamurthi A. Evaluating smooth muscle cells from CaCl2-induced rat aortal expansions as a surrogate culture model for study of elastogenic induction of human aneurysmal cells. Tissue Eng Part A. 2011 Aug;17(15–16):1945–58.

64. Morimoto K, Hasegawa T, Tanaka A, Wulan B, Yu J, Morimoto N, et al. Free-radical scavenger edaravone inhibits both formation and development of abdominal aortic aneurysm in rats. J Vasc Surg. 2012 Jun;55(6):1749–58.

65. Tong J, Schriefl AJ, Cohnert T, Holzapfel GA. Gender differences in biomechanical properties, thrombus age, mass fraction and clinical factors of abdominal aortic aneurysms. Eur J Vasc Endovasc Surg Off J Eur Soc Vasc Surg. 2013 Apr;45(4):364–72.

66. Mi T, Nie B, Zhang C, Zhou H. The elevated expression of osteopontin and NF-κB in human aortic aneurysms and its implication. J Huazhong Univ Sci Technol Med Sci Hua Zhong Ke Ji Xue Xue Bao Yi Xue Ying Wen Ban Huazhong Keji Daxue Xuebao Yixue Yingdewen Ban. 2011 Oct;31(5):602–7.

67. Tanaka A, Hasegawa T, Chen Z, Okita Y, Okada K. A novel rat model of abdominal aortic aneurysm using a combination of intraluminal elastase infusion and extraluminal calcium chloride exposure. J Vasc Surg. 2009 Dec;50(6):1423–32.

68. Yamanouchi D, Morgan S, Stair C, Seedial S, Lengfeld J, Kent KC, et al. Accelerated aneurysmal dilation associated with apoptosis and inflammation in a newly developed calcium phosphate rodent abdominal aortic aneurysm model. J Vasc Surg. 2012 Aug;56(2):455–61.

69. Gertz SD, Kurgan A, Eisenberg D. Aneurysm of the rabbit common carotid artery induced by periarterial application of calcium chloride in vivo. J Clin Invest. 1988 Mar;81(3):649–56.

70. Van Herck JL, De Meyer GRY, Martinet W, Van Hove CE, Foubert K, Theunis MH, et al. Impaired Fibrillin-1 Function Promotes Features of Plaque Instability in Apolipoprotein E–Deficient Mice. Circulation. 2009 Dec 15;120(24):2478–87.

71. Lerouge S, Bonneviot M-C, Salazkin I, Raymond J, Soulez G. Endothelial denudation combined with embolization in the prevention of endoleaks after endovascular aneurysm repair: an animal study. J Endovasc Ther Off J Int Soc Endovasc Spec. 2011 Oct;18(5):686–96.

72. Mestas J, Hughes CCW. Of Mice and Not Men: Differences between Mouse and Human Immunology. J Immunol. 2004 Jan 3;172(5):2731–8.

73. Shin SY, Kim JH, Baker A, Lim Y, Lee YH. Transcription factor Egr-1 is essential for maximal matrix metalloproteinase-9 transcription by tumor necrosis factor alpha. Mol Cancer Res MCR. 2010 Apr;8(4):507–19.

74. Shin I-S, Kim J-M, Kim KL, Jang SY, Jeon E-S, Choi SH, et al. Early growth response factor-1 is associated with intraluminal thrombus formation in human abdominal aortic aneurysm. J Am Coll Cardiol. 2009 Mar 3;53(9):792–9.

75. Xu Y, Toure F, Qu W, Lin L, Song F, Shen X, et al. Advanced glycation end product (AGE)-receptor for AGE (RAGE) signaling and up-regulation of Egr-1 in hypoxic macrophages. J Biol Chem. 2010 Jul 23;285(30):23233–40.

76. Miskolczi L, Guterman LR, Flaherty JD, Szikora I, Hopkins LN. Rapid saccular aneurysm induction by elastase application in vitro. Neurosurgery. 1997 Jul;41(1):220–8; discussion 228-229.

77. Yamashita O, Yoshimura K, Nagasawa A, Ueda K, Morikage N, Ikeda Y, et al. Periostin links mechanical strain to inflammation in abdominal aortic aneurysm. PloS One. 2013;8(11):e79753.

78. Malekzadeh S, Fraga-Silva RA, Trachet B, Montecucco F, Mach F, Stergiopulos N. Role of the renin-angiotensin system on abdominal aortic aneurysms. Eur J Clin Invest. 2013 Dec;43(12):1328–38.

79. Morris DR, Biros E, Cronin O, Kuivaniemi H, Golledge J. The association of genetic variants of matrix metalloproteinases with abdominal aortic aneurysm: a systematic review and meta-analysis. Heart Br Card Soc. 2013 Jun 27;

80. Tsui JC. Experimental Models of Abdominal Aortic Aneurysms. Open Cardiovasc Med J. 2010 Nov 26;4:221–30.

81. Marinov GR, Marois Y, Paˇris E, Rob P, Formichi M, Douville Y, et al. Can the Infusion of Elastase in the Abdominal Aorta of the Yucatán Miniature Swine

Consistently Produce Experimental Aneurysms? J Invest Surg. 1997 Jan;10(3):129–50.

82. Vijaynagar B, Bown MJ, Sayers RD, Choke E. Potential role for anti-angiogenic therapy in abdominal aortic aneurysms. Eur J Clin Invest. 2013 Jul;43(7):758–65.

83. Chen NX, O'Neill KD, Chen X, Kiattisunthorn K, Gattone VH, Moe SM. Activation of Arterial Matrix Metalloproteinases Leads to Vascular Calcification in Chronic Kidney Disease. Am J Nephrol. 2011 Sep;34(3):211–9.

84. Wang Y, Krishna S, Golledge J. The calcium chloride-induced rodent model of abdominal aortic aneurysm. Atherosclerosis. 2013 Jan 1;226(1):29–39.

85. Golledge J, Norman PE. Atherosclerosis and Abdominal Aortic Aneurysm Cause, Response, or Common Risk Factors? Arterioscler Thromb Vasc Biol. 2010 Jan 6;30(6):1075–7.

86. Shi G-P, Lindholt JS. Mast cells in abdominal aortic aneurysms. Curr Vasc Pharmacol. 2013 May;11(3):314–26.

87. Neumayer C. The role of neutrophils in abdominal aortic aneurysms. :1.

88. Akhavanpoor M, Wangler S, Gleissner CA, Korosoglou G, Katus HA, Erbel C. Adventitial inflammation and its interaction with intimal atherosclerotic lesions. Front Physiol [Internet]. 2014 Aug 8 [cited 2019 Dec 31];5. Available from: http://journal.frontiersin.org/article/10.3389/fphys.2014.00296/abstract

89. Spear R, Boytard L, Blervaque R, Chwastyniak M, Hot D, Vanhoutte J, et al. Adventitial Tertiary Lymphoid Organs as Potential Source of MicroRNA Biomarkers for Abdominal Aortic Aneurysm. Int J Mol Sci. 2015 May 18;16(12):11276–93.

90. Gräbner R, Lötzer K, Döpping S, Hildner M, Radke D, Beer M, et al. Lymphotoxin β receptor signaling promotes tertiary lymphoid organogenesis in the aorta adventitia of aged ApoE−/− mice. J Exp Med. 2009 Jan 16;206(1):233–48.

91. Rowe VL, Stevens SL, Reddick TT, Freeman MB, Donnell R, Carroll RC, et al. Vascular smooth muscle cell apoptosis in aneurysmal, occlusive, and normal human aortas. J Vasc Surg. 2000 Mar;31(3):567–76.

92. Cao X, Cai Z, Liu J, Zhao Y, Wang X, Li X, et al. miRNA-504 inhibits p53-dependent vascular smooth muscle cell apoptosis and may prevent aneurysm formation. Mol Med Rep. 2017 Mar;16(3):2570–8.

93. Lyon CA, Williams H, Bianco R, Simmonds SJ, Brown BA, Wadey KS, et al. Aneurysm Severity is Increased by Combined Mmp-7 Deletion and N-cadherin Mimetic (EC4-Fc) Over-Expression. Sci Rep. 2017 Dec;7(1):17342.

94. Yamanouchi D, Morgan S, Kato K, Lengfeld J, Zhang F, Liu B. Effects of Caspase Inhibitor on Angiotensin II-Induced Abdominal Aortic Aneurysm in Apolipoprotein E–Deficient Mice. Arterioscler Thromb Vasc Biol. 2010 Apr;30(4):702–7.

95. Wang Y-X, Martin-McNulty B, da Cunha V, Vincelette J, Lu X, Feng Q, et al. Fasudil, a Rho-Kinase Inhibitor, Attenuates Angiotensin II–Induced Abdominal Aortic Aneurysm in Apolipoprotein E–Deficient Mice by Inhibiting Apoptosis and Proteolysis. Circulation. 2005 May 3;111(17):2219–26.

96. Thrumurthy SG, Karthikesalingam A, Patterson BO, Holt PJE, Thompson MM. The diagnosis and management of aortic dissection. BMJ. 2011 Jan 11;344(jan11 1):d8290–d8290.

97. Gao Y, Li D, Cao Y, Zhu X, Zeng Z, Tang L. Prognostic value of serum albumin for patients with acute aortic dissection: A retrospective cohort study. Medicine (Baltimore). 2019 Feb;98(6):e14486.

98. Khan IA, Nair CK. Clinical, Diagnostic, and Management Perspectives of Aortic Dissection. Chest. 2002 Jul;122(1):311–28.

99. Cui J, Jing Z, Zhuang S, Qi S, Li L, Zhou J, et al. D-dimer as a Biomarker for Acute Aortic Dissection: A Systematic Review and Meta-analysis. Medicine (Baltimore). 2015 Jan;94(4):e471.

100. Ince H, Nienaber CA. Diagnosis and management of patients with aortic dissection. Heart. 2005 Dec 30;93(2):266–70.

101. Hagan PG, Nienaber CA, Isselbacher EM, Bruckman D, Karavite DJ, Russman PL, et al. The International Registry of Acute Aortic Dissection (IRAD): New Insights Into an Old Disease. JAMA. 2000 Feb 16;283(7):897.

102. Qiao Y, Zeng Y, Ding Y, Fan J, Luo K, Zhu T. Numerical simulation of two-phase non-Newtonian blood flow with fluid-structure interaction in aortic dissection. Comput Methods Biomech Biomed Engin. 2019 Mar;1–11.

103. Vianello E, Dozio E, Rigolini R, Marrocco-Trischitta MM, Tacchini L, Trimarchi S, et al. Acute phase of aortic dissection: a pilot study on CD40L, MPO, and MMP-1, -2, 9 and TIMP-1 circulating levels in elderly patients. Immun Ageing [Internet]. 2016 Dec [cited 2019 Mar 20];13(1). Available from: http://www.immunityageing.com/content/13/1/9

104. Pearman CM. Ehlers-Danlos with disease of the aorta and mitral valve. J Acute Med. 2012 Dec;2(4):128–30.

105. Wu D, Choi JC, Sameri A, Minard CG, Coselli JS, Shen YH, et al. Inflammatory Cell Infiltrates in Acute and Chronic Thoracic Aortic Dissection. AORTA. 2013 Dec 1;1(6):259–67.

106. Sbarouni E, Georgiadou P, Marathias A, Geroulanos S, Kremastinos DTh. D-dimer and BNP levels in acute aortic dissection. Int J Cardiol. 2007 Nov;122(2):170–2.

107. Tieu BC, Lee C, Sun H, Lejeune W, Recinos A, Ju X, et al. An adventitial IL-6/MCP1 amplification loop accelerates macrophage-mediated vascular inflammation leading to aortic dissection in mice. J Clin Invest. 2009 Dec;119(12):3637–51.

108. Caglayan AO, Dundar M. Inherited diseases and syndromes leading to aortic aneurysms and dissections. Eur J Cardiothorac Surg. 2009 Jun;35(6):931–40.

109. Kakko S, Räisänen T, Tamminen M, Airaksinen J, Groundstroem K, Juvonen T, et al. Candidate locus analysis of familial ascending aortic aneurysms and dissections confirms the linkage to the chromosome 5q13-14 in Finnish families. J Thorac Cardiovasc Surg. 2003 Jul;126(1):106–13.

110. van de Luijtgaarden KM, Heijsman D, Maugeri A, Weiss MM, Verhagen HJM, IJpma A, et al. First genetic analysis of aneurysm genes in familial and sporadic abdominal aortic aneurysm. Hum Genet. 2015 Aug;134(8):881–93.

111. Albornoz G, Coady MA, Roberts M, Davies RR, Tranquilli M, Rizzo JA, et al. Familial Thoracic Aortic Aneurysms and Dissections—Incidence, Modes of Inheritance, and Phenotypic Patterns. Ann Thorac Surg. 2006 Oct;82(4):1400–5.

112. Sawada H, Chen JZ, Wright BC, Sheppard MB, Lu HS, Daugherty A. Heterogeneity of aortic smooth muscle cells: A determinant for regional characteristics of thoracic aortic aneurysms? J Transl Intern Med. 2018 Oct 9;6(3):93–6.

113. Trigueros-Motos L, González-Granado JM, Cheung C, Fernández P, Sánchez-Cabo F, Dopazo A, et al. Embryological-Origin–Dependent Differences in Homeobox Expression in Adult Aorta: Role in Regional Phenotypic Variability and Regulation of NF-κB Activity. Arterioscler Thromb Vasc Biol. 2013 Jun;33(6):1248–56.

114. Sawada H, Rateri DL, Moorleghen JJ, Majesky MW, Daugherty A. Smooth Muscle Cells Derived From Second Heart Field and Cardiac Neural Crest Reside in Spatially Distinct Domains in the Media of the Ascending Aorta—Brief Report. Arterioscler Thromb Vasc Biol. 2017 Sep;37(9):1722–1726.

115. Robinson PN. The molecular genetics of Marfan syndrome and related microfibrillopathies. J Med Genet. 2000 Jan 1;37(1):9–25.

116. Cury M, Zeidan F, Lobato AC. Aortic Disease in the Young: Genetic Aneurysm Syndromes, Connective Tissue Disorders, and Familial Aortic Aneurysms and Dissections. Int J Vasc Med. 2013;2013:1–7.

117. Donato B, Ferreira MJ. Cardiovascular risk in Turner syndrome. Rev Port Cardiol. 2018 Jul;37(7):607–21.

118. Treasure T, Takkenberg JJM, Pepper J. Surgical management of aortic root disease in Marfan syndrome and other congenital disorders associated with aortic root aneurysms. Heart. 2014 Oct 15;100(20):1571–6.

119. Saeyeldin A, Zafar MA, Velasquez CA, Ip K, Gryaznov A, Brownstein AJ, et al. Natural history of aortic root aneurysms in Marfan syndrome. Ann Cardiothorac Surg. 2017 Nov;6(6):625–32.

120. D'hondt S, Van Damme T, Malfait F. Vascular phenotypes in nonvascular subtypes of the Ehlers-Danlos syndrome: a systematic review. Genet Med. 2018 Jun;20(6):562–73.

121. Gong Y, Chippada-Venkata UD, Oh WK. Roles of Matrix Metalloproteinases and Their Natural Inhibitors in Prostate Cancer Progression. Cancers. 2014 Jun 27;6(3):1298–327.

122. Zhang G, Miyake M, Lawton A, Goodison S, Rosser CJ. Matrix metalloproteinase-10 promotes tumor progression through regulation of angiogenic and apoptotic pathways in cervical tumors. BMC Cancer. 2014 May 3;14:310.

123. Mittal B, Mishra A, Srivastava A, Kumar S, Garg N. Matrix metalloproteinases in coronary artery disease. Adv Clin Chem. 2014;64:1–72.

124. Egeblad M, Werb Z. New functions for the matrix metalloproteinases in cancer progression. Nat Rev Cancer. 2002 Mar;2(3):161–74.

125. Jackson MT, Moradi B, Smith MM, Jackson CJ, Little CB. Activation of Matrix Metalloproteinases 2, 9, and 13 by Activated Protein C in Human Osteoarthritic Cartilage Chondrocytes. Arthritis Rheumatol. 2014 Jun 1;66(6):1525–36.

126. Bobryshev YV, Lord RS, Pärsson H. Immunophenotypic analysis of the aortic aneurysm wall suggests that vascular dendritic cells are involved in immune responses. Cardiovasc Surg Lond Engl. 1998 Jun;6(3):240–9.

127. Shelton L, Rada JS. Effects of cyclic mechanical stretch on extracellular matrix synthesis by human scleral fibroblasts. Exp Eye Res. 2007 Feb;84(2):314–22.

128. Wilson JS, Baek S, Humphrey JD. Parametric study of effects of collagen turnover on the natural history of abdominal aortic aneurysms. Proc Math Phys Eng Sci R Soc [Internet]. 2013 Feb 8 [cited 2014 May 10];469(2150). Available from: http://www.ncbi.nlm.nih.gov/pmc/articles/PMC3637002/

129. Xue M, McKelvey K, Shen K, Minhas N, March L, Park S-Y, et al. Endogenous MMP-9 and not MMP-2 promotes rheumatoid synovial fibroblast survival, inflammation and cartilage degradation. Rheumatol Oxf Engl. 2014 Jun 29;

130. Hu WS, Hu W. 220 ERK1/2 Mediates Lipopolysaccharide-upregulated FGF-2, UPA, MMP-2, MMP-9 and Cellular Migration in Primary Cardiac Fibroblasts. Heart Br Card Soc. 2014 Jun;100 Suppl 3:A120.

131. Ehrlichman LK, Ford JW, Roelofs KJ, Tedeschi-Filho W, Futchko JS, Ramacciotti E, et al. Gender-dependent differential phosphorylation in the ERK signaling pathway is associated with increased MMP2 activity in rat aortic smooth muscle cells. J Surg Res. 2010 May 1;160(1):18–24.

132. Zhang Y, Naggar JC, Welzig CM, Beasley D, Moulton KS, Park H-J, et al. Simvastatin inhibits angiotensin II-induced abdominal aortic aneurysm formation in apolipoprotein E-knockout mice: possible role of ERK. Arterioscler Thromb Vasc Biol. 2009 Nov;29(11):1764–71.

133. Jeong SH, Kim HJ, Ryu HJ, Ryu WI, Park Y-H, Bae HC, et al. ZnO nanoparticles induce TNF-α expression via ROS-ERK-Egr-1 pathway in human keratinocytes. J Dermatol Sci. 2013 Dec;72(3):263–73.

134. Charolidi N, Pirianov G, Torsney E, Pearce S, Laing K, Nohturfft A, et al. Pioglitazone Identifies a New Target for Aneurysm Treatment: Role of Egr1 in an Experimental Murine Model of Aortic Aneurysm. J Vasc Res. 2015 Jun 20;52(2):81–93.

135. Wu X-F, Zhang J, Paskauskas S, Xin S-J, Duan Z-Q. The role of estrogen in the formation of experimental abdominal aortic aneurysm. Am J Surg. 2009 Jan;197(1):49–54.

136. Thompson RW, Holmes DR, Mertens RA, Liao S, Botney MD, Mecham RP, et al. Production and localization of 92-kilodalton gelatinase in abdominal aortic aneurysms. An elastolytic metalloproteinase expressed by aneurysm-infiltrating macrophages. J Clin Invest. 1995 Jul;96(1):318–26.

137. Kim SC, Singh M, Huang J, Prestigiacomo CJ, Winfree CJ, Solomon RA, et al. Matrix metalloproteinase-9 in cerebral aneurysms. Neurosurgery. 1997 Sep;41(3):642–66; discussion 646-647.

138. Chen S-J, Ning H, Ishida W, Sodin-Semrl S, Takagawa S, Mori Y, et al. The Early-Immediate Gene EGR-1 Is Induced by Transforming Growth Factor-β and Mediates Stimulation of Collagen Gene Expression. J Biol Chem. 2006 Jul 28;281(30):21183–97.

139. Crist SA, Elzey BD, Ahmann MT, Ratliff TL. Early growth response-1 (EGR-1) and nuclear factor of activated T cells (NFAT) cooperate to mediate CD40L expression in megakaryocytes and platelets. J Biol Chem. 2013 Nov 22;288(47):33985–96.

140. Dollery CM, Owen CA, Sukhova GK, Krettek A, Shapiro SD, Libby P. Neutrophil Elastase in Human Atherosclerotic Plaques: Production by Macrophages. Circulation. 2003 Jun 10;107(22):2829–36.

141. Gardiner EE, Andrews RK. Neutrophil extracellular traps (NETs) and infection-related vascular dysfunction. Blood Rev. 2012 Nov;26(6):255–9.

142. Yan H, Zhou H-F, Akk A, Hu Y, Springer LE, Ennis TL, et al. Neutrophil Proteases Promote Experimental Abdominal Aortic Aneurysm via Extracellular Trap Release and Plasmacytoid Dendritic Cell ActivationHighlights. Arterioscler Thromb Vasc Biol. 2016 Aug 1;36(8):1660–9.

143. Jackson PL, Xu X, Wilson L, Weathington NM, Clancy JP, Blalock JE, et al. Human Neutrophil Elastase-Mediated Cleavage Sites of MMP-9 and TIMP-1: Implications to Cystic Fibrosis Proteolytic Dysfunction. :8.

144. Crisford H, Sapey E, Stockley RA. Proteinase 3; a potential target in chronic obstructive pulmonary disease and other chronic inflammatory diseases. Respir Res [Internet]. 2018 Dec [cited 2019 May 4];19(1). Available from: https://respiratory-research.biomedcentral.com/articles/10.1186/s12931-018-0883-z

145. Csernok E, Ernst M, Schmitt W, Bainton DF, Gross WL. Activated neutrophils express proteinase 3 on their plasma membrane in vitro and in vivo. Clin Exp Immunol. 2008 Jun 28;95(2):244–50.

146. Abdgawad M, Gunnarsson L, Bengtsson AA, Geborek P, Nilsson L, Segelmark M, et al. Elevated neutrophil membrane expression of proteinase 3 is dependent upon CD177 expression: Membrane PR3 depends on CD177 expression. Clin Exp Immunol. 2010 Jun;no-no.

147. Proteinase 3 and Serpin B1: a novel pathway in the regulation of caspase-3 activation, neutrophil spontaneous apoptosis, and inflammation. Inflamm Cell Signal [Internet]. 2014 Dec 1 [cited 2019 May 4]; Available from: http://www.smartscitech.com/index.php/ICS/article/view/462

148. Pham CTN. Neutrophil serine proteases: specific regulators of inflammation. Nat Rev Immunol. 2006 Jul;6(7):541–50.

149. Leskinen M, Wang Y, Leszczynski D, Lindstedt KA, Kovanen PT. Mast cell chymase induces apoptosis of vascular smooth muscle cells. Arterioscler Thromb Vasc Biol. 2001 Apr;21(4):516–22.

150. Thomas MP, Whangbo J, McCrossan G, Deutsch AJ, Martinod K, Walch M, et al. Leukocyte Protease Binding to Nucleic Acids Promotes Nuclear Localization and Cleavage of Nucleic Acid Binding Proteins. J Immunol. 2014 Jun 1;192(11):5390–7.

151. Spinosa M, Su G, Salmon MD, Lu G, Cullen JM, Fashandi AZ, et al. Resolvin D1 decreases abdominal aortic aneurysm formation by inhibiting NETosis in a mouse model. J Vasc Surg. 2018 Dec;68(6):93S-103S.

152. Blomkalns AL, Gavrila D, Thomas M, Neltner BS, Blanco VM, Benjamin SB, et al. CD14 directs adventitial macrophage precursor recruitment: role in early abdominal aortic aneurysm formation. J Am Heart Assoc. 2013 Apr;2(2):e000065.

153. Newby A. Matrix metalloproteinases regulate migration, proliferation, and death of vascular smooth muscle cells by degrading matrix and non-matrix substrates. Cardiovasc Res. 2006 Feb 15;69(3):614–24.

154. Korkmaz B, Horwitz MS, Jenne DE, Gauthier F. Neutrophil Elastase, Proteinase 3, and Cathepsin G as Therapeutic Targets in Human Diseases. Pharmacol Rev. 2010 Dec 1;62(4):726–59.

155. Folkesson M, Vorkapic E, Gulbins E, Japtok L, Kleuser B, Welander M, et al. Inflammatory cells, ceramides, and expression of proteases in perivascular adipose tissue adjacent to human abdominal aortic aneurysms. J Vasc Surg [Internet]. 2016 Mar 6 [cited 2017 Jan 10];0(0). Available from: http://www.jvascsurg.org/article/S0741-5214(16)00148-8/abstract

156. Sano M, Sasaki T, Hirakawa S, Sakabe J, Ogawa M, Baba S, et al. Lymphangiogenesis and Angiogenesis in Abdominal Aortic Aneurysm. PLOS ONE. 2014 Mar 20;9(3):e89830.

157. Villacorta L, Chang L. The role of perivascular adipose tissue in vasoconstriction, arterial stiffness, and aneurysm. Horm Mol Biol Clin Investig. 2015 Feb;21(2):137–47.

158. Verhagen SN, Visseren FLJ. Perivascular adipose tissue as a cause of atherosclerosis. Atherosclerosis. 2011 Jan 1;214(1):3–10.

159. Arts FA, Sciot R, Brichard B, Renard M, de Rocca Serra A, Dachy G, et al. PDGFRB gain-of-function mutations in sporadic infantile myofibromatosis. Hum Mol Genet. 2017 May 15;26(10):1801–10.

160. Nakayama A, Nakayama M, Turner CJ, Hoing S, Lepore JJ, Adams RH. Ephrin-B2 controls PDGFR internalization and signaling. Genes Dev. 2013 Dec 1;27(23):2576–89.

161. Wilkinson-Berka JL, Babic S, de Gooyer T, Stitt AW, Jaworski K, Ong LGT, et al. Inhibition of Platelet-Derived Growth Factor Promotes Pericyte Loss and Angiogenesis in Ischemic Retinopathy. Am J Pathol. 2004 Apr;164(4):1263–73.

162. Kuivaniemi H, Ryer EJ, Elmore JR, Tromp G. Understanding the pathogenesis of abdominal aortic aneurysms. Expert Rev Cardiovasc Ther. 2015 Sep 2;13(9):975–87.

163. Kugo H, Tanaka H, Moriyama T, Zaima N. Pathological Implication of Adipocytes in AAA Development and the Rupture. Ann Vasc Dis. 2018 Jun 25;11(2):159–68.

164. Garratt LW, Sutanto EN, Ling K-M, Looi K, Iosifidis T, Martinovich KM, et al. Matrix metalloproteinase activation by free neutrophil elastase contributes to bronchiectasis progression in early cystic fibrosis. Eur Respir J. 2015 Aug;46(2):384–94.

165. Geraghty P, Rogan MP, Greene CM, Boxio RMM, Poiriert T, O'Mahony M, et al. Neutrophil Elastase Up-Regulates Cathepsin B and Matrix Metalloprotease-2 Expression. J Immunol. 2007 May 1;178(9):5871–8.

166. Si-Tahar M, Pidard D, Balloy V, Moniatte M, Kieffer N, Van Dorsselaer A, et al. Human neutrophil elastase proteolytically activates the platelet integrin alphaIIbbeta3 through cleavage of the carboxyl terminus of the alphaIIb subunit heavy chain. Involvement in the potentiation of platelet aggregation. J Biol Chem. 1997 Apr 25;272(17):11636–47.

167. Wen G, An W, Chen J, Maguire EM, Chen Q, Yang F, et al. Genetic and Pharmacologic Inhibition of the Neutrophil Elastase Inhibits Experimental Atherosclerosis. J Am Heart Assoc [Internet]. 2018 Feb 20 [cited 2019 Feb 13];7(4). Available from: https://www.ahajournals.org/doi/10.1161/JAHA.117.008187

168. de Bont CM, Boelens WC, Pruijn GJM. NETosis, complement, and coagulation: a triangular relationship. Cell Mol Immunol. 2019 Jan;16(1):19–27.

169. Kaplan MJ, Radic M. Neutrophil Extracellular Traps: Double-Edged Swords of Innate Immunity. J Immunol. 2012 Sep 15;189(6):2689–95.

170. Bchir S, Nasr H ben, Bouchet S, Benzarti M, Garrouch A, Tabka Z, et al. Concomitant elevations of MMP-9, NGAL, proMMP-9/NGAL and neutrophil elastase in serum of smokers with chronic obstructive pulmonary disease. J Cell Mol Med. 2016 Dec 1;n/a-n/a.

171. Bihlet AR, Karsdal MA, Sand JMB, Leeming DJ, Roberts M, White W, et al. Biomarkers of extracellular matrix turnover are associated with emphysema and eosinophilic-bronchitis in COPD. Respir Res. 2017 Jan 19;18(1):22.

172. Kolaczkowska E, Kubes P. Neutrophil recruitment and function in health and inflammation. Nat Rev Immunol. 2013 Mar;13(3):159–75.

173. Benabid R, Wartelle J, Malleret L, Guyot N, Gangloff S, Lebargy F, et al. Neutrophil Elastase Modulates Cytokine Expression: CONTRIBUTION TO HOST DEFENSE AGAINST PSEUDOMONAS AERUGINOSA-INDUCED PNEUMONIA. J Biol Chem. 2012 Oct 12;287(42):34883–94.

174. Devaney JM, Greene CM, Taggart CC, Carroll TP, O'Neill SJ, McElvaney NG. Neutrophil elastase up-regulates interleukin-8 via toll-like receptor 4. FEBS Lett. 2003 Jun 5;544(1–3):129–32.

175. Strong M, Amenta P, Dumont A, Medel R. The role of leukocytes in the formation and rupture of intracranial aneurysms. Neuroimmunol Neuroinflammation. 2015;2(2):107.

176. Hannawa KK, Eliason JL, Woodrum DT, Pearce CG, Roelofs KJ, Grigoryants V, et al. L-Selectin–Mediated Neutrophil Recruitment in Experimental Rodent Aneurysm Formation. Circulation. 2005 Jul 12;112(2):241–7.

177. Kurihara T, Shimizu-Hirota R, Shimoda M, Adachi T, Shimizu H, Weiss SJ, et al. Neutrophil-Derived Matrix Metalloproteinase 9 Triggers Acute Aortic Dissection. Circulation. 2012 Dec 18;126(25):3070–80.

178. Cao RY, Amand T, Ford MD, Piomelli U, Funk CD. The Murine Angiotensin II-Induced Abdominal Aortic Aneurysm Model: Rupture Risk and Inflammatory Progression Patterns. Front Pharmacol. 2010;1:9.

179. Otterhag SN, Gottsäter A, Lindblad B, Acosta S. Decreasing incidence of ruptured abdominal aortic aneurysm already before start of screening. BMC Cardiovasc Disord. 2016 Feb 17;16:44.

180. Tang A, Kauffmann C, Tremblay-Paquet S, Elkouri S, Steinmetz O, Morin-Roy F, et al. Morphologic evaluation of ruptured and symptomatic abdominal aortic aneurysm by three-dimensional modeling. J Vasc Surg. 2014 Apr 1;59(4):894-902.e3.

181. Makowski MR, Wiethoff A, Ebersberger U, Blume U, Warley A, Jansen C, et al. Molecular assessment of aortic aneurysm wall integrity using an elastin-specific MR imaging probe. J Cardiovasc Magn Reson. 2013 Jan 30;15(1):O4.

182. Hatakeyama T, Shigematsu H, Muto T. Risk factors for rupture of abdominal aortic aneurysm based on three-dimensional study. J Vasc Surg. 2001 Mar 1;33(3):453–61.

183. Bartoli MA, Kober F, Cozzone P, Thompson RW, Alessi MC, Bernard M. In Vivo Assessment of Murine Elastase-induced Abdominal Aortic Aneurysm with High Resolution Magnetic Resonance Imaging. Eur J Vasc Endovasc Surg. 2012 Nov 1;44(5):475–81.

184. Klink A, Heynens J, Herranz B, Lobatto ME, Arias T, Sanders HMHF, et al. In Vivo Characterization of a New Abdominal Aortic Aneurysm Mouse Model With Conventional and Molecular Magnetic Resonance Imaging. J Am Coll Cardiol. 2011 Dec 6;58(24):2522–30.

185. Noone TC, Semelka RC, Chaney DM, Reinhold C. Abdominal imaging studies: comparison of diagnostic accuracies resulting from ultrasound, computed

tomography, and magnetic resonance imaging in the same individual. Magn Reson Imaging. 2004 Jan;22(1):19–24.

186. Cai H, Yang Z, Cao X, Xia W, Xu X. A new iterative triclass thresholding technique in image segmentation. IEEE Trans Image Process Publ IEEE Signal Process Soc. 2014 Mar;23(3):1038–46.

187. Habets J, Zandvoort HJA, Reitsma JB, Bartels LW, Moll FL, Leiner T, et al. Magnetic Resonance Imaging is More Sensitive than Computed Tomography Angiography for the Detection of Endoleaks after Endovascular Abdominal Aortic Aneurysm Repair: A Systematic Review. Eur J Vasc Endovasc Surg. 2013 Apr 1;45(4):340–50.

188. Otsu N. A Threshold Selection Method from Gray-Level Histograms. IEEE Trans Syst Man Cybern. 1979 Jan;9(1):62–6.

189. Arnaoutoglou E, Kouvelos G, Koutsoumpelis A, Patelis N, Lazaris A, Matsagkas M. An Update on the Inflammatory Response after Endovascular Repair for Abdominal Aortic Aneurysm. Mediators Inflamm. 2015;2015:1–6.

190. Marian AJ. On Genetics, Inflammation, and Abdominal Aortic Aneurysm: Can Single Nucleotide Polymorphisms Predict the Outcome? Circulation. 2001 May 8;103(18):2222–4.

191. Naba A, Pearce OMT, Rosario AD, Ma D, Ding H, Rajeeve V, et al. Characterization of the Extracellular Matrix of Normal and Diseased Tissues Using Proteomics. J Proteome Res. 2017 Jul 4;16(8):3083–91.

192. Yan H, Zhou H-F, Akk A, Hu Y, Springer LE, Ennis TL, et al. Neutrophil Proteases Promote Experimental Abdominal Aortic Aneurysm via Extracellular Trap Release and Plasmacytoid Dendritic Cell Activation. Arterioscler Thromb Vasc Biol. 2016 Aug;36(8):1660–9.

193. Jonathan Golledge MK. Reduced expansion rate of abdominal aortic aneurysms in patients with diabetes may be related to aberrant monocyte-matrix interactions. Eur Heart J. 2008;29(5):665–72.

194. Takayanagi T, Crawford KJ, Kobayashi T, Obama T, Tsuji T, Elliott KJ, et al. Caveolin 1 is critical for abdominal aortic aneurysm formation induced by angiotensin II and inhibition of lysyl oxidase. Clin Sci. 2014 Jun 1;126(11):785–800.

195. Heinen CA, Losekoot M, Sun Y, Watson PJ, Fairall L, Joustra SD, et al. Mutations in *TBL1X* Are Associated With Central Hypothyroidism. J Clin Endocrinol Metab. 2016 Dec;101(12):4564–73.

196. Tong L, Yuan Y, Wu S. Therapeutic microRNAs targeting the NF-kappa B signaling circuits of cancers. Adv Drug Deliv Rev. 2015 Jan;81:1–15.

197. Perissi V, Aggarwal A, Glass CK, Rose DW, Rosenfeld MG. A Corepressor/Coactivator Exchange Complex Required for Transcriptional Activation by Nuclear Receptors and Other Regulated Transcription Factors. Cell. 2004 Feb;116(4):511–26.

198. Niino T, Hata M, Sezai A, Yoshitake I, Unosawa S, Fujita K, et al. Efficacy of Neutrophil Elastase Inhibitor on Type A Acute Aortic Dissection. Thorac Cardiovasc Surg. 2010 Apr;58(03):164–8.

199. Furusawa T, Tsukioka K, Fukui D, Sakaguchi M, Seto T, Terasaki T, et al. The Effects of a Neutrophil Elastase Inhibitor on the Postoperative Respiratory Failure of Acute Aortic Dissection. Thorac Cardiovasc Surg. 2006 Sep;54(6):404–7.

200. Jia L-X, Zhang W-M, Zhang H-J, Li T-T, Wang Y-L, Qin Y-W, et al. Mechanical stretch-induced endoplasmic reticulum stress, apoptosis and inflammation contribute to thoracic aortic aneurysm and dissection: CHOP deficiency prevents thoracic aortic aneurysm/dissection. J Pathol. 2015 Jul;236(3):373–83.

201. Wen G, Zhang C, Chen Q, Luong LA, Mustafa A, Ye S, et al. A Novel Role of Matrix Metalloproteinase-8 in Macrophage Differentiation and Polarization. J Biol Chem. 2015 Jul 31;290(31):19158–72.

202. Darwood R, Earnshaw JJ, Turton G, Shaw E, Whyman M, Poskitt K, et al. Twenty-year review of abdominal aortic aneurysm screening in men in the county of Gloucestershire, United Kingdom. J Vasc Surg. 2012 Jul;56(1):8–13.

203. Satta J, Laurila A, Pääkkö P, Haukipuro K, Sormunen R, Parkkila S, et al. Chronic inflammation and elastin degradation in abdominal aortic aneurysm disease: an immunohistochemical and electron microscopic study. Eur J Vasc Endovasc Surg Off J Eur Soc Vasc Surg. 1998 Apr;15(4):313–9.

204. Itoh Y, Nagase H. Preferential Inactivation of Tissue Inhibitor of Metalloproteinases-1 That Is Bound to the Precursor of Matrix Metalloproteinase 9 (Progelatinase B) by Human Neutrophil Elastase. J Biol Chem. 1995 Jul 14;270(28):16518–21.

205. Sakalihasan N, Delvenne P, Nusgens BV, Limet R, Lapière CM. Activated forms of MMP2 and MMP9 in abdominal aortic aneurysms. J Vasc Surg. 1996 Jul;24(1):127–33.

206. Galis ZS, Khatri JJ. Matrix Metalloproteinases in Vascular Remodeling and Atherogenesis: The Good, the Bad, and the Ugly. Circ Res. 2002 Feb 22;90(3):251–62.

207. Ishibashi M, Sayers S, D'Armiento JM, Tall AR, Welch CL. TLR3 deficiency protects against collagen degradation and medial destruction in murine atherosclerotic plaques. Atherosclerosis. 2013 Jul;229(1):52–61.

208. An analysis of blood flow dynamics in AAA [Internet]. ResearchGate. [cited 2017 Mar 28]. Available from: https://www.researchgate.net/publication/221913868_An_analysis_of_blood_flow_dynamics_in_AAA

209. Wågsäter D, Johansson D, Fontaine V, Vorkapic E, Bäcklund A, Razuvaev A, et al. Serine protease inhibitor A3 in atherosclerosis and aneurysm disease. Int J Mol Med. 2012 Aug;30(2):288–94.

210. Paliogiannis P, Fois AG, Sotgia S, Mangoni AA, Zinellu E, Pirina P, et al. Neutrophil to lymphocyte ratio and clinical outcomes in COPD: recent evidence and future perspectives. Eur Respir Rev. 2018 Mar 31;27(147):170113.

14 APPENDIX

14.1 PROTEOMICS RESULTS FRACTION 1

Acc	Name	Mascot Score	No Unique Peptid	E3: NE Vs A	E2: NE Vs A	E1: NE Vs A	P value	E3: NE Vs A	E2: NE Vs A	E1: NE Vs A	P vaulue	E3: NE Vs A	E2: NE Vs A	E1: NE Vs A	ABS	log10 of p	log2 of FC
TBL1X_MOU	F-box-like/WD repeat-	234.38	4	-0.34586	0.213839	1		0.632923	0.714492	5.42E-05		0	0	1	1.492685	4.266366	0.577909577551201
KPRB_MOUS	Phosphoribosyl pyro	64.12	2	-8.0354	-0.01579	(11)		0.272041	0.980512	0.000851		0	0	1	11.44824	3.0703	3.51705331574394+4.532360141827191
K2C79_MOU	Keratin, type II cytosk	155.33	3	2.255864	2.090353	2		0.015292	0.204771	0.002536		1	0	1	2.28931	2.595773	1.19491311652675
IRGM1_MOU	Immunity-related GTP	114.92	3	-0.57343	1.446237	(3)		0.77077	0.051802	0.00412		0	0	1	2.614974	2.385089	1.38679640903029+4.532360141827191
COIA1_MOU	Collagen alpha-1(XVII	541.06	11	-0.76035	0.764304	1		0.046286	0.137781	0.005863		1	0	1	0.802348	2.231888	-0.3177006566288
NUPS4_MOU	Nuclear pore comple	224.92	8	-0.70081	-0.05784	(2)		0.228976	0.870941	0.006406		0	0	1	2.050748	2.193425	1.03615051867134+4.532360141827191
EIF3C_MOUS	Eukaryotic translation	82.46	8	1.485604	-0.07307	1		0.338005	0.726108	0.007373		0	0	1	0.860664	2.132346	-0.216477296772534
LKHA4_MOU	Leukotriene A-4 hydr	884.58	20	0.500149	-2.66682	(2)		0.635583	0.003242	0.007692		0	1	1	2.279126	2.11398	1.18848061175644+4.532360141827191
K2C75_MOU	Keratin, type II cytosk	401.1437	4	-0.28619	0.813816	2		0.544913	0.035793	0.009975		0	1	1	1.993644	2.0011	0.995408136671923
DIC_MOUSE	Mitochondrial dicarb	400.28	12	1.036198	0.11359	0		0.263142	0.62269	0.011065		0	0	1	0.342538	1.956047	-1.54566327797207
TLN2_MOUS	Talin-2 OS=Mus musc	153.17	11	-1.01916	1.256342	(1)		0.478909	0.123259	0.011084		0	0	1	1.204358	1.955298	0.268264179541011+4.532360141827191
SGCG_MOUS	Gamma-sarcoglycan C	161.05	4	0.00853	1.428512	(3)		0.995657	0.142625	0.01139		0	0	1	2.634651	1.943478	1.39761179532828+4.532360141827191
SRBS1_MOU	Sorbin and SH3 doma	158.4937	6	-4.05596	1.494575	1		0.083567	0.035247	0.011504		0	1	1	0.810954	1.939154	-0.302307668327417
DPP4_MOUS	Dipeptidyl peptidase	124.26	2	-3.51274	0.759489	1		0.181578	0.011751	0.012233		0	1	1	1.09541	1.912464	0.131471462393384
ACLY_MOUSE	ATP-citrate synthase C	1496.421	58	2.601298	-0.02769	1		0.062253	0.953392	0.012471		0	0	1	0.718788	1.904111	-0.476361377548627
ETFA_MOUSE	Electron transfer flavo	616.58	31	-2.16391	-0.5795	(1)		0.042894	0.17138	0.013152		1	0	1	1.298353	1.881025	0.376682981919671+4.532360141827191
VATH_MOUS	V-type proton ATPase	246.85	10	-2.92753	-0.22678	(1)		0.131856	0.502158	0.014227		0	0	1	1.251019	1.846894	0.323103837248184+4.532360141827191
CA198_MOU	Uncharacterized prote	58.78	1	-2.82808	-0.21448	(2)		0.354427	0.72454	0.016511		0	0	1	1.97568	1.782238	0.982349527438491+4.532360141827191
ASM3A_MOU	Acid sphingomyelina	130.38	5	-3.00412	-1.33047	(1)		0.018851	0.316986	0.017911		1	0	1	1.420881	1.746885	0.506785592420917+4.532360141827191
EIF3L_MOUS	Eukaryotic translation	88.08	7	-3.93403	-0.26112	0		0.060875	0.398331	0.018774		0	0	1	0.481518	1.726437	-1.05433730368725
CHM2B_MOU	Charged multivesicula	73.58	1	-11.0087	0.699134	(2)		0.053023	0.39615	0.019794		0	0	1	1.849488	1.703465	0.887126146520793+4.532360141827191
PCKGM_MOU	Phosphoenolpyruvat	74.89	5	-6.13386	0.424898	(3)		0.175736	0.171902	0.023003		0	0	1	3.040963	1.63821	1.60452829728939+4.532360141827191
ODBA_MOUS	2-oxoisovalerate dehy	353.6837	16	0.366117	-0.05819	1		0.397221	0.898251	0.023115		0	0	1	0.860185	1.636111	-0.217280183140906
NFH_MOUSE	Neurofilament heavy	64.88	5	2.550908	2.072499	2		0.122217	0.263297	0.024159		0	0	1	1.74705	1.61693	0.804921144983137
PEX19_MOU	Peroxisomal biogene	123.6	6	3.027589	0.556377	1		0.097568	0.216602	0.024162		0	0	1	1.125709	1.616869	0.17083351802847
KV3A5_MOU	Ig kappa chain V-III re	114.56	1	-7.86807	-0.13312	2		0.32243	0.868973	0.026549		0	0	1	1.523914	1.575952	0.6077811544654
H3C_MOUSE	Histone H3.3C OS=Mu	239.91	8	-4.48692	1.199794	(1)		0.0102	0.068912	0.029449		1	0	1	1.350728	1.530935	0.433737541836857+4.532360141827191
PLCL1_MOUSE		50.99	1	-2.42446	0.009587	(1)		0.391073	0.994149	0.029694		0	0	1	0.775698	1.527327	-0.366433034071424+4.532360141827191
RDH13_MOUSE		50.99	2	-2.42422	0.010231	(1)		0.391081	0.993727	0.030186		0	0	1	0.777619	1.520196	-0.362865008909254+4.532360141827191
COQ6_MOU	Ubiquinone biosynth	462.53	12	-2.83016	1.340995	(1)		0.153878	0.028258	0.030875		0	1	1	1.271285	1.510391	0.346287049004155+4.532360141827191
RD23A_MOU	UV excision repair pro	140.6	3	-5.71933	-0.56402	(1)		0.097404	0.208199	0.03116		0	0	1	0.658631	1.506399	-0.602458602535905+4.532360141827191
MPC1_MOU	Mitochondrial pyruva	87.39	3	1.20882	1.009402	1		0.095452	0.160946	0.032276		0	0	1	0.909764	1.491123	-0.136435960871983
PDLIS_MOU	PDZ and LIM domain	147.88	7	-5.69327	-0.43116	(1)		0.331093	0.346955	0.03295		0	0	1	0.748942	1.482142	-0.417073946953284+4.532360141827191
ILEUA_MOUS	Leukocyte elastase inh	426.28	22	-0.92958	-1.10128	(1)		0.144614	0.147837	0.039194		0	0	1	0.874402	1.406776	-0.193631058762863+4.532360141827191
RT31_MOUS	28S ribosomal protei	171.72	5	-2.05	-0.64113	(1)		0.118897	0.348339	0.039464		0	0	1	0.777754	1.4038	-0.362614945311374+4.532360141827191
RM18_MOU	39S ribosomal protei	93.52	3	-5.13579	0.436447	1		0.008235	0.003101	0.039677		1	1	1	1.157413	1.401461	0.210903183610051
DDX3L_MOU	Putative ATP-depende	153	4	-1.77387	0.255306	2		0.294054	0.362813	0.040255		0	0	1	1.723843	1.395182	0.78562880330012
K1C13_MOU	Keratin, type I cytoske	212.77	10	2.457555	0.27292	1		0.048862	0.724519	0.040608		1	0	1	1.095962	1.39139	0.132197855114077

14.2 PROTEOMICS RESULTS FRACTION 2

Acc	Name	Mascot Sc	No Uniqu	E3: NE Vs	E2: NE Vs	E1: NE Vs	P vaulue	E3: NE Vs	E2: NE Vs	E1: NE Vs	P vaulue	E3: NE Vs	E2: NE Vs	E1: NE Vs	FC	P
RAB10_MOU	Ras-related protein Rab-10	253.25	4	-0.361	1	0.23213		0.76536	0.00021	0.76252		0	1	0	1	3.68011
RMXL1_MOL	RNA binding motif protein	120.46	2	-0.0178	1	0.81201		0.98361	0.00039	0.20456		0	1	0	1	3.41003
CLIC5_MOUS	Chloride intracellular chan	60.91	2	-3.4019	(1)	-4.4171		0.3934	0.0004	0.38072		0	1	0	(1)	3.40252
UGDH_MOUS	UDP-glucose 6-dehydrogen	93.15	6	0.74795	0	-0.9334		0.19176	0.00055	0.59673		0	1	0	0	3.25771
REEP5_MOUS	Receptor expression-enhan	106.74	4	0.13821	1	0.35439		0.70078	0.00058	0.74877		0	1	0	1	3.23447
RS13_MOUSE	40S ribosomal protein S13	169.31	5	-6.0353	2	-0.2782		0.18977	0.00063	0.86548		0	1	0	2	3.20391
NPC2_MOUS	Epididymal secretory prote	80.62	3	0.34668	2	1.01423		0.77483	0.00063	0.07709		0	1	0	2	3.19835
CLM9_MOUS	CMRF35-like molecule 9 C	133.97	4	-0.0103	1	0.00584		0.97592	0.00091	0.98661		0	1	0	1	3.04296
FMO5_MOUS	Dimethylaniline monooxyg	68.45	2	-6.9191	2	0.77818		0.36272	0.00097	0.04543		0	1	1	2	3.01332
RUXF_MOUSE	Small nuclear ribonucleop	67.71	1	-9.5889	8	-2.7899		0.02206	0.00099	0.05369		1	1	0	8	3.00582
FIS1_MOUSE	Mitochondrial fission 1 pr	211.29	4	0.54543	1	1.21042		0.75741	0.00101	0.5833		0	1	0	1	2.99774
CNPY2_MOU	Protein canopy homolog 2	252.84	6	1.15543	3	-1.0282		0.22937	0.00101	0.2155		0	1	0	3	2.99504
TIM16_MOU	Mitochondrial import inne	92.83	2	-6.4411	2	0.77818		0.32103	0.00105	0.04543		0	1	1	2	2.97938
RAB18_MOU	Ras-related protein Rab-18	97.25	2	1.0548	2	0.77818		0.01057	0.00119	0.04543		1	1	1	2	2.92324
P2RX1_MOU	P2X purinoceptor 1 OS=M	72.22	2	0.85125	2	-0.0821		0.52165	0.00121	0.94326		0	1	0	2	2.91705
ATP5L_MOUS	ATP synthase subunit g, m	77.63	4	0.49163	1	-2.23		0.7949	0.00147	0.06488		0	1	0	1	2.83334
ATPD_MOUSE	ATP synthase subunit delta	142.73	2	-1.744	2	-0.0903		0.02326	0.00157	0.8277		1	1	0	2	2.80481
RAB2A_MOU	Ras-related protein Rab-2A	295.15	10	-2.5996	1	0.09035		0.0249	0.00164	0.79126		1	1	0	1	2.78412
MUP2_MOUS	Major urinary protein 2 OS	170.29	6	1.86355	3	0.59587		0.16292	0.00174	0.78599		0	1	0	3	2.75991
RLA1_MOUSE	60S acidic ribosomal prote	82.02	2	-3.9725	1	-0.6455		0.04268	0.0018	0.5583		1	1	0	1	2.74511
UK114_MOU	Ribonuclease UK114 OS=M	75.59	2	-8.0371	2	0.77818		0.22213	0.00184	0.04543		0	1	1	2	2.73503
ATP5I_MOUS	ATP synthase subunit e, m	120.28	2	-6.0164	1	-0.9951		0.12164	0.00185	0.51759		0	1	0	1	2.73363
PPIC_MOUSE	Peptidyl-prolyl cis-trans is	187.99	5	-2.7664	1	3.0836		0.16904	0.00196	0.14424		0	1	0	1	2.70786
ARL1_MOUSE	ADP-ribosylation factor-lik	130.91	2	1.0548	2	5.65079		0.01057	0.00201	0.36594		1	1	0	2	2.6959
RAB5B_MOU	Ras-related protein Rab-5B	232.74	5	0.95245	1	-0.031		0.0157	0.00207	0.98308		1	1	0	1	2.68411
TIM23_MOU	Mitochondrial import inne	144.14	2	-4.5661	2	-2.4491		0.01421	0.00207	0.40424		1	1	0	2	2.68399
TPM2_MOUS	Tropomyosin beta chain O	1805.35	72	0.11545	1	0.56714		0.82625	0.00218	0.447		0	1	0	1	2.66236
AN32A_MOU	Acidic leucine-rich nuclear	236.9	13	-2.4941	(1)	-0.5299		0.07708	0.0022	0.15265		0	1	0	(1)	2.65771
LRRF1_MOUS	Leucine-rich repeat flightle	128.92	7	0.56292	(1)	-0.0378		0.06242	0.00234	0.94135		0	1	0	(1)	2.6317
RS18_MOUSE	40S ribosomal protein S18	267.55	10	-3.6868	1	-0.4184		0.03338	0.00236	0.57884		1	1	0	1	2.62677
SC61B_MOU	Protein transport protein S	126.22	2	2.87836	2	5.35159		0.43753	0.00238	0.32852		0	1	0	2	2.62282
GPX41_MOU	Phospholipid hydroperoxi	201.39	7	-3.3812	1	-0.9588		0.03424	0.00254	0.4854		1	1	0	1	2.59464
ARPC4_MOU	Actin-related protein 2/3 c	219.32	4	-2.4291	1	0.1265		0.00767	0.00278	0.81052		1	1	0	1	2.55568
INSR_MOUSE	Insulin receptor OS=Mus m	54.93	3	-0.3684	3	2.16526		0.78301	0.0028	0.40437		0	1	0	3	2.55256
SF3B6_MOUS	Splicing factor 3B subunit	81.73	1	1.0548	1	0.77818		0.01057	0.003	0.04543		1	1	1	1	2.52315
RM18_MOUS	39S ribosomal protein L18	93.52	3	-5.1358	0	1.15741		0.00824	0.0031	0.03968		1	1	1	0	2.50855
RL30_MOUSE	60S ribosomal protein L30	146.97	3	-4.3755	1	0.04123		0.01258	0.00314	0.96234		1	1	0	1	2.50341
LKHA4_MOU	Leukotriene A-4 hydrolase	884.58	20	0.50015	(3)	-2.2791		0.63558	0.00324	0.00769		0	1	1	(3)	2.48924
SRSF4_MOUS	Serine/arginine-rich splicin	84.99	3	-0.2027	2	-0.1653		0.81049	0.00357	0.70881		0	1	0	2	2.44765
COMD3_MOU	COMM domain-containing	50.87	2	-8.8308	2	-0.2282		0.11827	0.00362	0.91582		0	1	0	2	2.44175
TM109_MOL	Transmembrane protein 10	118.16	4	-0.7214	1	-0.4294		0.55561	0.00383	0.49889		0	1	0	1	2.41702
TPM1_MOUS	Tropomyosin alpha-1 chai	1591.23	52	-0.1055	1	0.17753		0.86186	0.00394	0.80358		0	1	0	1	2.40481
GPR98_MOU	G-protein coupled receptor	52.83	3	1.1419	1	0.94066		0.04872	0.00411	0.18347		1	1	0	1	2.38651
GBG12_MOU	Guanine nucleotide-bindir	115.87	7	-3.1898	2	-0.3939		0.18176	0.0042	0.63297		0	1	0	2	2.3766
AT2A2_MOU	Sarcoplasmic/endoplasmi	1134.24	18	1.01737	1	1.12677		0.19421	0.00451	0.26693		0	1	0	1	2.34558
THR8_MOUSE	Prothrombin OS=Mus mus	240.801	18	-2.6951	(0)	-0.6082		0.00704	0.00455	0.25768		1	1	0	(0)	2.34242
TPM3_MOUS	Tropomyosin alpha-3 chai	1333.56	67	0.32968	1	0.57722		0.48338	0.00463	0.42703		0	1	0	1	2.33419
FUBP2_MOU	Far upstream element-bind	115.45	3	-6.5926	(3)	-0.6838		0.20274	0.00469	0.32714		0	1	0	(3)	2.32841
UD17C_MOU	UDP-glucuronosyltransfera	116.98	1	1.0548	3	0.77818		0.01057	0.0047	0.04543		1	1	1	3	2.32753

14.3 PROTEOMICS RESULTS FRACTION 3

Acc	Name	Mascot Sc	No Uniqu	E3: NE Vs	E2: NE Vs	E1: NE Vs	P vaulue	E3: NE Vs	E2: NE Vs	E1: NE Vs	P vaulue	E3: NE Vs	E2: NE Vs	E1: NE Vs	FC	
HNRPC_MOUS	Heterogeneous nuclear ribonucle	323.01	14	-3.1131	0.58969	-0.04323		5.87E-07	0.16798	0.93524		1	0	0	-3.1131	6.23131
H2B1C_MOUSE	Histone H2B type 1-C/E/G OS=M	292.05	7	-3.64791	1.35624	-1.38406		1.67E-05	0.04666	0.06375		1	1	0	-3.64791	4.77631
SNP23_MOUSE	Synaptosomal-associated protein	53.82	2	-10.8548	1.37066	-0.97658		1.93E-05	0.02185	0.4741		1	1	0	-10.8548	4.714
MFAP4_MOUSE		75.38	6	-3.116	1.25469	0.13362		8.29E-05	0.09978	0.72594		1	0	0	-3.116	4.08132
PSB8_MOUSE	Proteasome subunit beta type-8	101.76	5	-3.21951	0.75742	1.06037		0.000116	0.31949	0.35696		1	0	0	-3.21951	3.93578
LMNB1_MOUS	Lamin-B1 OS=Mus musculus GN	1193.42	43	-2.40318	0.96451	-0.23932		0.000123	0.06073	0.71514		1	0	0	-2.40318	3.90922
OPA1_MOUSE	Dynamin-like 120 kDa protein, m	992.35	31	-2.24188	-0.02738	-0.50607		0.000129	0.9324	0.39704		1	0	0	-2.24188	3.88949
DDHD2_MOUSE	Phospholipase DDHD2 OS=Mus	158.05	7	-5.65703	-0.35909	0.73417		0.00014	0.47905	0.10131		1	0	0	-5.65703	3.85525
NDUS3_MOUSE	NADH dehydrogenase [ubiquinon	324.88	9	-4.17494	0.33963	-0.6186		0.000198	0.45002	0.51395		1	0	0	-4.17494	3.70387
DUS3_MOUSE	Dual specificity protein phospha	103.32	12	-4.17957	0.34207	-0.61375		0.000202	0.44108	0.50739		1	0	0	-4.17957	3.69384
PBIP1_MOUSE	Pre-B-cell leukemia transcription	57.67	1	-9.96578	0.60656	-0.13891		0.000222	0.68526	0.85344		1	0	0	-9.96578	3.6531
SCLY_MOUSE	Selenocysteine lyase OS=Mus mu	54.47	1	-9.04103	-0.32845	-1.23447		0.000293	0.49746	0.0715		1	0	0	-9.04103	3.53249
EIF3I_MOUSE	Eukaryotic translation initiation f	174.09	10	-3.72813	0.05312	0.0952		0.000305	0.91205	0.85227		1	0	0	-3.72813	3.51589
ACTY_MOUSE	Beta-centractin OS=Mus musculu	349.38	8	-6.29753	0.16585	-2.90033		0.000342	0.44702	0.3673		1	0	0	-6.29753	3.46629
ISLR_MOUSE	Immunoglobulin superfamily co	211.71	6	-5.22717	0.21603	-1.53441		0.000371	0.5703	0.29232		1	0	0	-5.22717	3.43021
ETHE1_MOUSE	Persulfide dioxygenase ETHE1, m	131.56	7	-3.72027	0.35002	-1.08358		0.000372	0.32365	0.22495		1	0	0	-3.72027	3.4292
SPB6_MOUSE	Serpin B6 OS=Mus musculus GN	361.25	29	-3.24279	-0.60757	-1.01896		0.000419	0.35703	0.35027		1	0	0	-3.24279	3.37751
RBBP7_MOUSE	Histone-binding protein RBBP7 (	225.22	7	-3.48882	-0.01163	-0.21771		0.000525	0.97662	0.42338		1	0	0	-3.48882	3.28015
CD97_MOUSE	CD97 antigen OS=Mus musculus	311.46	7	-2.81015	-0.49204	-3.05407		0.000537	0.70598	0.32679		1	0	0	-2.81015	3.27043
CDC37_MOUSE	Hsp90 co-chaperone Cdc37 OS=I	152.66	5	-1.739	0.17015	-0.12532		0.000554	0.4981	0.82468		1	0	0	-1.739	3.25625
PSA5_MOUSE	Proteasome subunit alpha type-5	263.21	11	-3.32233	-0.39836	-0.07484		0.000591	0.27011	0.81284		1	0	0	-3.32233	3.2283
CTNB1_MOUSE	Catenin beta-1 OS=Mus musculu	465.24	18	2.903824	-0.17334	0.45614		0.000591	0.59291	0.29583		1	0	0	2.90382	3.22806
MECP2_MOUS	Methyl-CpG-binding protein 2 O	211.7	5	-3.44951	5.28746	0.43336		0.000618	0.10209	0.27803		1	0	0	-3.44951	3.2091
GMPPB_MOUS	Mannose-1-phosphate guanyltra	54.49	3	2.578488	-0.49845	-0.52138		0.000633	0.08669	0.34679		1	0	0	2.57849	3.19864
RL24_MOUSE	60S ribosomal protein L24 OS=M	72.73	1	-12.1115	0.74865	1.5758		0.000646	0.09256	0.56232		1	0	0	-12.1115	3.18989
GORS2_MOUSE	Golgi reassembly-stacking protein	96.23	6	2.539137	-0.25163	-0.06057		0.000702	0.56157	0.92985		1	0	0	2.53914	3.15369
VWA8_MOUSE	von Willebrand factor A domain-	649.62	15	3.162046	0.3515	-0.38275		0.000707	0.85452	0.07536		1	0	0	3.16205	3.15079
NNRD_MOUSE	ATP-dependent (S)-NAD(P)H-hydr	355.98	14	-9.48993	-0.39106	-0.79739		0.000718	0.04696	0.26983		1	1	0	-9.48993	3.14358
CSN8_MOUSE	COP9 signalosome complex sub	52.33	2	3.703205	1.18185	4.37147		0.000724	0.35143	0.10572		1	0	0	3.70321	3.13998
NID1_MOUSE	Nidogen-1 OS=Mus musculus GI	673.2	43	-3.7231	0.69331	-0.5824		0.000739	0.29768	0.27382		1	0	0	-3.7231	3.13164
MIME_MOUSE	Mimecan OS=Mus musculus GN	632.21	24	-3.13736	0.10179	-0.94013		0.000745	0.72323	0.05272		1	0	0	-3.13736	3.12813
SEC13_MOUSE	Protein SEC13 homolog OS=Mus	115.76	7	-1.29883	-0.23496	-0.60206		0.000765	0.46083	0.24407		1	0	0	-1.29883	3.11628
GBB2_MOUSE	Guanine nucleotide-binding prot	494.3	8	-3.48051	0.58584	-0.41814		0.000815	0.07227	0.44372		1	0	0	-3.48051	3.08873
TMOD3_MOUS	Tropomodulin-3 OS=Mus muscu	590.35	19	-3.00538	-0.20065	-0.04081		0.00091	0.51381	0.85892		1	0	0	-3.00538	3.04078
PHB2_MOUSE	Prohibitin-2 OS=Mus musculus	780.5	29	-5.54635	0.77314	-0.77495		0.000977	0.2405	0.08154		1	0	0	-5.54635	3.01003
NDUS8_MOUSE	NADH dehydrogenase [ubiquinon	299.75	8	-3.88738	0.5217	-1.24826		0.001068	0.32919	0.40366		1	0	0	-3.88738	2.97146
ACTB_MOUSE	Serine beta-lactamase-like protein	55.49	38	-1.69366	1.2939	0.05743		0.001075	0.12707	0.86106		1	0	0	-1.69366	2.96859
SEPT8_MOUSE	Septin-8 OS=Mus musculus GN=	192.35	8	-3.87496	0.11609	-0.35049		0.001084	0.72207	0.55604		1	0	0	-3.87496	2.96491
PLBL2_MOUSE	Putative phospholipase B-like 2	212.79	4	-3.17338	0.01694	-0.39265		0.001179	0.96214	0.32971		1	0	0	-3.17338	2.92857
MIC19_MOUSE	MICOS complex subunit Mic19	967.04	24	-2.499	0.86019	-0.63588		0.001196	0.16405	0.66039		1	0	0	-2.499	2.92222
ACS2L_MOUSE	Acetyl-coenzyme A synthetase 2-l	335.56	16	3.586525	-0.57561	1.4282		0.001274	0.12874	0.10235		1	0	0	3.58653	2.89482
B4GT5_MOUSE	Beta-1,4-galactosyltransferase 5 C	69.4637	2	-3.24248	-0.04231	-0.16497		0.001319	0.93822	0.74775		1	0	0	-3.24248	2.87974
ARC1B_MOUSE	Actin-related protein 2/3 comple	80.91	12	-5.18429	0.21775	-0.00209		0.00135	0.5936	0.99704		1	0	0	-5.18429	2.86962
PRDX4_MOUSE	Peroxiredoxin-4 OS=Mus muscul	182.04	8	-1.61415	0.10795	0.04274		0.001354	0.60511	0.92631		1	0	0	-1.61415	2.86847